MECHANICS OF CLOSED-DIE FORGING (PHASE II)

James R. Douglas, et al

Battelle Columbus Laboratories

Prepared for:

Army Materials and Mechanics Research Center

November 1972

AMMRC CTR 72-25

A STUDY OF MECHANICS OF CLOSED-DIE FORGING PHASE II

November 1972

JAMES R. DOUGLAS and TAYLAN ALTAN

BATTELLE
Columbus Laboratories
505 King Avenue
Columbus, Ohio 43201

Final Report - Contract DAAG46-71-C-0095

Prepared for

ARMY MATERIALS AND MECHANICS RESEARCH CENTER
Watertown, Massachusetts 02172

Unclassified

Security Classification

DOCUMENT CONTROL DATA - R & D

(Security classification of title, body of abstract and indexing annotation must be entered when the overall report is classified)

1 ORIGINATING ACTIVITY (Corporate author) Battelle, Columbus Laboratories 505 King Avenue Columbus, Ohio 43201	2a. REPORT SECURITY CLASSIFICATION Unclassified 2b. GROUP

3 REPORT TITLE

Mechanics of Closed-Die Forging (Phase II)

4 DESCRIPTIVE NOTES (Type of report and inclusive dates)

Final Report, March 22, 1971 - September 21, 1972

5 AUTHOR(S) (First name, middle initial, last name)

James R. Douglas and Taylan Altan

6 REPORT DATE November 1972	7a. TOTAL NO OF PAGES 112	7b NO OF REFS
8a. CONTRACT OR GRANT NO DAAG46-71-C-0095 b. PROJECT NO D/A Project 6062 c. AMCMS Code 4097.92.1.P6062 (XC1) d.	9a ORIGINATOR'S REPORT NUMBER(S) AMMRC CTR 72-25 9b. OTHER REPORT NO(S) (Any other numbers that may be assigned this report)	

10 DISTRIBUTION STATEMENT

Approved for public release, distribution unlimited.

11 SUPPLEMENTARY NOTES	12. SPONSORING MILITARY ACTIVITY Army Materials and Mechanics Research Center Watertown, Massachusetts 02170

13 ABSTRACT

This report represents the result of Phase II work completed under this manufacturing improvement program. ~~Phase II of~~ the program covered the following specific areas (a) flow stresses of metals, (b) instrumentation of forging presses, (c) evaluation and comparison of screw presses and mechanical presses for forging, (d) uniform compression tests and ring tests for determining the flow stress of metals, and (e) methods for predicting and measuring forging load under production conditions. It is expected that the information developed in this program will contribute to the improvement in the design and execution of forging operations.

1a

DD FORM 1 NOV 68 1473 REPLACES DD FORM 1473, 1 JAN 64, WHICH IS OBSOLETE FOR ARMY USE.

Unclassified

Security Classification

14 KEY WORDS	LINK A		LINK B		LINK C	
	ROLE	WT	ROLE	WT	ROLE	WT
Forging						
Die forging						
Deformation						
Forging presses						
Hydraulic press						
Flow stress						
Instrumentation						
Stainless steel						
Titanium alloys						

16

AMMRC CTR 72 25

A STUDY OF MECHANICS OF CLOSED DIE FORGING (PHASE II)

Technical Report by
JAMES R DOUGLAS AND TAYLAN ALTAN
BATTELLE
Columbus Laboratories
505 King Avenue
Columbus, Ohio 43201

NOVEMBER 1972

FINAL REPORT Contract No. DAAG46-71-C-0095

D/A Project 6062
AMCMS Code 4097.92.1.P6062 (XC1)
Title of Project: Materials Manufacturing and Technology

Prepared for

ARMY MATERIALS AND MECHANICS RESEARCH CENTER
Watertown, Massachusetts 02172

FOREWORD

This final report on "A Study of Mechanics of Closed-Die Forging (Phase II)" covers the work performed under Contract DAAG 46-71-C-0095 with Battelle's Columbus Laboratories, from March 22, 1971, to September 22, 1972.

The technical supervision of this work was by Mr. Roger Gagne of the Army Materials and Mechanics Research Center, Watertown, Massachusetts 02172.

This project has been accomplished as part of the U.S. Army Manufacturing Methods and Technology Program, which has as its objective the timely establishment of manufacturing processes, techniques or equipment to insure the efficient production of current or future defense programs.

This program has been conducted at Battelle's Columbus Laboratories under the overall supervision of Mr. R. J. Fiorentino, Chief of the Metalworking Division. The principal investigators in the program are Mr. J. R. Douglas, Research Metallurgist, and Dr. T. Altan, Fellow. Others who contributed to the program are Mr. D. E. Nichols in data preparation, Mr. Gerald Crist in experimentation, Mr. Frank A. Syler in instrumentation, and Dr. N. Akgerman in computer programming. Mr. F. W. Boulger, Senior Technical Advisor, and Mr. H. J. Henning, Associate Chief, contributed to the quality of the work by making significant suggestions in various parts of the program. Mr. Carl R. Spilker edited the final report and contributed to its preparation.

ACKNOWLEDGMENTS

The present work was supported by the Army Materials and Mechanics Research Center, Watertown, Massachusetts, and by the U.S. Army Aviation Material Command, St. Louis, Missouri. The technical supervisor was Mr. Roger Gagne of AMMRC. The authors gratefully acknowledge the continuous encouragement and assistance given by Mr. Roger Gagne of AMMRC and Mr. John S. Willison of USAMMC throughout this work.

The program has been conducted with the combined efforts of various individuals from Battelle's Columbus Laboratories and from companies participating in the program. Several companies: Ontario Corporation of Muncie, Indiana; Steel Improvement and Forge Company of Cleveland, Ohio; Westinghouse Electric Corporation, Turbine Components Plant of Winston-Salem, North Carolina; The Accurate Brass Corporation of Bristol, Connecticut; and the Acheson Colloids Company of Port Huron, Michigan, contributed to the success of this program by supplying equipment and tooling time, manpower, materials, and assistance during the experimental studies.

The authors of this report gratefully acknowledge the assistance they received from Messrs. Michael G. Pasotti, Hal Glass, and William Barber of Ontario Corporation; Messrs. Otto Brass, Alex Axt, and Gursharan Singh of Westinghouse; Messrs. Nick Ruggiero, Ken Jackman, Richard Philpot, and Lou DeLuca of the Steel Improvement and Forge Company; Messrs. George C. Venter, William Shamansky, and Charles Riggs of the Accurate Brass Corporation; Mr. J. Szinyei of Bridgeport Brass Company; Mr. Richard C. Doehring of Acheson Colloids Company; Messrs. Ned B. Plecas and Ron Kasaback of Erie Foundry Company. Mr. Jon E. Jenson, Executive Director of the Forging Industry Education and Research Foundation (FIERF) took part in various discussions concerning the direction and objective of the program. His interest is also acknowledged.

PROGRAM SUMMARY

The overall objective of this manufacturing improvement program was to develop technical information for improving the efficiency and productivity in design and control of forging processes. This was accomplished by establishing and determining the influence of forging variables, such as material properties, friction conditions, and equipment characteristics, upon the forging process.

The success of any manufacturing improvement program depends mainly upon two factors:

(1) The technical quality and the usefulness of the research and development work

(2) The acceptance, the application, and the use of the results developed in the program by the industry and by other research centers active in that field.

Therefore, in addition to conducting practical and applied research work to advance forging technology, a major objective of the program was to disseminate the developed information to industry and to other research centers active in forging. As a part of this objective, Battelle has been working closely with various forging companies and individuals, well-known within the forging industry and interested in the progress of forging technology.

Phase I Work

The present final report covers the work done in Phase II of the program on "A Study of the Mechanics of Closed-Die Forging". Phase I of this program was completed in August, 1970, and the final report on Phase I, authored by Altan, et al, is available under number AD711544 from

National Technical Information Service
Springfield, Virginia 22151

The Phase I report consists of the following separate chapters:

1 - Shape-Difficulty Factor and Flash Design in Closed-Die Forging of Round Steel Parts

2 - The Use of Model Materials in Predicting Forming Loads in Metalworking

3 - Prediction of Loads and Stresses in Closed-Die Forging

4 - Computer Simulation to Predict Load, Stresses, and Metal Flow in an Axisymmetric Closed-Die Forging

5 - Temperature Effects in Closed-Die Forging

6 - Important Factors in Selection and Use of Equipment for Forging

7 - Experimental Determination of Process Variables in Closed-Die Forging

8 - Instrumentation and Calibration of Forging Presses for Monitoring Processing Variables

9 - Use of Standardized Copper Cylinders for Determining Load and Energy in Forging Equipment.

Various parts of these studies have been received with considerable interest by the industry and by professional engineering societies. A list of publications, prepared by using Phase I studies, is given below.

- Altan, T., and Sabroff, A. M., "Important Factors in the Selection and Use of Equipment for Forging", Parts I, II, III, and IV, paper published in Precision Metal, June, July, August, and September, 1970.
- Altan, T., Sabroff, A. M., "Closed-Die Forging – Recent Developments in Research", Precision Metal, May 1970, p. 44.
- Altan, T., et al, "The Use of Model Materials in Predicting Forming Loads in Metalworking", ASME Transactions, J. of Eng. for Industry, May 1970, p. 444.
- Altan, T., and Gerds, A. F., "Temperature Effects in Closed-Die Forging", ASM Report No. C70-30.1, presented at the 1970 Conference in Cleveland, Ohio, October 20, 1970. Also Metals Engineering Quarterly, August 1971, p. 44.
- Altan, T., and Fiorentino, R. J., "Prediction of Loads and Stresses in Closed-Die Forging", ASME Transactions, J. of Eng. for Industry, May 1971, p. 477.
- Altan, T., "Computer Simulation to Predict Load, Stress, and Metal Flow in an Axisymmetric Closed-Die Forging", in Metalforming: Interrelation Between Theory and Practice, A. L. Hoffmanner (editor), Plenum Publishing Corporation, 1971.
- Altan, T., and Henning, H. J., "Closed-Die Forging of Round Shapes: Flash Design and Material Savings", Metallurgia and Metalforming, March 1972, p. 83.
- Altan, T., "Important Factors in Selection and Use of Equipment for Metalworking", contributed to 2nd Inter-American Conference on Materials Technology, Mexico City, August 24, 1970, published in Proceedings.
- Altan, T., and Nichols, D., "The Use of Standard Copper Samples for Determining Load and Energy in Forging Equipment", ASME Trans., J. Eng. Industry, Vol. 94, No. 3, August 1972, p. 769.

The studies in Phase I were conducted in close cooperation with four forging companies: Aluminum Company of America, Steel Improvement and Forge Company, Ontario Corporation, and Wyman-Gordon Company.

Phase II Work

Based on the results of the Phase I studies, Phase II work concentrated on material and equipment characteristics that directly influence the predictions on metal flow, load, and energy in forging processes. For this purpose, studies were conducted on (a) determining and comparing the characteristics of presses, (b) determining the flow stress and friction in forging of various materials. This final report consists of seven separate chapters which are essentially independent of each other. The titles of these chapters are:

1 - Flow Stresses of Metals in Forging

2 - Instrumentation and Monitoring of Forging Presses

3 - Mechanical Presses and Screw Presses for Closed-Die Forging: Designs, Applications, and Comparisons

4 - Characteristics of Hydraulic, Mechanical, and Screw Presses for Forging: Determination and Comparison

5 - Isothermal Uniform Compression Tests for Determining Flow Stress of Metals at Forging Temperatures

6 - Ring Compression Tests for Determining Flow Stress and Friction at Forging Temperatures

7 - Prediction and Measurement of Forging Load Under Production Conditions.

Each chapter can be read separately, without having to go through the entire report in order to find a specific piece of information.

Program Significance

The present work, Phases I and II, sponsored by the Army, represents a major research and development effort on the engineering fundamentals and applications of closed-die forging. This work appears to be the single significant program of its kind conducted in this country during recent years. The program is unique in that a number of fundamental aspects of forging have been studied. Each aspect is reported as a chapter of the report. Thus, the information obtained in the program is easily studied because each chapter is complete in itself, and proper interpretation of the information does not necessarily require examination of the entire report.

Studies, such as those conducted in the present program, are not directly related to a specific hardware. However, they help to improve the state of the art, and supply to the industry engineering data and procedures for more efficient and productive manufacturing. For example, using the techniques developed in the present program, several companies have instrumented their forging presses. One company started to manufacture strain-bars of a new design for use in metalworking industry for monitoring forming loads. The equipment studies have been of interest to forging-press manufacturers as well as to users. The data generated on various difficult-to-form materials are being used by several companies in improving existing forging operations. These improvements consist of reducing costs or improving quality and reliability. The forging companies supply various manufacturers of military hardware and components. Thus, the results of this program, sponsored by the Army, are beneficial in procurement of military hardware.

The present work is far from having exhausted the problem areas of forging technology requiring investigation. Problems such as die wear and die-life improvement, optimization of heating and lubrication techniques, reduction of flash and scrap losses, development of engineering guidelines for preforming, development of techniques for precision forging aerospace alloys, and many other areas still represent needed development efforts. Studies of the mechanics of other significant metalforming processes, such as extrusion and drawing of bar, tube, and shapes, rolling of sheet and shapes, ironing and reducing of shell-type components, would also advance metalforming technology and improve efficiency and productivity in hardware manufacture.

An interesting observation made throughout this study is that, in the U. S., the advancement of metalforming technology, as an engineering discipline, has not kept pace with advances made in other countries, specifically in Japan, Soviet-Union, and West Germany. As a result, the competitive technological position of the U. S. metalforming industry has worsened. This fact is reflected in increased imports of European-made metalforming equipment such as screw presses, automatic mechanical forging presses for large production series, high-speed hydraulic hammers and presses, extrusion presses, and radial forging machines for axle and gun-barrel production. Similarly, most advanced forging processes such as precision forging of turbine and compressor blades and gears have been successfully developed and used in Europe and Japan. The number of universities and research institutes active in teaching and researching metalforming technology is significantly larger than that of U. S. institutions. As a result, the number of people trained in manufacturing and metalforming technologies and the information available in the technical literature is further advanced in other countries. Therefore, research and development efforts are required in these areas so that the leading position of the U. S. in manufacturing technology can be maintained.

TABLE OF CONTENTS

CHAPTER 1

FLOW STRESS OF METALS IN FORGING

by

T. Altan, D. E. Nichols, and F. W. Boulger

TABLE OF CONTENTS

CHAPTER 1

FLOW STRESSES OF METALS IN FORGING

by

T. Altan, D. E. Nichols, and F. W. Boulger

ABSTRACT

Forging load and energy can be determined if the flow stress of the forged material is known at the temperature and strain-rate conditions existing during the process. In this study domestic and foreign metalforming articles were reviewed and the available flow stress data have been presented for selected carbon, stainless, and tool steels; aluminum, copper, and titanium alloys; magnesium, uranium, Zircaloy, molybdenum, tungsten, tantalum, and niobium. Whenever possible, data are presented by calculating and tabulating coefficients K and n to express strain hardening (flow stress $\bar{\sigma} = K\bar{\epsilon}^n$), and C and m to express strain-rate dependency ($\bar{\sigma} = C\dot{\bar{\epsilon}}^m$).

Examples are given to illustrate the use of flow-stress data with simple formulas in predicting pressures in upset forging, closed-die forging, and cold extrusion.

INTRODUCTION

In planning and scheduling a given forging operation, it is necessary to estimate the maximum forging load, the forging energy, and the die stresses. In order to determine these variables it is necessary to know (1) the flow stress of the material being forged, and (2) the friction coefficient or the friction factor at the die-material interface. The values of both must be known at the temperature and strain-rate conditions that exist during deformation.

For a given metal, the flow stress is most commonly obtained by conducting a homogeneous upset test (without barrelling) or a torsion test at the temperature and strain-rates of interest. The widely known tensile test does not supply the flow-stress data for large strains necessary in analyzing forging processes. That is because, in a tensile test, the material deforms locally, or necks, and the sample fails before any significant overall homogeneous deformation occurs.

The compression and torsion tests provide flow-stress data at higher strains but require special equipment and carefully controlled laboratory conditions that are not generally available in practice. It is therefore useful to summarize all the available flow-stress data on various materials. Thus, the practicing forging engineer can use these data in predicting forging loads, energies, and stresses without having to conduct his own tests to measure the flow stress of the forg material.

FACTORS INFLUENCING THE FLOW STRESS OF METALS

Plastic deformation begins when applied external stresses induce a critical shear stress within the material. Assuming that the material follows the von Mises flow rule, this condition can be expressed as

$$\sigma_y - \sigma_x = \frac{2}{\sqrt{3}}\,\bar{\sigma} \qquad (1\text{-}1a)$$

and for axisymmetric deformation

$$\sigma_z - \sigma_r = \bar{\sigma} \qquad (1\text{-}1b)$$

where,

$\bar{\sigma}$ = flow stress

σ_z, σ_r = axial and radial principal stresses, respectively, in axisymmetric case

σ_y, σ_x = longitudinal and lateral stresses, respectively, in plane-strain case.

In Equation (1-1b), if σ_r is zero, a so-called "uniaxial state of stress" is achieved and the flow stress, $\bar{\sigma}$, is equal to the axial stress, σ_z. The homogeneous upset test without barrelling represents a practical method of creating a uniaxial state of stress. Thus, by measuring the instantaneous upsetting pressure, the flow stress, $\bar{\sigma}$, is obtained under the conditions of the test.

The flow stress of a metal is influenced by:

- Factors unrelated to the deformation process, such as chemical composition, metallurgical structure, phases, grain size, segregation, prior strain history

- Factors explicitly related to the deformation process:

  (1) Temperature of deformation (θ)

  (2) Degree of deformation or strain ($\bar{\epsilon}$)

  (3) Rate of deformation or strain rate ($\dot{\bar{\epsilon}}$).

Thus, the flow stress $\bar{\sigma}$ can be expressed as a function of temperature θ, strain $\bar{\epsilon}$, and strain rate $\dot{\bar{\epsilon}}$:

$$\bar{\sigma} = f(\theta, \bar{\epsilon}, \dot{\bar{\epsilon}}) \quad . \qquad (1\text{-}2)$$

In hot forging of metals at temperatures above the recrystallization temperature, the influence of strain upon flow stress is insignificant, and the influence of strain rate (i.e., rate of deformation) becomes increasingly important. Conversely, at room temperature (i.e., in cold forming), the effect of strain rate upon flow stress is negligible and the effect of strain upon flow stress (i.e., strain hardening) is most important.

The degree of dependency of the flow stress upon temperature varies largely for different metals and alloys. Therefore, changes in temperature during closed-die forging (due to die chilling, excessive cooling in handling, or internal heat generated by deformation) can have quite different effects in load requirements and in metal flow for different materials. For instance, a drop of approximately 100 F in forging temperature would result in a 40 percent increase in flow stress for the titanium alloy Ti-8Al-1Mo-1V. The increase in flow stress for the same temperature drop, 100 F, would be only about 15 percent for AISI steel 4340.[1]

DETERMINATION OF FLOW-STRESS DATA

To be useful in analyzing hot-forging processes, the flow stress of the forged material must be determined at various temperatures and strain rates. Tests such as plane strain and axisymmetric compression, tensile and torsion are used for this purpose.

Fundamentals of the Uniform Upset Test

In most research centers, the isothermal cylinder-upset test is the most widely used method of obtaining practical flow-stress data at various temperatures and strain rates. This test is commonly conducted using a fixture similar to the one illustrated in Figure 1-1[2]. This type of device, being built for the present program, will be used for determining the flow stress of selected materials. The platens and the cylindrical sample are maintained at the same temperature so that die chilling and its influence upon the metal flow is prevented. To be applicable without errors or corrections, the cylindrical sample must be upset without any barrelling, i.e., the state of uniform stress in the sample must be maintained.[3] Barrelling is prevented by using adequate lubrication, for instance graphite in oil for aluminum alloys, glass for steel, titanium, and high-temperature alloys.

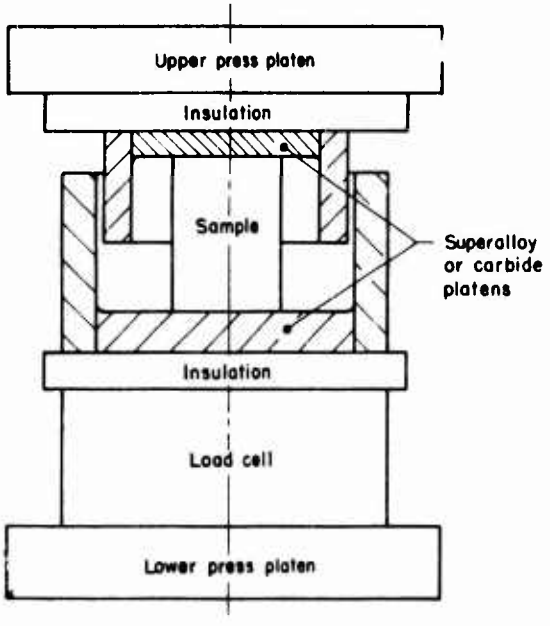

FIGURE 1-1. TOOL SETUP FOR ISOTHERMAL COMPRESSION TESTS TO ESTABLISH FLOW-STRESS DATA[2]

In analyzing metal-forming problems, it is useful to define the magnitude of deformation in terms of "logarithmic" strain $\bar{\epsilon}$. In uniform upset test:

$$\bar{\epsilon} = \int_{h_1}^{h_o} \frac{dh}{h} = \ln \frac{h_o}{h_1} \qquad (1\text{-}3)$$

where,

h_o = initial sample height

h_1 = sample height at the end of upsetting.

The strain-rate $\dot{\bar{\epsilon}}$ is the derivation of strain $\bar{\epsilon}$ with respect to time or:

$$\dot{\bar{\epsilon}} = \frac{d\epsilon}{dt} = \frac{dh}{hdt} = \frac{V}{h} \qquad (1\text{-}4)$$

where,

V = instantaneous upsetting speed

h = instantaneous height.

In all forging operations, except in uniform upsetting, $\bar{\epsilon}$ and $\dot{\bar{\epsilon}}$ values vary within the deforming material. Consequently, in using strains and strain-rates in practical forging operations, average values must be employed.

The forging temperature, as commonly specified, represents the temperature of the

sample, or of the forging, prior to deformation. However, during deformation, a very large portion of the deformation energy (about 95 percent) is transformed into heat. Thus, the temperature of the deforming material may increase appreciably during the upset test, or forging operation. The change is given by:

$$\Delta\theta = \frac{A\bar{\epsilon}\bar{\sigma}_a}{c\delta} \qquad (1\text{-}5)$$

where,

$\bar{\sigma}_a$ = average flow stress

c = heat capacity

δ = specific gravity

A = conversion factor from mechanical to thermal energy.

In a practical forging operation, heat generation due to interface friction also may be significant. However, due to the optimum lubrication conditions of the test, it can be neglected in the upset test.

In upsetting the cylindrical sample, the load and the displacement versus time are recorded. Thus, the maximum normal stress, or the flow stress, $\bar{\sigma}$, is obtained by dividing the instantaneous load P by the surface area F. F is determined by dividing the volume of the san ple by its instantaneous height.

Representation of Flow Stress Data

At room temperature, the influence of strain rate upon flow stress is insignificant in most metals. Lead, having a recrystallization temperature near room temperature, represents a major exception. It was empirically found that the effect of strain upon flow stress for most materials (i.e., the strain-hardening effect) can be expressed in the following exponential form:

$$\bar{\sigma} = K\bar{\epsilon}^n \qquad (1\text{-}6)$$

where,

K = flow stress $\bar{\sigma}$ when strain $\bar{\epsilon}$ = 1

n = strain-hardening coefficient.

At higher temperatures, above the recrystallization temperature, the effect of strain hardening is minimal for most materials. Consequently, at a given temperature, it is possible to approximate the variation of flow stress $\bar{\sigma}$ in function of strain rate $\dot{\bar{\epsilon}}$ by :

$$\bar{\sigma} = C\dot{\bar{\epsilon}}^m \qquad (1\text{-}7)$$

where,

C = flow stress $\bar{\sigma}$ when strain-rate $\dot{\bar{\epsilon}}$ = 1

m = strain-rate coefficient.

It is seen from Equation (1-4) that, in upsetting under conventional forging machines, strain rate $\dot{\bar{\epsilon}}$ varies during the test since both the ram speed V and the sample height vary. A few laboratories around the world have developed machines called "plastometers" which have cam-operated rams and which upset samples under constant strain-rate conditions.[3-8] The cam shape programs ram speed to give the desired strain rate. Upset tests conducted at various temperatures and constant strain rates under a plastometer make it possible to determine the coefficients C and m of Equation (1-7) for various materials directly from experimental data.

SUMMARY OF FLOW-STRESS DATA FOR VARIOUS MATERIALS

Although there is hardly any published flow-stress (or true stress versus true strain) data in U. S. literature, British, German, and Japanese investigators have conducted many investigations on flow stress of metals.

Most investigators used plastometers in their studies and obtained, for a given material, flow stress $\bar{\sigma}$ versus strain $\bar{\epsilon}$ (true strain) at a constant strain rate under isothermal conditions. At room temperature, where the effect of strain rate can be neglected for most materials, some of the flow-stress data were obtained at low testing-machine speeds.[10] Thus, these data are usually given in form of curves, $\bar{\sigma}$ versus $\bar{\epsilon}$, for constant temperature and strain rate. This representation, though very useful in discussing the data for few materials and test conditions, takes too much space when used for discussing a large number of materials. Therefore, the data obtained from the literature have been used to calculate, by a least-mean-square-fit technique, the coefficients K and n of Equation (1-6) (for strain dependency) and C and m of Equation (1-7) for strain-rate dependency. A computer program was used for processing all the data. The results are seen in Tables 1-1 through 1-8.

For a few materials and a few test conditions, slightly different results were obtained by using the data from various sources. These differences may be due to material composition or errors in calculating the stress-strain curves from the test results. Unless otherwise indicated, all of the data presented were obtained in continuous-upset tests. Thus, the specified temperatures are the initial temperatures of the samples and do not include the temperature increase due to deformation, as indicated by Equation (1-5).

Strain-Dependent Flow-Stress Data

Steels, aluminum alloys, and copper alloys are, within engineering approximations, strain dependent only at room temperature and lower

forging temperature ranges. The K and n values of the expression $\bar{\sigma} = K\bar{\varepsilon}^n$ calculated for steels, aluminum alloys, and copper alloys are given in Tables 1-1, 1-2, and 1-3, respectively. Each table also gives

- The material composition
- The U. S. standard material number which corresponds approximately to that composition
- The test temperature
- The strain rate
- The literature reference for the data
- The range of strain used in calculations
- K and n values calculated from the original data by least-mean-square fit.

TABLE 1-1. SUMMARY OF K AND n VALUES DESCRIBING THE FLOW STRESS-STRAIN RELATION, $\bar{\sigma} = K(\bar{\varepsilon})^n$, FOR VARIOUS STEELS

Material	Composition, percent												Temperature		Strain Rate, 1/sec	K, 10^3 psi	n	Reference	Strain Range	Material History[a]
	C	Mn	P	S	Si	N	Al	V	Ni	Cr	Mo	W	F	C						
Armco Iron	0.02	0.03	0.021	0.010	tr[c]								68	20	T.M.[d]	88.2	0.25	10	0.1-0.7	A
1006	0.06	0.29	0.02	0.042	tr	0.009							68	20	Ditto	89.6	0.31	10	0.1-0.7	A
1008	0.08	0.36	0.023	0.031	0.06	0.007							68	20	"	95.3	0.24	10	0.1-0.7	A
	0.07	0.28			0.27								68	20	"	95.3	0.17	10	0.1-0.7	A
1010	0.13	0.31	0.010	0.022	0.23	0.004							68	20	"	103.8	0.22	10	0.1-0.7	A
1015	0.15	0.40	0.01	0.016	tr								32	0	30	91.4	0.116	8	0.2-0.7	F-A
1015[b]	0.15	0.40	0.045	0.045	0.25								68	20	1.6	113.8	0.10	11		A
1015	0.15	0.40	0.01	0.016	tr								390	200	30	73.7	0.140	8	0.2-0.7	F-A
1015[b]	0.15	0.40	0.045	0.045	0.25								572	300	1.6	115.2	0.11	11		A
1020	0.22	0.44	0.017	0.043	tr	0.005							68	20	T.M.	108.1	0.20	10	0.1-0.7	A
1035	0.36	0.69	0.025	0.032	0.27	0.004							68	20	Ditto	130.8	0.17	10	0.1-0.7	A
													68	20	1.6	139.4	0.11	11		A
1035	0.36	0.69	0.025	0.032	0.27	0.004							57	300	1.6	122.3	0.16	11		A
1045[b]	0.45	0.65	0.045	0.045	0.25								68	20	1.6	147.9	0.11	11		A
													68	20	1.5	137.9	0.14	11		A
1045[b]													572	300	1.6	126.6	0.15	11		A
About 1050	0.51	0.55	0.016	0.041	0.28	0.0062	0.03						68	20	T.M.	140.8	0.16	10	0.1-0.7	A
1060													68	20	1.6	163.5	0.09	11		A
													68	20	1.5	157.8	0.12	11		A
About 2317	0.19	0.55	0.057	0.023	0.26	0.016							68	20	T.M.	111.2	0.170	10	0.2-1.0	A
5115	0.14	0.53	0.028	0.027	0.37					0.71			68	20	Ditto	115.2	0.18	10	0.1-0.7	A
													68	20	1.6	123.7	0.09	11		A
5115	0.14	0.53	0.028	0.027	0.37					0.71			572	300	1.6	102.4	0.15	11		A
About 5120	0.18	1.13	0.019	0.023	0.27					0.86			68	20	T.M.	126.6	0.18	10	0.1-0.7	A
													68	20	1.6	116.6	0.09	11		A
About 5120	0.18	1.13	0.019	0.023	0.27					0.86			572	300	1.6	98.1	0.16	11		A
5140	0.41	0.67	0.04	0.019	0.35					1.07			68	20	T.M.	125.1	0.15	10	0.1-0.7	A
													68	20	1.6	133.7	0.09	11		A
5140	0.41	0.67	0.04	0.019	0.35					1.07			572	300	1.6	112.3	0.12	11		A
About D2 tool steel	1.60	0.45			0.24		0.46		11.70		0.75	0.59	68	20	T.M.	191.0	0.157	10	0.2-1.0	A
L6 tool steel	0.56						0.14	1.60		1.21	0.47		68	20	Ditto	170.2	0.128	10	0.2-1.0	A
W1-1.0C special	1.05	0.21			0.16								68	20	"	135.6	0.179	10	0.2-1.0	A
302 SS	0.08	1.06	0.037	0.005	0.49				9.16	18.37			32	0	10	185.7	0.295	8	0.25-0.7	HR-A
302 SS	0.053	1.08	0.027	0.015	0.47				10.2	17.8			68	20	T.M.	210.5	0.6	10	0.1-0.7	A
302 SS	0.08	1.06	0.037	0.005	0.49				9.16	18.37			390	200	30	120.8	0.278	8	0.25-0.7	HR-A
302 SS	0.08	1.06	0.037	0.005	0.49				9.16	18.37			750	400	30	92.7	0.279	8	0.25-0.7	HR-A
About 304 SS	0.030	1.05	0.023	0.014	0.47				10.6	18.7			68	20	T.M.	210.5	0.6	10	0.1-0.7	A
316 SS	0.055	0.92	0.030	0.008	0.49				12.9	18.1	2.05		68	20	Ditto	182.0	0.59	10	0.1-0.7	A
410 SS	0.093	0.31	0.026	0.012	0.33					13.8			68	20	"	119.4	0.2	10	0.1-0.7	A
													68	20	1.6	137.9	0.09	11		A
431 SS	0.23	0.38	0.020	0.006	0.42				1.72	16.32			68	20	T.M.	189.1	0.11	10	0.1-0.7	A

(a) HR - hot rolled, A - annealed, F - forged
(b) Analysis not given in original reference, - table shows nominal composition
(c) tr - trace
(d) T.M. - testing machine - no specific rate given, low speed

TABLE 1-2. SUMMARY OF K AND n VALUES DESCRIBING THE FLOW STRESS-STRAIN RELATION, $\bar{\sigma} = K(\bar{\varepsilon})^n$, FOR VARIOUS ALUMINUM ALLOYS

Material	Composition, percent										Temperature		Strain Rate[e], 1/sec	K, 10^3 psi	n	Reference	Strain Range	Material History[a]
	Al	Cu	Si	Fe	Mn	Mg	Zn	Ti	Cr	Pb	F	C						
1100	99.0	0.10	0.15	0.50	0.01	0.01					32	0	10	25.2	0.304	8	0.25-0.7	CD-A
1100	Bal[d]	0.01	0.10	0.16	0.01	0.01	0.01				68	20	T.M.	17.3	0.297	10	0.2-1.0	A
EC	99.5	0.01	0.092	0.23	0.026	0.033	0.01				68	20	4	22.4	0.204	9	0.2-0.8	A[b]
2017	Bal	4.04	0.70	0.45	0.55	0.76	0.22			0.06	68	20	T.M.	45.2	0.180	10	0.2-1.0	A
About 2024	Bal	4.48	0.60	0.46	0.87	1.12	0.20			0.056	68	20	T.M.	56.1	0.154	10	0.2-1.0	A
5052	Bal	0.068	0.10	0.19	0.04	2.74	0.01	0.003			68	20	4	29.4	0.134	9	0.2-0.8	A[c]
About 5052	Bal	0.09	0.13	0.16	0.23	2.50	0.05				68	20	T.M.	55.6	0.189	10	0.2-1.0	A
5056	Bal	0.036	0.15	0.22	0.04	4.83	0.01		0.14		68	20	4	57.0	0.130	9	0.2-0.7	A[c]
5083	Bal	0.01	0.10	0.16	0.77	4.41	0.01	0.002	0.13		68	20	4	65.2	0.131	9	0.2-0.8	A[c]
5454	Bal	0.065	0.12	0.18	0.81	2.45	<0.01	0.002			68	20	4	49.9	0.137	9	0.2-0.8	A[c]
About 6062	Bal	0.03	0.63	0.20	0.63	0.68	0.065	0.08			68	20	T.M.	29.7	0.122	10	0.2-1.0	A

(a) CD - cold drawn, A - annealed.
(b) Annealed 4 hr at 752 F (400 C)
(c) Annealed 4 hr at 788 F (420 C)
(d) Bal - balance.
(e) T.M. - testing machine, no specific rate given, low speed.

After determining K and n values, the flow stress was calculated by using Equation (1-6). The difference between the original and the calculated flow-stress value was always less than 10 percent, and in most cases less than 5 percent. Thus, K and n values can be used for estimating forging loads and stresses for practical purposes.

Strain-Rate Dependent Flow-Stress Data

At higher forging temperatures, generally above the recrystallization temperatures, the flow stress of metals is, for all practical purposes, strain-rate dependent. However, for some intermediate temperatures, between room and recrystallization temperatures, the effect of strain may be considerable for some materials. This factor was considered in presenting the Tables 1-4 through 1-8 where C and m values, of the expression $\bar{\sigma} = C\dot{\bar{\varepsilon}}^m$, are given for various materials at various temperatures and strains. The C and m values, calculated from published experimental data, are given in Tables 1-4 through 1-8 for steels, aluminum alloys, copper alloys, titanium alloys, and other forging materials. Each table contains

- The material composition
- The material history
- The test temperature
- The strain at which C and m values were calculated

TABLE 1-3. SUMMARY OF K AND n VALUES DESCRIBING THE FLOW STRESS-STRAIN RELATION, $\bar{\sigma} = K(\bar{\varepsilon})^n$, FOR VARIOUS COPPER ALLOYS

Material[a]	Composition, percent										Temperature		Strain Rate[b], 1/sec	K, 10^3 psi	n	Reference	Strain Range	Material History[c]
	Al	Cu	Si	Fe	Sb	Sn	Zn	S	Pb	Ni	F	C						
CDA110		99.94		0.0025	0.0003			0.0012	0.0012	0.001	64	18	2.5	65.5	0.328	8	0.25-0.7	HR-A
CDA110											68	20	T.M.	54.0	0.275	10	0.2-1.0	F
CDA230		84.3					15.7				68	20	T.M.	76.7	0.373	10	0.2-1.0	A
CDA260		70.8					29.2				68	20	T.M.	98.1	0.412	10	0.2-1.0	A
CDA260		70.05		tr[d]		tr[d]	Bal				390	200		71.7	0.414	8	0.25-0.7	HR-A
CDA272		63.3					36.7				68	20	T.M.	103.9	0.394	10	0.2-1.0	A
CDA377		58.6		tr[d]			39.6		1.7		68	20	T.M.	115.3	0.334	10	0.2-1.0	A
About CDA521		91.0				9.0					68	20	T.M.	130.8	0.486	10	0.2-1.0	F
CDA647		97.0	0.5							2.0	68	20	T.M.	67.2	0.282	10	0.2-1.0	F
CDA757		65.1					22.4		<0.05	12.4	68	20	T.M.	101.8	0.401	10	0.2-1.0	A
CDA794		61.7		tr[d]			20.6		tr[d]	17.5	68	20	T.M.	107.0	0.336	10	0.2-1.0	A

(a) CDA is Copper Development Association.
(b) T.M. - testing machine, no specific rate given, low speed.
(c) HR - hot rolled, A - annealed, F - forged.
(d) tr - trace

TABLE 1-4. SUMMARY OF C AND m VALUES DESCRIBING THE FLOW STRESS-STRAIN RATE RELATION, $\bar{\sigma} = C(\dot{\bar{\epsilon}})^m$, FOR STEELS AT VARIOUS TEMPERATURES (C is in 10^3 psi)

Material	Material History	Strain	C	m	C	m	C	m	C	m	C	m	Reference	Strain Rate Range, 1/sec
Test Temperature, F(C)			1110(600)		1470(800)		1830(1000)		2190(1200)					
1015	Forged,	0.2	36.8	0.112									4	0.2-50
0.15 C, tr Si, 0.40 Mn,	annealed	0.25			19.9	0.105	17.0	0.045	7.2	0.137				
0.01 P, 0.016 S		0.4	40.6	0.131										
		0.5			21.5	0.104	18.8	0.058	6.8	0.169				
		0.6	40.0	0.121										
		0.7	39.5	0.114	21.1	0.109	18.3	0.068	5.7	0.181				
Test Temperature, F(C)			1650(900)		1830(1000)		2010(1100)		2190(1200)					
1016	Hot rolled,	0.10	16.6	0.092	13.4	0.100	9.9	0.124	7.5	0.143			6	1.5-100
0.15 C, 0.12 Si, 0.68 Mn,	annealed	0.30	22.7	0.082	18.2	0.085	13.3	0.115	9.4	0.153				
0.034 S, 0.025 P		0.50	23.7	0.087	18.2	0.104	12.7	0.146	8.5	0.191				
		0.70	23.1	0.099	16.7	0.147	11.0	0.166	7.5	0.218				
1016	Hot rolled,	0.05	11.8	0.133	10.7	0.124	9.0	0.117	6.4	0.150			13	
0.15 C, 0.12 Si, 0.68 Mn,	annealed	0.1	16.5	0.099	13.7	0.099	9.7	0.130	7.1	0.157				
0.034 S, 0.025 P		0.2	20.8	0.082	16.5	0.090	12.1	0.119	9.1	0.140				
		0.3	22.6	0.085	18.2	0.088	13.4	0.109	9.5	0.148				
		0.4	23.0	0.084	18.2	0.098	12.9	0.126	9.1	0.164				
		0.5	23.9	0.088	18.1	0.109	12.5	0.141	8.2	0.189				
		0.6	23.3	0.097	16.9	0.127	12.1	0.156	7.8	0.205				
		0.7	22.8	0.104	17.1	0.127	12.4	0.151	8.1	0.196				
Test Temperature, F(C)			1600(870)		1800(980)		2000(1090)		2200(1205)		2150(1180)			
1018			25.2	0.07	15.8	0.152	11.0	0.192	9.2	0.20			15	
1025	Forged,	0.25			33.7	0.004	16.2	0.075	9.3	0.077			8	3.5-30
0.25 C, 0.08 Si, 0.45 Mn,	annealed	0.50			41.4	0.032	17.2	0.080	9.6	0.094				
0.012 P, 0.025 S		0.70			41.6	0.032	17.5	0.082	8.8	0.105				
1043	Hot rolled, as received	0.3/0.5/0.7									10.8	0.21	20	0.1-100
Test Temperature, F(C)			1650(900)		1830(1000)		2010(1100)		2190(1200)					
About 1045		0.05	25.4	0.080	15.1	0.089	11.2	0.100	8.0	0.175			13	
0.46 C, 0.29 Si, 0.73 Mn,		0.10	28.9	0.082	18.8	0.103	13.5	0.125	9.6	0.168				
0.018 P, 0.021 S, 0.08 Cr,		0.20	33.3	0.086	22.8	0.108	15.4	0.128	10.5	0.167				
0.01 Mo, 0.04 Ni		0.30	35.4	0.083	24.6	0.110	15.8	0.162	10.8	0.180				
		0.40	35.4	0.105	24.7	0.134	15.5	0.173	10.8	0.188				
Test Temperature, F(C)			1110(600)		1470(800)		1830(1000)		2190(1200)					
1055	Forged,				29.4	0.087	14.9	0.126	7.4	0.145			8	3.5-30
0.55 C, 0.24 Si, 0.73 Mn,	annealed				32.5	0.076	14.3	0.191	7.4	0.178				
0.014 P, 0.016 S					32.7	0.066	11.5	0.237	6.4	0.229				
Test Temperature, F(C)			1650(900)		1830(1000)		2010(1100)		2190(1200)					
About 1060	Hot rolled,	0.10	18.5	0.127	13.3	0.143	10.1	0.147	7.4	0.172			6	1.5-100
0.56 C, 0.26 Si, 0.28 Mn,	annealed	0.30	23.3	0.114	16.9	0.123	12.6	0.135	8.9	0.158				
0.014 S, 0.013 P, 0.12 Cr,		0.50	23.3	0.118	16.4	0.139	12.0	0.158	8.6	0.180				
0.09 Ni		0.70	21.3	0.132	14.9	0.161	10.4	0.193	7.8	0.207				
About 1060		0.05	16.2	0.128	10.8	0.168	8.7	0.161	6.5	0.190			13	
0.56 C, 0.26 Si, 0.28 Mn,		0.10	18.3	0.127	13.2	0.145	10.1	0.149	7.5	0.165				
0.014 S, 0.013 P, 0.12 Cr,		0.20	21.8	0.119	16.1	0.125	12.1	0.126	8.5	0.157				
0.09 Ni		0.30	23.3	0.114	17.1	0.125	12.8	0.127	8.8	0.164				
		0.40	23.7	0.112	16.8	0.128	12.5	0.148	[illegible]	0.171				
		0.50	23.6	0.110	16.6	0.133	12.7	0.143	8.7	0.176				
		0.60	22.8	0.129	17.1	0.127	11.7	0.169	8.4	0.189				
		0.70	21.3	0.129	16.2	0.138	10.7	0.181	7.8	0.204				
About 1095	Hot rolled,	0.10	18.3	0.146	13.9	0.143	9.8	0.159	7.1	0.184			6	1.5-100
1.00 C, 0.19 Si, 0.17 Mn,	annealed	0.30	21.9	0.133	16.6	0.132	11.7	0.147	8.0	0.183				
0.027 S, 0.023 P, 0.10 Cr,		0.50	21.8	0.130	15.7	0.151	10.6	0.176	7.3	0.209				
0.09 Ni		0.70	21.0	0.128	13.6	0.179	9.7	0.191	6.5	0.232				
Test Temperature, F(C)			1705(930)		1830(1000)		1940(1060)		2075(1135)		2190(1200)			
1115	Hot rolled,	0.105	16.3	0.088	13.0	0.108	10.9	0.112	9.1	0.123	7.6	0.116	7	4.4-23.1
0.17 C, 0.153 Si, 0.62 Mn,	as received	0.223	19.4	0.084	15.6	0.100	12.9	0.107	10.5	0.129	8.6	0.122		
0.054 S, 0.032 P		0.338	20.4	0.094	17.3	0.090	14.0	0.117	11.2	0.138	8.8	0.141		
		0.512	20.9	0.099	18.0	0.093	14.4	0.127	11.0	0.159	8.3	0.173		
		0.695	20.9	0.105	18.9	0.122	13.6	0.150	9.9	0.198	7.6	0.196		
Test Temperature, F(C)			1650(900)		1830(1000)		2010(1100)		2190(1200)					
Alloy steel		0.05	16.6	0.102	12.2	0.125	9.4	0.150	7.4	0.161			13	
0.35 C, 0.27 Si, 1.49 Mn,		0.10	19.9	0.091	14.8	0.111	11.5	0.121	8.1	0.149				
0.041 S, 0.037 P, 0.03 Cr,		0.20	23.0	0.094	17.6	0.094	13.5	0.100	9.4	0.139				
0.11 Ni, 0.28 Mo		0.30	24.9	0.092	19.1	0.093	14.4	0.105	10.2	0.130				
		0.40	26.0	0.088	19.6	0.095	14.5	0.112	10.4	0.139				
		0.50	25.9	0.091	19.6	0.100	14.4	0.112	10.1	0.147				
		0.60	25.9	0.094	19.5	0.105	14.2	0.122	9.7	0.159				
		0.70	25.5	0.099	19.2	0.107	13.9	0.126	9.2	0.165				
About 4337	Hot rolled,	0.10	22.1	0.080	16.6	0.109	12.1	0.115	8.2	0.165			6	1.5-100
0.35 C, 0.27 Si, 0.66 Mn,	annealed	0.30	28.1	0.077	20.8	0.098	15.0	0.111	10.7	0.138				
0.023 S, 0.029 P, 0.59 Cr,		0.50	29.2	0.075	21.8	0.096	15.7	0.112	11.3	0.133				
2.45 Ni, 0.59 Mo		0.70	28.1	0.080	21.3	0.102	15.5	0.122	11.3	0.135				
About 9261	Hot rolled,	0.10	22.9	0.109	17.1	0.106	11.8	0.152	8.6	0.168			6	1.5-100
0.61 C, 1.58 Si, 0.94 Mn,	annealed	0.30	28.2	0.101	20.4	0.106	14.3	0.140	10.1	0.162				
0.038 S, 0.035 P, 0.12 Cr,		0.50	27.8	0.104	20.0	0.120	13.8	0.154	9.1	0.193				
0.27 Ni, 0.06 Mo		0.70	25.8	0.112	18.2	0.146	11.8	0.179	7.5	0.235				
About 50100		0.05	16.1	0.155	12.4	0.155	8.2	0.175	6.3	0.199			13	
1.00 C, 0.19 Si, 0.17 Mn,		0.10	18.6	0.145	14.1	0.142	9.5	0.164	6.8	0.191				
0.027 S, 0.023 S, 0.10 Cr,		0.20	20.9	0.135	15.9	0.134	11.4	0.141	8.1	0.167				
0.09 Ni		0.30	21.8	0.135	16.6	0.134	11.7	0.142	8.0	0.174				
		0.40	22.0	0.134	16.8	0.134	11.2	0.155	8.4	0.164				
		0.50	21.5	0.131	15.6	0.150	11.1	0.158	7.4	0.199				
		0.60	21.3	0.132	14.6	0.163	10.0	0.184	7.0	0.212				
		0.70	20.9	0.131	13.5	0.176	9.7	0.183	6.7	0.220				
52100	Hot rolled,	0.10	20.9	0.123	14.3	0.146	9.5	0.169	6.7	0.203			6	1.5-100
1.06 C, 0.22 Si, 0.46 Mn,	annealed	0.30	25.5	0.107	17.7	0.127	12.0	0.143	8.3	0.171				
0.019 S, 0.031 P, 1.41 Cr,		0.50	25.9	0.107	17.7	0.129	12.3	0.143	8.3	0.178				
0.17 Ni		0.70	23.3	0.131	16.8	0.134	12.0	0.148	7.7	0.192				

TABLE 1-4. (Continued)

Material	Material History	Strain	C	m	C	m	C	m	C	m	C	m	Reference	Strain Rate Range, 1/sec
Test Temperature, F(C):			1650(900)		1830(1000)		2010(1100)		2190(1200)					
Mn-Si steel		0.05	19.2	0.117	14.8	0.119	9.7	0.172	7.5	0.181			13	
0.61 C, 1.58 Si, 0.94 Mn,		0.10	22.6	0.112	17.1	0.108	11.8	0.151	8.7	0.166				
0.038 S, 0.035 P, 0.12 Cr,		0.20	25.7	0.108	19.5	0.101	13.5	0.139	9.7	0.160				
0.27 Ni, 0.06 Mo		0.30	27.6	0.108	20.5	0.109	14.8	0.126	10.0	0.161				
		0.40	27.6	0.114	20.2	0.114	14.4	0.141	9.5	0.179				
		0.50	27.2	0.113	19.8	0.125	14.1	0.144	9.1	0.188				
		0.60	26.0	0.121	18.8	0.137	12.8	0.162	8.2	0.209				
		0.70	24.7	0.130	17.8	0.152	11.9	0.178	7.5	0.228				
Cr-Si steel		0.05	19.9	0.118	23.9	0.104	15.1	0.167	10.0	0.206			13	
0.47 C, 3.74 Si, 0.58 Mn,		0.10	19.9	0.136	25.6	0.120	16.8	0.162	11.1	0.189				
8.20 Cr, 0.20 Ni		0.20	19.9	0.143	27.6	0.121	18.5	0.153	11.9	0.184				
		0.30	19.9	0.144	28.4	0.119	19.1	0.148	12.1	0.182				
		0.40	19.3	0.150	28.2	0.125	18.9	0.150	12.1	0.178				
		0.50	18.5	0.155	26.6	0.132	18.5	0.155	11.8	0.182				
		0.60	17.5	0.160	25.2	0.142	17.5	0.160	11.5	0.182				
		0.70	16.1	0.163	23.3	0.158	16.1	0.162	10.7	0.199				
About D3	Hot rolled,	0.10	39.2	0.087	29.0	0.108	21.0	0.123	14.6	0.121			6	1.5-100
2.23 C, 0.43 Si, 0.37 Mn,	annealed	0.30	43.7	0.087	30.4	0.114	21.0	0.139	13.9	0.130				
13.10 Cr, 0.33 Ni		0.50	39.7	0.101	27.1	0.125	18.4	0.155	12.2	0.124				
		0.70	33.3	0.131	22.5	0.145	15.3	0.168	10.7	0.108				
Test Temperature, F(C)			1290(700)		1510(820)		1650(900)		1830(1000)					
H-13		0.1	19.1	0.232	10.2	0.305	6.0	0.373	4.8	0.374			12	290-906
0.39 C, 1.02Si, 0.60 Mn,		0.2	30.1	0.179	13.7	0.275	8.2	0.341	9.0	0.295				
0.016 P, 0.020 S, 5.29 Cr,		0.3	31.0	0.179	15.1	0.265	10.8	0.305	11.6	0.267				
0.04 Ni, 1.35 Mo, 0.027 N,		0.4	25.9	0.204	12.3	0.295	12.5	0.287	11.8	0.269				
0.83 V														
Test Temperature, F(C)			1650(900)		1830(1000)		2010(1100)		2190(1200)					
About H-26	Hot rolled,	0.10	46.7	0.058	37.4	0.072	26.2	0.106	18.7	0.125			6	1.5-100
0.80 C, 0.28 Si, 0.32 Mn,	annealed	0.30	49.6	0.075	38.1	0.087	26.0	0.121	18.3	0.140				
4.30 Cr, 0.18 Ni, 0.55 Mo,		0.50	44.6	0.096	33.7	0.102	23.6	0.131	16.2	0.151				
18.40 W, 1.54 V		0.70	39.1	0.115	27.9	0.124	20.1	0.149	13.8	0.162				
Test Temperature, F(C)			1110(600)		1470(800)		1830(1000)		2190(1200)					
About 301 SS	Hot rolled,	0.25			40.5	0.051	16.3	0.117	7.6	0.161			8	0.8-100
0.08 C, 0.93 Si, 1.10 Mn,	annealed	0.50			39.3	0.062	17.8	0.108	7.6	0.177				
0.009 P, 0.014 S, 16.99 Cr,		0.70			37.8	0.069	17.4	0.102	6.6	0.192				
6.96 Ni, 0.31 Mo, 0.93 Al,														
0.02 N, 0.063 Se														
302 SS	Hot rolled,	0.25	26.5	0.147	25.1	0.129	11.0	0.206	4.6	0.281			8	310-460
0.07 C, 0.71 Si, 1.07 Mn,	annealed	0.40	31.3	0.153	30.0	0.121	13.5	0.188	4.7	0.284				
0.03 P, 0.005 S, 18.34 Cr,		0.60	17.5	0.270	45.4	0.063	16.8	0.161	4.1	0.310				
9.56 Ni														
302 SS	Hot rolled,	0.25	52.2	0.031	36.6	0.042	23.1	0.040	12.8	0.082			8	0.2-30
0.08 C, 0.49 Si, 1.06 Mn,	annealed	0.40	58.9	0.022	40.4	0.032	24.7	0.050	13.6	0.083				
0.037 P, 0.005 S, 18.37 Cr,		0.60	63.2	0.020	41.9	0.030	24.9	0.053	13.5	0.091				
9.16 Ni		0.70	64.0	0.023	42.0	0.031	24.7	0.052	13.4	0.096				
Test Temperature, F(C)			1650(900)		1830(1000)		2010(1100)		2190(1200)					
302 SS		0.05	24.6	0.023	16.8	0.079	13.7	0.093	9.7	0.139			13	1.5-100
0.07 C, 0.43 Si, 0.48 Mn,		0.10	28.4	0.026	21.2	0.068	15.6	0.091	11.1	0.127				
18.60 Cr, 7.70 Ni		0.20	33.6	0.031	25.2	0.067	18.1	0.089	12.5	0.120				
		0.30	35.3	0.042	26.3	0.074	19.5	0.089	13.5	0.115				
		0.40	35.6	0.055	26.9	0.084	19.9	0.094	14.2	0.110				
		0.50	35.6	0.060	27.0	0.093	19.6	0.098	14.2	0.115				
		0.60	34.1	0.068	26.4	0.092	19.3	0.102	13.8	0.118				
		0.70	33.6	0.072	25.7	0.102	18.9	0.108	13.9	0.120				
Test Temperature, F(C)			1110(600)		1470(800)		1830(1000)		2190(1200)					
309 SS	Hot drawn,	0.25			39.4	0.079			8.7	0.184			8	200-525
0.13 C, 0.42 Si, 1.30 Mn,	annealed	0.40			45.1	0.074			9.6	0.176				
0.023 P, 0.008 S, 22.30 Cr,		0.60			48.1	0.076			9.5	0.185				
12.99 Ni														
310 SS	Hot drawn,	0.25	50.3	0.080	32.3	0.127	27.5	0.101	12.0	0.154			8	310-460
0.12 C, 1.26 Si, 1.56 Mn,	annealed	0.40	56.5	0.060	32.2	0.142	22.8	0.143	10.8	0.175				
0.01 P, 0.009 S, 25.49 Cr,		0.60	61.8	0.067	21.9	0.212	9.7	0.284	4.5	0.326				
21.28 Ni														
316 SS	Hot drawn,	0.25	13.5	0.263	22.2	0.149	6.4	0.317	8.0	0.204			8	310-460
0.06 C, 0.52 Si, 1.40 Mn,	annealed	0.40	28.8	0.162	26.8	0.138	3.7	0.435	7.4	0.227				
0.035 P, 0.005 S, 17.25 Cr,		0.60	39.3	0.128	30.1	0.133	6.1	0.365	6.5	0.254				
12.23 Ni, 2.17 Mo														
403 SS	Hot rolled,	0.25			26.3	0.079	15.4	0.125	7.3	0.157			8	0.8-100
0.16 C, 0.37 Si, 0.44 Mn,	annealed	0.50			26.9	0.076	16.0	0.142	7.8	0.152				
0.024 P, 0.007 S, 12.62 Cr		0.70			24.6	0.090	15.3	0.158	7.5	0.155				
			1110(600)		1470(800)		1830(1000)		2190(1200)		1650(900)			
SS	Hot rolled,	0.25			28.7	0.082	17.2	0.082	11.9	0.079			8	0.8-100
0.12 C, 0.12 Si, 0.29 Mn,	annealed	0.50			29.1	0.093	20.7	0.073	11.6	0.117				
0.014 P, 0.016 S, 12.11 Cr,		0.70			28.7	0.096	22.5	0.067	11.2	0.131				
0.50 Ni, 0.45 Mo														
SS	Hot rolled,	0.25					19.5	0.099	8.9	0.128	28.3	0.114	8	3.5-30
0.08 C, 0.45 Si, 0.43 Mn,	annealed	0.50					22.3	0.097	9.5	0.145	34.9	0.105		
0.031 P, 0.005 S, 17.38 Cr,		0.70					23.2	0.098	9.2	0.158	37.1	0.107		
0.31 Ni														
Test Temperature, F(C):			1600(870)		1700(925)		1800(980)		2000(1095)		2100(1150)			
Maraging 300			43.4	0.077	36.4	0.095	30.6	0.113	21.5	0.145	18.0	0.165	15	
Test Temperature, F(C):			2200(1205)											
Maraging 300			12.8	0.185									15	

- The strain-rate range used in calculations
- The literature reference for the data
- C and m values calculated by least-mean-square fit from the original data at a given strain and temperature.

As for strain-dependent data, the calculated C and m values were used to predict the flow-stress values using Equation (1-7). The difference between the original and the calculated flow stress value was always less than 10 percent, and in most cases less than 5 percent.

Useful ranges for average strain rates are, for hydraulic presses 2-5 1/sec., mechanical and screw presses 10-25 1/sec., and for hammers 100-200 1/sec.

Flow-Stress Data for Uranium, Molybdenum, Tungsten, Tantalum, and Niobium

For some materials, the flow stress could not be expressed in exponential forms. Those data are presented in form of curves.

Uranium is strain-rate dependent even at room temperature. Therefore, for uranium C and m values are given for room temperature at

TABLE 1-5. SUMMARY OF C AND m VALUES DESCRIBING THE FLOW STRESS-STRAIN RATE RELATION, $\bar{\sigma} = C(\dot{\bar{\epsilon}})^m$, FOR ALUMINUM ALLOYS AT VARIOUS TEMPERATURES (C is in 10^3 psi)

Material	Material History	Strain	C	m	C	m	C	m	C	m	C	m	Reference	Strain Rate Range, 1/sec
Test Temperature, F(C):			390(200)		570(300)		750(400)		930(500)		1110(600)			
Super-pure	Cold rolled,												14	0.4-311
99.38 Al, 0.0017 Cu,	annealed 1/2 hr	0.288	5.7	0.110	4.3	0.120	2.8	0.140	1.6	0.155	0.6	0.230		
0.0026 Si, 0.0033 Fe,	at 1110 F	2.88	8.7	0.050	4.9	0.095	2.8	0.125	1.8	0.175	0.6	0.215		
0.006 Mn														
Test Temperature, F(C):			465(240)		645(340)		825(480)							
EC	Annealed 3 hr												9	0.25-63
0.01 Cu, 0.026 Mn,	at 750 F	0.20	10.9	0.066	5.4	0.141	3.4	0.168						
0.033 Mg, 0.092 Si,		0.40	12.3	0.064	6.3	0.146	3.5	0.169						
0.23 Fe, 0.01 Zn,		0.60	13.1	0.067	6.4	0.147	3.2	0.173						
99.5 Al		0.80	13.8	0.064	6.7	0.135	3.4	0.161						
Test Temperature, F(C):			390(200)		750(400)		930(500)							
1100	Cold drawn,												8	0.25-40
99.0 Al(Min), 0.10 Cu,	annealed	0.25	9.9	0.064	4.2	0.115	2.1	0.211						
0.15 Si, 0.50 Fe,		0.50	11.4	0.071	4.4	0.132	2.1	0.227						
0.01 Mn, 0.01 Mg		0.70	12.2	0.075	4.5	0.141	2.1	0.224						
Test Temperature, F(C):			300(150)		480(250)		660(350)		840(450)		1020(550)			
About 1100	Extruded, an-												7	4-40
0.10 Cu, 0.20 Si,	nealed 1 hr at	0.105	11.4	0.022	9.1	0.026	6.3	0.055	3.9	0.100	2.2	0.130		
0.02 Mn, 0.46 Fe,	750 F	0.223	13.5	0.022	10.5	0.031	6.9	0.061	4.3	0.098	2.4	0.130		
0.01 Zn, Bal Al		0.338	15.0	0.021	11.4	0.035	7.2	0.073	4.5	0.100	2.5	0.141		
		0.512	16.1	0.024	11.9	0.041	7.3	0.084	4.4	0.116	2.4	0.156		
		0.695	17.0	0.026	12.3	0.041	7.4	0.088	4.3	0.130	2.4	0.155		
Test Temperature, F(C):			390(200)		750(400)		930(500)							
2017	Cold drawn,												8	0.2-30
94.95 Al, 3.50 Cu,	annealed	0.250	34.5	0.014	14.8	0.110	5.8	0.126						
0.10 Si, 0.50 Fe,		0.500	32.2	-0.025	13.2	0.121	5.2	0.121						
0.50 Mn, 0.45 Mg		0.700	29.5	-0.038	12.5	0.128	5.1	0.119						
Test Temperature, F(C):			570(300)		660(350)		750(400)		840(450)		930(500)			
About 2017	Solution treated												14	0.4-311
0.89 Mg, 4.17 Cu,	1 hr at 950 F,	0.115	10.8	0.035	9.1	0.100	7.5	0.110	6.2	0.145	5.1	0.155		
0.61 Si, 0.41 Fe, 0.80 Mn,	water quenched,	2.660	10.0	0.100	9.2	0.100	7.7	0.080	6.8	0.090	4.6	0.155		
0.052 Zn, 0.01 Pb,	annealed 4 hr													
92.9 Al	at 750 F													
Test Temperature, F(C):			465(240)		645(340)		825(480)							
5052	Annealed 3 hr												9	0.25-63
0.068 Cu, 0.04 Mn,	at 790 F	0.20	14.3	0.038	8.9	0.087	5.6	0.125						
2.74 Mg, 0.10 Si,		0.40	15.3	0.035	9.3	0.071	5.3	0.130						
0.19 Fe, 0.01 Zn,		0.60	16.8	0.035	9.0	0.068	5.1	0.134						
0.003 Ti, Bal Al		0.80	17.5	0.038	9.4	0.088	5.0	0.125						
5056	Annealed 3 hr												9	0.25-63
0.036 Cu, 0.04 Mn,	at 790 F	0.20	42.6	-0.032	20.9	0.138	11.7	0.200						
4.83 Mg, 0.15 Si,		0.40	44.0	-0.032	20.8	0.138	10.5	0.205						
0.22 Fe, 0.01 Zn,		0.60	44.9	-0.031	19.9	0.145	10.3	0.202						
0.14 Cr, Bal Al		0.70	45.6	-0.034	20.3	0.144	10.3	0.203						
5083	Annealed 3 hr												9	0.25-63
0.01 Cu, 0.77 Mn,	at 790 F	0.20	43.6	-0.006	20.5	0.095	9.3	0.182						
4.41 Mg, 0.10 Si,		0.40	43.6	-0.001	19.7	0.108	8.3	0.208						
0.16 Fe, 0.01 Zn,		0.60	41.9	0.003	18.8	0.111	8.5	0.201						
0.13 Cr, 0.002 Ti,		0.80	40.2	0.002	19.1	0.105	9.7	0.161						
Bal Al														
5454	Annealed 3 hr												9	0.25-63
0.065 Cu, 0.81 Mn,	at 790 F	0.20	33.6	-0.005	16.8	0.093	10.8	0.182						
2.45 Mg, 0.12 Si,		0.40	36.0	-0.009	16.3	0.104	10.7	0.188						
0.18 Fe, <0.01 Zn,		0.60	36.9	-0.009	16.0	0.102	10.0	0.191						
0.002 Ti, Bal Al		0.80	37.0	-0.009	16.2	0.097	10.2	0.183						
Test Temperature, F(C):			750(400)		840(450)		930(500)		1020(550)					
About 7075	Sol. treat 1 hr												14	0.4-311
89.6 Al, 1.31 Cu,	at 870 F, water	0.115	10.0	0.090	6.0	0.135	3.9	0.150	2.4	0.170				
2.21 Mg, 0.21 Si,	quenched, aged	2.66	9.7	0.115	6.2	0.120	4.8	0.115	2.7	0.115				
0.30 Fe, 0.34 Mn,	at 285 F for													
5.75 Zn, 0.01 Pb	16 hr													

TABLE 1-6. SUMMARY OF C AND m VALUES DESCRIBING THE FLOW STRESS-STRAIN RATE RELATION, $\bar{\sigma} = C(\dot{\bar{\epsilon}})^m$, FOR COPPER ALLOYS AT VARIOUS TEMPERATURES (C is in 10^3 psi)

Material	Material History	Strain	C	m	C	m	C	m	C	m	C	m	Reference	Strain Rate Range, 1/sec
Test Temperature, F(C):			570(300)		840(450)		1110(600)		1380(750)		1650(900)			
Copper	Cold drawn,	0.105	20.2	0.016	17.0	0.010	12.7	0.050	7.6	0.096	4.7	0.134	7	4-40
0.018 P, 0.0010 Ni, 0.0003 Sn,	annealed 2 hr	0.223	26.5	0.018	23.5	0.004	16.8	0.043	9.7	0.097	6.3	0.110		
0.0002 Sb, 0.0005 Pb	at 1110 F	0.338	30.2	0.017	25.1	0.008	18.9	0.041	10.0	0.128	6.1	0.154		
0.0010 Fe, 0.0020 Mn,		0.512	32.2	0.025	26.6	0.014	19.4	0.056	8.5	0.186	5.5	0.195		
<0.0005 Mg, <0.0005 As,		0.695	34.4	0.024	26.8	0.031	19.0	0.078	8.2	0.182	5.2	0.190		
<0.0001 Bi, 0.0014 S, less														
than 0.003 O_2, Se + Te not														
detected														
Test Temperature, F(C):			800(427)											
OFHC Copper			26.7	0.0413									15	
Test Temperature, F(C):			750(400)		930(500)		1110(600)							
CDA 110	Hot rolled,	0.25	23.0	0.046	12.9	0.136	6.6	0.160					8	0.25-40
99.94 Cu, 0.0003 Sb, 0.0012 Pb,	annealed	0.50	27.4	0.049	13.7	0.150	6.9	0.168						
0.0012 S, 0.007 Fe, 0.001 Ni		0.70	28.8	0.057	13.3	0.165	6.8	0.176						
Test Temperature, F(C):			390(200)		750(400)		1110(600)		1470(800)					
CDA 220	Extruded, cold	0.25	41.0	0.017	34.1	0.018	22.6	0.061	11.2	0.134			8	0.1-10
90.06 Cu, 0.033 Fe, 0.004 Pb,	drawn 10%,	0.50	46.7	0.029	39.9	0.032	24.4	0.084	11.0	0.156				
0.003 Sn, Bal Zn	annealed 650 C,	0.70	48.1	0.034	40.7	0.024	24.6	0.086	11.4	0.140				
	90 min													
CDA 260	Hot rolled,	0.25			34.9	0.036	16.0	0.194	7.1	0.144			8	3.5-30
70.05 Cu, tr Fe + Sn	annealed	0.50			42.3	0.031	14.8	0.247	7.0	0.148				
Bal Zn		0.70			42.4	0.045	14.3	0.228	6.3	0.151				
CDA 280	Hot rolled,	0.25	49.0	0.028	26.9	0.083	7.6	0.189	3.1	0.228			8	3.5-30
60.44 Cu, 0.01 Pb, 0.02 Fe,	annealed	0.50	58.6	0.027	28.6	0.075	5.4	0.281	2.8	0.239				
tr Sn, Bal Zn		0.70	60.3	0.027	26.7	0.081	4.7	0.291	2.7	0.220				
CDA 365	Hot rolled,	0.25	45.8	0.038	28.6	0.065	9.8	0.106	2.4	0.166			8	3.5-30
59.78 Cu, 0.30 Pb, 0.02 Fe,	annealed	0.50	57.2	0.032	28.9	0.085	8.5	0.137	2.1	0.197				
tr Sn, Bal Zn		0.70	59.1	0.035	26.6	0.078	8.4	0.113	1.8	0.222				

TABLE 1-7. SUMMARY OF C AND m VALUES DESCRIBING THE FLOW STRESS-STRAIN RATE RELATION, $\bar{\sigma} = C(\dot{\bar{\epsilon}})^m$, FOR TITANIUM ALLOYS AT VARIOUS TEMPERATURES (C is in 10^3 psi)

Material	Material History	Strain	C	m	C	m	C	m	C	m	C	m	C	m	Reference	Strain Rate Range, 1/sec
Test Temperature, F(C):			68(20)		392(200)		752(400)		1112(600)		1472(800)		1652(900)		1832(1000)			
Type 1	Annealed 15 min	0.2	92.8	0.029	60.9	0.046	39.8	0.074	25.3	0.097	12.8	0.167	5.4	0.230	3.0	0.382	16	0.25-16.0
0.04 Fe, 0.02 C,	at 1200 F in	0.4	113.7	0.029	73.3	0.056	48.8	0.061	29.6	0.115	14.6	0.181	5.5	0.248	3.6	0.289		
0.005 H_2, 0.01 N_2,	high vacuum	0.6	129.6	0.028	82.2	0.056	53.9	0.049	32.1	0.105	14.9	0.195	5.5	0.248	3.5	0.289		
0.04 O_2, Bal Ti		0.8	142.5	0.027	87.7	0.058	56.3	0.042	32.7	0.099	15.4	0.180	5.9	0.186	3.2	0.264		
		1.0	150.6	0.027	90.7	0.054	56.6	0.044	32.5	0.099	15.9	0.173	5.9	0.167	3.0	0.264		
Type 2	Annealed 15 min	0.2	143.3	0.021	92.7	0.043	54.5	0.051	33.6	0.092	17.5	0.167	6.9	0.135	4.2	0.220	16	0.25-16.0
0.15 Fe, 0.02 C,	at 1200 F in	0.4	173.2	0.021	112.1	0.042	63.1	0.047	36.3	0.101	18.4	0.190	7.2	0.151	4.9	0.167		
0.005 H_2, 0.02 N_2,	high vacuum	0.6	193.8	0.024	125.3	0.045	65.6	0.047	36.9	0.104	18.4	0.190	7.8	0.138	4.5	0.167		
0.12 O_2, Bal Ti		0.8	208.0	0.023	131.9	0.051	66.0	0.045	37.0	0.089	18.4	0.190	7.6	0.106	3.9	0.195		
		1.0	216.8	0.023	134.8	0.056	65.3	0.045	36.9	0.092	18.6	0.190	6.8	0.097	3.7	0.167		
Test Temperature, F(C):			1110(600)		1290(700)		1470(800)		1650(900)									
Unalloyed	Hot rolled,	0.25	23.4	0.062	14.3	0.115	8.2	0.236	1.8	0.324							8	0.1-10
0.03 Fe, 0.0084 N,	annealed 800 C,	0.50	27.9	0.066	17.8	0.111	10.0	0.242	2.1	0.326								
0.0025 H, Bal Ti	90 min	0.70	30.1	0.065	20.0	0.098	12.2	0.185	2.5	0.310								
Test Temperature, F(C):			68(20)		392(200)		752(400)		1112(600)		1472(800)		1652(900)		1832(1000)			
Ti-5Al-2.5Sn	Annealed 30 min	0.1	173.6	0.046	125.6	0.028	97.6	0.028									16	0.25-16.0
5.1 Al, 2.5 Sn, 0.06 Fe,	at 1470 F in	0.2	197.9	0.048	138.8	0.022	107.4	0.026	86.1	0.025	58.5	0.034	44.2	0.069	5.4	0.308		
0.03 C, 0.01 H_2,	high vacuum	0.3	215.6	0.046	147.4	0.021	112.5	0.027	92.8	0.020								
0.03 N_2, 0.1 O_2, Bal Ti		0.4	230.6	0.039	151.4	0.022	116.0	0.022	95.6	0.019	58.7	0.040	44.8	0.082	5.1	0.294		
		0.5							96.7	0.021								
		0.6							96.6	0.024	55.6	0.042	43.0	0.078	5.2	0.264		
		0.8									50.2	0.033	39.1	0.073	5.2	0.264		
		0.9									46.8	0.025						
		1.0											35.2	0.056	5.3	0.280		
Ti-6Al-4V	Annealed 120 min	0.1	203.3	0.017	143.8	0.024	119.4	0.025									16	0.25-16.0
6.4 Al, 4.0 V, 0.14 Fe	at 1400 F in	0.2	209.7	0.015	151.0	0.021	127.6	0.022	94.6	0.004	61.3	0.146	23.3	0.143	9.6	0.131		
0.05 C, 0.01 H_2,	high vacuum	0.3	206.0	0.015	152.0	0.017	126.2	0.017	91.2	0.073								
0.015 N_2, 0.1 O_2, Bal Ti		0.4					118.7	0.014	84.7	0.079	39.8	0.175	21.4	0.147	9.4	0.118		
		0.5							77.9	0.080								
		0.6									40.4	0.205	20.0	0.161	9.6	0.118		
		0.8									26.6	0.199	19.5	0.172	9.3	0.154		
		0.9									24.9	0.201						
		1.0											20.3	0.146	8.9	0.192		
Test Temperature, F(C):			1550(843)		1750(954)		1800(982)											
Ti-6Al-4V			38.0	0.064	12.3	0.24	9.4	0.29									15	
Test Temperature, F(C):			68(20)		392(200)		752(400)		1112(600)		1472(800)		1652(900)		1832(1000)			
Ti-13V-11Cr-3Al	Annealed 30 min	0.1	173.1	0.041													16	0.25-16.0
3.6 Al, 14.1 V, 10.6 Cr,	at 1290 F in	0.2	188.2	0.037	150.5	0.030	130.5	0.035	118.4	0.040	65.4	0.097	44.6	0.147	32.4	0.153		
0.27 Fe, 0.02 C,	high vacuum	0.3	202.3	0.034														
0.014 H_2, 0.03 N_2,		0.4	215.2	0.029	174.2	0.024	153.9	0.030	107.5	0.039	59.5	0.096	42.1	0.139	30.9	0.142		
0.11 O_2, Bal Ti		0.5	226.3	0.026	181.1	0.023												
		0.6			183.5	026	147.9	0.046	92.8	0.045	56.7	0.088	40.9	0.127	29.2	0.155		
		0.7			181.4	0.029												
		0.8					136.3	0.045	84.7	0.036	53.9	0.081	39.3	0.125	27.8	0.167		
		0.9									52.9	0.080						
		1.0											38.8	0.127	28.0	0.159		

various strains in Table 1-8. The data for uranium were obtained by conducting stepwise compression tests between 68 and 392 F. Thus, the upsetting of the samples was conducted for a strain of $\bar{\epsilon} = 0.2$, the test was stopped, the sample and the platens relubricated, and the test continued.[17] Therefore, it can be assumed these test values neglect the effect of heat generation during deformation. This point is particularly significant in uranium because its flow stress is extremely temperature dependent (as seen from C values given in Table 1-8). The deformation behavior of uranium drastically changes at 760 C (1400 F) when the rhombic α structure is transformed into brittle β structure. Near 800 C (1470 F), uranium is transformed into γ structure which represents relatively good formability. The extraordinary flow stress and fracture behavior of uranium at 760 C (1400 F) is shown in Figure 1-2 in function of strain and strain rate.[17]

The flow stress data for tungsten, molybdenum, tantalum, and niobium could not be, without large errors, approximated in exponential forms because these materials exhibit strain and strain-rate dependency at low and high temperatures. Therefore, the data for these materials are given in form of curves in Figures 1-3 through 1-6. Tungsten has very little ductility at temperatures below 400 C (750 F). In some cases, many high-temperature materials exhibit certain amount

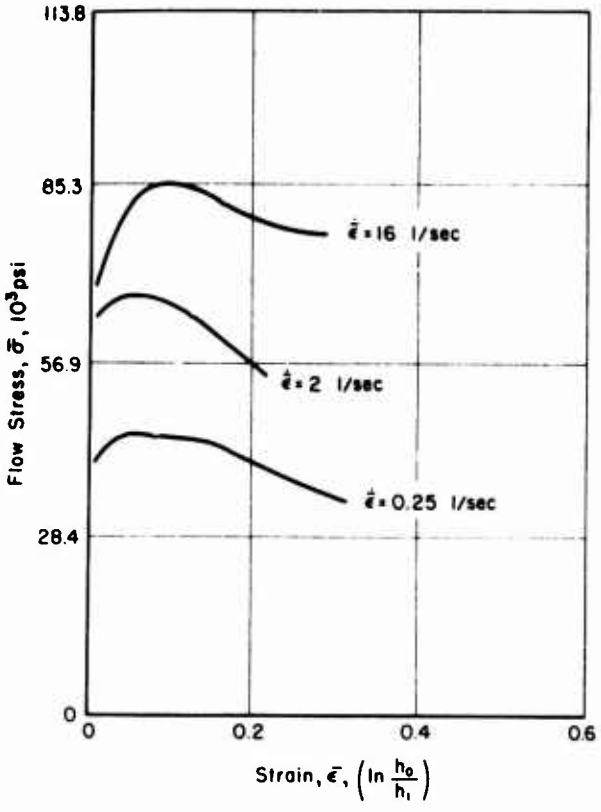

FIGURE 1-2. FLOW STRESS AND FRACTURE LIMIT OF URANIUM AT 760 C (1400 F) AND AT VARIOUS STRAIN-RATES[17]

(Composition is given in Table 1-8.)

TABLE 1-8. SUMMARY OF C AND m VALUES DESCRIBING THE FLOW STRESS-STRAIN RATE RELATION, $\bar{\sigma} = C(\dot{\bar{\epsilon}})^m$, FOR VARIOUS MATERIALS (C is in 10^3 psi)

Material	Material History	Strain	C	m	C	m	C	m	C	m	C	m	C	m	Reference	Strain Rate Range, 1/sec
Test Temperature, F(C):			72(22)		230(110)		335(170)		415(215)		500(260)		570(300)			
Lead		0.115	2.0	0.040	1.56	0.065	1.21	0.085	0.70	0.130	0.47	0.160	0.40	0.180	14	
99.98 Pb, 0.003 Cu, 0.003 Fe, 0.002 Zn, 0.002 Ag		2.66	4.0	0.055	1.47	0.100	1.04	0.125	0.55	0.135	0.36	0.180	0.28	0.225		
Test Temperature, F(C):			390(200)		570(300)		750(400)		930(400)							
Magnesium	Extruded, cold		(13)		(14)		(13)		(14)						8	0.1-10
0.010 Al, 0.003 Zn, 0.008 Mn, 0.004 Si, 0.004 Cu, 0.0008 Ni, Bal Mg	drawn 15%, annealed 350 C, 90 min	0.25	19.1	0.069	9.8	0.215	4.1	0.243	1.7	0.337						
		0.50	17.2	0.093	8.4	0.211	4.0	0.234	1.7	0.302						
		0.70	15.5	0.094	8.3	0.152	4.3	0.215	2.1	0.210						
Test Temperature, F(C):			1975(1080)		2030(1166)											
U-700			26.6	0.21	22.1	0.21									15	
Test Temperature, F(C):			68(20)		392(200)		752(400)		1112(600)		1472(800)		1652(900)		1832(1000)		16	0.25-16.0
Zirconium	Annealed 15 min at 1380 F in high vacuum	0.2	117.4	0.041	74.0	0.052	40.2	0.050	23.8	0.069	16.8	0.069	6.8	0.227	4.0	0.301
99.8 Zr, 0.009 Hf, 0.008 Al, 0.038 Fe, 0.0006 H_2, 0.0025 N_2, 0.0825 O_2, 0.0 Ni		0.3	143.7	0.022	92.2	0.058										
		0.4	159.5	0.017	105.1	0.046	54.4	0.085	29.4	0.091	18.2	0.116	7.1	0.252	4.0	0.387
		0.5	169.3	0.017	112.8	0.041	58.2	0.093								
		0.6			118.5	0.042	60.2	0.095	33.3	0.089	18.8	0.118	7.2	0.264	4.0	0.387
		0.7					61.9	0.095								
		0.8							32.0	0.081	19.4	0.101	6.9	0.252	4.1	0.403
		1.0							32.1	0.085	19.7	0.108	6.9	0.252	4.1	0.403
Zircaloy 2	Annealed 15 min at 1380 F in high vacuum	0.1	96.8	0.031	65.9	0.046									16	0.25-16.0
98.35 Zr, 0.015 Hf, 1.4 Zn, 0.01 Al, 0.06 Fe, 0.045 Ni, 0.0006 H_2, 0.0023 N_2, 0.0765 O_2		0.2	136.9	0.025	105.8	0.035	58.3	0.065	40.4	0.049	16.6	0.147	7.5	0.425	3.9	0.362
		0.3	178.5	0.034	131.4	0.035	67.9	0.056								
		0.4	202.7	0.027	145.4	0.036	73.5	0.056	37.8	0.053	18.7	0.172	7.8	0.342	4.0	0.487
		0.5			154.2	0.034	77.3	0.057								
		0.6					79.9	0.055	39.2	0.053	18.8	0.178	7.2	0.387	4.0	0.387
		0.8							40.4	0.057	18.8	0.178	7.9	0.442	4.8	0.533
		1.0							40.7	0.053	18.8	0.178	8.5	0.310	4.8	0.533
Test Temperature, F(C):			68(20)		212(100)		392(200)		572(300)		932(500)		1292(900)		1652(900)			
Uranium[a]	Annealed 2 hr at 1130 F in high vacuum	0.2	151.0	0.043	113.0	0.042	77.4	0.034	45.9	0.044	31.9	0.051	16.0	0.081	4.5	0.069	17	0.25-16.0
99.8 U, 0.0012 Mn, 0.0012 Ni, 0.00974 O_2, 0.00072 Cr, 0.0001 Co, 0.0047 H_2, 0.0041 N_2, 0.1760 O_2 (free of cadmium and boron)		0.4	173.4	0.033	132.7	0.049	91.0	0.041	54.5	0.047	33.1	0.059	16.1	0.089	4.5	0.069		
	high vacuum	0.6	184.4	0.023	143.1	0.047	98.1	0.032	56.0	0.056	33.4	0.054	16.1	0.089	4.5	0.069		
		0.8	189.8	0.018	149.5	0.048	102.6	0.036	58.3	0.057	33.3	0.049	16.2	0.097	4.5	0.069		
		1.0							59.0	0.056	32.5	0.055	16.4	0.097	4.5	0.069		

(a) See text for additional information.

of formability under compression, but they fracture at higher strains. These cases are indicated in figures where the flow-stress curve for a given temperature could not be extended beyond the strain where the sample fractured.

Few flow-stress data in function of temperature and strain rate exist for alloys of refractory materials or for cobalt- and nickel-base superalloys. Very useful data on forging pressures at various forging conditions, however, are available in a recent book published by Battelle staff members.[1] This information, since it is readily available in the U. S., has not been included in the present report.

APPLICATION OF FLOW-STRESS DATA IN PREDICTING FORGING LOADS AND STRESSES

A number of methods are used in analyzing metalforming and forging problems. The most commonly used method for predicting forging stresses and loads is the so-called "Slab" or "Sachs" method. The principles and the details of this method are described in various publications[18] and they have been applied to practical forging problems earlier in this program.[19] At this time it is useful to illustrate, with a few examples, how the flow-stress data summarized in this report can be used for predicting stress and loads in forging operations.

Upset Forging of a Ring or a Cylinder

The upset forging of a ring with an internal radius r_b, external radius r_e, and height, h, is schematically illustrated in Figure 1-7. The axial stress distribution, σ_z, as shown in Figure 1-7, is given by:[19]

$$\sigma_z = \frac{2\tau}{h}(r_e - r_b) + \overline{\sigma} \quad . \qquad (1\text{-}8)$$

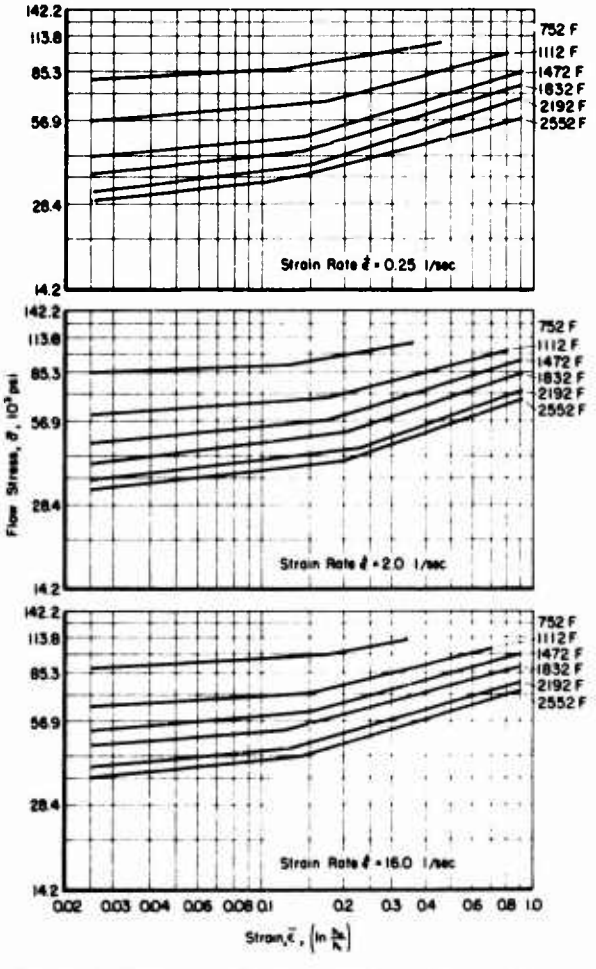

FIGURE 1-3. FLOW STRESS-STRAIN CURVES FOR TUNGSTEN AT VARIOUS TEMPERATURES AND STRAIN-RATES[16]

(99.96 W, tr Mo, 0.004 Fe, 0.008 C, 0.001 H_2, 0.003 N_2, 0.003 O_2; annealed 60 min at 1920 F in high vacuum)

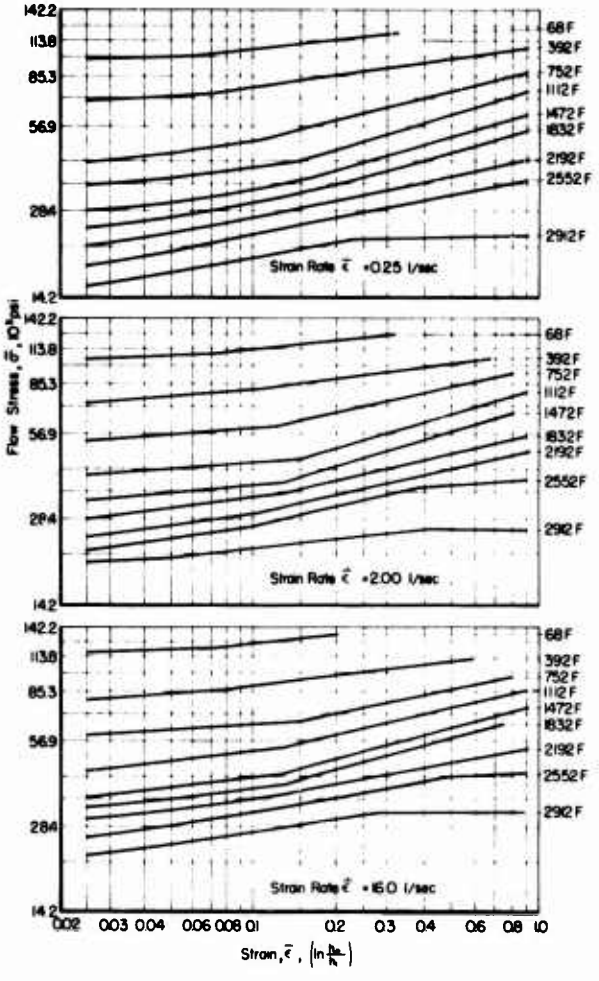

FIGURE 1-4. FLOW STRESS-STRAIN CURVES FOR MOLYBDENUM AT VARIOUS TEMPERATURES AND STRAIN-RATES[16]

(99.95 Mo, tr Nb, 0.01 Fe, 0.005 C, 0.001 H_2, 0.001 N_2, 0.005 O_2; annealed 60 min at 1740 F in high vacuum)

The forging load, P, for upsetting the ring is

$$P = 2\pi \left[-\frac{2\tau}{h} \left(\frac{r_e^3 - r_b^3}{3} \right) + \left(\frac{2\tau}{h} r_e + \overline{\sigma} \right) \frac{r_e^2 - r_b^2}{2} \right] \qquad (1\text{-}9)$$

where,

σ_z = axial stress distribution

P = forging load

$\tau = f \cdot \overline{\sigma}$, friction shear stress

f = friction factor, $0.15 \leq f \leq 0.3$ in hot forging

$\overline{\sigma}$ = flow stress of the material t temperature and strain-rate conditio is present during forging

h, r_e, r_b = dimensions of the ring as shown in Figure 1-7.

Equations (1-8) and (1-9) are also valid for a cylinder. In that case, the value $r_b = 0$ must be substituted in the expressions.

For example, let us consider the upset forging of a 1043 steel cylinder of final height $h_1 = 0.5$ inch, and final radius of 2 inches under a hydraulic press of 2 in./sec constant ram speed at 1180 C (2160 F). From the height of the sample and from the ram speed, the strain rate, $\dot{\bar{\epsilon}}$, near the end of forging is obtained using Equation (1-4):

$$\dot{\bar{\epsilon}} = \frac{V}{h_1} = \frac{2}{0.5} = 4 \text{ sec}^{-1} .$$

For 1043 steel, at 1180 C (2160 F), from Table 1-4, we obtain the values C = 10,800 and

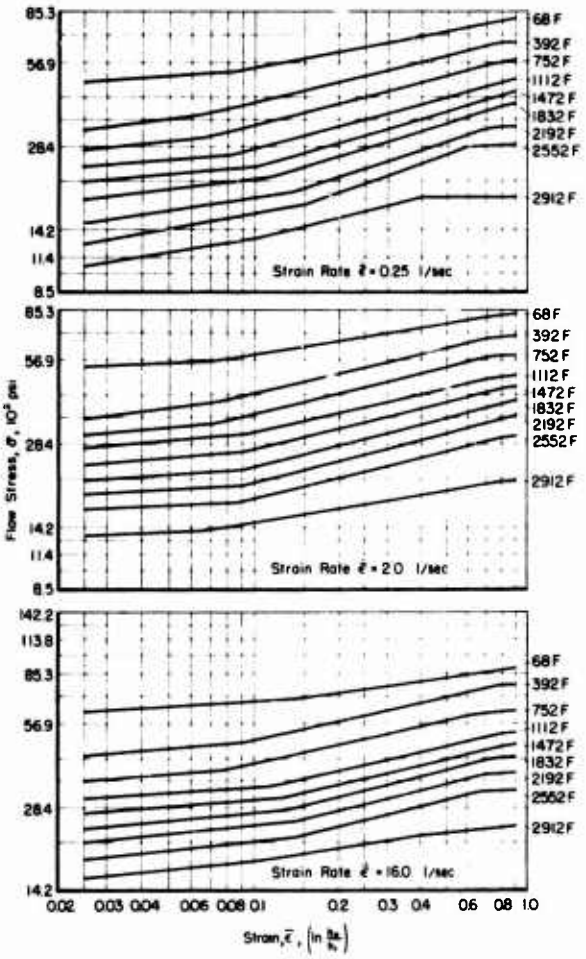

FIGURE 1-5. FLOW STRESS-STRAIN CURVES FOR TANTALUM AT VARIOUS TEMPERATURES AND STRAIN-RATES[16]

(0.12 Nb, 99.8 Ta, free of U, 0.03 Fe, free of Ti, 0.001 H_2, 0.031 N_2, 0.003 O_2; annealed 60 min at 2190 F in high vacuum)

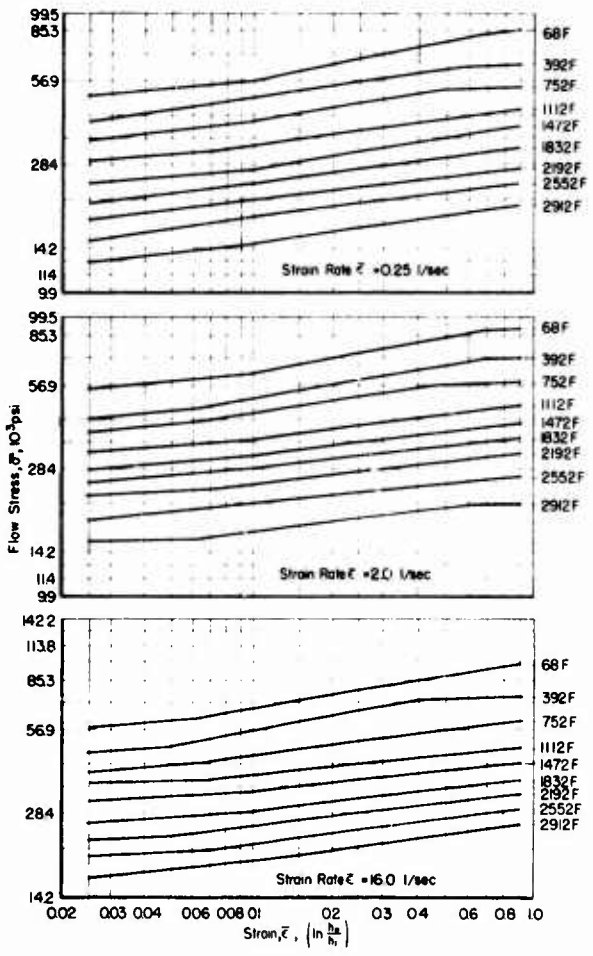

FIGURE 1-6. FLOW STRESS-STRAIN CURVES FOR NIOBIUM AT VARIOUS TEMPERATURES AND STRAIN-RATES[16]

(99.86 Nb, 0.02 Ta, 0.05 Fe, 0.008 Ti, 0.005 C, 0.001 H_2, 0.03 N_2, 0.02 O_2; annealed 60 min at 2190 F in high vacuum)

m = 0.21. Thus, the flow stress $\bar{\sigma}$ towards the end of forging is

$$\bar{\sigma} = C\dot{\bar{\epsilon}}^{m} = 10,800(4)^{0.21} = 14,450 \text{ psi.}$$

Thus, with $r_b = 0$, and estimating the friction factor f = 0.3, the forging load is obtained by evaluating Equation (1-9), or

$$P = 2\pi\left[\frac{\tau r_e^3}{3h} + \frac{\bar{\sigma} r_e^2}{2}\right] = 2\pi\bar{\sigma}\,(2.6) = 5.2\,\pi\bar{\sigma}$$

P = 246,000 pounds.

Round Closed-Die Forging With Flash

The forging schematically illustrated in Figure 1-8 was earlier investigated in Phase I of this program.[19] At that time, detailed mathematical expressions were derived and applied to several forgings including the one seen in Figure 1-8. In the present report the application of an approximate, but very simple, method of predicting the forging load will be illustrated.

This technique was initially suggested by Siebel[21]. The flash stress, σ_{z2}, at the entrance to die cavity is obtained by considering the flash as a ring and by using the dimensions given in Figure 1-3. It is then assumed that the normal pressure acting on the entire forging, including the flash, would be approximately constant and equal to the flash stress σ_{z2}, at the entrance to the die cavity. Thus, by assuming a friction factor f = 0.25, which is typical for hot forging, and by using the dimensions given in Figure 1-8, Equation (1-8) gives:

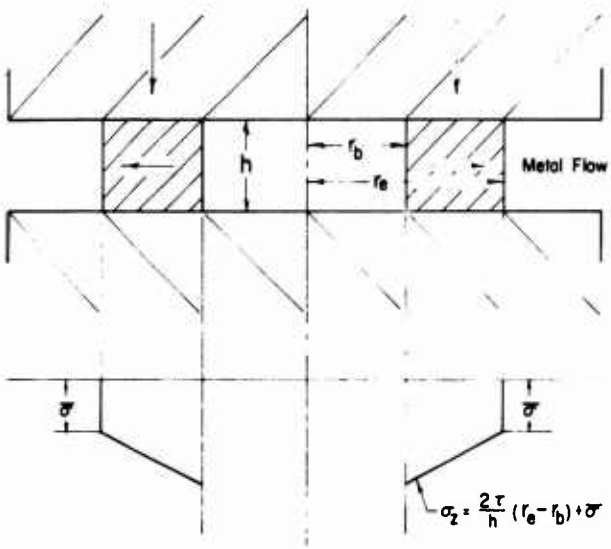

FIGURE 1-7. STRESS DISTRIBUTION IN UPSET FORGING A RING WITH METAL FLOWING OUTWARD

$$\sigma_{z2} = \frac{2 \times 0.25 \times \bar{\sigma}}{0.079}(1.181 - 0.787) + \bar{\sigma} = 3.5\,\bar{\sigma}\ .$$

For a ram velocity of 1.02 in./sec, the strain rate in the flash near the end of the forging is

$$\dot{\bar{\epsilon}} = \frac{V}{h} = \frac{1.02}{0.079} = 12.9 \text{ sec}^{-1}\ .$$

The corresponding flow stress for 1043 steel at 2160 F is obtained by using the corresponding coefficients C = 10,800 and m = 0.21 from Table 1-4. Thus,

$$\bar{\sigma} = 10,800\,(12.9)^{0.21} = 18,400 \text{ psi}\ .$$

The total forging load is now given by:

$$P = \sigma_{z2} \cdot \pi r_1^2 = 3.5\,\bar{\sigma}\pi\,(1.181)^2 = 282,000 \text{ lbs}\ .$$

This value is for practical purposes close to the actual load, 264,000 lbs, measured in forging the part illustrated in Figure 1-8.[19,20]

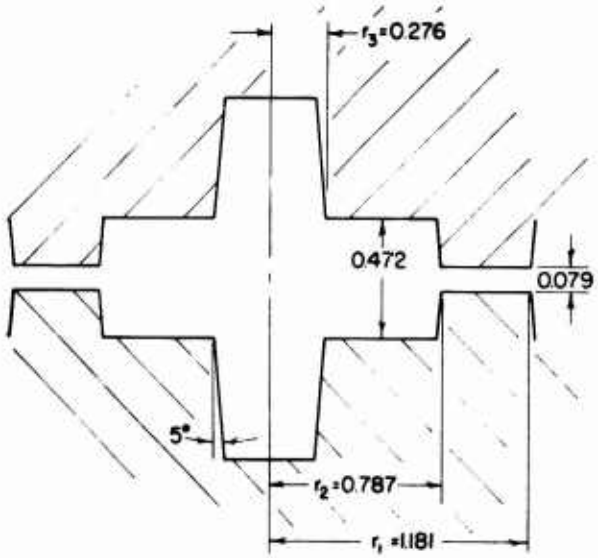

FIGURE 1-8. SCHEMATIC ILLUSTRATION OF ROUND CLOSED-DIE FORGING WITH FLASH[20]

Prediction of Temperatures in Hot Forging

The accuracy of estimating the flow-stress values in forging depends significantly upon the prediction of average values of strain rate and temperature. As discussed above, the average strain rate is calculated from the known average thickness of the forging and from the average deformation velocity of the equipment. Often it is desirable to calculate average temperatures in a forging, or in various zones of a given forging.

Detailed discussion of temperatures in forging processes, and the method of predicting them are given elsewhere.[22] In estimating

average temperatures in a forging, it is necessary to consider the initial stock temperature, θ_s, the temperature increase due to deformation, θ_d, and the temperature drop due to heat losses into the dies, θ_c. As a first approximation, the temperature increase due to friction, θ_f, may be neglected because it can be assumed that the friction contributes to achieve an average uniform temperature across the forging.

Calculation of temperatures in a forging can be illustrated by considering the 6061 aluminum forging seen in Figure 1-9[23, 24]. This

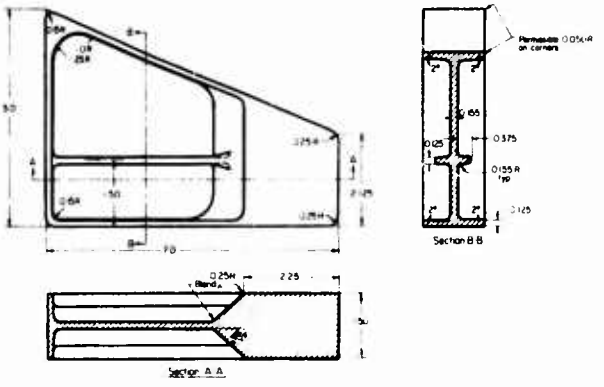

FIGURE 1-9. EXAMPLE FORGING FROM 6061 ALUMINUM[23]

part has a thinner zone on the left and a thicker zone on the right. The average temperatures of the forged material in these zones are calculated separately. In simplifying the analysis, a reasonable approximation is to neglect the temperature gradients and consider different parts of the forging as separate plates with average uniform temperatures, cooled symmetrically from both sides. Thus, the heat balance gives[22]:

$$\theta = \theta_1 + (\theta_s - \theta_1) \exp\left(-\frac{\alpha T}{c\rho t}\right), \quad (1\text{-}10)$$

where

θ_1 = initial die-surface temperature = 400 F = 204 C

θ = instantaneous average temperature of the forging

θ_s = initial stock temperature = 850 F = 454 C

α = heat-transfer coefficient between the forging and the dies, ≃15,000 kcal/in.^{2}-hr-°C, estimated from values obtained in forging steel[22]

T = time of contact estimated from press speed (T_L = 0.6 sec for left side, T_R = 0.5 sec for right side)

c = specific heat of forged material ≃0.2114 + 0.000133 θ (cal/g-°C)

ρ = density of forged material ≃2.71 g/cm^3

t = thickness of the plate, measured on actual forging (t_L = 0.195 in. = 0.495 cm for left side, t_R = 1.517 in. = 3.85 cm for right side).

Left Side. Applying Equation (1-10) to the left side of the forging, Figure 1-9, gives the temperature in the forging after cooling in the dies θ_L = 309 C. The temperature increases due to deformation is given by

$$\theta_d = A\bar{\sigma}_a\bar{\epsilon}_a/c\rho \quad , \quad (1\text{-}11)$$

where, in addition to the previously defined symbols,

A = factor for conversion from mechanical energy into heat energy, 3.238 x 10^{-4} kcal/ft-lb, or 2.342 x 10^{-3} kcal/m-kg

$\bar{\sigma}_a$ = average flow stress (estimated for 309 C to be about 11,500 psi)

$\bar{\epsilon}_a$ = average strain, estimated from initial and final thicknesses ($\bar{\epsilon}_{aL}$ = 0.5 for left side).

The evaluation of Equation (1-11) gives θ_{dL} ≃17 C. Thus, the average temperature of the thin side of the forging is,

$$\theta_{FL} \simeq 309\ C + 17\ C = 326\ C \simeq 620\ F.$$

Right Side. The thick side of the forging was subject to a very small amount of deformation because its preform thickness was nearly equal to finish thickness. Consequently, we can neglect the temperature increases due to deformation and friction. The average temperature of the forging at the end of stroke θ_R, is estimated by evaluating Equation (1-10) with the appropriate constants. Thus,

$$\theta_{FR} \simeq 432\ F = 810\ F.$$

These temperatures can now be used for predicting the flow stress at both right and left zones of the forging.

Forward Extrusion at Room Temperature

Various formulas predict the punch pressure in forward extrusion. The expression, originally suggested by Siebel, is:[21]

$$p = \bar{\sigma}_a \ln R + \frac{2}{3}\alpha\bar{\sigma}_a + \frac{\bar{\sigma}_a \ln Rf}{\cos\alpha \sin\alpha} + \pi DL\bar{\sigma}_o f \quad (1\text{-}12)$$

where,

p = punch pressure

$\bar{\sigma}_a$ = average flow stress in the deformation zone, including strain hardening

α = die half angle, in radians

R = reduction in area = cross-sectional area of slug/cross-sectional area of product

f = friction factor, assumed to be 0.04 in cold extrusion

D = diameter of slug

L = length of slug

$\bar{\sigma}_o$ = yield stress of slug material, or flow stress at small strain.

In the deformation zone under the extrusion die, the strain, and consequently the flow stress, varies with location. The material strain hardens as it approaches the exit of the die. A reasonable approximation for the average flow stress $\bar{\sigma}_a$ can be obtained by integrating the flow-stress curve along the strain ln R and by taking the average value, or

$$\bar{\sigma}_a = \frac{1}{\ln R} \int_o^{\ln R} \bar{\sigma} d\epsilon = \frac{K(\ln R)^n}{r+1} \qquad (1-13)$$

where the coefficients K and n are obtained from Tables 1-1 through 1-3. For example, in cold extruding 1018 hot-rolled steel at room temperature (K = 117,000 psi, n = 0.224), the extrusion pressure was calculated for various reductions by using Equations (1-10) and (1-11). A friction factor f = 0.04 (which is typical for cold forging), was assumed and the half die angle, $\alpha = 60°$, was the same for all reductions. The predicted and measured punch pressures are given below:

Reduction in Area, percent	Calculated Punch Pressure, 10^3 psi	Measured Punch Pressure, 10^3 psi
20	118.0	110.8
50	183.4	186.0
60	212.4	204.6

These results indicate that extrusion pressures, predicted by using an appropriate formula, a corresponding friction factor f, and K and n values of the extruded material, are within useful agreement with actual data.

CONCLUSIONS AND FUTURE WORK

In this chapter a thorough review of the domestic and foreign literature on the fundamentals of metalforming was conducted, and flow-stress data dependence on strain, strain rate and temperature were compiled for various materials. These data, presented for steels, aluminum, copper, and titanium alloys, and for high-temperature materials, are extremely useful in designing forging processes and predicting forging loads and energies.

In forging, the load and energy required to carry out the process are determined by the flow stress of the forged material, by the frictional conditions, and by the geometrical shape of the forging. Thus, in addition to the flow stress of the forged material, the values of the friction factor, and the equations for predicting the stresses and loads must also be available. In this chapter, application of flow stress data in predicting forging pressures have been illustrated by using examples of upset forging, closed-die forging, and cold extrusion.

Future studies related to material flow-stress data and forging-load predictions, will include (a) the design, construction, and use of a device for determining flow-stress data of various materials of interest, (b) derivation and representation of simple formulas for predicting pressures, loads, and energies in various forging operations, within useful approximations, and (c) the determination of friction factors for selected forging operations.

REFERENCES

(1) Sabroff, A. M., Boulger, F. W., and Henning, H. J., Forging Materials and Practices, Rheinhold Book Corporation (1968).

(2) Watnough, T., et al, "Manufacture of Large Precision-Cast Dies for Heated Die Forging of Titanium Alloys", Progress reports prepared under Air Force Contract No. F33615-67-C-1722, IITRI.

(3) Meyer-Nolkemper, H., "On the Relationship Between Flow Stress and Its Factors of Influence" (in German), Industrie-Anzeiger, June 17, 1966, p. 153.

(4) Kienzle, O., and Bühler, H., "The Plastometer, A Material Testing Machine for the Compressive Characteristics of Metals" (in German), Zt. f. Metallkunde, 55 (1969), pp. 668-673.

(5) Dunstan, G. R., Evans, R. W., "A Technique for Simulating the Hot Rolling of Metals", Metallurgia, March 1969, p. 96.

(6) Cook, P. M., "True Stress-Strain Curves for Steel in Compression at High Temperatures and Strain Rates, for Application to the Calculation of Load and Torque in Hot Rolling", Institution of Mech. Engr. Conf. on Properties of Materials at High Rates of Strain, May 1957.

(7) Alder, J. F., Phillips, V. A., "The Effect of Strain-Rate and Temperature on The

Resistance of Aluminum, Copper, and Steel to Compression", J. Inst. of Metals, 83 (1954-55), p. 80.

(8) Suzuki, H., et al, "Studies on Flow Stress of Metals and Alloys", 18 (3), Serial No. 117, Reports by the Institute of Industrial Sciences, University of Tokyo, March 1968.

(9) Bühler, H., et al, "The Flow Stress of Aluminum and of Some Aluminum Alloys" (in German), Bänder, Beche, Rohre, 11 (1970), No. 12, p. 645.

(10) Verein Deutscher Ingenieure, "Flow Curves of Metallic Materials" (in German), VDI Data Sheets 3200, 3201, and 3202, April 1964.

(11) Schwandt, S., "Flow Curves of Carbon and Alloy Steels" (in German), Industrie-Anzeiger, 90, 1968, No. 19, p. 366.

(12) Samanta, S. K., "Effect of Strain-Rate on Compressive Strength of Tool Steel at Elevated Temperatures", Proc. Conf. on Deformations Under Hot Working Conditions, The Iron and Steel Institute, p. 122, London, 1968.

(13) Hinkfoth, R., Konig, H. D., "Calculation of Flow Stress in Warmforming With the Help of Coefficients" (in German), Neue Hutte, 12 (1967), p. 212.

(14) Bailey, J. A., Singer, A.R.E., "Effect of Strain Rate and Temperature on the Resistance to Deformation of Aluminum, Two Aluminum Alloys, and Lead", J. Inst. of Metals, 92 (1963-64), p. 404.

(15) DePierre, V., "Experimental Measurement of Forces During Extrusion and Correlation With Theory", ASME Paper 69-WA/Lub-6.

(16) Wagener, H., "The Compressive Characteristics of Reactive and High Temperature Metals" (in German), Doctoral Dissertation, Technical University Hannover, 1965.

(17) Bühler, H., and Wagener, H. W., "The Compressive Characteristics of Natural Uranium" (in German), Z. für Metallkunde, 57 (1966), p. 825.

(18) Thomsen, E. G., et al, "Mechanics of Plastic Deformation in Metal Processing", The MacMillan Company, New York (1965).

(19) Altan, T., et al, "A Study of Mechanics of Closed-Die Forging", Final Report to Army Materials and Mechanics Research Center, Watertown, Mass., August 1970, AD 711544, Chapters 3 and 4, also Altan, T., and Fiorentino, R., "Prediction of Loads and Stresses in Closed-Die Forging", ASME Trans. J. Engr. Industry, May 1971, p. 477.

(20) Brill, K., "Model Materials for Forging of Metals" (in German), Doctoral Dissertation, Technical University Hannover, 1963.

(21) Siebel, E., "Fundamentals and Concepts of Forming" (in German), Werkstattstechnik and Maschinenbau, 40, 1950, p. 373.

(22) Altan, T., and Gerds, A. F., "Temperature Effects in Closed-Die Forging", ASM Technical Report No. C70-30-1, October, 1970.

(23) Becker, J. R., Douglas, J. R., and Simonen, F. A., "Effective Tooling Designs for Production of Precision Forging", Air Force Contract No. F33615-70-C-1437. Final Report, Battelle's Columbus Laboratories, June, 1972, AFML-TR-72-89.

(24) Akgerman, N., and Altan, T., "Modular Analysis of Geometry and Stresses in Closed-Die Forging: Application to a Structural Part", ASME Paper 72-Prod-9.

CHAPTER 2

INSTRUMENTATION AND MONITORING OF FORGING PRESSES

by

J. R. Douglas, T. Altan, and R. J. Fiorentino

TABLE OF CONTENTS

2-1

INSTRUMENTATION AND MONITORING OF FORGING PRESSES

by

J. R. Douglas, T. Altan, and R. J. Fiorentino

ABSTRACT

The successful forging operation requires a certain amount of energy and a certain magnitude of load. For the efficient use of existing forging equipment, it is necessary to know whether the loads and the energies required by the process are within the available capacity of the equipment. It is also useful to know if the required load exceeds the machine or tooling design limits, thus enhancing the possibility of failure. Only by using monitoring instrumentation is it possible to accurately determine the actual required load and energy of a process.

The various approaches to forging-load measurement that are discussed in this chapter include (1) measurement with load cells, (2) measurement via press-frame deflection, and (3) measurement via hydraulic pressure (for hydraulic presses). Techniques explored for monitoring the displacement of the moving press ram include use of (1) linear variable-differential transformers, (2) resistance-based potentiometric transducers, and (3) high-speed photography. Methods of determining velocity, acceleration, and energy are covered, and it is shown that they can be calculated on the basis of load and displacement measurements.

INTRODUCTION

The efficient use of forging equipment and the improvement of existing forging processes require quantitative determination of process variables. For a given material, forging temperature, and part configuration a certain amount of forging energy and a certain magnitude of forging load are required in order to successfully carry out the forging process. Figure 2-1 shows a typical forging load plotted versus the forging stroke. The surface area under the curve is the deformation energy necessary to complete the process. Thus, a successful forging operation requires that

- The load available at the machine be larger than the load required by the process during one stroke cycle.
- The energy available in the machine be larger than the energy required by the process during one stroke cycle.

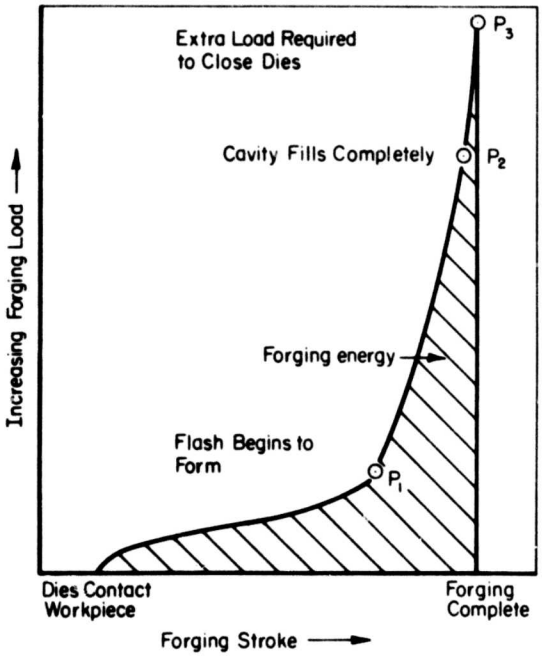

FIGURE 2.1. TYPICAL FORGING-LOAD CURVE FOR CLOSED-DIE FORGING SHOWING THREE DISTINCT STAGES

For economic use of existing forging equipment, it is necessary to know whether the loads and the energies required and supplied by the machine are adequate for the forging operation. Ideally, the machine should be used at or near its maximum load and energy capacities without being overloaded. As most forging machines are designed with large safety factors, they can be subjected at times to slight overloads. However, continuous overloading of equipment may result in blocking (in a mechanical press), breakage of tooling, decreased life of moving machine members, and in high maintenance costs and downtime. Instrumentation and monitoring of forging equipment assists in preventing damage from overloading, permits greater reproducibility in forged parts, and provides information for improvement of the specific forging operation.

FORGING VARIABLES AND THEIR MEASUREMENT

In press forging, with mechanical, hydraulic, or screw presses, the most significant

variable to know is the maximum forging load – it determines whether the equipment is being used below or above its load capacity. In mechanical presses, the energy required by the process determines the flywheel slowdown and the number of strokes per minute under production conditions. The ram speed determines the rate of deformation and the contact time under load. Thus, the ram speed influences the flow stress of the deforming material, the friction conditions, and die wear.

The principal objectives in instrumenting forging equipment can be summarized in the following categories:

(1) In practical situations, the most significant variable is usually the forging load. Here one or several load-measuring devices on the press are necessary, and monitoring or recording equipment need only show peak loads. Excessive and off-center loading conditions may result in damage to the press and tooling, and in excessive tool wear. At times it may be necessary to monitor the load at each of four columns to determine the degree of off-center loading.

(2) In starting a new forging operation, or developing a preform design, it is useful to know the variation of the load during the forging stroke. Thus, the energy necessary for forging can also be obtained from the surface area under the load-stroke curve, Figure 2-1. For this purpose, in addition to a load measuring device, a displacement transducer will also be necessary. The output from both load and displacement measuring devices can be used in a X-Y recorder to obtain directly the load-stroke curve during the forging process.

(3) In developing a new forging process (new material, unusual part configuration) and in precision forging of gears, air foils, and aircraft structural parts, exact knowledge of forging conditions is needed. For these applications, ram velocity, time of contact between dies, time of forging under pressure, and die temperatures may have to be recorded in addition to load and displacement. Various types of transducers and recorders can be used for this purpose. If load and displacement are recorded versus time, the velocity and the contact times can be easily obtained from this recording.

In this chapter no attempt has been made to discuss the instrumentation that might be used in monitoring or control of temperature. While temperature is a most important factor in forging, it is not included in this chapter because it would be better covered as a sole topic of a chapter. In earlier work conducted at Battelle, this topic has been treated in detail(1)*. The objective of the present report is to provide useful information about current practice that could be applicable to forging. No attempt has been made to provide a complete review of measurement technology since many techniques would be impractical for measuring forging variables. A number of texts treat measurement technology in more detail. (2, 3) Discussed here are the most important methods for monitoring and recording these variables in practical forging operations. Special emphasis has been placed on monitoring load and displacement because of their importance.

MEASUREMENT OF FORGING LOAD

Although there are various types of load transducers based on piezoelectric, capacitive, and inductive effects, a large majority of devices used for measuring loads, i.e., load transducers, employ electrical-resistance strain gages in one manner or another. The operation of the strain gage is based on the physical effect that the electrical resistance of metals change in direct proportion to the amount of strain. Since strain is proportional to stress, strain gages are logical devices for determining stress for eventual conversion to load. The most common load-measuring device, a load cell, designed on this basis is schematically illustrated in Figure 2-2.

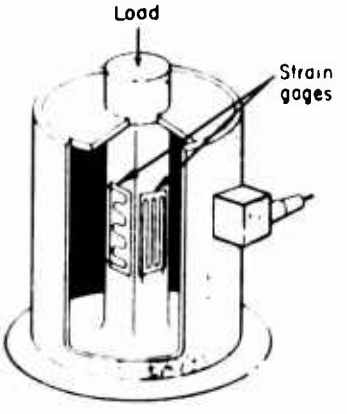

FIGURE 2-2. REPRESENTATION OF A TYPICAL LOAD CELL WHERE STRAIN GAGES ARE USED TO SENSE LOAD(2)

Since the resistance change due to strain is usually quite small, it is necessary to use sensitive electrical circuitry to detect these minor changes in resistance (3) The most common electrical circuit used for this purpose is known as the Wheatstone bridge Figures 2-3 and 2-4 illustrate schematically the Wheatstone bridge and show how strain gages are used to make up the bridge

Load transducers are usually designed with a degree of temperature compensation built into

*See Reference Section.

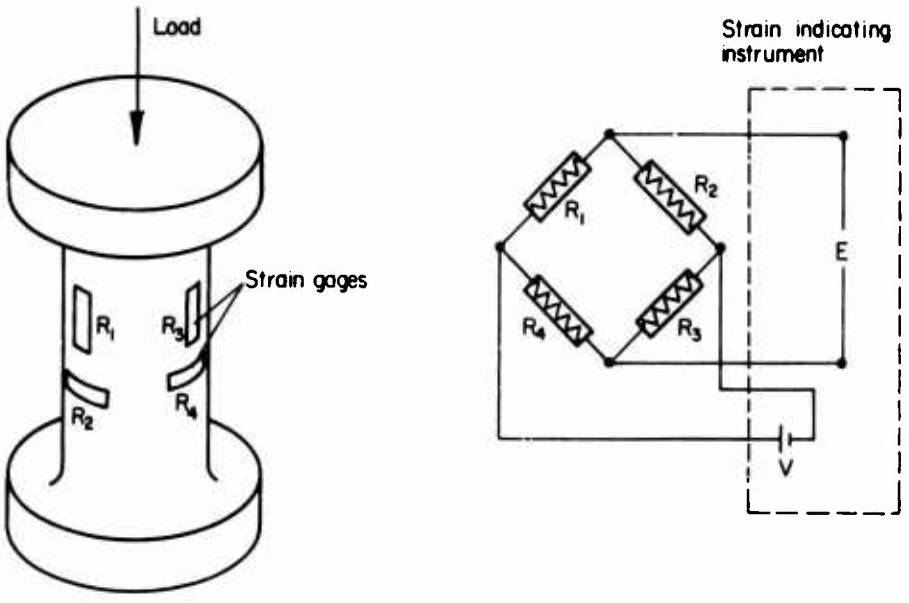

FIGURE 2-3. SCHEMATIC OF A FULL WHEATSTONE BRIDGE

V = Excitation Voltage, E = Output Voltage.

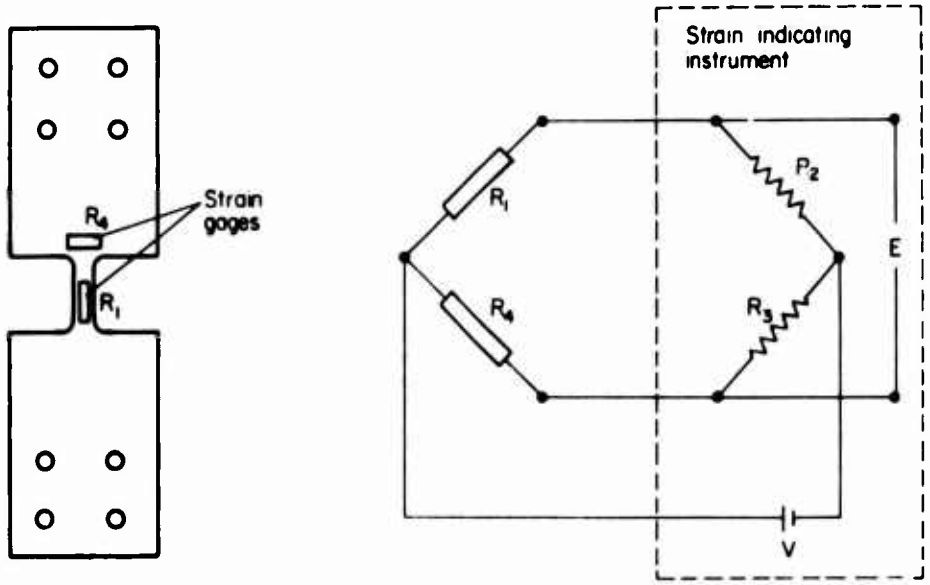

FIGURE 2-4. SCHEMATIC OF A HALF WHEATSTONE BRIDGE IN USING A STRAIN BAR

V = Excitation Voltage, E = Output Voltage.

them. This is accomplished by using compensating strain gages which are usually placed perpendicular to the strain measuring gages. As seen in Figure 2-3, the temperature compensating gages are always placed in Arms R2 and R4 and nullify the effect of temperature-caused strains in the gages in Arms R1 and R3.

It is usually preferable to form a full Wheatstone bridge arrangement as seen in Figure 2-3. If, however, a full bridge arrangement is not practical, the strain gages can be used to make up a half bridge, with the other half of the bridge supplied as part of the monitoring operation as shown in Figure 2-4. Any number of identical strain gages can be used to form the arms of the Wheatstone bridge. The four arms must, however, be balanced (equal number of gages in each arm) and the compensating gages must be in Arms R2 and R4 as shown in Figure 2-3.

Load Measurement With Load Cells

The most accurate load transducer is the load cell. Most load cells include a load-carrying member that is designed so that the strain at the point where the gages are attached varies linearly with load, Figure 2-2.[2] The load cell must be calibrated so that the resistance change of the strain gates can be related to load. For use in minitoring forging loads, the load cell is usually placed under the tooling in a position to carry the full forging load. The load cell is often used in research and development studies in forging where accurate load measurement is important.[4, 5] Usually, however, the accuracy obtainable with load cells is not required, and other simpler methods can be used for measuring load with useful accuracy.

In the present study a 3000-ton load cell was built and calibrated at the National Bureau of Standards. The details of the design and the calibration of this load cell are described in Appendix 2 C.

Load Measurement Via Tooling Stresses

Another approach to load measurement during forging is to place strain gages on a strategic portion of the tooling. This is a particularly useful technique where symmetrical tooling is being used and where uniform loading of the tooling can be assumed. In practical hot-forging operations, however, it is not possible to apply strain gages to tooling because of the severe environmental conditions; thus, some indirect method is necessary for measuring loads.

Load Measurement Via Press-Frame Deflection

Press-frame deflection can be used in a number of ways for determining the load during a forging operation. All of these techniques are based on the fact that the press frame must support the entire forging load. Under load, the press frame will strain in proportion to the load, and this strain can be measured and used to re-represent directly the magnitude of the load.

The classical approach to measuring loads via press deflection involves steel bands that extend from the bottom to the top of the press. For protection, the bands are usually placed inside of the hollow tie rods of the press. Strain gages, attached to the bands, reflect the strain in the tie rods and, after calibration, the load can be directly obtained from this strain.

Strain gages can be attached directly to the columns of the press frame and used to monitor forging load. Frequently, however, the amount of strain in the columns or tie rods is small and difficult to measure accurately with directly applied strain gages, even at maximum tonnage. Excessive electrical interference could alter the output of directly applied strain gages. In these instances, strain bars may be used to amplify the strain mechanical and to minimize external electrical interference.

Strain bars are designed to give a mechanically induced strain amplification. Figure 2-5 illustrates a strain bar designed at Battelle for use in an earlier program.[1] Strain bars are usually made of a high-strength material and designed so that strain, where the gages are attached, is amplified due to stress concentration. Thus, the strain gages, which are attached at the point of stress concentration, will be subjected to a much larger strain than exists in the press frame. This strain will still be proportional to the load in the press and will be easily measured. Strain bars of various designs are available commercially (see Appendix 2-A).

Another approach to load measurement using press-frame deflection involves fixing one end of a long bar at the top of the press frame. The other end of the bar is free of the press and is at some location near the bottom of the press frame. As load is applied, the press frame strains and there will be relative movement between the bottom end of the bar and the adjacent part of the press frame. This movement is proportional to the load and strain in the frame, and, when calibrated, can be used to monitor load. Most often, dial indicators are used to read load directly. However, sensitive displacement transducers could also be used to provide input for recording devices.

Load Measurement Via Hydraulic Pressure

In hydraulic presses, forging loads can be monitored by measuring the fluid pressure of the hydraulic system. The pressure transducer is usually located in some convenient position on the hydraulic system where the fluid pressure is identical to that of the main cylinder(s) of the press. Neglecting cylinder friction losses, the fluid pressure will always be proportional to the load. However, this method of measuring loads is less accurate than the others described because the cylinder friction losses may vary with time and, at high-speed operations, vibrations in the hydraulic system may distort the pressure measurements.

Calibration of Load Transducers

With all of the load-measuring techniques, it is necessary to obtain a calibration so that the electrical output of the transducer (load cell,

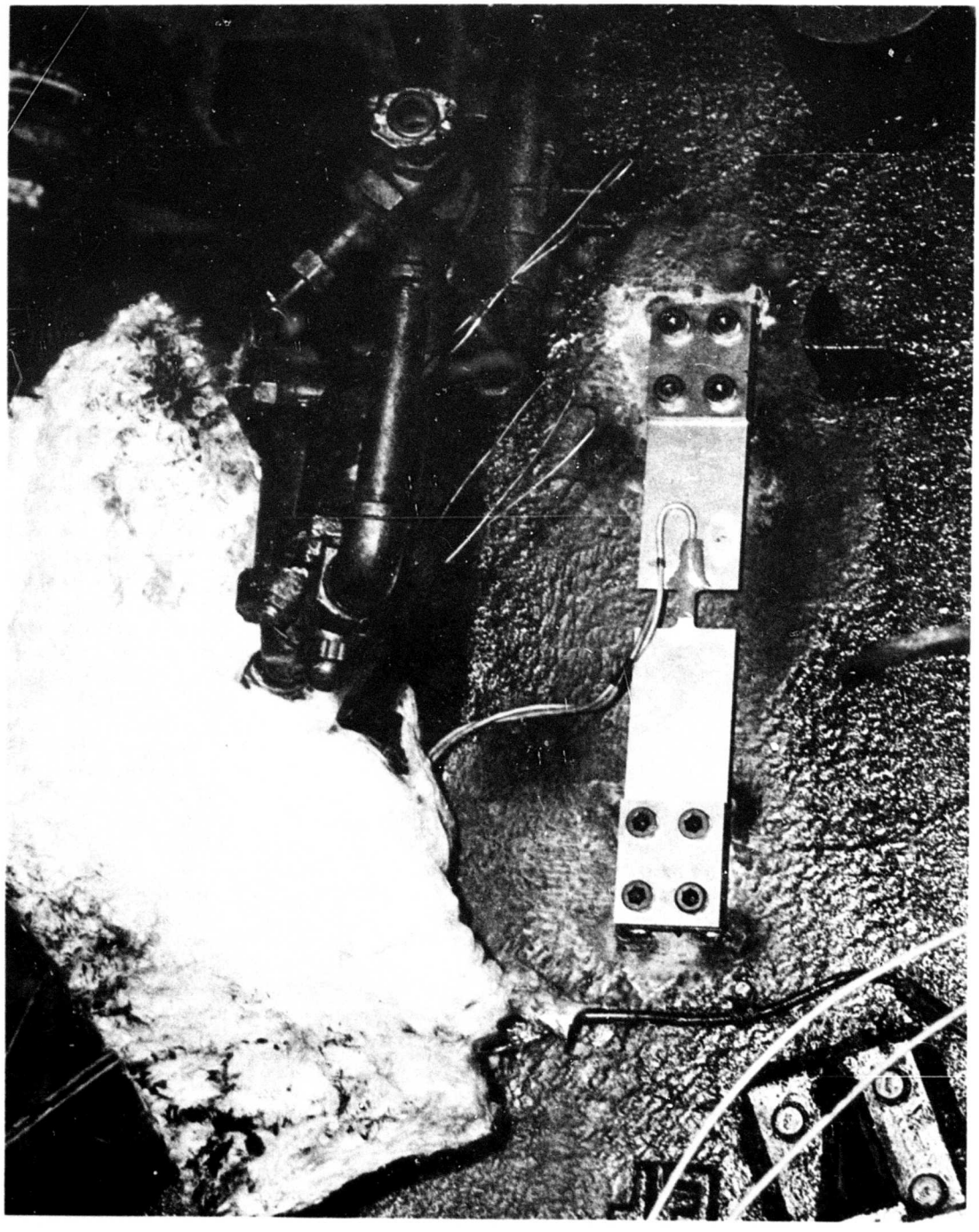

FIGURE 2-5. STRAIN BAR ATTACHED TO PRESS POST ON A PRODUCTION MECHANICAL PRESS

Fiberglass insulation shown at left of photograph was used to cover the strain bars to minimize temperature fluctuations.

strain bar, or pressure transducer) can be directly related to the load. When the Wheatstone bridge is used, application of load will cause the bridge to become unbalanced and result in a small output voltage. Since this output voltage is proportional to the strain in the load transducer and to the load in the press, it is plotted as a function of load and serves as the calibration record, Figure 2-6.

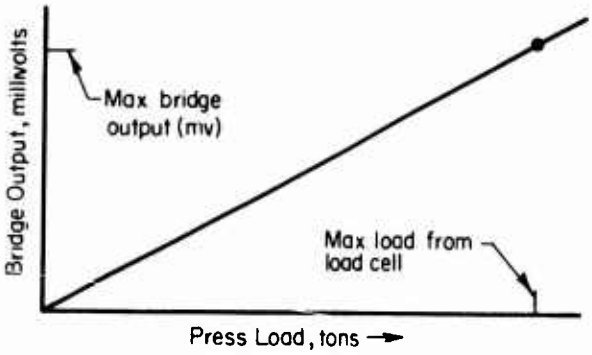

FIGURE 2-6. ILLUSTRATION OF CALIBRATION PLOT WHERE WHEATSTONE BRIDGE OUTPUT DETERMINES PRESS LOAD

The most direct and best approach to calibration is to load the press against a precalibrated load cell and then relate a maximum load to maximum output of the Wheatstone bridge. It is assumed that a linear relationship exists between the output of the transducer and the applied loads. (This linear relationship should be a basic requirement of any load-measurement system used.) Thus, calibration at a single load can be used although it is good practice to verify the linearity of the measuring system by determining the transducer output at a number of loads.

Load cells to about 750 tons are catalog items and can be purchased without difficulty (see Appendix 7-A). When a large press is to be calibrated, it is sometimes possible to place two or more load cells, of the same height, in the press and add the tonnage measured by each of the load cells. This total load will be accurate and can be related to the bridge output voltage to serve as the calibration for the press load transducers.

Special care is required in calibrating mechanical presses in order to prevent the possibility of blocking. A mechanical press has a fixed stroke and cannot be loaded incrementally. Therefore, the calibration, for example of strain bars attached on press frame, is conducted as follows. The load cell is placed upon the lower platen and the ram is brought to its bottom-dead-center (BDC) position. The space between the load cell and the ram is filled with spacers or shims. Before each following stroke, additional shims are placed on the load cell so that the press load is increased gradually from one stroke to the next. Thus, the load is measured after each stroke and the overloading, or blocking, of the press is prevented.

The second technique that can be used for forging-press calibration involves upsetting copper samples of known flow-stress characteristics. Copper was originally selected by German researchers, because of its uniformity and availability for measuring the available energy in forging machines.(6) This technique, further developed at Battelle(1) in Phase I of the present program, was found to be sufficiently accurate. The preferred approach when using this technique is to select copper samples from a lot (preferably from the same bar) that has been cast, worked, and heat treated together. One of the samples can then be upset in a calibrated press equipped with strain bars or a load cell to determine the flow-stress curve for that lot of material. It is usually sufficient to upset the material to about 50 percent. Other pieces of the same lot are then upset together in the forging press to be calibrated. The load used should approach at least half the capacity of the press (this can be controlled by the number of pieces upset simultaneously); however, the reduction should not exceed that obtained on the single sample upset in the calibrated press. Based then on the reduction and on the flow stress curve of the material, it is possible to determine the maximum load and to relate this single value to the maximum output of the load transducers during upsetting. Assuming linearity of transducer output to load, it is now possible to construct the calibration curve, similar to that in Figure 2-6, for the press load measuring system. To verify the linearity it may be desirable to upset specimens to other press loads which will give a second data point at a different load and at different load-transducer output.

MEASUREMENT OF RAM DISPLACEMENT

The three physical effects most commonly used to sense displacement in commercially available displacement transducers are resistance, inductance, and capacitance. Available capacitance devices offer high displacement sensitivity, but they often require somewhat complicated associated instrumentation. Resistance devices have disadvantages in maintaining linearity and must ordinarily rely on a stepping mechanism. Displacement transducers based on inductance seem to offer the best combination of operating characteristics for use in forging applications.

Linear Variable Differential Transformer (LVDT)

The most common displacement transducer based on inductance is the linear variable differential transformer (LVDT).

An LVDT consists of a primary winding and two secondary windings as shown in Figure 2-7. The windings are arranged concentrically over a hollow mandrel which is usually of a nonmagnetic and insulated material. A ferromagnetic sensing core is attached to the transformer shaft and slides freely within the hollow portion of the transducer.[7] The cross-sectional view of a

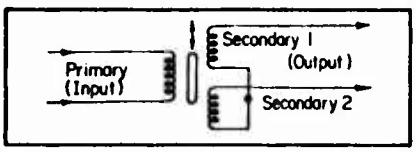

FIGURE 2-7. SCHEMATIC REPRESENTATION OF THE LVDT[1]

typical LVDT is shown in Figure 2-8. When the LVDT is properly energized, the position of the core relative to a null or balance position produces a voltage proportional to the distance from that null position.

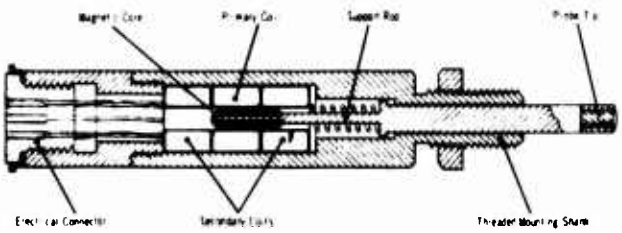

FIGURE 2-8. CROSS-SECTIONAL VIEW OF A TYPICAL SPRING-LOADED LVDT[8]

The LVDT has been found to be a dependable and accurate instrument for monitoring displacement. Its usefulness stems largely from its linear response to displacement and is enhanced by the lack of contact between parts in its function, thereby minimizing deterioration by wear. The single disadvantage of the LVDT is that it is usually limited to relatively short displacement (4-6 inches maximum).

Potentiometric Displacement Transducers

Potentiometric displacement transducers are based on variation of a resistance and usually involve a sliding contact that moves over the resistance element, as shown in Figure 2-9.

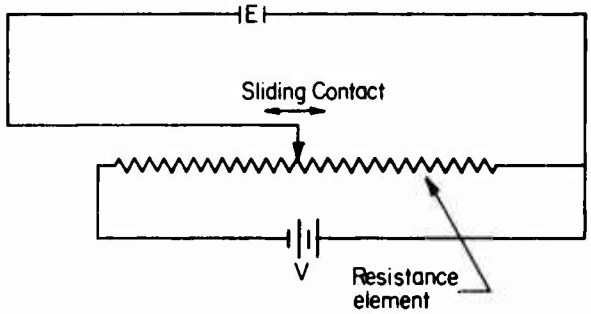

FIGURE 2-9. SCHEMATIC OF THE ELECTRICAL CIRCUITRY OF A RESISTANCE-BASED POTENTIOMETRIC DISPLACEMENT TRANSDUCER

V = Excitation Voltage, E = Output Voltage

The sliding contact is mechanically linked to the moving press platen and thus moves in proportion to the platen displacement. The output voltage is proportional to position of the sliding contact and, when calibrated, can be used to monitor displacement.

Resistance displacement transducers with rotary potentiometers are available for monitoring displacement over a distance of several feet.

High-Speed Photography

Special displacement-measuring techniques such as high-speed photography must be used for forging in high-energy-rate machines and hammers. Displacement transducers that rely on a mechanical link between the moving platen and the transducer are unreliable and easily damaged at high speed and under impact conditions.

Although somewhat more expensive than displacement transducers discussed above, the high-speed camera is simple in principle, and it is accurate in measuring displacement. Normally, the camera is focused to observe the moving press platen when the forging begins. A measuring scale may be placed in the camera view so that the edge of the platen acts as a position marker on the scale. Then, at each frame the advance of the platen can be noted and, since the camera takes a fixed number of frames per second, it is a simple matter to convert the platen advance to a plot of position versus time. This plot will be similar to the record of output obtained from the transducers, and it can be used to determine velocity, contact time, dwell, and other parameters.

Calibration of Displacement Transducers

All of the displacement measuring transducers must be calibrated so that the output of the transducer can be accurately related to displacement. Displacement transducers are usually calibrated each time the monitoring equipment is set up. It is most convenient to relate a fixed displacement at the transducer with a galvanometer deflection, pen or light beam movement, at the monitoring or recording equipment.

A simple example can be used to illustrate the calibration of a displacement transducer. Assume that an LVDT is being used to monitor the platen displacement in a forging press. First, the LVDT should be placed so that the core moves with the upper platen. Care should be taken so that the transducer output is proportional to platen displacement during forging. (Output of an LVDT may not be proportional to core movement when the core moves outside of the linear range for which the LVDT was designed.) If an oscillograph is being used for recording, the galvanometer driven pen, or light beam, should be adjusted so that it registers near the zero on the chart. The core of the LVDT should be moved upward some exact distance, for example, 1 inch. Motion of the oscillograph marker will then occur and the gain on the LVDT signal-conditioning equipment can be adjusted to control the amount of pen or light-beam motion or sweep. It is thus possible to obtain a 1-inch sweep on the oscillograph chart for a 1-inch motion of the transducer core. If greater resolution of the displacement is needed, the gain can be adjusted so that a larger chart displacement is obtained (the ratio of chart sweep to ram displacement may be 5 to 1 or more).

Obtaining a precise 1-inch movement at the displacement transducer can be accomplished in a number of ways. If the zero position is determined with the upper and lower die faces or platen fully in contact, precision-ground 1-inch plates or spacers can be placed between them to obtain an exact 1-inch displacement. It is also possible to obtain mechanical devices which can be used with LVDT's to control precisely the core movement and thus assist in calibration. (7)

MEASUREMENT OF OTHER PROCESS VARIABLES

Velocity

Velocity-measuring transducers are most often of the generator type, in which linear or angular velocity is converted to d-c voltage. A common type linear velocity transducer has a coil in a stainless steel housing and a coaxial cylindrical permanent magnet core attached to a motion-sensing shaft. The magnetic core moves freely within the coil via its attachment to the moving press platen. The voltage output from the coil in this transducer is linear with the velocity of the core. These devices have the disadvantage of a limited linear range.

Velocity can also be determined by differentiating a displacement-versus-time curve with respect to time. This can be done either mechanically or electronically, or by graphically evaluating the displacement-versus-time recording of an oscillograph.

Acceleration

In general, acceleration is measured by a spring mass system with the spring fixed to the case of the instrument which is, in turn, attached to the structure whose acceleration is to be measured. For forging processes, it is usually adequate to calculate the acceleration by double differentiation of displacement with respect to time.

Energy

It is important to determine the energy consumed in a forging process since proper use of forging equipment is based in part on the ability of equipment to deliver the necessary energy. The determination is also useful since a comparison of energy consumed by the process and energy lost by the forging press will reveal the efficiency of that particular forging press.

Consumption of energy by a forging process cannot be measured directly. It is usually determined by making a plot of load and displacement, similar to that shown in Figure 2-1, and then calculating the area within the curve. This area in terms of foot-pounds, will be an accurate representation of the energy consumed by the forging process.

The energy lost by the forging press must also be calculated. For mechanical presses, this energy is usually determined on the basis of loss of velocity of the flywheel. Prior to forging, the flywheel of the press is turning at a constant angular velocity and its velocity and inertia determine the amount of energy stored by the flywheel. Upon completion of the forging operation, the flywheel velocity and the residual energy in the flywheel will have been reduced. The difference between the initial stored energy and the residual energy after the forging operation is the energy consumed (a) to carry out the forging process and (b) to overcome friction and inertia

losses in the machine. These energy characteristics of various forging machines have been extensively reviewed in Phase I of this program. (1)

RECORDING INSTRUMENTS

The instrumentation for measuring and recording forging parameters must be properly suited to the work being conducted. It should be able to reproduce the output signal of the particular transducer as accurately as is needed within the limitations of the transducer. The first criterion in selecting the type of voltage-measuring instrumentation is adequate frequency response. Forging, because it is a dynamic operation, cannot make use of null-balance type of measuring equipment. It is, thus, necessary to use galvanometer-based oscillographs. In this category, the two general classes of recording instruments are the galvanometer-driven pen oscillograph and the light-beam oscillograph in which a galvanometer-driven mirror reflects a light beam onto light sensitive paper (Figure 2-10).

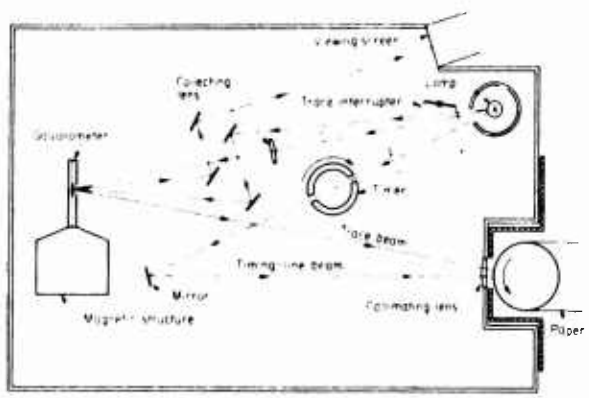

FIGURE 2-10. SCHEMATIC OF THE LIGHT-BEAM OSCILLOGRAPH

The pen recorder is limited to a frequency of about 40 Hz because of the relatively large mass of the pen that must be driven by a galvanometer. The light-beam oscillograph can be used to a frequency of 2000 Hz since the galvanometer must drive only a mirror whose mass can be quite small.

The selection of a recording instrument can depend on a number of factors. As mentioned above, the frequency response of the two instruments varies considerably and for events which cannot be adequately captured at 40 Hz (where a significant development may occur within a time space of 0.025 second), it will be necessary to use the faster light-beam oscillograph. Unlike the pen recorder, the light-beam recorder uses the full width of the chart for all channels. Thus greater resolution of the recorded data is usually possible with the light-beam oscillograph. Figure 2-10 illustrates schematically the operating principle of the light-beam oscillograph.

SUMMARY

Determination of process variables is necessary for efficient use of forging equipment and improvement of an existing forging process. The most important variables are the load and energy required by the forging process, and it is imperative that the forging press deliver adequate load and energy to carry out the process. Efficient use of forging equipment is based on maximum utilization of its capabilities without exceeding its design limits.

Usually, measurement of load and displacement is adequate for determination of the process variables. Displacement can be monitored using either a potentiometric displacement transducer or a linear variable differential transformer (LVDT). The LVDT seems to offer the best combination of operating characteristics for most press-forging operations. In hammer or in high-energy-rate forging, high-speed photography is the most practical method of measuring displacement. Load is most conveniently measured by using strain bars that detect press-frame deflections when attached to the press columns.

Devices are available for monitoring ram velocity. However, it is usually adequate to differentiate the displacement with respect to time. Similarly, acceleration can also be determined by the double differentiation of displacement with respect to time.

Next to load, energy is the most important process variable in forging and it cannot be directly measured. It is usually determined from the area under load-versus-displacement plot obtained from a forging experiment.

In order to facilitate the purchase and the use of forging press instrumentation, a partial list of instrumentation suppliers is given in Appendix 2A, while typical forging instrumentation is described, as an example, in Appendix 2B.

REFERENCES

(1) Altan, T., et al, "A Study of the Mechanics of Closed-Die Forging", Final Report, Chapters 1, 5, and 8, D/A Project 6331, Contract DAAG46-68-C-0111, AMMRC, Watertown, Massachusetts (1970), AD711-599.

(2) Chapin, W. E., and Mitchell, R. K., "A Summary of Force-Transducer Technology: Measurement Techniques Calibration, Element Design, Availability, and Research Activity", TIC Summary Report No. 2, April, 1966.

(3) Norton, H. N., Handbook of Transducers for Electronic Measuring Systems, Prentice-Hall, Inc., Englewood Cliffs, New Jersey (1969).

(4) Jain, S. C., and Bramley, A. N., "Characteristics of the High-Speed Hot Forging Process", Proceedings of the 9th International MTDR Conference, University of Birmingham, England, Part I (1968), p. 95.

(5) Slater, R.A.C., Johnson, W., and Aku, S. T., "Fast Upsetting of Short Circular Cylinders of Plain Medium Carbon (0.55% C) Steel at Room Temperature", Proceedings of the 9th International MTDR Conference.

(6) Waterman, D., "Determination of the Energy of Hammers and Presses With Copper Cylinders" (in German), Werkstatttechnik, 52 (2), 1962, pp. 95-102.

(7) Schaevitz Engineering Technical Bulletin AA-1b.

(8) Daytronic Corporation Catalog 70-D.

(9) ISA Transducer Compendium, Glenn F. Harvey, Editor, Second Edition, Part 2, Instrument Society of America, Pittsburgh (1970).

(10) Jain, S. C., and Amini, E., "Development of a Short Load Cell for Metal-Forming Application", Proceedings of the 11th International MTDR Conference, University of Birmingham, England, (1970), p. 229.

APPENDIX 2A

INSTRUMENT AND TRANSDUCER MANUFACTURERS

This appendix includes a partial list of manufacturers of the various transducers and instruments discussed in this report. The list is by no means complete and it should not be considered a list of recommended manufacturers. It is merely offered in hopes that it will assist in purchasing monitoring instrumentation. A more complete listing of transducers, their specifications and manufacturers is contained in the ISA Transducer Compendium.(9)

Load Cells (250 tons and larger)

Transducers Inc.
11971 East Rivera Road
Santa Fe Springs, California 90670

Morehouse Instrument Company
1742 Sixth Avenue
York, Pennsylaniva 17403

Lebow Associates, Inc.
1728 Mapletown Road
Troy, Michigan 48084

Asea Electric, Inc.
400 W. Madison Street
Chicago, Illinois 60606

GSE Incorporated
30675 West Eight Mile Road
Livonia, Michigan 48152

Strain Bars

GSE Incorporated
30675 West Eight Mile Road
Livonia, Michigan 48152

LeBow Associates, Inc.
1728 Mapletown Road
Troy, Michigan 48084

Displacement Transducers (LVDT)

Daytronic Corporation
2875 Culver Avenue
Dayton, Ohio 45429

Schaevitz Engineering
U. S. Route 130 and Union Avenue
Pennsauken, New Jersey

Hewlett-Packard
Waltham Division
175 Wyman Street
Waltham, Massachusetts 02154

Transducer Technology, Inc.
74 Eastern Boulevard
Glastonbury, Connecticut 06033

G. L. Collins Corporation
5875 Obispo Avenue
Long Beach, California 90805

Displacement Transducers (Potentiometric)

Bourns, Inc.
6135 Magnolia Avenue
Riverside, California 92506

Computer Instruments Corporation
92 Madison Avenue
Hempstead, L. I., New York 11550

Servonic Instruments
Division of Gulton Industries
1644 Whittier Avenue
Costa Mesa, California

Research, Inc.
P. O. Box 6164
Minneapolis, Minnesota

Recorders and Signal Conditioning Equipment

Brush Instruments Division
Gould Inc.
3631 Perkins Avenue
Cleveland, Ohio 44114

Century Electronics and Instruments, Inc.
6540 East Apache Street
Tulsa, Oklahoma 74115

Hewlett-Packard
Waltham Division
175 Wyman Street
Waltham, Massachusetts 02154

BLH Electronics, Inc.
42 Fourth Avenue
Waltham, Massachusetts 02154

Honeywell, Inc.
2701 4th Avenue South
Minneapolis, Minnesota 55408

APPENDIX 2B

TYPICAL FORGING INSTRUMENTATION

Figure 2B-1 shows the block diagram of an instrumentation setup used on a forging press. Most important is the load-monitoring strain bridge which, in many cases, may be the only instrumentation necessary. The other instrumentation shown may be added as required.

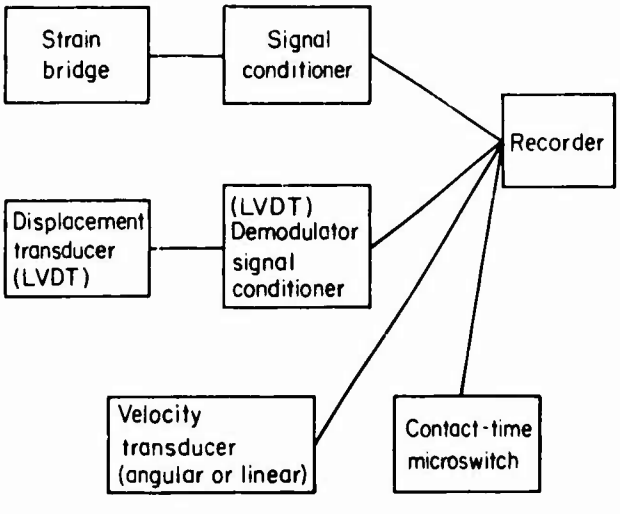

FIGURE 2B-1. BLOCK DIAGRAM OF AN INSTRUMENTATION SETUP

Below is a discussion of each of the blocks for a more complete understanding of the instrumentation arrangement.

Strain Bridge - Regardless of the load transducer used it will very likely be constructed using strain gages in either a half- or full-Wheatstone-bridge arrangement.

Signal Conditioning - Assuming that a full- or half-bridge arrangement exists in the load transducer, the signal conditioning equipment will excite the bridge and amplify the bridge output for the recorder. When a peak meter is used, the excitation, amplification and the meter may be contained in the same instrument.

Displacement Transducer - Signal conditioning for the displacement transducer will vary depending on the type of transducer. When a LVDT is used, it is necessary to excite it with 2-10 volts ac at 60 to 10,000 cps. The output of the LVDT usually must be demodulated and amplified for recording. Again the excitation and demodulation is usually carried out in a single instrument designed for this purpose.

Angular Velocity - Most velocity devices are of the self-generating type and, thus, do not require excitation. The velocity transducers usually generate a d-c voltage that is proportional to the velocity and may be used as direct input to the recorder.

Contact Time - Contact time can be easily determined using a microswitch. The switch

should be placed so that fine adjustment can be made in its position and contact time can be determined accurately. Almost any excitation can be used including d-c dry-cell batteries. The excitation should be large enough to drive the recording galvanometer to an easily read deflection.

Interpretation of Recorded Data

Figure 2B-2 illustrates, in an abbreviated form, a possible tracing from a light-beam oscillograph obtained using instrumentation on a mechanical press. Recorded on the oscillograph are flywheel velocity, displacement, load and die-contact time. Also on Figure 2B-2 several significant events are noted. The significance of these events is discussed below.

Prior to t_1 the reference position for flywheel velocity and load are recorded. These positions represent maximum flywheel velocity and zero load and, at later positions on the chart, the flywheel velocity and load can be determined as a function of distance from this reference position.

At t_1 the downstroke of the ram begins and some energy is lost from the flywheel due to inertia and friction in the press. From t_1 to t_2 the energy losses are rather modest since the actual forging has not begun.

From t_2 to t_3 the forging is completed as indicated by the rapidly increasing load that peaks at t_3. Flywheel velocity continues to decrease through this time period indicating that energy is being lost to the forging process. The bottom-dead-center (BDC) position of the ram is reached at t_3 (as illustrated by the displacement tracing and by the peak load).

Energy continues to be lost from the flywheel until the t_4 position is reached. This is well after the BDC position and after the completion of the forging. The extra energy loss results from the effect of the inertia of the flywheel, and of the heavy ram which was in the down position and had to be accelerated upward. Recovery of the flywheel to its original speed and energy begins at t_4 and is completed at t_5.

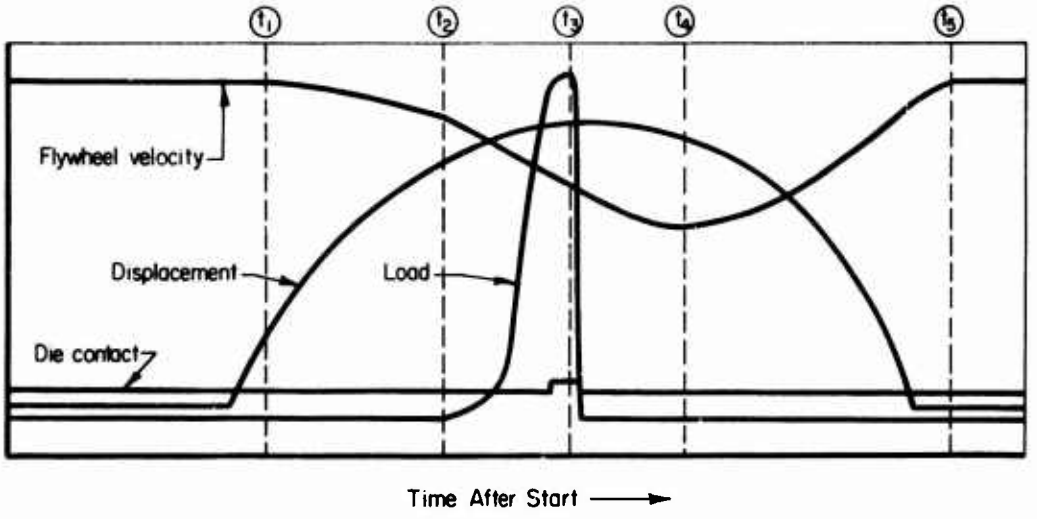

FIGURE 2B-2. TYPICAL LIGHT-BEAM OSCILLOGRAPH RECORDING

Note: t_1 - Beginning of ram downstroke
t_2 - Contact of upper die with forging-forging start
t_3 - Bottom dead center (BDC) - forging completed
t_4 - Lowest flywheel velocity
t_5 - Return of flywheel to normal velocity-energy restored.

APPENDIX 2C

DESIGN AND CALIBRATION OF A 3000-TON LOAD CELL

Some of the work in this program was to be conducted in production forging presses in the plants of forging manufacturers. Since, in this work, the measurements of loads and displacements were required, it was necessary to attach transducers to the press to monitor these parameters. Prior to use, the load transducers must be calibrated so that the electrical output of the transducers can be related to forging load. This calibration can be most effectively accomplished by loading the press against a load cell whose electrical output-load relationship is known.

Load cells in the sizes required for this purpose are not generally available. It was also determined, after contacting several manufacturers, that a large load cell might be purchased on a special-order basis but that the cost would be prohibitive. It was then decided to design and build a load cell at Battelle which would be adequate for forging press calibration required in this program.

Design

Most load-sensing devices employ electrical strain gages whose resistance changes when strained. When the gages are connected in a Wheatstone bridge arrangement and properly energized, the change in resistance is reflected in a voltage output from the initially balanced bridge. The voltage output is proportional to the strain in the strain gages and to the stress in the member to which the gage is attached. Since the output is proportional to the stress in the loaded member, it is also proportional to the load, and the device can be calibrated so that output is read directly as load.

The load cell built in this program was to be used in a number of presses, including those having small shut heights. Therefore, it was decided to construct a load cell with a minimum possible height. However, low-profile load cells are undesirable since they normally do not have a linear electrical response with load. One investigator,[10] who also desired to build a minimum-height load cell, showed that a ring configuration was more suitable than a solid disk for minimizing the nonlinearity effects. It was on this basis that it was decided to build the load cell shown in Figure 2C-1.

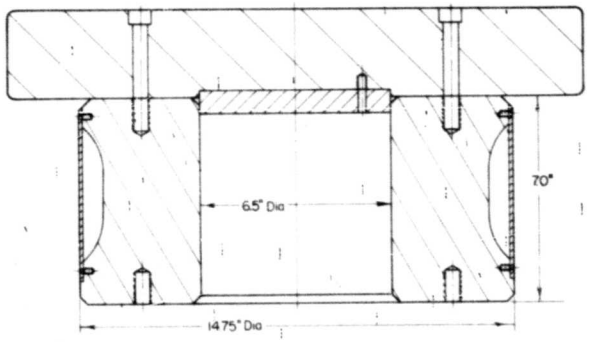

FIGURE 2C-1. SCHEMATIC OF THE LOAD CELL DESIGNED AND BUILT IN THIS PROGRAM

Forged AISI 4340 steel rings were used for the load cell. This material was heat treated to a hardness of R_C 38-40 so that relatively high stress levels could be used and the weight of the cell would be minimized. At this hardness level, the material has a yield strength of about 150,000 to 160,000 psi; it can be used at the design stress of 60,000 psi (for 3000 tons) and still have a safe overload capacity of 100 percent. (A material with a yield strength of 150,000 psi will actually begin to deform slightly at a stress somewhat below the yield strength. However, it is not expected that the stress at which distortion begins, proof stress, will be below 120,000 psi.

End plates were designed so that the end load could be distributed over a larger area. Thus, the load cell could be used on mild-steel press platens and the maximum compressive stress would be about 20,000 psi. To minimize the possibility of eccentric loading, the load cell and the end plates were manufactured with close tolerances to maintain the parallelity of the top and bottom surfaces.

Strain gages were placed at eight locations around the outside surface of the ring-shaped load cell. The gages were wired such that the total output of the load cell represent an average value of the individual outputs registered at the eight different locations. Thus, the measured stress would be an average of the stresses at all of the eight locations and the effects of nonsymmetric loading would be minimized. Two strain gages were mounted at each location; one gage to measure the compressive strain and the other to compensate for temperature changes and Poisson's effect.

As shown in Figure 2C-2, two Wheatstone bridges were wired from the gages attached to the load cell. The arms of each bridge were made up of two strain gages connected in series. The two bridges were connected in parallel; thus, with 350-ohm strain gages, a nominal resistance of 350 ohms was obtained across each arm of the completed bridge.

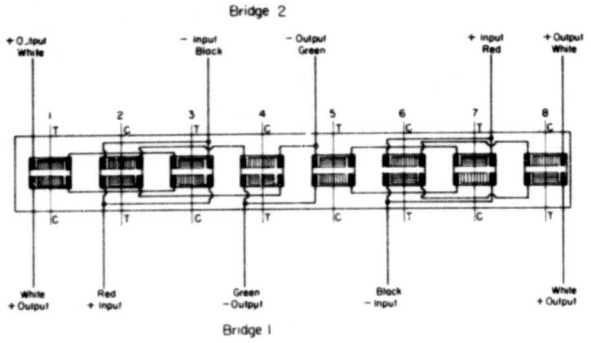

FIGURE 2C-2. SCHEMATIC OF THE STRAIN-GAGE LAYOUT ON THE 3000-TON LOAD CELL DESIGNED AND BUILT IN THIS PROGRAM

Bridges 1 and 2 are wired in parallel to complete the electrical design.

Calibration

The load cell was calibrated in the 12-million-pound testing machine of The National Bureau of Standards. This machine is hydraulically operated and the accuracy of the applied loads is within 0.5 percent.

Prior to the actual calibration, the load cell was loaded several times to a tonnage about 10 percent greater than its design limit. The purpose of this overloading was to insure that the top and bottom plates of the load cell were well seated and to strain the gages beyond the maximum that they would be subject to in service. Thus, it could be expected that, having been loaded to this high level, the output of the load cell should be consistent from one trial to another.

To calibrate, the resistive unbalance in the strain gage bridge was measured as the ratio of the d-c output voltage to the input voltage. The ratio measurements were made with Gilmore Millivolt per Volt Indicator No. 4751. The uncertainty attributed to the Gilmore instrument was estimated to be less than 0.001 millivolt per volt.

The load cell was loaded several times to its 6,000,000-pound capacity. The first loading was done to exercise the load cell and to verify the bridge output under no load. Then the load cell was carefully loaded and output measurements were recorded at 400,000-pound increments. Thus, 15 data points were obtained during each of the two calibration runs. After the second calibration run, the load cell was again cycled to various loads and data recorded. A plot of representative data obtained in this calibration is shown in Figure 2C-3.

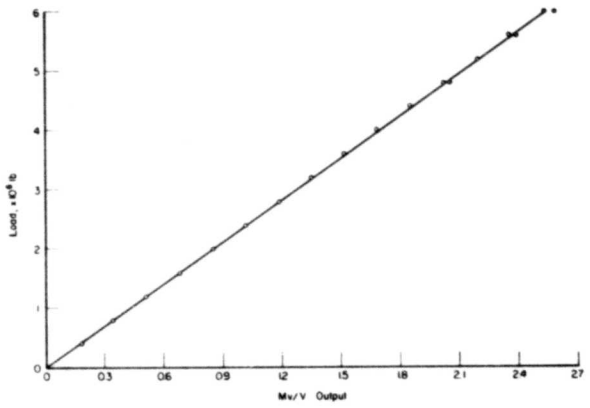

FIGURE 2C-3. REPRESENTATIVE CALIBRATION DATA OBTAINED AT THE NATIONAL BUREAU OF STANDARDS

When setting up instrumentation for use with a load cell, it is helpful to be able to artificially induce an output of the load cell for a specific load. This is easily done by shunting a resistance across an arm of the bridge containing the compensating strain gages. The output from the bridge will vary inversely with the size of the resistance, and it is possible to determine a calibration shunt for a specific load. A decade box was used as the resistance shunt and the bridge output monitored on a millivolt per volt meter. The decade box was adjusted until the output from the cell corresponded to that for a specific load. The shunt resistance that simulated the output at 6,000,000 pounds load was determined to be 34,700 ohm.

Since the shunt resistance will vary inversely with the load, it can be determined for any load by using a simple linear relationship. Here, the relationship would be as follows:

$$R_{SH} = \frac{(6,000,000)(34,700)}{L} = \frac{2.08 \times 10^{11}}{L},$$

where R_{SH} = Shunt resistance for a given load L

L = Load in pounds.

CHAPTER 3

MECHANICAL PRESSES AND SCREW PRESSES FOR CLOSED-DIE FORGING: DESIGNS, APPLICATIONS, AND COMPARISONS

by

T. Altan, J. R. Douglas, and R. J. Fiorentino

TABLE OF CONTENTS

MECHANICAL PRESSES AND SCREW PRESSES FOR CLOSED-DIE FORGING: DESIGNS, APPLICATIONS, AND COMPARISONS

by

T. Altan, J. R. Douglas, and R. J. Fiorentino

ABSTRACT

The design and the kinematics of mechanical and screw presses are drastically different. The application of each type of press for a specific forging operation and its optimum use requires a thorough understanding of the equipment characteristics. This report reviews the various types of screw and mechanical presses, the maximum available capacities, and the new developments in design. The characteristics of both types of presses are compared in terms of load and energy, time dependent parameters, and forging tolerances. This discussion indicates that each type of machine has its specific optimum field of application depending on the type, dimensions, production volume, and material of the parts forged.

INTRODUCTION

The mechanical press with crank or eccentric drive has proved to be an efficient and versatile machine and, next to hammers, is the most widely used equipment for closed-die forging in the United States. The screw (or percussion) press is used in this country for forging and coining by only a few companies. In the European forging industry, screw presses are more widely known and their application in closed-die forging of ferrous and nonferrous alloys is increasing steadily. In some shops, the screw press is replacing hammers[1] and in others it competes strongly with mechanical presses. A statistical survey made in 1960 in W-Germany showed that, in forge shops with a monthly production larger than 1000 metric ton (1,120 U. S. ton), the screw press was, after the hammer, the most common machine and represented 12.5 percent of all machinery used in a forge shop.[2] While no major suppliers of screw presses are in the U. S., approximately a dozen companies are manufacturing screw presses in Europe.

The capabilities and the applications of mechanical presses, hammers, and upsetters are well known in the U. S., but we have relatively little experience and practical information on screw presses. Plans for new investment, modernization, and automation in forging industry require a thorough knowledge and consideration of the technical and economic aspects of all types of equipment. It is, therefore, useful and timely to discuss the characteristics and the use of screw and mechanical presses. For this purpose the basic principles of both forging machines are considered with respect to hot-closed-die forging. It should be noted, however, that both machines are also used for cold forging and coining operations.

THE MECHANICAL PRESS

The drive of most mechanical presses (crank or eccentric) is based on the slider-crank mechanism which translates rotary into reciprocating linear motion. The eccentric shaft is connected through a clutch and brake system directly to the flywheel. In designs for larger capacities the flywheel is located on the pinion shaft which drives the eccentric shaft. The constant clutch torque (M) is available at the eccentric shaft which transmits the torque and the flywheel energy to the slide through the pitman arm, or the connecting rod, as illustrated in Figure 3-1. The flywheel stores energy that is used only during a small portion of the crank revolution, namely during deformation.

Recent developments in mechanical-press design indicates a strong emphasis on (a) large capacities, (b) increased forging accuracy under on- and off-center conditions, and (c) high forging speed, not necessarily in terms of production rate but rather in terms of contact time and its effects on die wear.

A new type mechanical press, the wedge-type press, is claimed to reduce tilting under off-center loading in both directions (front to back and left to right) and to offer increased overall stiffness. The principle of the wedge-type press is shown in Figure 3-2. In this press, the load acting upon the ram is supported by the wedge wnich is driven by a two-point crank mechanism. This design greatly reduces the deflection of the drive mechanism (to about 1/4 of a single-point drive) so that the total deflection of the press is only about 60 percent of a one-point eccentric press.[3] The eccentric

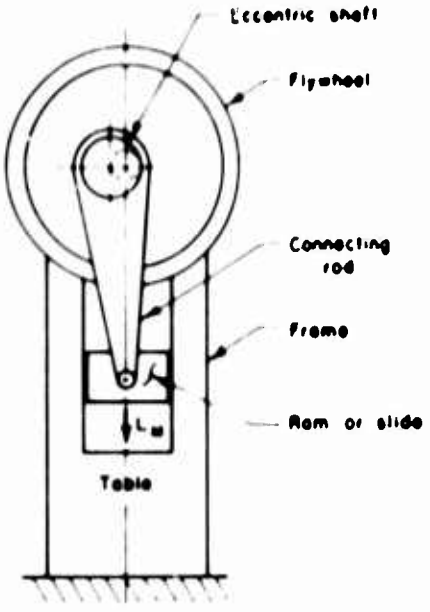

FIGURE 3-1 SCHEMATIC OF A MECHANICAL FORGING PRESS WITH ECCENTRIC DRIVE

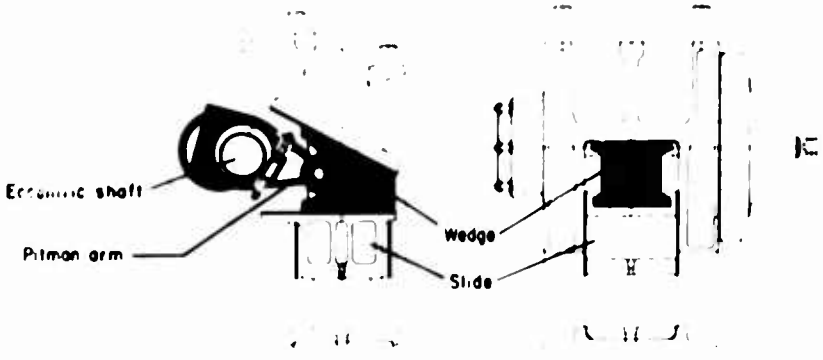

FIGURE 3-2 PRINCIPLE OF THE WEDGE-TYPE MECHANICAL PRESS[3]

mechanism driving the wedge includes an eccentric bushing that can be rotated through a worm gear. Thus, the shut height, or the forging thickness, can be adjusted by using this mechanism instead of the more commonly used wedge adjustment at the press bed. More than 50 forging presses of this type are operating; the largest, with 8000-ton capacity, is in a West German forge plant.

In conventional mechanical forging presses the eccentric shaft is located from left to right of the press. (This is not so for some sheet metal and trimming presses.) A novel forging press design locates the eccentric shaft front to back and offers the following principal advantages:[4] (a) the shaft is shorter and deflects less, (b) during off-center forging both eccentric shaft bearings, being located in front and back, are loaded evenly, (c) the ram guides are built in one piece and they are longer than in a conventional design, Figure 3-3, (d) the pitman is connected to the ram through an eccentric pin. By slight swivelling of the eccentric pin, the ram-to-bolster distance can be finely adjusted without modifying the lateral positioning of the dies. The eccentric pin can also be rotated hydraulically and can be used to free the press if it is overloaded and blocked.

The scotch-yoke type design represents a well-established and proven drive mechanism for forging presses. In this design, illustrated in Figure 3-4, the ram contains top and bottom eccentric blocks that contain the eccentric shaft. As the shaft rotates, the eccentric blocks move both horizontally and vertically and the ram is actuated by the eccentric blocks only vertically.[5] This design compares very favorably with that for the wedge-type press drive and offers rigid guiding and good off-center loading capacity.

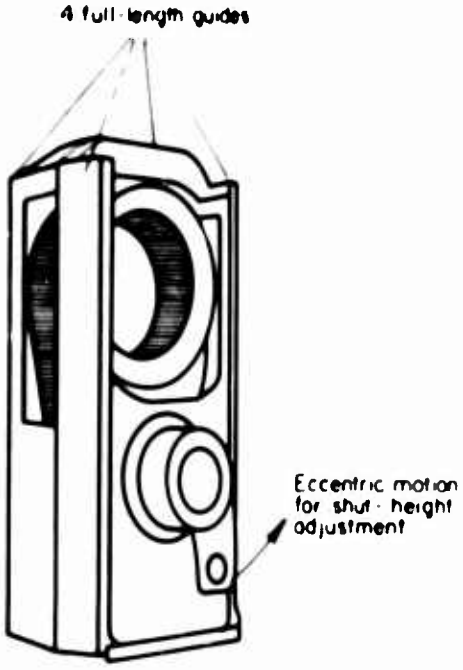

FIGURE 3-3 RAM-PITMAN ASSEMBLY AND SHUT-HEIGHT ADJUSTMENT IN A MECHANICAL PRESS WITH FRONT-TO-BACK ECCENTRIC SHAFT[4]

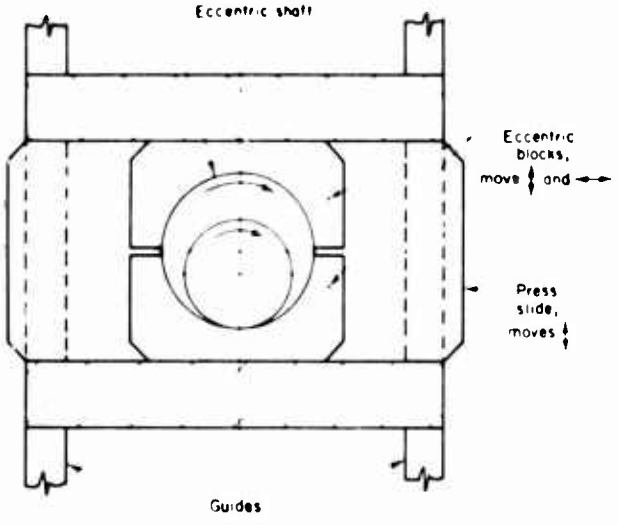

FIGURE 3-4 PRINCIPLE OF THE SCOTCH-YOKE TYPE DRIVE FOR MECHANICAL PRESSES[5]

The trend in increased capacity requirements is reflected in the presses built in the past few years. Recently the largest mechanical presses available in the U. S. were the three 8000-ton Maxipresses built by National Machinery. An 11,000-ton Maxipress, based on National's design and built by Sumitomo in Japan for forging large crankshafts (Figure 3-5), went into operation late in 1971. The first 8,000-ton wedge press, built by Eumuco of West Germany, went into operation during 1970. The world's largest mechanical press with 12,000 ton capacity will have a scotch-yoke design, Figure 3-6. It was built by Erie Foundry for installation at TRW in Cleveland during 1972.

THE SCREW PRESS

The screw press, used for various types of forging and coining operations, offers distinct advantages in some processes such as precision forging of gears and air foils. In the past few years a large number of screw presses of modern design have been installed in Europe, Japan, and in the Soviet Union. Various U. S. companies are also showing interest in these forging machines.

Principles of Screw Press Design

The screw press uses friction, gear, electric, or hydraulic drives to accelerate the flywheel and the screw assembly and it converts the angular kinetic energy into the linear energy of the ram. Figure 3-7 shows three basic designs of screw presses.[6,7] In the friction-drive press, the driving disks are mounted on a horizontal shaft and are rotated continuously. For a downstroke, one of the driving disks is pressed against the flywheel by a servomotor. The flywheel, which is connected to the screw either positively or by a friction slip clutch, is accelerated by this driving disk through friction. The flywheel energy and the slide speed continue to increase until the slide hits the workpiece. Thus, the load necessary for forging is built up and transmitted through the slide, the screw, and the bed to the press frame. When the entire energy in the flywheel is used in deforming the workpiece and elastically deflecting the press, the flywheel, the screw, and the slide stop. At this moment, the servomotor activates the horizontal shaft and presses the upstroke driving disk wheel against the flywheel. Thus, the flywheel and the screw are accelerated in the reverse direction and the slide is lifted to its top position. In the direct electric drive press, a reversible electric motor is built directly on the screw and on the frame, above the flywheel. The screw is threaded into the ram and does not move vertically. To change the direction of flywheel rotation, the electric motor is reversed after each downstroke and upstroke. The gear drive with slip clutch is a variation of the direct electric drive used in large capacity presses.[7] The flywheel is in two parts; the smaller inner wheel is connected positively to the screw shaft. The outer ring, in which the larger portion of the energy is stored, is

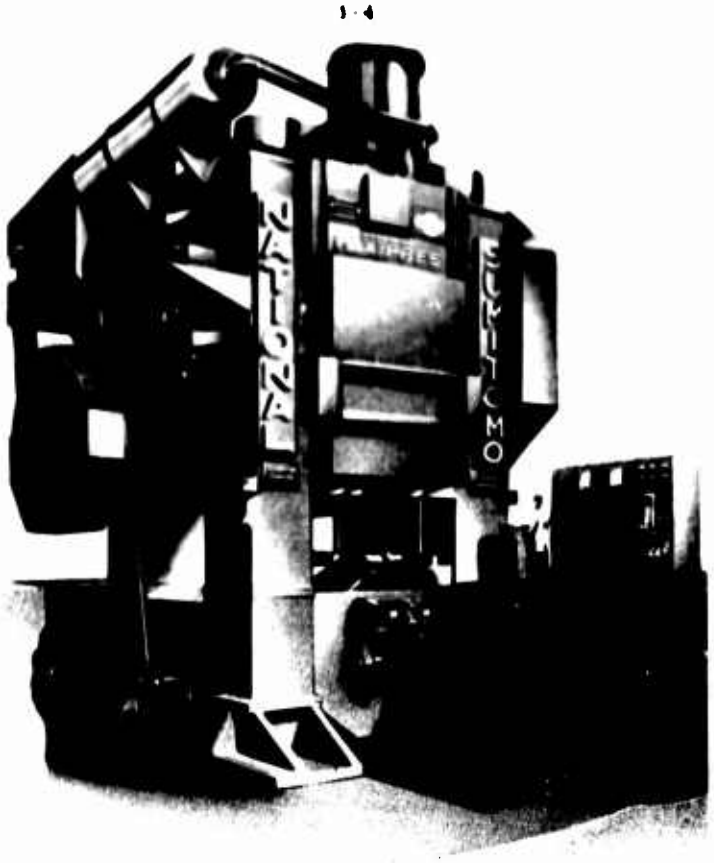

FIGURE 3-5. ARTIST'S CONCEPTION OF THE 11,000-TON PITMAN TYPE MAXIPRESS BUILT BY SUMITOMO OF JAPAN ACCORDING TO NATIONAL MACHINERY'S DESIGN (COURTESY OF NATIONAL MACHINERY)

connected to the inner flywheel by a slipping clutch. Thus, the total torque is limited and, during operation, the drive gears and the screw are protected from overloading.

New Developments, Capacities, and Applications

While there is no U. S. manufacturer of modern screw presses, a number of suppliers in Europe are developing various drives and designs of screw presses in all capacities. The emphasis appears to be on (a) improving the overall efficiency of the press drive, (b) electronic energy metering for successive blows, and (c) manufacturing larger capacity presses.

The conventional friction drive, Figure 3-7a, results in considerable friction slip losses and wear at start of up and downstrokes. The more-modern electric drives that use reversing electric motors, require a large amount of electric power to overcome the extensive losses associated with the reversing of the motors.[8] Thus, several new designs based on hydraulic drives have been developed. The hydraulic screw press drive seen in Figure 3-8 has proved itself for several years under various forging conditions.[9] The drive is placed on top of press frame. Pressure from the hydraulic accumulator pushes the axial screw downward and starts its rotation. The rotary motion is transmitted through a coupling to the flywheel and to the main screw without any axial loading. Figure 3-9 illustrates a screw press with underfloor drive and 4,400-ton nominal capacity.[9] In this design, the flywheel remains axially stationary and it is driven by several hydraulic motors through gear drives. This design lends itself for further development to obtain larger capacities.

The principle of another hydraulic drive is illustrated in Figure 3-10.[10] The ram is moved up and down through a relatively low capacity hydraulic cylinder placed on top of the press frame. The vertical motion of the ram rotates the flywheel through the screw and nut. The kinetic energy which is thus built up in the flywheel is then transmitted through the screw and ram to the deforming material. Essentially the same drive principle is used in the double-screw press illustrated in Figure 3-11. In this design, two screws are mechanically synchronized through the gears on the flywheel. Hydraulic cylinders on either side of the press, as shown in

FIGURE 3-6. ARTIST'S CONCEPTION OF THE 12,000-TON SCOTCH-YOKE MECHANICAL FORGING PRESS (COURTESY ERIE FOUNDRY)

Figure 11, actuate the slide vertically. This motion rotates the flywheels and, thus, generates the kinetic energy. Being essentially a true two-point design, this press is capable of sustaining large off-center loads.(11)

A large hydraulically driven screw press, with 3500-ton nominal (7,000 ton maximum) capacity built by Hasenclever of West Germany, was installed in 1971 at Steel Improvement and Forge Company, in Cleveland. The world's largest screw press is being built by Weingarten of West Germany for Westinghouse Electric Corporation. This press, illustrated in Figure 3-12, will use the drive system seen in Figure 3-7c with four reversing electric motors. The press, with the nominal capacity of 8,000 ton (maximum 16,000 tons), will be installed during 1972.

EVALUATION OF LOAD AND ENERGY CHARACTERISTICS

From the description of the basic kinematics of screw and mechanical presses it is seen that the manner of supplying load and energy to the forging process is significantly different in the machine types. Therefore, it is necessary to discuss equipment characteristics affecting the forging process with respect to the design of each machine.

The following conditions must be satisfied in order to carry out a forging process:

$$L_M \geq L_p \text{ at any time during a stroke} \quad (3\text{-}1)$$

$$E_M \geq E_p \text{ for an entire forging stroke.} \quad (3\text{-}2)$$

Equation (3-1) states that the load available from the machine (L_M) at any stroke position must be larger than the load (L_p) required by the forging process. Equation (3-2) states that the available energy (E_M) during a stroke must be larger than the energy (E_p) required by the forging process.

Mechanical Press

In a mechanical press the constant torque (M) at the eccentric shaft is transformed to the slide load (L_M) through a slider-crank mechanism as seen in Figure 3-13. The symbols defined in the force diagram of the slider-crank mechanism (Figure 3-13) can be used to show that the slide

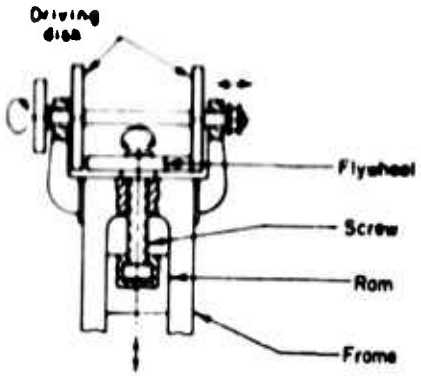

(a) Friction Drive

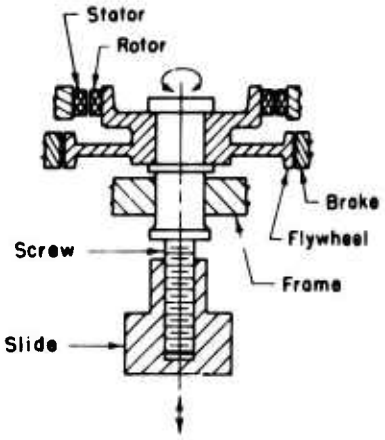

(b) Direct Electric Drive

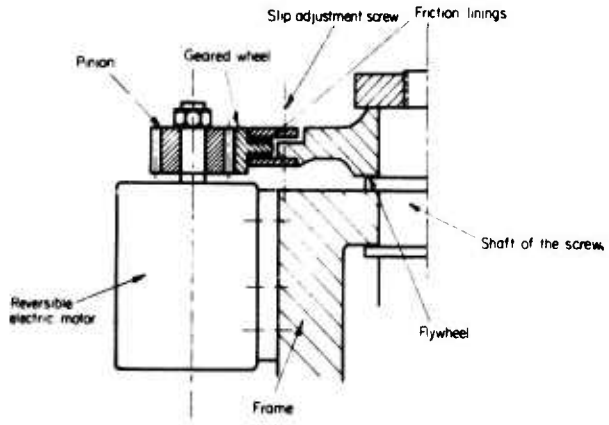

(c) Gear Drive With Slipping Clutch

FIGURE 3-7. SCREW PRESS DRIVES[6, 7]

load (L_M) can be approximately expressed in the following form:

$$L_M = \frac{2\,M}{S \sin \alpha} \quad . \qquad (3\text{-}3)$$

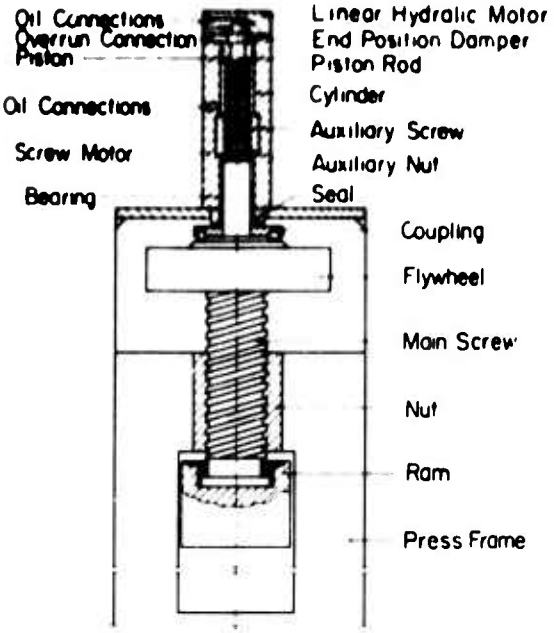

FIGURE 3-8. HYDRAULIC SCREW-PRESS DRIVE PLACED ON TOP OF PRESS FRAME[9]

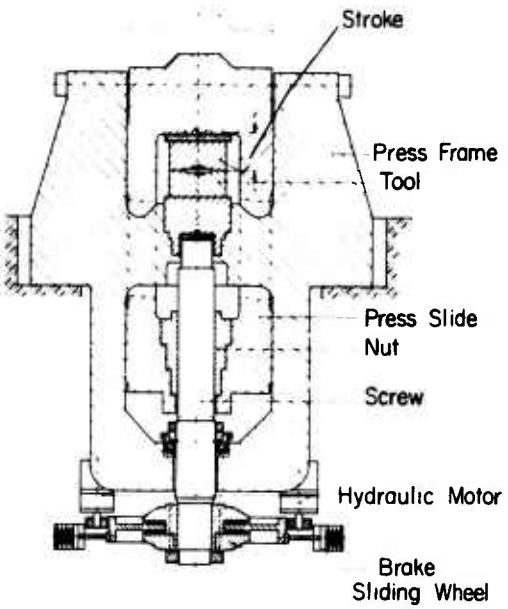

FIGURE 3-9. HYDRAULIC SCREW PRESS WITH UNDERFLOOR DRIVE[9]

Equation (3-3) illustrates the variation of the slide load (L_M) with the crank angle (α) before bottom dead center, BDC, for given torque (M) and stroke (S) of the press. The torque (M) at the clutch has a constant value for which the drive mechanism (i.e., eccentric shaft, pinion gear, clutch, brake, etc.) is designed. It is seen that in a mechanical press the nominal slide load (L_M) is available only toward the end of the

stroke. Therefore, the nominal load of a mechanical press is always specified for a certain crank angle or distance, before BDC, usually 1/2 inch.

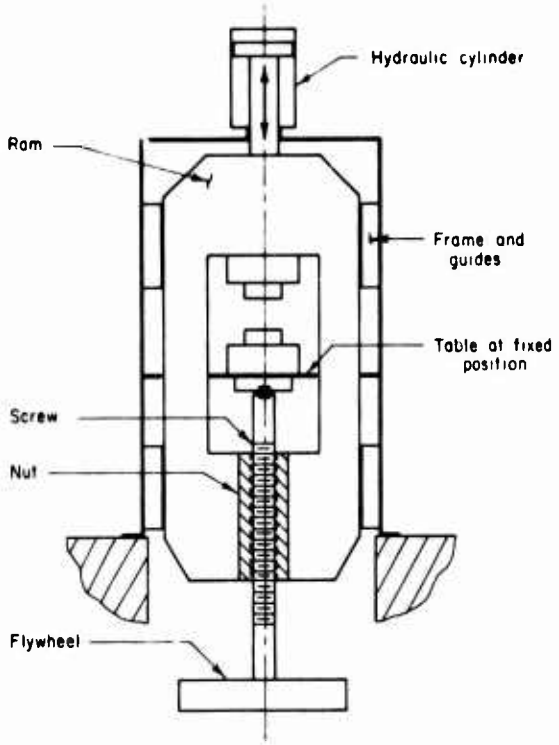

FIGURE 3-10. HYDRAULICALLY DRIVEN SCREW PRESS WITH UNDERFLOOR FLYWHEEL[10]

Equation (3-3) also illustrates that as the angle (α) approaches zero, the load (L_M) may become infinitely large without exceeding the clutch torque (M), i.e., without causing the friction clutch to slip. In this case the press stalls or "blocks", the flywheel stops, and the entire flywheel energy is transformed into deflection energy by straining the press frame, the pitman arm, and the drive mechanism.

The flywheel of the mechanical press, which stores energy, has its idle speed (n_o) at the beginning of a stroke. During a stroke, the flywheel supplies, as needed, the energy for the forging process (E_p), the energy for overcoming machine friction (E_F), and the energy necessary for elastic deflection of the press (E_d). The total available energy during one stroke ($E_T = E_p + E_F + E_d$) is determined by the allowable slowdown of the flywheel, which has the moment of inertia (I), from the idle speed (n_o) to the slowed-down speed (n_1). The total energy per stroke (E_T) is given by:

$$E_T = \frac{1}{2}\left(\frac{\pi}{30}\right)^2 (n_o^2 - n_1^2) \quad . \qquad (3\text{-}4)$$

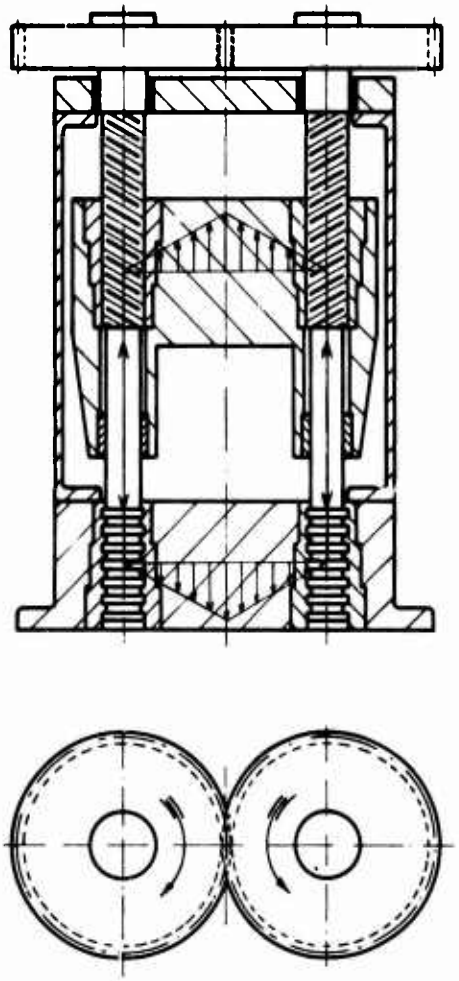

FIGURE 3-11. SCHEMATIC OF DOUBLE SCREW PRESS WITH HYDRAULIC DRIVE[1]

(Hydraulic system is not shown.)

At the end of a forging stroke, the electric motor must bring the flywheel from its slowed-down speed (n_1) to its idle speed (n_o) before the next forging stroke starts. Consequently, in a continuously operating mechanical press, if the electric motor driving the flywheel is not powerful enough, the number of strokes per minute under load (n_p) may well depend upon the energy (E_p) required by the forging process.

Screw Press

In a screw press the forging load is transmitted through the slide, screw, and bed to the press frame. The available load at a given stroke position is supplied by the energy stored in the flywheel. At the end of a forging stroke, the flywheel and the screw come to a standstill before starting their reversed rotation. Thus, the total flywheel energy (E_T) is transformed, as in a mechanical press, into available energy for the

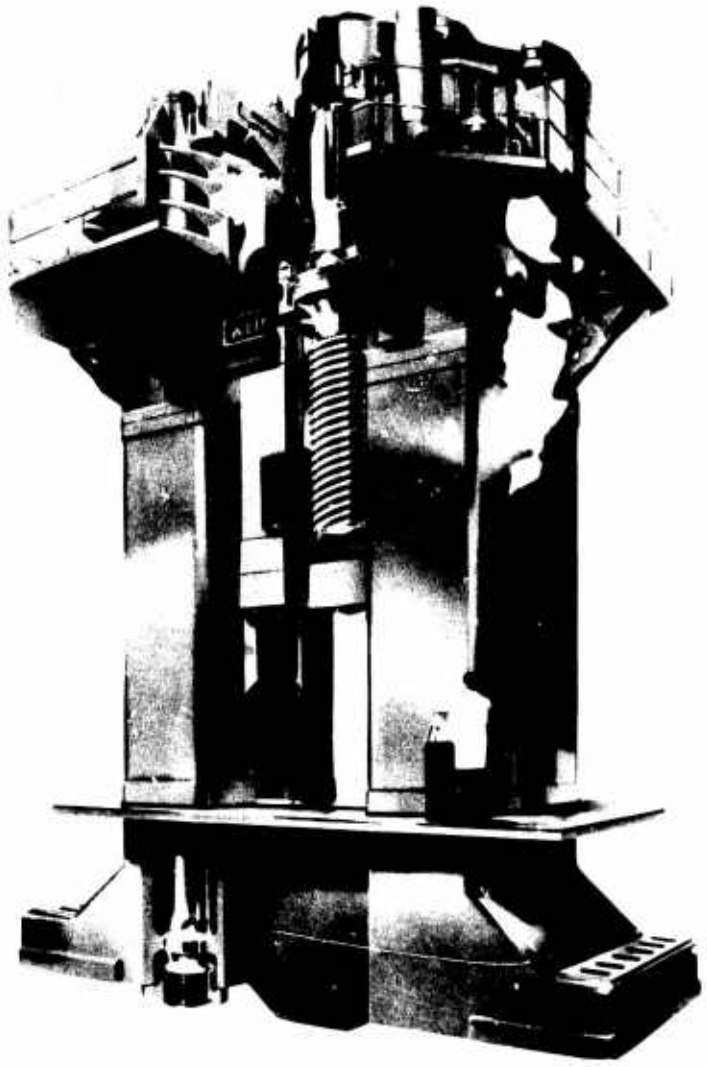

FIGURE 3-12. ARTIST'S CONCEPTION OF THE WORLD'S LARGEST SCREW PRESS BUILT FOR PRECISION FORGING OF TURBINE BLADES (COURTESY WEINGARTEN)

process (E_p), energy to overcome machine friction (E_F), and energy to elastically deflect the machine (E_d). If the total flywheel energy (E_T) is larger than necessary for overcoming machine losses and for carrying out the forging process, the excess energy is transformed into additional deflection energy and both the die and the press are subjected to unnecessary high load. This is illustrated in Figure 3-14. In order to eliminate the excess energy which results in increased die wear and noise, the modern screw press is equipped with an energy-metering device that controls the flywheel velocity and regulates the total flywheel energy. The energy metering can also be programmed so that the machine supplies different amounts of energy during successive blows.

In a screw press, which is essentially an energy-bound machine like a hammer, the load and the energy are in direct relation with each other. For a given press (i.e., for the same friction losses, elastic deflection properties and available flywheel energy) the load available at the end of the stroke depends mainly upon the deformation energy required by the process (i.e., on the shape, temperature, and material of the workpiece). Thus, for a constant flywheel energy, low deformation energy (E_p) results in high end load (L_M), and high deformation energy (E_p) results in low end load (L_M). These relations are illustrated in the "load-energy diagram" of a screw press as shown in Figure 3-15.[12] The energy-load curve has a parabolic shape. This is due to the fact that the deflection energy (E_d) is given by the second-order equation

$$E_d = L_M^2/2C \quad , \qquad (3\text{-}5)$$

in which L_M is machine load and C is total press stiffness.

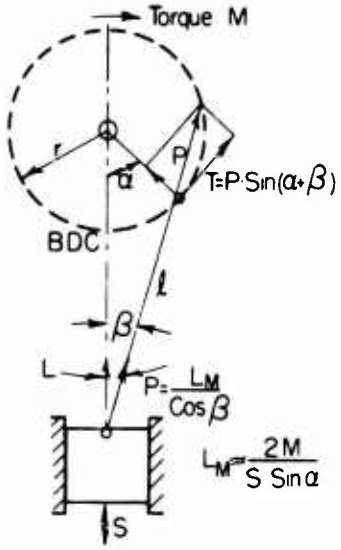

FIGURE 3-13. THE BASIC SLIDER-CRANK MECHANISM OF MECHANICAL PRESSES

(S = Stroke, α = Crank-Angle Before BDC, L_M = Machine Load)

A screw press designed for forging operations, where large energies (E_M) are needed, can also be used for coining where smaller energies are required. For coining, however, a friction clutch is built between the flywheel and the screw. When the ram load reaches the nominal load, this clutch starts slipping and uses up a part of the flywheel energy as friction heat energy (E_c) at the clutch. Consequently, the maximum load at the end of downstroke is reduced from (L) to (L_{max}) and the press is protected from overloading, Figure 3-15.

Comparison of Screw and Mechanical Presses in Terms of Load and Energy

An objective and detailed comparison of two forging machines can be made only by considering a specific part to be forged. This comparison requires that the load and energy (or load-displacement curve) necessary for forging must be known. Therefore, in the present discussion, only a general comparison can be made by pointing out which forging variables are more significant than others. From the description of the two presses, the following conclusions are drawn:

(1) During one working stroke the screw press delivers all the flywheel energy; if this energy is insufficient to forge the part, a second blow might be used to complete the operation. As the mechanical press usually has excess energy in the flywheel, it can be overloaded in terms of energy (but not load). No successive blows, however, can be used for the same operation.

(2) In a screw press, load and energy are in direct relationship. Consequently, for determining the overall capacity of the machine, it is necessary to have the load-energy diagram as seen in Figure 3-15. In a mechanical press the available slide load varies with the slide position, and the flywheel stores more energy than necessary for a forging process. Consequently, the

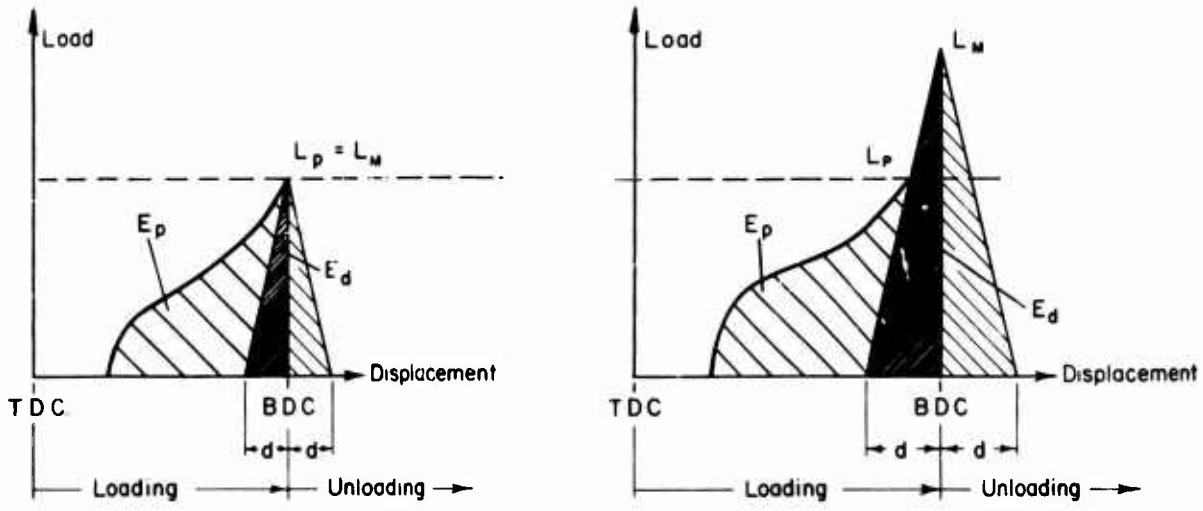

(a) With Energy or Load Metering

(b) Without Energy or Load Metering

FIGURE 3-14. LOAD AND ENERGIES IN CLOSED-DIE FORGING IN A PRESS

(E_p = energy required by process, L_p = load required by process, L_M = maximum machine load, E_d = elastic deflection energy, d = press deflection)

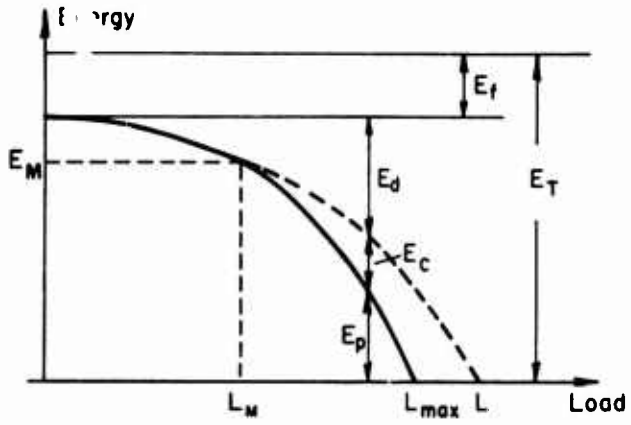

--- without friction clutch at flywheel
—— with slipping friction clutch at flywheel
E_T = total flywheel energy
E_f = friction energy
E_d = deflection energy
E_p = energy required by process
E_c = energy lost in slipping clutch
L_M = nominal machine load
L_{max} = maximum load
E_M = nominal machine energy available for forging.

FIGURE 3-15. LOAD AND ENERGY RELATIONSHIP IN A SCREW PRESS[12]

overall capacity of the machine is determined by the load-slide displacement (or load-crank angle) curve of the press.

(3) Modern screw presses are equipped with energy-metering devices and with a friction clutch at the flywheel, which slips when a preset slide load is reached. Therefore, a screw press can not be overloaded and does not "block". A mechanical press may "block", and the press and the tooling may be overloaded (in terms of pressure and temperature) if the load required by the process exceeds the design load of the press and if no overload safety device is provided. This difference is significant because "blocking" of a mechanical press is more frequent when small production lots are forged and when the magnitude of the maximum forging load can not be estimated easily.

(4) A screw press, equipped with an energy metering device, supplies the same reproducible amount of energy in forging each part. Consequently, variations in tolerances or in die-filling have to be the result of variations in stock weight, stock material or stock temperature. Thus, with a screw press, closer control of forging parameters is possible. In a mechanical press, forging load and energy can be monitored by using various types of devices. This monitoring, though very useful, will not prevent the press from being overloaded because of low forging temperature or oversize stocks.

(5) In general the same part requires less load for forging under a screw press then under a mechanical press. This is due to higher slide velocity of the screw press as discussed below.

EVALUATION OF SLIDE VELOCITY AND CONTACT TIME UNDER PRESSURE

Since the kinematics of screw and mechanical presses are different, the slide velocity and its variation also differ significantly for both machines.

Mechanical Press

From the geometry of the slider-crank mechanism illustrated in Figure 3-13, the approximate relations describing the variation of the slide velocity can be obtained.[13, 19]

The distance (W) of the slide from the BDC, is mainly determined by the press stroke (S) and the crank-angle (α) before BDC as follows:

$$W = \frac{S}{2}(1 - \cos\alpha) \qquad (3\text{-}6)$$

The slide velocity under load (V_p) depends essentially upon the press stroke (S), the number of strokes per minute (n), and the crank-angle (α) before BDC as follows:

$$V_p = \frac{S\pi n}{60}\sin\alpha \qquad (3\text{-}7)$$

The slide velocity (V_p) with respect to the distance (W) of the slide from BDC is given by:

$$V_p = \frac{W\pi n}{30}\sqrt{\frac{S}{W} - 1} \qquad (3\text{-}8)$$

From Equations (3-7) and (3-8), it is seen that for a given stroke (S) the slide velocity (V_p) depends only upon the number of strokes per minute (n). The variation of (V_p) with respect to slide position is schematically illustrated in Figure 3-16. The slide velocity under pressure

(V_p) of a mechanical press is essentially independent of the geometry and the load-energy requirements of the forging. (This is not strictly true since the elastic deflection of the press, which is determined by the maximum forging load, slightly influences the velocity (V_p)).

The number of strokes per minute under load (n_p) is essentially influenced by the velocity-displacement diagram, and by the capacity of the electric motor to bring the flywheel back into its idle speed before the next stroke starts. This point was discussed in reviewing the energy behavior of a mechanical press.

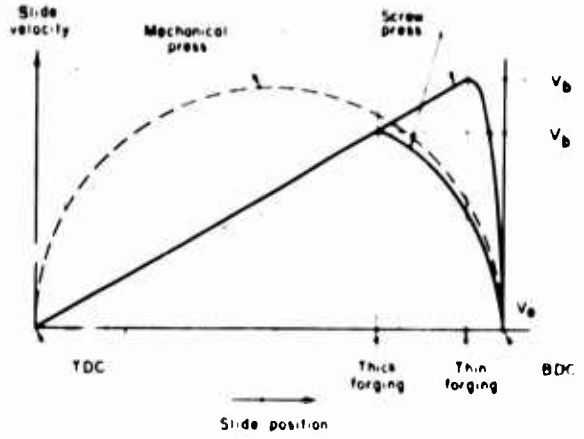

FIGURE 3-16. REPRESENTATION OF SLIDE VELOCITIES FOR MECHANICAL AND SCREW PRESSES IN FORGING A THICK AND A THIN PART

Screw Press

In a screw press the number of strokes per minute under load (n_p) largely depends upon both the energy required by the specific forging process and the capacity of the drive mechanism to accelerate the screw and the flywheel

During a downstroke, the velocity under pressure (V_p) increases until the slide hits the forging blank, as illustrated in Figure 3-16. In this respect the screw press behaves like a hammer. After the forging starts, the velocity of the slide decreases according with the energy requirements of the processes. Thus, the velocity (V_p) is greatly influenced by the geometry of the stock and of the forging. In most forging operations under a screw press, the slide velocity (V_p) decreases from the velocity (V_b) at the beginning of forging to $V_e = 0$, at the end of forging, in a parabolic manner as seen in Figure 3-16. The average slide velocity under pressure (V_{ave}) is given by:[12]

$$V_{ave} = 2V_b/3 \qquad (3\text{-}9)$$

Comparison of Mechanical and Screw Presses in Terms of Time-Dependent Parameters

From the discussion given above the following conclusions are drawn:

(1) In a given screw or mechanical press, the number of strokes per minute under pressure (n_p) depends upon the amount of energy required by the forging process When a press will be operated continuously, for instance in an automated forging line, it is necessary for the user to have a diagram describing the number of strokes per minute (n_p) as a function of forging energy required from the machine.

In general, mechanical presses provide 3 to 5 times more strokes per minute than screw presses, if both machines were to be operated continuously Thus, for large-volume production the mechanical press has a larger production rate, particularly if automated forging lines are considered. Often the loading and unloading sequences, however, require that the press be operated intermittently Then the production-rate advantage of the mechanical press over the screw press is reduced.

(2) The contact time under load (t_p) is the time during which the forging remains under pressure and in contact with the dies The magnitude of t_p greatly influences the cooling of the forging, the metal flow in filling cavities, the forging pressure, and the wear and the washout of dies. These effects are more pronounced if parts with a large surface-to-volume ratio are forged (Large surface area encourages heat transfer, small volume means small heat capacity.) Thus, the magnitude of the contact time (t_p) is very important in precision forging, in forging of thin parts such as air-foils, and in deforming the flash. In both mechanical and screw presses, t_p is influenced primarily by the slide velocity (V_p). In a screw press the contact times (t_p) are usually shorter than in a mechanical press.

(3) In both mechanical and screw presses, the press elastically deflects under load, and the length of deformation stroke increases The amount of deflection is inversely proportional to the stiffness of the press Therefore, the total stiffness of the machine also influences the contact time (t_p). The stiffer the press, the smaller is the deflection and the shorter is the contact time.

(4) The screw press has in general a larger slide velocity which results in higher deformation rates Therefore, at the same temperature the flow stress of the forged material

is higher in a screw press. The high slide velocity, however, also results in shorter contact times and die-chilling effects are usually smaller than in a mechanical press. In most forging operations, die chilling has the overriding effect of increasing the forging load and reducing die fill. Consequently, the load required for forging a part is usually smaller in a screw press than in a mechanical press, especially for thinner parts having a large surface-to-volume ratio.

EVALUATION OF MECHANICAL AND SCREW PRESSES IN TERMS OF OPERATION AND FORGING TOLERANCES

After reviewing the load-energy and time-dependent characteristics of mechanical and screw presses, it is useful to consider the operation of the machines.

The dimensional accuracies of a press under unloaded condition, such as parallelism of slide and bed surfaces, clearances in the gibs, etc., have basically the same significance in the operation of both presses.

The screw press and the mechanical press are both pushbutton operated. Thus, the operator does not have to be very skilled and he can not influence the forging process after it has been initiated. Both presses may be equipped with powerful mechanical or hydraulic ejectors or other accessories.

The major operating differences of the mechanical and screw type presses include:

(1) The possibility of automation is somewhat easier with a mechanical press.

(2) A screw press is operated like a hammer, i.e., the top and bottom dies "kiss" at each blow. This is not the usual practice in forging under a mechanical press. This basic difference in operation has two important consequences:

(a) Die set-up times are longer with a mechanical press because the flash and the forging thickness are obtained by adjusting the slide and the bed positions. In a screw press, die set-up is relatively simple because, as in hammer dies, no adjustment for flash is necessary. During a forging run the mechanical press may require additional adjustments of the stroke because the slide position may vary during the forging run due to heat buildup.

(b) In forging under a mechanical press, the load variations caused by variations in stock weight and stock temperature influence the deflection of the press.(17) The stiffer the press, the smaller are the deflection variations due to unreproducible forging conditions. The deflection of the mechanical press, however, influences the thickness tolerances of the forging. This situation, which may be very important in precision forging, does not exist in a screw press where the dies "kiss" at each blow.

(c) A mechanical press can be operated so that the dies "kiss", but then either the press is operated well under capacity or the possibility of "blocking" the press is increased.

(d) The off-center loading capacity of the press influences the possibility of having skewed surfaces in forgings. This capacity is increased in modern presses by having long gibs and by finish forging at the die center, whenever possible. The mechanical press can sustain off-center loads better than the screw press.

Therefore, in addition to finish forging, other operations such as descaling, preforming and trimming can be carried out under the same mechanical press. The capacity of the screw press for off-center loading is limited. Consequently, additional machines are usually necessary for preforming and trimming when finish forging under a screw press.

CONCLUSIONS

A detailed comparison of two types of forging machines is best made by considering a specific part to be forged. It is possible, however, to point out the most important characteristics of the two machines and how they influence the forging process. In this review, the mechanical and screw presses for closed-die forging are compared with respect to load, energy, slide velocity, contact times and tolerances.

In selecting a specific piece of equipment for forging a part, the most important factors are load and energy requirements. Therefore, approximate predictions must be made during the process design stage unless experimental data, obtained in forging the same part, are already available.

In closed-die forging, metal flow and load-energy requirements are influenced by heat transfer and cooling effects. Often die-chilling effects cannot be separated from lubrication and friction conditions. It is therefore very useful to obtain detailed information on actual slide velocity and contact times for both machines before a final selection is made.

The deflection behavior of the press is important if the machine will be subject to off-center loading and if close-tolerance parts will be forged. Practical considerations such as die set-up times, possibility of attaching automatic feeding and unloading devices, experience in die design for a given machine, etc., must also be considered in selecting a forging press.

It is apparent that an objective and optimum selection of a forging press requires detailed and systematic knowledge both of the specific forging process under consideration, and of the characteristics of the machines considered. Studies as presented in this paper should also be made for other types of forging equipment, such as hammers and hydraulic presses, in order to help the forging engineer in making an optimum equipment selection.

REFERENCES

(1) Schieferdecker, F. D., "Experiences in Forging With the Screw Press" (in German), Werkstattstechnik und Maschinen bau, April, 1958. p. 243.

(2) Meier, R., "The Distribution of Machine Types in the Die Forging Shops in W-Germany" (in German), Werkstattstechnik, 51 (1961), p. 212.

(3) Rau G., "A Die Forging Press With a New Drive", Metal Forming, July, 1967, p. 194.

(4) Bayer, F., "Czech Vertical Hot Forging Presses", Metal Forming, 37, July, 1970, p. 197.

(5) Erie Foundry Company, "Features of the Erie Forging Press", Forging Press Literature, Erie, Pennsylvania.

(6) Mäkelt, H., "Mechanical Presses" (in German), Carl Hansen Verlag, Munich, 1961.

(7) Bohringer, H., and Kilp, K. H., "Development of the Direct-Drive Percussion Press", Sheet Metal Industries, 43, November, 1966, p. 857.

(8) Hammersen, H., "Comparative Investigations on the Behavior of Various Types of Screw Presses" (in German), Werkstattstechnik und Maschinenbau, 48, 1958, p. 237.

(9) Lange, K., "Metalforming in Production Technology, Trends and Techniques in Machines", SME Technical Paper, MF71-199.

(10) Husek, J., "Czech Forming Machines at 10th International Fair in Brünn, 1968" (in German), Industrie-Anzeiger, 91, November 12, 1968, p. 2000.

(11) Georg, O., "Double-Screw Press" (in German), Industrie-Anzeiger, 93, February 2, 1971, p. 190.

(12) Klaprodt, Th., "Comparison of Some Characteristics of Mechanical and Screw Presses for Die Forging" (in German), Industrie-Anzeiger, 90, 1968, pp. 1423.

(13) Altan, T., and Sabroff, A. M., "Important Factors in the Selection and Use of Equipment for Forging", Part I, II, III, and IV, Precision Metal, June, July, August, and September, 1970.

(14) Altan, T., et al., "A Study of Mechanics of Closed-Die Forging", Final Report Prepared for Army Materials and Mechanics Research Center, Watertown, Mass., Battelle Memorial Institute, Contract No. DAAG46-68-C-0111 (1970), AD711-599.

CHAPTER 4

CHARACTERISTICS OF HYDRAULIC, MECHANICAL, AND SCREW PRESSES FOR FORGING: DETERMINATION AND COMPARISON

by

J. R. Douglas, T. Altan, and R. J. Fiorentino

TABLE OF CONTENTS

CHARACTERISTICS OF HYDRAULIC, MECHANICAL, AND SCREW PRESSES FOR FORGING: DETERMINATION AND COMPARISON

by

J. R. Douglas, T. Altan, and R. J. Fiorentino

ABSTRACT

The behavior of forging equipment greatly influences the variables in forging process. Therefore, the characteristics of forging presses must be known in terms of load and energy capacities, accuracy, and time-dependent parameters. To reflect the actual conditions, press characteristics must be determined under dynamic conditions, where speeds, loads, and energies are comparable to those found in practical forging operations.

This study discusses the important characteristics of forging presses and describes methods for determining them. A 700-ton hydraulic press, a newly installed 500-ton mechanical press of scotch yoke design, and a 400-ton screw press were used in the study. High-temperature ring-upset tests were conducted in all three presses to determine the practical effect of press speed upon die chilling, metal flow, and load requirements. In the mechanical press, room-temperature copper upset tests were used to determine the dynamic press stiffness, the off-center loading characteristics, the flatness of ram and bolster surfaces under load, and the available energy capacity at various production rates.

The methods employed in the present study can be used for evaluation, comparison, and standardization of forging presses under practical production conditions.

INTRODUCTION

Developments in the forging industry are greatly influenced by the worldwide requirements for manufacturing larger, more-complex components from more-difficult-to-forge materials with closer tolerances. The present and future needs of aerospace industry, the increase in demand for stationary power systems, jet engines, and aircraft components require continuous upgrading of today's technology. Thus, the more efficient use of existing forging equipment and the installation of more sophisticated machinery have become unavoidable necessities.

The selection of new forging equipment, and the efficient use of various types of existing equipment, require a thorough understanding of the effect of equipment characteristics upon the forging operations, the load and energy requirements of the specific forging operation, and the capabilities and characteristics of the specific forging machine used for that operation. Today, the trend is to install presses, especially mechanical or screw presses, instead of hammers except for very large capacities. The hammer, although it is the least-expensive forging machine, offers several disadvantages such as limited accuracy, noise pollution, and difficulty in automation. The mechanical forging press is most effectively used for large production series, where tool changes and setups are required infrequently. The screw press, well known in Europe, but far less common in the U.S., competes with hammers and with mechanical presses, especially in forging relatively thin parts with great accuracy. Hydraulic presses are mostly used for open-die forging. For closed-die forging operations, the hydraulic press is, in general, too slow, gives long contact times, and causes the die chilling. Consequently, the hydraulic press is practical only for forging aluminum and magnesium alloys, where dies are heated and no excessive die chilling is present, and for forging very large parts requiring forging loads above 6,000 to 8,000 tons.

Plans for new investment, modernization, and automation in forging industry require a thorough knowledge and consideration of the technical and economic aspects of all types of equipment. It is, therefore, useful and timely to discuss the characteristics of the hydraulic, mechanical, and screw presses for forging. For this purpose, the basic principles of these machines were compared with respect to requirements for hot-closed-die forging operations. It should be noted, however, all three types of presses are also being used for cold-forging and coining operations.

INTERACTION BETWEEN PROCESS AND EQUIPMENT IN FORGING

The principal process and equipment variables and their interactions in hot forging in

presses are indicated in Figure 4-1, in which a line between two blocks shows that one variable influences the other.[1,2]

As seen in the left side of Figure 4-1, the flow stress ($\bar{\sigma}$), the interface friction conditions, and the forging geometry (dimensions, shape) determine both the load (L_p) at each position of the stroke, and the energy (E_p) required by the forging process. The flow stress ($\bar{\sigma}$) increases with increasing deformation rate ($\dot{\bar{\epsilon}}$) and with decreasing temperature (θ). The magnitude of these variations depends upon the specific workpiece material. The friction conditions deteriorate with increasing die chilling.

As indicated by lines connected to the temperature block, for a given initial stock temperature, the temperature variations in the forging are largely influenced by the surface area of contact between dies and forging, the part thickness or volume, the die temperature, the amount of heat generated by deformation and friction, and the contact time under pressure. During deformation, heat transfer from the hot forging to the colder dies is nearly perfect with graphite-base lubricants. With glass-base lubricants, however, the heat transfer is greatly reduced depending upon the interface temperature and the thickness and type of glass coating.

The velocity of the slide under pressure (V_p) determines mainly the contact time under pressure (t_p) and the deformation rate ($\dot{\bar{\epsilon}}$). The number of strokes per minute under no-load conditions (n_o), the machine energy (E_M), and the deformation energy (E_p) required by the process all influence the slide velocity under load (V_p) and the number of strokes under load (n_p); (n_p) determines the maximum number of parts forged per minute (i.e., the production rate) provided the feeding and unloading of the machine can be carried out at that speed.

The load-displacement curves, for hot forging a steel part with different types of forging equipment, are shown in Figure 4-2.[2] These curves illustrate that, due to strain rate and temperature effects, for the same forging, different forging loads and energies are required by different machines. In the hammer, the forging load is initially higher, due to strain-rate effects, but the maximum load is lower than in either hydraulic or screw presses. This is because, in the presses, the extruded flash cools rapidly, while in the hammer the flash temperature remains nearly the same as the initial stock temperature.

Thus, the material flow stress and the interface friction conditions vary with the rate of deformation and with die-chilling effects.

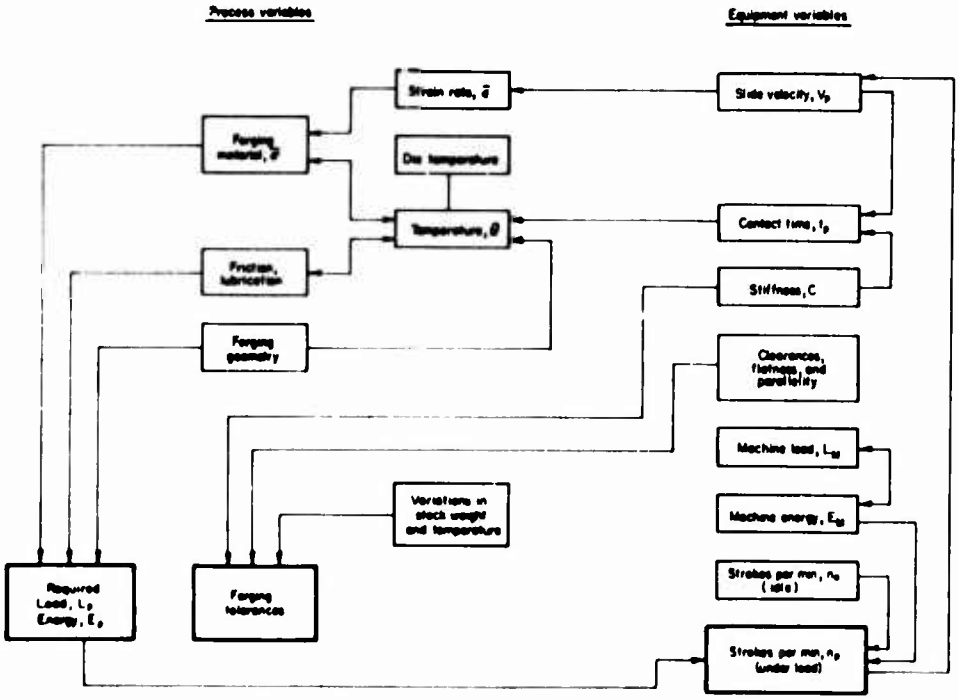

FIGURE 4-1. RELATIONSHIPS BETWEEN PROCESS AND EQUIPMENT VARIABLES IN CLOSED-DIE FORGING IN PRESSES[1]

Consequently, the velocity behavior of the forging equipment used determines the forging load and energy required by the process. This fact is not always clearly acknowledged although it is of paramount importance in understanding the relationship between process and equipment.

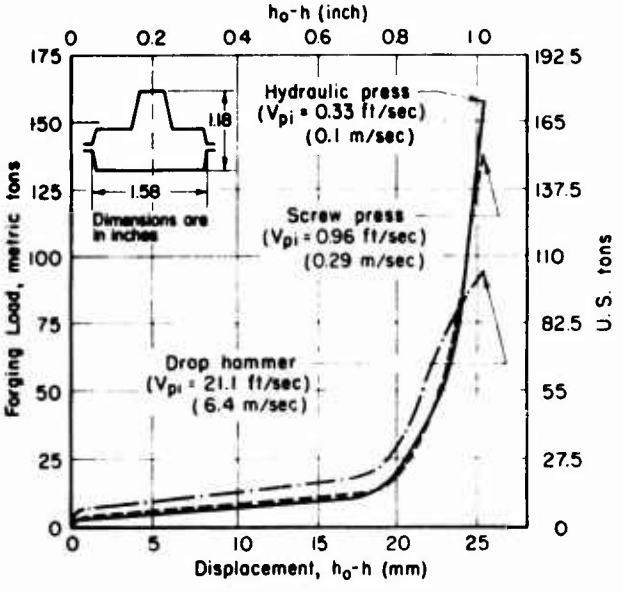

FIGURE 4-2. LOAD-VERSUS-DISPLACEMENT CURVES OBTAINED IN CLOSED-DIE FORGING AN AXISYMMETRIC STEEL PART AT 2012 F UNDER THREE MACHINES WITH DIFFERENT RAM VELOCITIES[2]

As indicated in Figure 4-1, the stiffness of the press influences the contact time under pressure. The stiffness also influences the thickness tolerance of forged parts in mechanical-press forging in which the upper and lower dies usually do not touch or "kiss" during a forging stroke. The flatness and parallelism of upper and lower die surfaces determine the degree of "tilt" and contribute to mismatch in the forged part. Therefore, these characteristics are also important for evaluating the overall performance of a forging press. In hydraulic and screw presses, the stiffness does not affect forging tolerances.

SIGNIFICANT CHARACTERISTICS OF FORGING PRESSES

In discussing characteristics of specific equipment, it is useful to classify forging machinery with respect to principle of operation.[3, 4] Hydraulic presses are load-restricted machines, i.e., capability for carrying out a forming operation is limited mainly by the maximum load capacity. Mechanical (eccentric or crank) presses are stroke-restricted machines since the length of the press stroke and the available load at various stroke positions represent their capability. Screw presses are essentially energy-restricted machines since deformation results from dissipating the kinetic energy of the press ram. As with hydraulic and mechanical presses, the frame of a screw press not only guides the ram, but also is subjected to loading during a forging stroke.

Characteristics of a machine consist of all design and performance data on that machine which are pertinent to its economical use.[3] These data are necessary for optimum selection of equipment for a given process. The characteristic data for forging equipment can be classified into three groups: those for load and energy, those that are time dependent, and those for accuracy.[3, 4]

Characteristic Data for Load and Energy

Available energy (E_M) (ft-lb or kgm) is the energy supplied by the machine to carry out the deformation during an entire stroke. Available energy (E_M) does not include either (E_f), the energy necessary to overcome the friction in the bearings and slides, or (E_d), the energy lost because of elastic deflections in the frame, crown, bed, and driving system.

Available load (L_M) (tons) is the load available at the ram to carry out the deformation process. This load can be essentially constant as in hydraulic presses, it may vary with the slide position in respect to "bottom-dead-center" (BDC) as in mechanical presses, or it may be directly related to the available energy (E_M) as in screw presses.

The following conditions must be satisfied to complete a forging operation:[1, 2]

$$L_M \geq L_p \text{ (Load Required by Process)} \quad (4\text{-}1)$$
at any time during the working stroke

and

$$E_M \geq E_p \text{ (Energy Required by Process)} \quad (4\text{-}2)$$
for an entire stroke.

Time-Dependent Characteristic Data

Number of strokes per minute under load (n_p) is the most important characteristic of any machine since it determines the permissible

production rate. When a part is forged with multiple and consecutive blows (in hammers, open-die hydraulic presses, and screw presses), the n_p of the machine greatly influences the ability to forge a part without reheating.

Contact time under pressure (t_p) is the time during which the forging remains in the die under deformation load. The heat transfer between the hotter forged part and the cooler dies occurs most rapidly under pressure.[5] With increasing t_p, the die wear increases. In addition, cooling of the workpiece results in higher forging load requirements.

Velocity under pressure (V_p) is the velocity of the slide under load. This is an important variable because it determines both the contact time under pressure and the rate of deformation or the strain rate. The strain rate influences the flow stress of the forged material and consequently affects the load and energy required for forging.

Characteristic Data for Accuracy

Under unloaded conditions, the stationary surfaces and their relative positions are established by clearance in the gibs, parallelism of upper and lower beds, flatness of upper and lower beds, perpendicularity of slide motion with respect to lower bed, and concentricity of tool holders.[3] All these machine characteristics affect the tolerances in the forged part. However, characteristics under load and under dynamic conditions are much more significant. The tilting of the ram and deflections of the ram and frame, particularly under off-center loading, may result in excessive wear of the gibs, in thickness deviations in the forged part, and in excessive tool wear.

The stiffness of a press (C), i.e., the ratio of the load (L_M) to the total elastic deflection (d) between the upper and lower beds, can influence the forging process as follows:[6]

- The deflection energy (E_d) stored in a press during a forging stroke is given by

  $$E_d = dL_M/2 = L_M^2/2C \quad . \qquad (4\text{-}3)$$

  Consequently, with decreasing stiffness, C, the amount of energy lost into deflection, E_d, increases. This is particularly significant in mechanical and screw presses.

- The stiffness influences the velocity-versus-time curve under load. Since a less-stiff machine takes more time to build up and remove pressure, the contact time under pressure (t_p) is longer. This fact contributes to the reduction of tool life in hot forging.

- The higher the stiffness, the lower the the deflection of the press. Consequently, in mechanical presses, deviations in forging thickness, due to volume or temperature variations in the stock, are also smaller in a stiffer press.

Very often the stiffness of a press, given in tons/inch, is measured under static loading conditions. Such measurements are misleading, and for practical use the stiffness of a press must be determined under dynamic loading conditions.

DESCRIPTION OF EXPERIMENTAL WORK, EQUIPMENT, AND INSTRUMENTATION

Purpose and Scope of Experimental Work

The purpose of the present investigations is to develop test methods and to demonstrate their application determine the most significart characteristics of the forging presses. These tests must be practical and relatively simple so that they can be conducted easily by the press manufacturers as well as by the press users in a forge shop. The test methods will allow the objective comparison of two machines of the same type but of different makes (such as two hydraulic presses) or of two different machines, such as a screw and a mechanical press. Press characteristics must be determined under conditions which exist during forging. For example, the parallelism of the press ram and bed determined under unloaded conditions and the press stiffness determined under static conditions are of little value in evaluating the performance of a press under dynamic loading conditions.

Three different presses were used in the experimental portion of the present investigation. A 700-ton hydraulic press and a 500-ton mechanical press with scotch yoke design which are installed at the Metalworking Laboratory of Battelle's Columbus Laboratories were used. The 400-ton screw press was a production press in the Brave, Pennsylvania plant of the Accurate Brass Corporation.

The following significant press characteristics were evaluated for the three presses:

Characteristics	Press		
	Hydraulic	Mechanical	Screw
Capacity, tons	700	500	400
Dynamic Stiffness		X	X
Production Rate/ Energy		X	
Ram Tilting, Load Increase in Off-Center Loading		X	
Ram Speed, Contact Time	X	X	X

Hydraulic Press

The vertical 700-ton hydraulic press shown in Figure 4-3 is direct driven, uses hydraulic oil as working medium, and the ram speed is adjustable between 0.1 and 80 ipm. A typical sequence of operations in this press is as follows. The upper ram falls under gravity and oil is drawn from the reservoir into the ram cylinder by the suction created in the free fall. When the ram contacts the workpiece, the valve between the ram cylinder and the reservoir is closed and the pump builds up pressure in the ram cylinder. When the ram reaches a predetermined position, or when the pressure reaches a certain value, the pressure is released and diverted to lift the ram. There is a certain dwell time after the ram touches the workpiece and before the deformation proceeds. Another dwell time exists after the stroke is completed and before the ram is lifted up. A typical oscillograph recording, illustrating the variation of ram displacement and of the press load, is given in Figure 4-4.

This press was instrumented* with two displacement trandsducers: a resistance type with 36-inch travel and an inductive type (LVDT) for 4-inch travel. For load measurement, four strain bars were attached on the columns of the

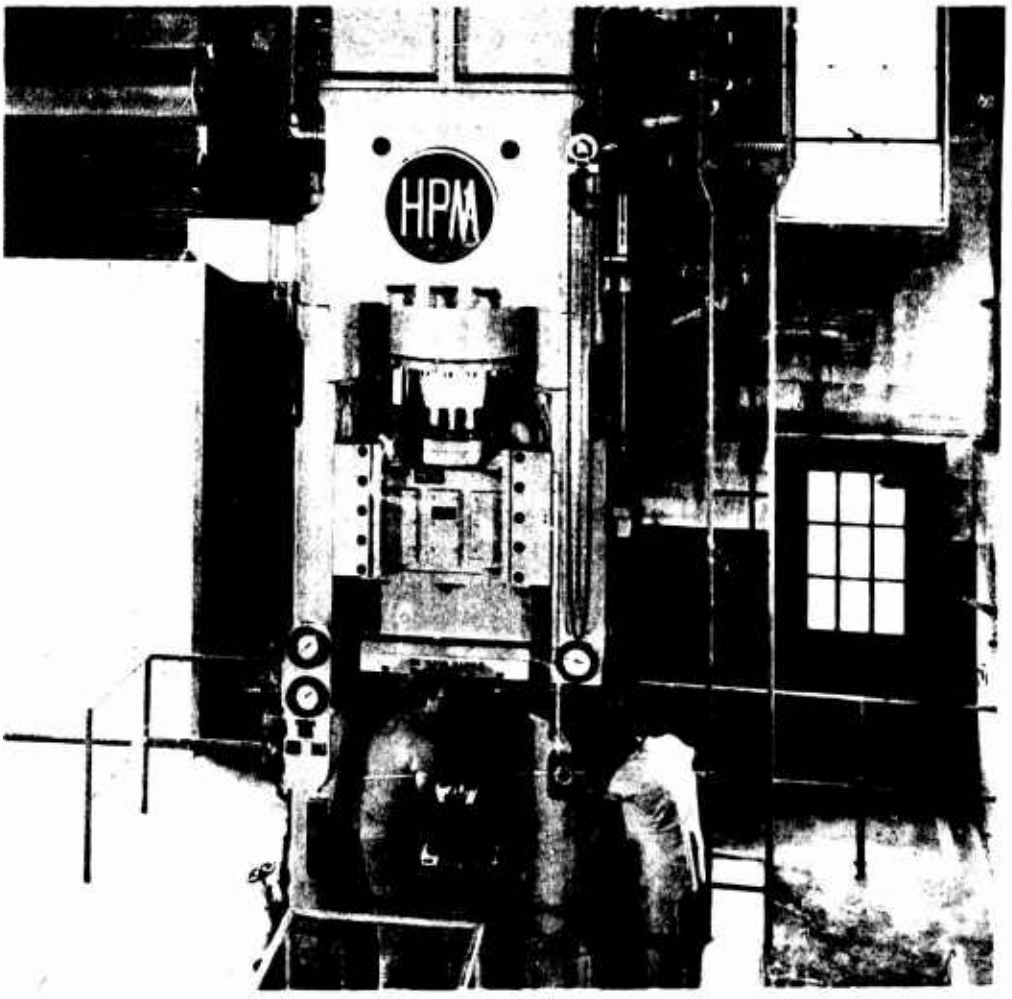

FIGURE 4-3. BATTELLE'S 700-TON, DIRECT-DRIVE, VARIABLE-SPEED HYDRAULIC PRESS USED IN FORGING TRIALS

* Details of instrumentation are described in Chapter 2 (topical report).

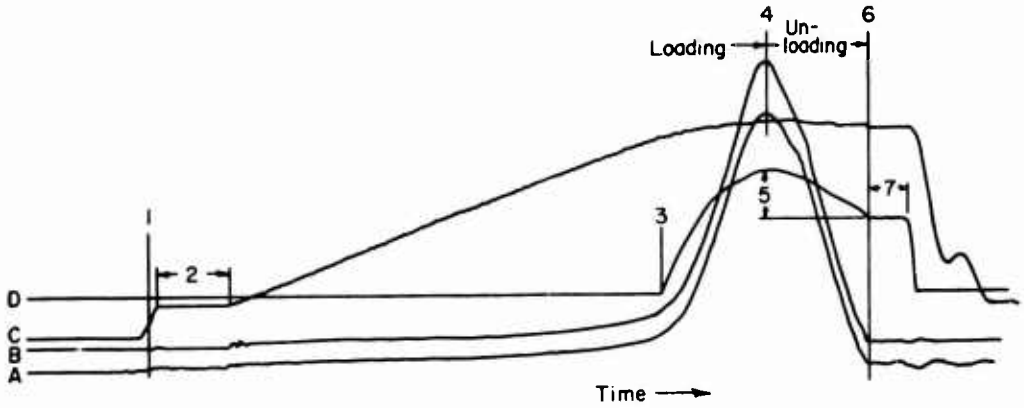

Curves:
- A – Load from column strain gages trace
- B – Load from BLH hydraulic pressure transducer trace
- C – 36-inch displacement transducer trace
- D – 1-inch displacement transducer trace

Lines:
1. Specimen contact
2. Dwell before deformation
3. Activation of 1-inch transducer
4. Maximum load
5. Press deflection
6. Unloaded press
7. Dwell before ram retraction

FIGURE 4-4. A TYPICAL OSCILLOGRAPH RECORDING OBTAINED DURING FORGING IN THE 700-TON HYDRAULIC PRESS

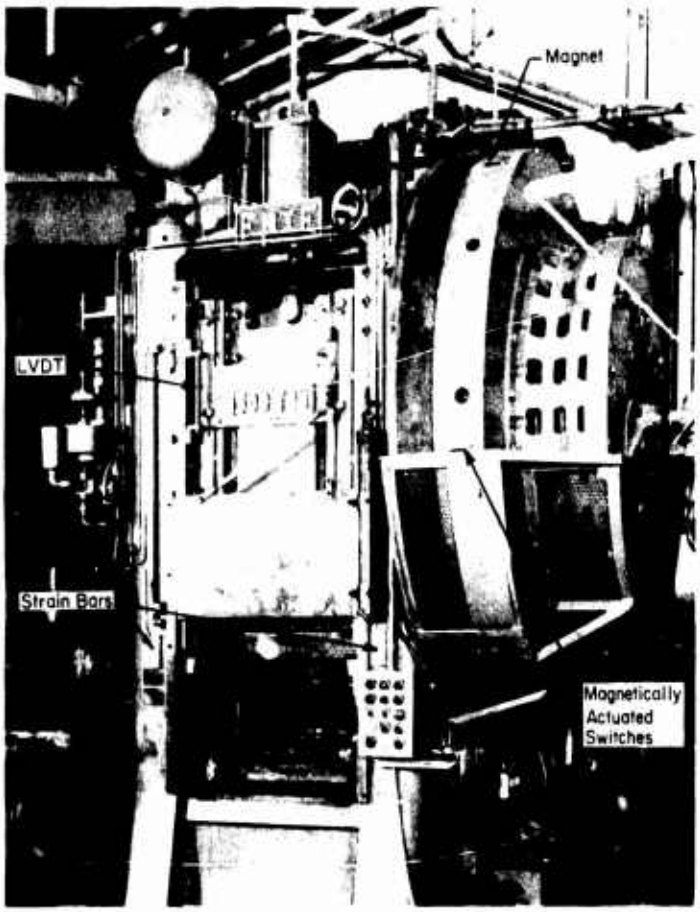

FIGURE 4-5. BATTELLE'S 500-TON SCOTCH YOKE MECHANICAL PRESS WITH THE STRAIN BARS AND LVDT

press and calibrated by using a 700-ton precalibrated load cell. A strain bar acts as a mechanical amplifier. The elongation, which occurs during loading of the press along the length of the bar, is concentrated mainly on the reduced section of the bar where strain gages are located. Thus, good strain response without signal noise is obtained in recordings.

Mechanical Press

The mechanical press used in the present study is the newly installed 500-ton eccentric Erie press with scotch yoke design shown in Figure 4-5. As in all mechanical presses, the drive of this press is basically a slider-crank mechanism that translates rotary into reciprocating linear motion. The eccentric shaft is connected through an air-operated, multiplate friction clutch directly to the flywheel (seen on the right side of the press in Figure 4-5). The flywheel, driven by an electric motor and "V" belts, stores energy that is used only during a small portion of the eccenter revolution, namely during deformation of the forged material. The constant clutch torque is available at the eccentric shaft which transmits the torque and the flywheel energy to the slide through the scotch yoke mechanism, illustrated in Figure 4-6.[1] In this design, the ram contains a top and bottom eccentric block which retain the eccentric shaft. As the shaft rotates, the eccentric blocks move in both horizontal (front to back), and vertical directions while the ram is actuated by the eccentric blocks only in vertical direction.

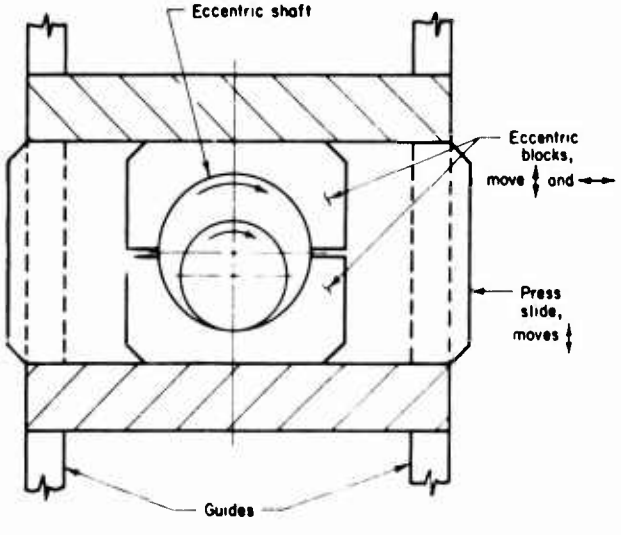

FIGURE 4-6. PRINCIPLE OF THE SCOTCH YOKE TYPE DRIVE FOR ERIE'S MECHANICAL FORGING PRESSES[1]

This mechanical press, rated 500 ton at 0.25 inch before bottom dead center, is a high-speed forging press. It has a stroke of 10 inches and a nominal idle speed of 90 strokes/minute. The press was instrumented to measure displace- with an inductive transducer (LVDT), and load with strain bars attached on the four columns of the press, as indicated in Figure 4-5. The LVDT was calibrated by comparing the known displacement of its core with the voltage output obtained on an oscillograph recording. The strain bars, each consisting of a full strain-gage bridge with four active arms, were wired in parallel arrangement, seen in Figure 4-7. Thus, four of the 350-ohm strain gages (one from each strain bar) make up each arm of the resulting bridge. This bridge, formed by the four strain bars, was calibrated using a load cell. During calibration, shims of gradually increasing thickness were placed upon the load cell and a press blow was struck. Thus, at each new stroke a gradual increase in load and comparison between the outputs of the load cell and the strain bars were

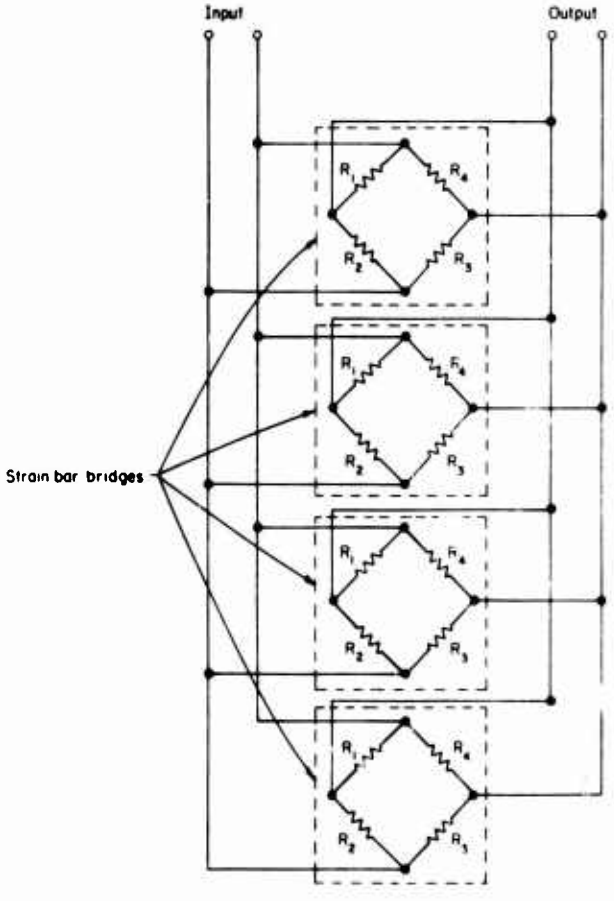

FIGURE 4-7. ARRANGEMENT OF WHEATSTONE BRIDGES ON THE FOUR STRAIN BARS ATTACHED TO BATTELLE'S 500-TON MECHANICAL PRESS

(Under load, gages R_1 and R_3 are in tension and gages R_2 and R_4 are in compression.)

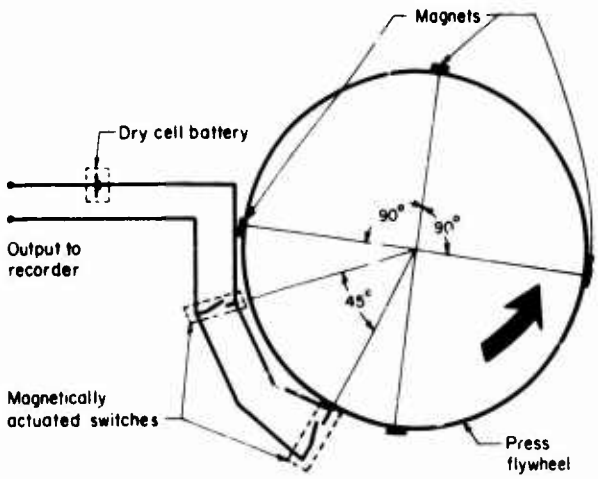

FIGURE 4-8. ILLUSTRATION OF THE TECHNIQUE USED FOR MEASURING FLYWHEEL VELOCITY IN THE MECHANICAL PRESS

(The magnets attached to the flywheel pass by the switches and send eight signals to the recorder during each revolution.)

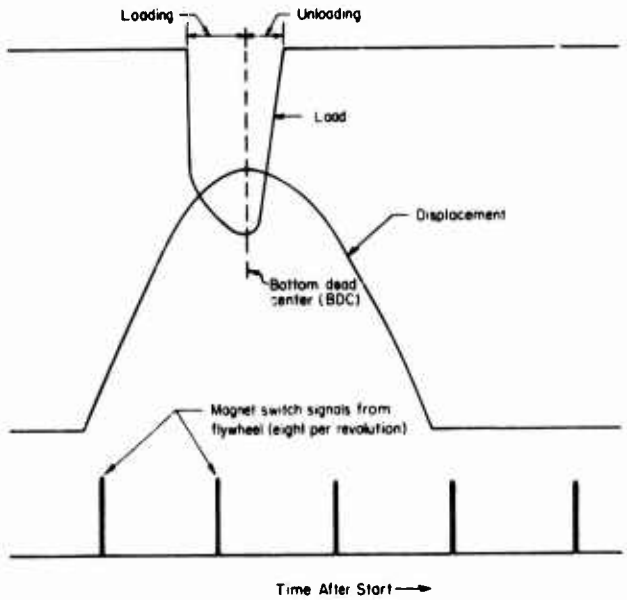

FIGURE 4-9. A TYPICAL OSCILLOGRAPH RECORDING IN AN ECCENTRIC-TYPE MECHANICAL FORGING PRESS

obtained. To measure the flywheel speed, two magnetically operated switches were placed on the housing of the flywheel, and four magnets were attached to the flywheel of the press. The principle of this arrangement and the circuitry used are seen in Figure 4-8. With this very simple setup, a signal on the oscillograph was obtained at every 1/8 revolution of the flywheel. Using the time marker of the oscillograph, the distance or the time lapse between two signals was measured and thus, the variation of the flywheel velocity was obtained. A typical oscillograph recording, obtained during forging in the mechanical press, is illustrated in Figure 4-9.

Screw Press

The screw press used in present investigations is a Weingarten PSS 225 with direct electric drive, as shown in Figure 4-10. This press, using an electric drive to accelerate the flywheel and the screw assembly, converts the angular kinetic energy into the linear energy of the ram. As illustrated in Figure 4-11, a reversible electric motor is built directly on the screw and on the frame, above the flywheel.[7] The screw is threaded into the ram and does not move vertically. During a downstroke, the motor accelerates the flywheel and the screw, and the ram starts its downward motion. The flywheel energy and the ram speed continue to increase until the ram hits the workpiece. Thus, the load necessary for forging is built up and transmitted through the ram, the screw, and the bed to the press frame. When the entire energy of the flywheel is used in deforming the workpiece and elastically deflecting the press, the flywheel, the screw, and the ram stop. Axial elastic loading of the frame and axial and torsional straining of the screw rotate the screw in the reverse direction and the ram disengages from the workpiece. At this time the electric motor is reversed and lifts up the ram to its initial position.

This screw press has a nominal rating of 400 tons load (2250 m-kg), 97.2 in.-tons energy, with a production rate of approximately 30 strokes/minute. The manufacturer specifies a maximum ram velocity of (0.64 m/sec) 2.1 ft/sec at a maximum stroke of 15.8 inch. The static stiffness of the press is given as (300 ton/mm) 8400 tons/inch. The press was instrumented with an LVDT for recording the ram displacement versus time. The load was measured by means of a load cell placed directly under the lower die. A typical oscillograph recording, obtained during forging in the screw press, is given in Figure 4-12.

DYNAMIC PRESS STIFFNESS

Provided the oil pressure is adequate for supplying the forging load, the hydraulic press always has sufficient energy to perform the forging operation. Closed-die forging, in hydraulic presses, is done usually with "kissing" dies. Thus, the stiffness of a hydraulic press is of minor significance because it does not influence the part tolerances or the energy behavior.

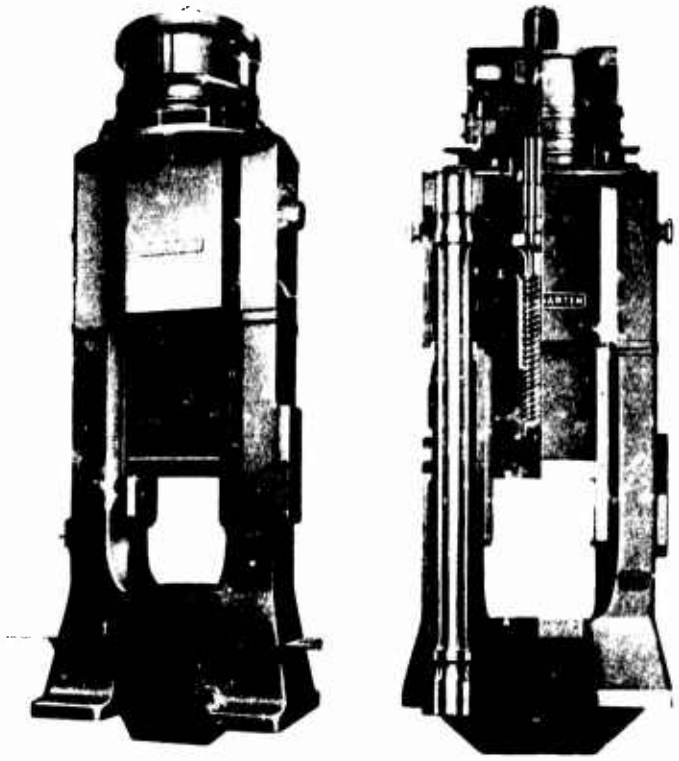

FIGURE 4-10. WEINGARTEN SCREW PRESS WITH DIRECT ELECTRIC DRIVE AND REVERSING MOTOR (Courtesy Weingarten)

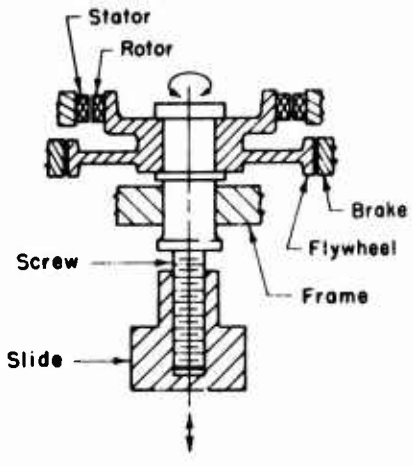

FIGURE 4-11. SCHEMATIC OF THE DIRECT ELECTRIC DRIVE SCREW PRESS WITH REVERSING MOTOR

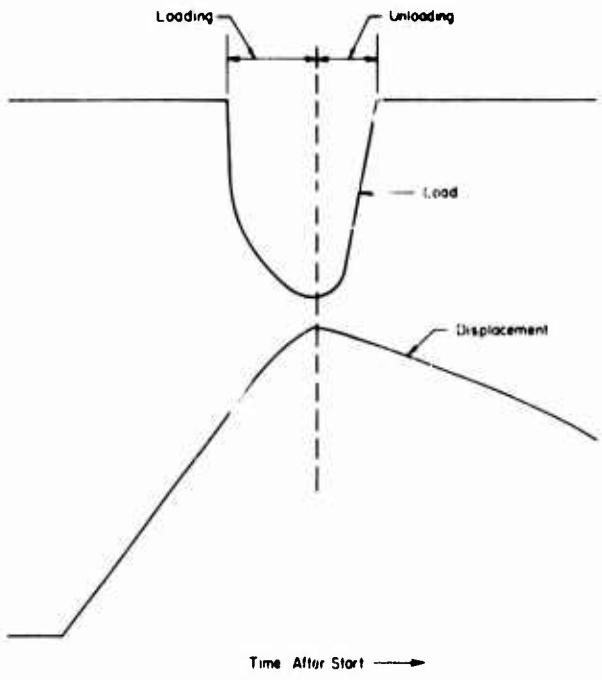

FIGURE 4-12. A TYPICAL OSCILLOGRAPHIC RECORDING OBTAINED DURING FORGING IN A SCREW PRESS

Determination of Dynamic Stiffness in the Mechanical Press

The dynamic stiffness is particularly significant in a mechanical press since it influences thickness tolerances of forged parts attributable to fluctuations in stock temperature, volume, and load variations between forging strokes. Close forging tolerances are obtained in a mechanical press operated with "kissing" dies. The press must be preloaded so that the dies still "kiss" at the bottom dead center despite the elastic stretching of the press during forging. The amount of required preloading increases with decreasing press stiffness.

The total elastic deflection of the press, i.e., the separation of the top and bottom dies from each other under load, is influenced by the bending of the press crown and bed, the stretching of the press frame, and the deflection of the drive mechanism. Because of its scotch yoke design, the press evaluated in the present study was expected to be stiffer than comparable forging presses.

In order to measure the dynamic stiffness of the mechanical press, 2-inch-high copper samples of various diameters were forged under on-center conditions to the final height of approximately 1 inch, Table 4-1. As in other investigations, the samples were made of wrought pure electrolytic copper, annealed 1 hour at 900 F.[8, 9] The press setup was not changed during the tests. Lead samples, about 1 inch square and 1.5 inches high, were placed approximately 5 inches to the side of the copper sample. As indicated in Table 4-1, increasing the specimen diameter increased the load required for forging the copper samples. After each trial, the final height of the forged lead sample was measured. This height was compared to the final height of a lead sample forged alone (thus requiring practically no load). These differences in the heights of lead samples gave the total press deflection as a function of load.

The variation of total press deflection versus forging load, obtained from these experiments, is illustrated in Figure 4-13. During the initial nonlinear portion of the curve, the play in the press driving system is taken up. The linear portion, beginning at approximately 50 tons, represents the actual elastic deflection of the press components. The slope of the linear curve is the dynamic stiffness which was determined to be 5800 tons/inch for the 500 ton Erie forging press.

The method, described above, requires the measurement of the load in forging annealed copper samples. When instrumentation for load and displacement would be impractical for forge shop measurements, the flow stress of the copper can be used for estimating the load and the energy for a given reduction in height. The details of this approximate approach are given elsewhere.[9]

TABLE 4-1. COPPER SAMPLES FORGED UNDER ON-CENTER CONDITION IN THE 500-TON MECHANICAL PRESS

Reduction in height = 50 percent.

Sample	Sample Size, inches		Predicted[1] Load, tons	Forged Height[3] of lead, inches	Measured Load, tons	Predicted[2] Energy, in.-tons	Measured Energy, in.-tons
	Height	Diameter					
1	2.00	1.102	48	0.993	45	24	29
2	2.00	1.560	96	1.008	106	48	60
3	2.00	2.241	197	1.027	210	98	120
4	2.00	2.510	247	1.034	253	124	140
5	2.00	2.715	289	1.043	290	144	163
6	2.00	2.995	352	1.052	350	176	175

(1) Based on an estimate of 50,000 psi flow stress for copper at 50 percent reduction in height.
(2) Estimated by assuming that the load-displacement curve has a triangular shape, i.e., energy = 0.5 x load x displacement.
(3) Press-deflection measurements were based on these values and on the forged height of small lead sample (0.972 inch) which was forged alone and required less than 5 tons.

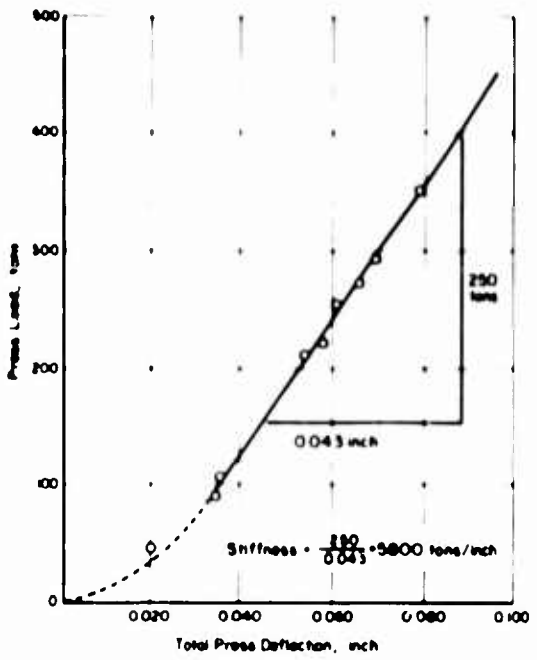

FIGURE 4-13. TOTAL PRESS DEFLECTION VERSUS PRESS LOADING OBTAINED UNDER DYNAMIC FORGING CONDITIONS FOR A 500-TON ERIE SCOTCH-YOKE PRESS

Dynamic Stiffness in the Screw Press

Usually, in forging in a screw press, the dies "kiss" during each blow. Thus, while the stiffness of the press does not influence the thickness tolerances of the forged part, it determines the amount of energy lost into press deflection and it influences the contact time.

The static stiffness of the 400 ton Weingarten screw press, used in the present study, was given by the manufacturer as 8400 tons/inch. This stiffness is measured by the manufacturer, by loading the press statically with a hydraulic jack, and measuring the separation of the dies at various load levels.[10] Thus, this stiffness does not include an allowance for the torsional stiffness of the screw which occurs under dynamic conditions. As pointed out by Waterman[11], who conducted an extensive study on the efficiency of screw presses, the torsional deflection of the screw may contribute up to 30 percent of the total losses at maximum load (about 2.5 times nominal load). In this case, the axial deflection of the screw may contribute 50 percent, and the friction in the screw 20 percent to the total losses in the machine. On the basis of experiments conducted in a smaller Weingarten press (Model P160, nominal load 180 metric tons, energy 800 kg-m), Watermann concluded that the dynamic stiffness was 0.7 times the static stiffness.[11] Assuming that this ratio is approximately valid for the present press, the dynamic stiffness is 0.7 x 8400 = 5900 tons/inch.

During a downstroke, the total energy supplied by a screw press (E_T) is equal to the sum of machine energy available for deformation (E_M), energy necessary to overcome friction in the press drive (E_F), and energy necessary to elastically deflect the press (E_D). Thus,

$$E_T = E_M + E_F + E_D \quad . \qquad (4-4)$$

Using Equation (4-3) to express E_D, in terms of press stiffness, C, Equation (4-4) can be written as

$$E_T - E_F = E_M + L_M^2/2C \qquad (4-5)$$

In a forging test, the energy used for deformation (E_M) (surface area under the load displacement curve) and the maximum forging load (L_M) can be obtained from oscillograph recordings. By considering simultaneously two tests, conducted at the same energy setting, and by assuming that E_F remains constant during these tests, one equation with one unknown, C, can be derived from Equation (4-5). However, in order to obtain reasonable accuracy, it is necessary that in both tests considerable press deflection be obtained, i.e., high loads (L_M) and low deformation energies (E_M) are measured. Thus, the errors in calculating E_M do not impair the accuracy of the stiffness calculations.

The practical procedure, described above, could not be used in the present study because the capacity of the load cell used in screw-press experiments was limited to 500 tons and the press should be loaded in 800-1000 ton range in order to obtain reasonably accurate stiffness values from Equation (4-5). However, using the approximate dynamic stiffness value, C = 5900 tons/inch, and the results of a copper-upset test, the approximate energy distribution can be estimated from Equation (4-5). With E_M = 79.7 in.-ton, L_M = 212 tons (obtained from experiment), E_T = 97.2 in.-ton (manufacturer's specification), and C = 5900 ton-inch, the following values are obtained:

Deflection energy,
$E_D = L_M^2/2C = 3.8$ in.-tons

Friction energy,
$E_F = E_T - E_M - E_D = 13.7$ in.-tons .

Thus, for this specific experiment the friction energy (E_F) consisted of about 14 percent, and the deflection energy (E_D) of about 4 percent of the total energy while the rest was consumed in deforming the part.

PRODUCTION RATE VERSUS ENERGY IN THE MECHANICAL PRESS

In hydraulic and screw presses, the maximum production rate of the press, i.e., number of strokes per minute, depends largely on the stroke length used and it is not significantly influenced by the energy required by the deforming material. In mechanical presses, however, the flywheel slows down during each stroke and supplies the energy available for the process (E_M), the energy necessary to overcome the inertial and frictional resistance in the drive mechanism (E_F), and the energy necessary to deflect the press (E_D). The time necessary for the flywheel to reach its idle speed, before starting the next stroke, will be prolonged if too much energy is lost from the flywheel. Therefore, the energy capacity of a mechanical press is known only if a curve describing the actual stroking rate versus available energy per stroke is known.[9, 12]

For this purpose, the results of the on-center copper-forging tests, given in Table 4-1, were used. During each stroke, the time required by the flywheel to recover 99 percent of its original velocity was measured. The deformation energy and the maximum load required by each sample were obtained from the oscillograph recordings. This information was sufficient to obtain the possible production-rate-versus-energy curve, given in Figure 4-14.

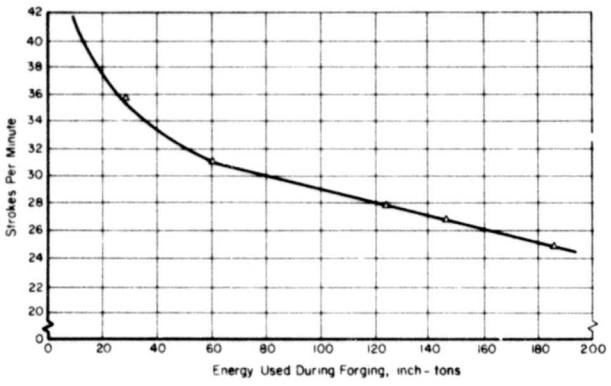

FIGURE 4-14. MAXIMUM STROKES PER MINUTE VERSUS ENERGY AVAILABLE IN THE 500-TON MECHANICAL ERIE PRESS

This curve also includes the energy necessary to deflect the press. During a forging stroke, in order to overcome inertial and frictional resistance, the flywheel slows down before hitting the part. This slowdown corresponds to an energy loss of about 7 percent of the total flywheel energy of 1170 in.-tons (calculated for a flywheel rpm of 92 from the moment of inertia of rotating parts). Thus, approximately 82 ton-inch energy is required to overcome the frictional and inertial resistance during a downstroke.

RAM TILTING AND LOAD INCREASE IN OFF-CENTER FORGING

Off-center loading conditions occur often when several forging operations are performed in the same mechanical press. Especially in automated mechanical presses, the finish blow which requires the highest load occurs on one side of the press. Consequently, the investigation of off-center forging is particularly significant for mechanical presses.

The off-center loading characteristics of the 500-ton mechanical press were evaluated in four tests as follows. Copper specimens, which required 220 tons to forge, were forged 5 inches from the press center in each of four directions, i.e., left, right, front, and back. Lead specimens, which required not more than 5 tons for forging, were placed an equal distance on the opposite sides of the center. The comparison of the final height of the copper and lead forged during the same blow gave a good indication of the nonparallelism of the ram and bolster surfaces over a 10-inch span. The results are given below:

Position of Copper Specimen	Difference in Deflection (10-Inch Span), inch
Front	0.035
Back	0.032
Right	0.032
Left	0.029

In conducting this comparison, the local elastic deflection of the dies in forging copper must be considered. Therefore, the final thicknesses of the copper samples were corrected to counteract this local die deflection before calculating the difference in deflection.

It is seen that, in off-center loading with 220 tons (or 44 percent of nominal capacity), an average ram-bed nonparallelism of 0.038 inch/foot was measured. In comparison, the nonparallelism under unloaded conditions was about 0.002 inch/foot. Before conducting the experiments described above, the clearance in the press gibs was set to 0.010 inch. The nonparallelism in off-center forging would increase with increasing gib clearance.

During off-center loading, the ram tilts and the diagonally opposed corners of the ram

are pressed against the gibs. The tilting of the ram causes a moment and additional friction forces in the gibs, as seen in Figure 4-15. Thus, at these corners the gibs are elastically deformed and the press frame is also stretched and bent. Watermann has investigated a screw press in detail.[13] By assuming that the horizontal forces on the gibs are point loads, it is possible to estimate the increase in press load from the static force and torque equilibrium.[16] These estimations, however, are rather approximate. An accurate picture of the press deflection and loads in off-center forging can be obtained only through extensive experimental studies and stress analyses.[13]

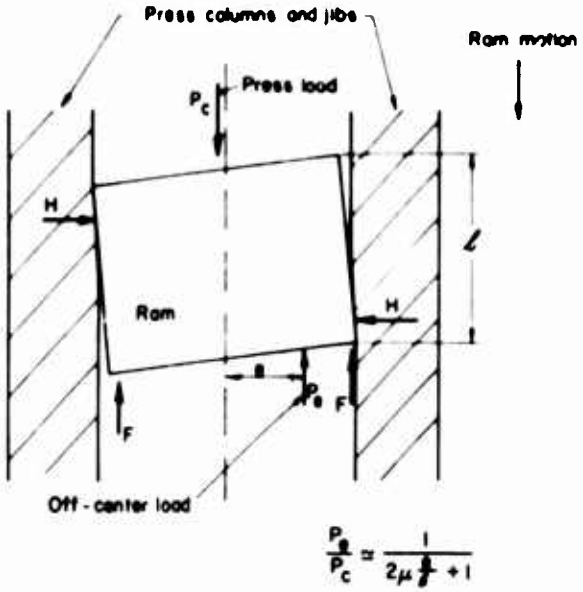

FIGURE 4-15. SCHEMATIC OF FORCES IN OFF-CENTER LOADING OF A PRESS[14]

(μ = coefficient of friction.)

EVALUATION OF RAM SPEED AND CONTACT TIME

In forging, increased contact times may result in increased friction, more severe cooling of the surface layers of the forging by contact with the dies, and in increased flow stress of the forged material because of excessive cooling. The ram speeds and the contact times can be readily obtained from oscillograph recordings. However, to evaluate the direct effect upon the forging process, it is necessary to investigate how metal flow and flow stress varies with contact time and ram speed. For this purpose, the well-known ring-compression test was used.

Principles and Application of the Ring Test

The ring test is used primarily for investigating friction in forging,[15, 16] and for evaluating forging lubricants at various forging conditions.[17] Recently, however, it is also being used for determining the flow stress of forged materials.[16, 18] The test consists of upsetting a flat, ring-shaped specimen to a known reduction. The change in internal and external diameters of the forged ring is very much dependent upon the friction at the tool-specimen interface. The internal diameter of the ring is reduced if the interface friction is large, and it is increased if the friction is low. Thus, the change in the internal ring diameter, before and after upsetting, represents a simple method for evaluating interface friction.

The interface friction shear stress (τ) is expressed by

$$\tau = f\bar{\sigma} = \frac{m}{\sqrt{3}}\bar{\sigma}, \qquad (4\text{-}6)$$

where

f = friction factor $= \frac{m}{\sqrt{3}}$, $0 \le f \le 0.577$

m = shear factor, $0 \le m \le 1$

$\bar{\sigma}$ = flow stress of forged material.

To obtain the magnitude of the friction factor, the internal diameter of the upset ring must be compared with the values predicted by using various friction factors. The present study used a computer program, developed at Battelle's Columbus Laboratories.[16] This computer program simulates the ring-upsetting process for given shear factors (m) by including the bulging of the free surfaces. Thus, ring dimensions for various reductions and shear factors (m) can be determined, and theoretical calibration curves can be generated for rings of different dimensions. Calibration curves are given in Figures 4-16, 4-17, and 4-18 for the rings having OD x ID x thickness ratio of 6:3:2, 6:3:1, and 6:3:1/2, respectively. Rings having these dimensional ratios were used in the present study.

The computer program, simulating the ring-upsetting test, can be used for predicting the average flow stress of the forged ring material, provided the forging load has been measured during the test.[16] For this purpose, the ratio of the forging load to the average instantaneous flow stress (Load/$\bar{\sigma}_{ave}$) is calculated for various shear factors, m, and for

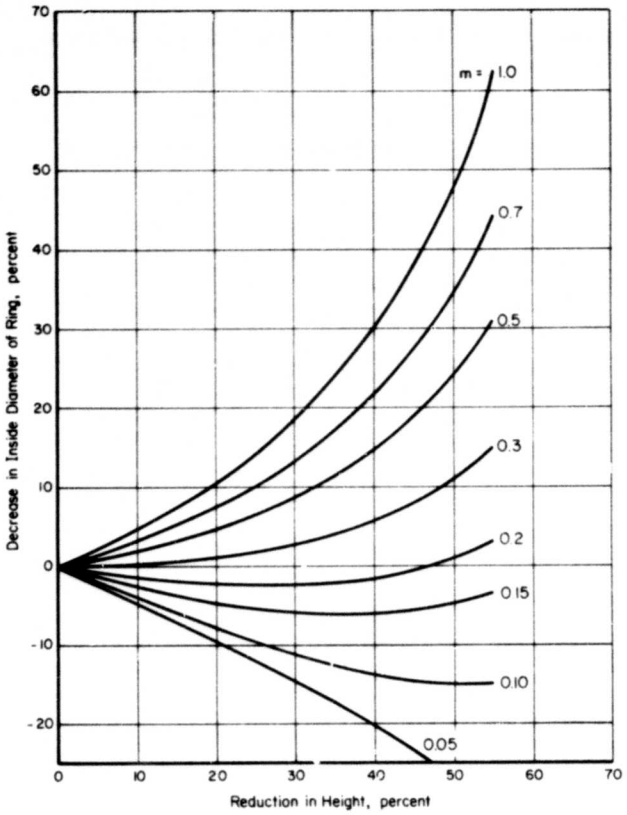

FIGURE 4-16. THEORETICAL CALIBRATION CURVES FOR UPSETTING A RING HAVING OD, ID, AND THICKNESS DIMENSIONS IN A RATIO OF 6:3:2

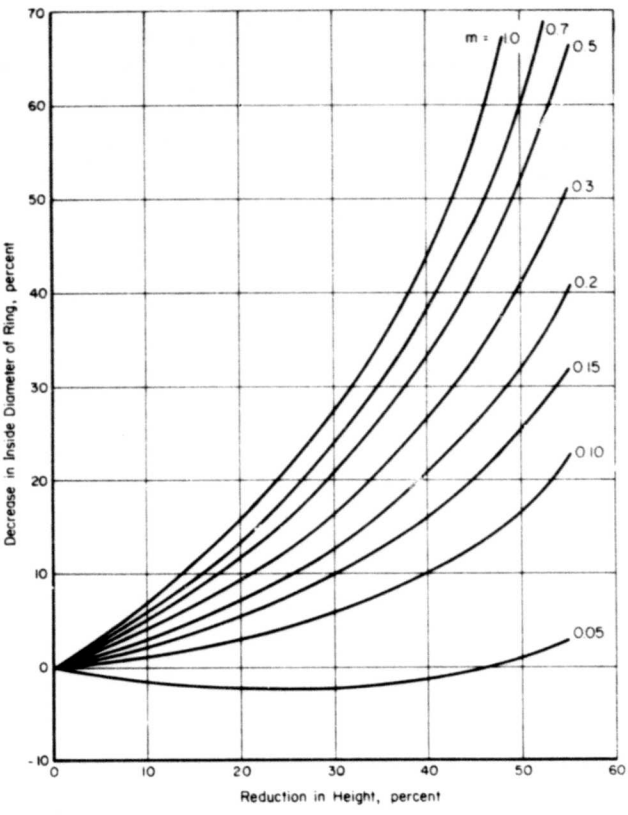

FIGURE 4-18. THEORETICAL CALIBRATION CURVES FOR UPSETTING A RING HAVING OD, ID, AND THICKNESS DIMENSIONS IN A RATIO OF 6:3:1/2

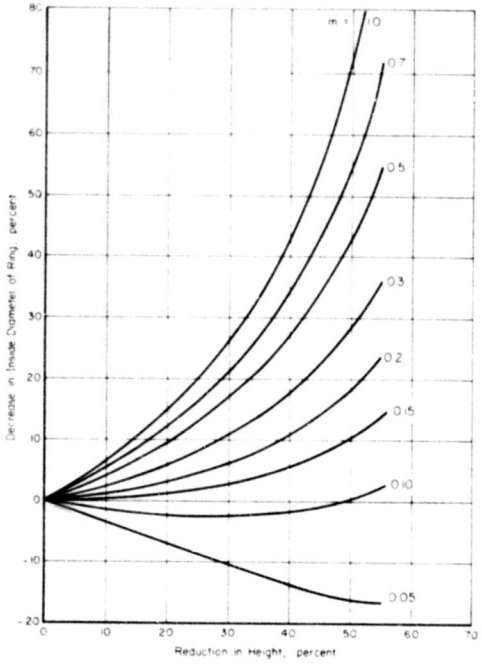

FIGURE 4.17. THEORETICAL CALIBRATION CURVES FOR UPSETTING A RING HAVING OD, ID, AND THICKNESS DIMENSIONS IN A RATIO OF 6:3:1

various reductions. Figures 4-19, 4-20, and 4-21 illustrate the Load/$\bar{\tau}_{avg}$ values calculated for 6:3:2, 6:3:1, and 6:3:1/2 rings, respectively. The shear factors, used in generating these data, were selected from experimental results.

The ring-compression tests, conducted in all three presses, are listed in Table 4-2. In the hydraulic press two speed settings, 20 and 80 in./min, were used. The mechanical press could be operated at only one speed. In the screw press, the maximum energy setting was used but tooling height limited the maximum stroke to 13.5 inches (the maximum press stroke was 15.8 inches). The ring materials were selected such that variations in heat conductivity (titanium versus aluminum) and various degrees of flow stress versus temperature and strain-rate dependencies (titanium versus stainless steel and aluminum) could be obtained. The lubrication and the sample and die temperatures were kept unchanged in tests conducted in all three presses. Lubricants, recommended by one supplier, were selected without any effort to optimize lubrication conditions, and usual commercial practice was followed in lubricating the samples and the dies. (Samples were dipped in the coatings and the dies, at 300 F, were sprayed with graphite-base lubricant.)

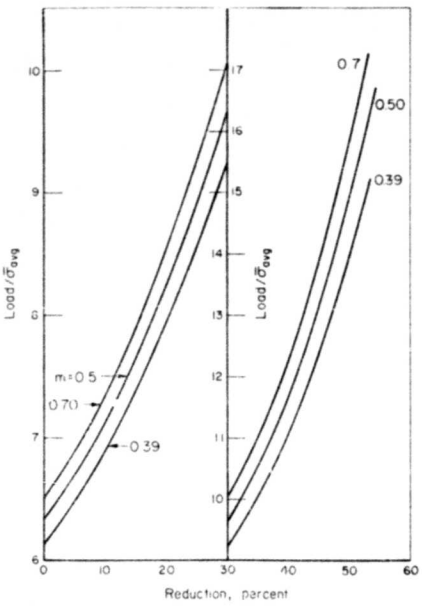

FIGURE 4-19. LOAD/$\bar{\sigma}_{avg}$ DATA CALCULATED FOR 6:3:2 RING AT VARIOUS SHEAR FACTORS (m)

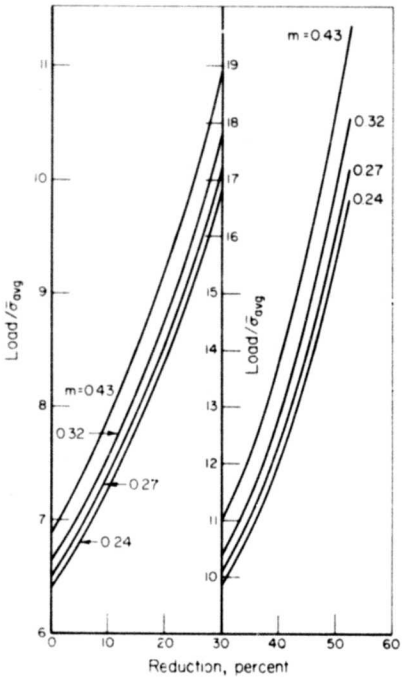

FIGURE 4-20. LOAD/$\bar{\sigma}_{avg}$ DATA CALCULATED FOR 6:3:1 RING AT VARIOUS SHEAR FACTORS (m)

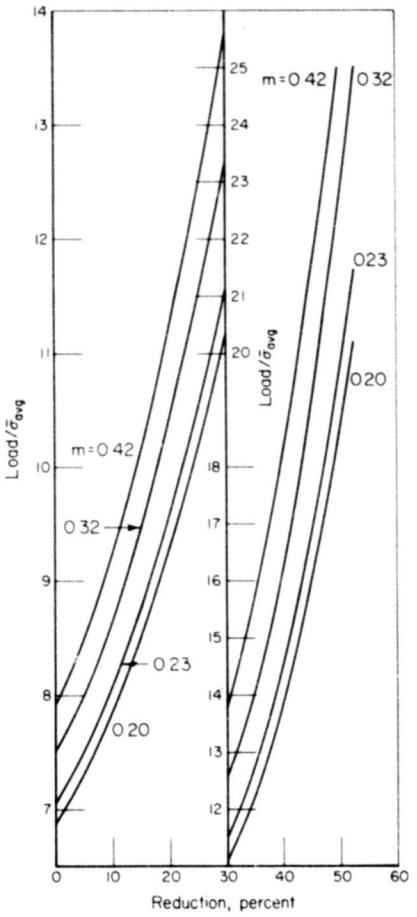

FIGURE 4-21. LOAD/$\bar{\sigma}_{avg}$ DATA CALCULATED FOR 6:3:1/2 RING AT VARIOUS SHEAR FACTORS (m)

All the samples were placed on the lower die, on top of 0.030-inch-diameter mild-steel wire, in order to prevent die chilling prior to deformation. The transfer time (time necessary to take a sample from the furnace and to place it on the lower die) was approximately 3 seconds in mechanical and hydraulic press trials. However, in screw press trials, conducted in a forging plant, the furnace was farther from the press and the transfer time was approximately 10 seconds. The effect of this difference in transfer times, upon the test results, is discussed later.

Results of Ring Forging Experiments

The forging conditions for these experiments are given in Table 4-2. The dimensions of the samples were selected such that the maximum forging load in forging the thinnest samples would be in the range of 500 tons. Thus, the capacities of all three presses were sufficient to perform the experiments.

TABLE 4-2. MATERIALS AND CONDITIONS FOR RING-COMPRESSION TESTS CONDUCTED IN A 700-TON HYDRAULIC PRESS, 500-TON MECHANICAL PRESS, AND 400-TON SCREW PRESS

(The same hot work tool steel dies were used in all tests, temperature - 300 F, surface finish - 25 microinches.)

Sample Material:	6061 Aluminum	AISI 403 Stainless Steel	Ti-7Al-4Mo
Sample Temperatures, F:	800	1800	1750
Ring Dimensions, inch (OD x ID x Thickness)	6 x 3 x 2 6 x 3 x 1 6 x 3 x 0.5[b]	3 x 1.5 x 1[a] 3 x 1.5 x 0.5[a] 3 x 1.5 x 0.25[b]	3 x 1.5 x 1 3 x 1.5 x 0.5 3 x 1.5 x 0.25[b]
Approximate Reduction in Height, percent	50	50	50
Lubrication System:			
Dies	Graphite spray[c]	Graphite spray[e]	Graphite spray[e]
Specimen	Caustic precoat + graphite[d]	Glass-base coating[f]	Glass-base coating[f]

(a) Due to excessive scaling, these tests, conducted in the hydraulic press, were not evaluated.
(b) These tests were not conducted in the hydraulic press.
(c) Deltaforge 105 (Acheson Colloids Company).
(d) Dag 137 (Acheson Colloids Company).
(e) Deltaforge 43 (Acheson Colloids Company).
(f) Deltaforge 347 (Acheson Colloids Company), glass-base lubricant diluted in isopropanol with solid content of 15 percent by weight, samples were dipped into the solution prior to heating.

The results obtained in forging aluminum, titanium, and stainless steel rings to reductions of 50 percent in height are given in Table 4-3. Most data represent the average for two samples. The results for these samples did not differ more than 5 to 10 percent. The reduction was obtained from the initial and final sample dimensions; the load and the contact times were obtained from oscillograph recordings, the contact velocity was calculated as the slope of the displacement-versus-time-curve at the start of forging. The shear-factor values were obtained from the final dimensions of the rings by using the calibration curves given in Figures 4-16 through 4-18. The average flow-stress data at maximum reduction, calculated for some of the titanium and stainless steel samples, were obtained by using the measured forging load and the curves given in Figures 4-19 through 4-21.

6061 Aluminum Rings

The results obtained in forging 6061 aluminum rings are given in Table 4-3. From these data, the following observations and conclusions are made:

- The shear factor (m) is not influenced by contact time and deformation speed. This indicates that temperature gradients through the thickness of the ring samples were not steep enough to give significantly stiffer interface surfaces. This is because aluminum is an excellent heat conductor and the temperature was probably reduced somewhat uniformly throughout the samples.

- The transfer time, 4 seconds in the mechanical and hydraulic press and 10 seconds in the screw press, does not appear to have any major influence on shear factors and load. In these experiments the samples had large volume-to-surface ratios and cooling in air was less significant than it would be for smaller samples. In fact, specimens subjected to longer transfer time could be forged with smaller loads.

- In forging rings with 6:3:2 ratio, which have large ratio of volume to interface contact area, the effect of die chilling appears to be balanced by the effect of strain rate. Consequently, the load does not vary drastically with contact time (compare the results for samples A-1, A-2, and A-3).

- The contact times (loading and unloading) are shorter in the screw press for rings having 6:3:1 and 6:3:1/2 ratios, as seen for samples A-7, A-8, A-9, and A-10. For rings with

TABLE 4-3. DATA OBTAINED WHILE FORGING RINGS IN A HYDRAULIC PRESS, MECHANICAL PRESS, AND SCREW PRESS

Experimental conditions are given in Table 4-2; the data represent the average for two samples.

Test	Press	Reduction, percent	Load, tons	Shear Factor, m	Contact Time, sec: Dwell[a]	Loading	Unloading	Total	Contact Velocity, in./sec	Flow Stress, 10^3 psi
6061 Aluminum										
6:3:2 Ring Ratio										
A-1	Hydraulic[b,e]	51.0	285	0.63	1.00	3.60	0.32	4.92	(d)	
A-2	Hydraulic[c,e]	51.2	250	0.65	0.44	0.83	0.29	1.56	(d)	
A-3	Mechanical[e]	51.0	260	0.53	--	0.079	0.018	0.097	26	
A-4	Screw[f]	34.9	160	0.49	--	0.051	0.035	0.086	19	
6:3:1 Ring Ratio										
A-5	Hydraulic[b,e]	50.2	465	0.48	0.92	2.56	0.42	3.90	(d)	
A-6	Hydraulic[c,e]	51.0	386	0.42	0.47	0.53	0.35	1.35	(d)	
A-7	Mechanical[e]	49.8	338	0.31	--	0.047	0.029	0.076	19	
A-8	Screw[f]	47.0	275	0.35	--	0.041	0.021	0.062	22	
6:3:1/2 Ring Ratio										
A-9	Mechanical[e]	45.7	520	0.40	--	0.038	0.027	0.065	14	
A-10	Screw[f]	45.6	400	0.34	--	0.023	0.017	0.040	22	
Ti-7Al-4Mo										
6:3:2 Ring Ratio										
T-1	Hydraulic[b,e]	51.0	255	0.72	1.03	2.16	0.31	3.50	(d)	
T-2	Hydraulic[c,e]	52.2	215	0.40	0.43	0.49	0.29	1.21	(d)	
T-3	Mechanical[e]	49.0	225	0.70	--	0.056	0.018	0.074	22	29.1
T-4	Screw[f]	40.0	250	0.64	--	0.043	0.019	0.062	20	41.0
6:3:1 Ring Ratio										
T-5	Hydraulic[b,e]	47.7	690	0.26	1.57	0.99	0.69	3.25	(d)	92.0
T-6	Hydraulic[c,e]	48.8	335	0.28	0.50	0.33	0.37	1.20	(d)	43.1
T-7	Mechanical[e]	46.2	275	0.42	--	0.044	0.017	0.061	17	33.6
T-8	Screw[f]	44.8	365	0.44	--	0.024	0.021	0.045	22	46.5
6:3:1/2 Ring Ratio										
T-9	Mechanical[e]	30.8	400	.42	--	0.033	0.020	0.053	15	56.7
T-10	Screw[f]	37.6	445	.20	--	0.019	0.018	0.037	22	68.0
AISI 403 Stainless Steel										
6:3:2 Ring Ratio										
S-1	Mechanical[e]	51.1	225	.34	--	0.047	0.028	0.075	20	31.3
S-2	Screw[f]	47.3	270	.50	--	0.040	0.022	0.062	21	38.2
6-3-1 Ring Ratio										
S-3	Mechanical[e]	51.2	275	.24	--	0.037	0.025	0.062	16	34.2
S-4	Screw[f]	45.6	330	.32	--	0.026	0.015	0.041	22	44.6
6:3:1/2 Ring Ratio										
S-5	Mechanical[e]	46.1	330	.23	--	0.029	0.023	0.052	11	38.0
S-6	Screw[f]	40.0	390	.32	--	0.020	0.016	0.036	23	47.5

(a) This dwell, which occurs only in the hydraulic press, is the length of time that the ram is in contact with the specimen before deformation begins.

(b) Nominal ram speed: 20 in./min.

(c) Nominal ram speed: 80 in./min.

(d) In the hydraulic press, the contact velocity depends upon the free fall of the ram. This velocity averaged about 20 in./sec.

(e) The transfer time from the furnace to the press for both the hydraulic press and the mechanical press was about 4 seconds.

(f) The transfer time from the furnace to the screw press was about 10 seconds due to the greater distance of the furnace from the press.

6:3:2 ratios, a direct comparison of the mechanical and the screw press, in terms of contact times, is not possible because of the difference in reductions. However, the results clearly indicate that, for actual forging strokes of 1 inch or less, the screw press gives definitely a shorter contact time than the mechanical press.

- The comparison of forging loads for samples A-5 and A-6, A-7 and A-8, A-9, and A-10 indicates that, although the shear factors, the strain rates, and the reductions are approximately the same, the load decreases with decreasing contact time and increasing deformation speed. This trend appears to be stronger for thinner samples, as it can be seen by comparing the load variations for samples A-7 and A-8 (6:3:1 ratio) and A-9 and A-10 (6:3:1/2 ratio).

  Thus, in forging aluminum (which is an excellent heat conducting material) with graphite-base lubricants (which insure good heat transfer at tool-material interface) the effect of die-chilling on raising loads is significant while the effect of strain-rate is not significant. This observation agrees with the emperical and practical information available in forging practice and explains the extensive use of screw presses (up to 30 percent of Weingarten presses in use in forge shops[7]) for hot forging of aluminum and copper alloys.

- During unloading, the ram of the screw press is pushed back by the elastic energy stored in the frame and the screw. Therefore, in the screw press, the unloading time is shorter for larger loads, as it is seen from samples A-4, A-8, and A-10.

Ti-7Al-4Mo Rings

The results obtained in forging Ti-7Al-4Mo rings are summarized in Table 4-3. From these data, the following observations and conclusions are made:

- The transfer time, 10 seconds for the screw press and 4 seconds for the other presses significantly influenced the cooling of the samples in the air because these samples were small and had large surface to volume ratios. The calculated flow stresses and measured loads are higher for specimens forged in the screw press than for those upset in the mechanical press for all sample sizes. These differences can not be explained by strain rate because the strain rate does not vary significantly between operations in the two presses.

- For a particular ram velocity and reduction, strain rate increases as specimen thickness decreases. So does the tendency for the die to lower the average temperature of the workpiece. Both higher strain rates and colder specimen temperatures result in higher flow strengths. The combined effects are shown by comparing flow stresses for samples T-3, T-7, and T-9 or for samples T-4, T-8, and T-10.

- The shear factor (m) does not appear to be influenced by cooling time in air and by small contact time differences found in screw and mechanical-press trials.

- In hydraulic-press trials, the shear factor varies with press speed and contact time for the 6:3:2 samples but not for the 6:3:1 rings. For the latter, the forging load increases drastically with increasing contact time. Thus, it appears that the 6:3:1 samples reach a lower but more uniform temperature at both speeds. Therefore the shear factors, determined for the 6:3:1 samples do not reflect the effects of die chilling.

- The contact times are lower in screw press for all sample sizes. As discussed for aluminum samples, the unloading time in the screw press decreases with increasing forging load. A similar trend is not recognizable in the mechanical press.

403 Stainless Steel Rings

The results obtained in forging 403 stainless steel rings are summarized in Table 4-3. From these data the following observations and conclusions are made:

- Both the flow stress and the shear factors are larger in the screw press. This is due to larger transfer and cooling times in air (10 seconds for the screw press and 4 seconds for the mechanical press). In order to verify that the increase in shear factor in the screw press was due to increased transfer time (lower specimen temperatures), additional experiments were conducted in the mechanical and in the screw press. In these tests a scale-preventing coating, Turco Pretreat, was used instead of the glass-base coating, Acheson 347, and the transfer times were kept at 10 seconds. The shear factor values are given below:

Ring Ratio	Press	Reduction, percent	Shear Factor, m
6:3:2	Mechanical	49.9	0.37
6:3:2	Screw	45.8	0.42
6:3:1	Mechanical	44.1	0.26
6:3:1	Screw	44.0	0.25
6:3:1/2	Mechanical	34.0	0.30
6:3:1/2	Screw	37.6	0.20

These results indicate that there is no significant difference in shear factors, provided the transfer time is the same for both presses. (The data for 6:3:1/2 ring cannot be used for a reliable conclusion since the difference in reductions is considerable.)

- The contact times are shorter in the screw press. Again, in the screw press, the unloading time decreases with increasing load.

- The combined strain rate and die chilling effect is seen from samples S-1, S-3, and S-5 for the mechanical press and from samples S-2, S-4, and S-6 for the screw press. The increase in flow stress with decreasing sample thickness is more pronounced for titanium and stainless steel samples. Particularly, the comparison of 6:3:1 and 6:3:1/2 rings indicates that die chilling must have a far more significant effect in titanium than in stainless steel. This is valid for both presses and it is explained by the fact that the flow stress of titanium is more temperature dependent than the stainless steel.

SUMMARY AND CONCLUSIONS

The present work was conducted for the purpose of developing simple and useful methods for evaluating presses for closed-die forging. The effect of equipment behavior upon the forging process has been reviewed and the most significant characteristics of hydraulic, mechanical, and screw presses have been investigated.

For evaluating and comparing the performance of mechanical presses, practical test methods have been developed for determining the dynamic stiffness under forging conditions, for determining the maximum possible production rate versus available energy for deformation, and for evaluating the ram and bed parallelism in off-center loading conditions. The application of these methods has been demonstrated on a high-speed, 500-ton mechanical press. These tests can be used for comparing different mechanical presses, for evaluating the performance of used presses, and to establish the necessity and the schedule for preventive maintenance.

The dynamic stiffness of a screw press has been discussed and a practical method for its determination has been suggested. However, due to capacity limitation of the load cell, used in screw press trials, the practical application of the suggested technique could not be carried out.

The principles of the ring-upset test have been reviewed and its application for determining friction shear factors and flow-stress values has been discussed. 6061 aluminum, Ti-7Al-4Mo, and 403 stainless steel rings of various dimensions with 6:3:2, 6:3:1, and 6:3:1/2 ratios have been forged in a hydraulic, a mechanical, and a screw press of comparable capacities. For all these tests, ram speeds, contact times, and forging loads have been measured. The shear factors and flow-stress values have been calculated by using the experimental results and the theoretical calibration curves which give the shear factor versus reduction and load/average flow stress versus reduction. These curves have been obtained from computer programs which simulate the ring-upset test by taking bulging of free surfaces into account.

The results of the ring-upset tests give useful practical information for comparing the time-dependent characteristics of the hydraulic, screw, and mechanical presses investigated in the present study. From these results the following observations and conclusions are made:

- For actual forging strokes of 1 inch or less, the screw press exhibits shorter contact times in this study than the mechanical and the hydraulic presses.

- During unloading, the ram of the screw press is lifted through elastic energy stored in the frame and in the screw. Therefore, in the screw press the unloading time decreases with increasing forging load. A similar trend was not detected in experiments with the mechanical press.

- The influence of transfer time, 4 seconds in mechanical and hydraulic presses and 10 seconds in screw press, upon friction and load is not significant in large aluminum rings (6 inch O D x 3 inch O D). However, this influence was considerable in the smaller titanium and stainless steel rings. In the screw press, calculated flow stress and measured load values are larger than in the mechanical press, for all ring thicknesses. These differences were due to larger transfer times in screw-press trials and cannot be explained by strain-rate because the strain rate does not differ significantly in both presses.

- The differences in contact times and deformation speeds, between mechanical and screw presses, do not affect the friction shear factor (m) in aluminum, titanium, or stainless steel ring-compression tests. (For stainless steel the trials conducted with "Turco Pretreat" and 10-sec transfer time must be used for comparison.

- In aluminum rings, the load decreases with decreasing contact time and increasing deformation speed. Thus, in forging aluminum (an excellent heat conductor) with graphite-base lubricants (insure good heat transfer at die-material interface), the effect of die chilling is significant while the effect of strain-rate is negligible. This observation explains the extensive use of screw presses in hot forging of aluminum and copper alloys.

- A combined effect of increasing strain rate and decreasing temperature upon forging load is shown by forging rams with different thicknesses in the same press. The increase in flow stress with decreasing ring thickness is particularly significant between 6:3:1 and 6:3:1/2 rings. These results, for stainless steel and titanium rings, indicate that die chilling must have a far more significant effect in titanium than in stainless steel. This is valid for both mechanical and screw presses and it is explained by the fact that the flow stress of titanium is more temperature dependent than that of stainless steel.

In summary, the ring tests indicate that, except for aluminum alloys, the differences in contact time and deformation rate, which existed in the mechanical and screw press used in the present study, are not expected to influence appreciably the metal flow and forging load. However, shorter contact times in the screw press may result in lower die wear in practical forging operations. This point was not further investigated in the present study.

REFERENCES

(1) Altan, T., and Sabroff, A. M., "Comparison of Mechanical Presses and Screw Presses for Closed-Die Forging", SME Technical Paper MF70-125.

(2) Stöter, J., "Investigation of the Forging Process in Hammer and Press, Particularly as Related to Die Fill", (in German), Doctoral Dissertation, Technical University, Hannover, 1959.

(3) Kienzle, O., "Characteristics of Data in Machine Tools for Closed-Die Forging" (in German), Werkstattstechnik, 55, 1965, p. 509.

(4) Altan, T., and Sabroff, A. M., "Important Factors in the Selection and Use of Equipment for Forging", 28, Part I, II, III, and IV, Precision Metal, June, p. 54, July, August, and September, 1970.

(5) Klafs, U., "On the Determination of Temperature Distribution in Dies and Workpiece During Warmforming" (in German), Doctoral Dissertation, Technical University, Hannover, 1969.

(6) Kienzle, O., "Development Trends in Forming Equipment" (in German), Werkstattstechnik, 49, 1959, p. 479.

(7) Knauss, P., "The Design and Application of the Modern Percussion Press", Sheet Metal Industries, February, 1970, p. 137.

(8) Watermann, D., "Determination of Available Energy in Hammers and Presses With Copper Cylinders" (in German), Werkstattstechnik, 52, 1962, p. 95.

(9) Altan, T., and Nichols, D. E., "Use of Standardized Copper Cylinders for Determining Load and Energy in Forging Equipment", ASME Paper 71-WA/Prod-3.

(10) Bohringer, H., and Kilp, K. H., "The Significant Characteristics of Percussion Presses and Their Measurement", Sheet Metal Industries, May, 1968, p. 335.

(11) Watermann, H. D., "The Blow Efficiency in Hammers and Screw Presses", (in German) Industrie-Anzeiger, No. 77, September 24, 1963, p. 53.

(12) Klaprodt, Th., "Comparison of Characteristics of Screw and Crank Presses for Die Forging" (in German), Industrie-Anzeiger, 90, 1968, p. 1423.

(13) Watermann, H. D., "The Work Accuracy of Hammers and Screw Presses in Off-Center Loading", (in German), Werkstattstechnik, 53, (8), 1963, p. 413.

(14) Makelt, H., "The Mechanical Presses" (in German) Carl Hanser Verlag, Munich, 1961.

(15) Male, A. T., and De Pierre, V., "The Validity of Mathematical Solutions for Determining Friction From the Ring Compression Test", ASME Paper No. 69-WA/Lub-8.

(16) Lee, C. H., and Altan, T., "Influence of Flow Stress and Friction Upon Metal Flow in Upset Forging of Rings and Cylinders", ASME Paper 71/WA/Prod-9.

(17) Jain, S. C. and Bramley, A. N., "Speed and Frictional Effects in Hot Forming" Proceedings of the Institution of Mechanical Engineers, 182, Part I, (39), 1967-68, p. 783.

(18) Saul, G., Male, A. T., and De Pierre, V., "A New Method for the Determination of Material Flow Stress Values Under Metalworking Conditions", Technical Report AFML-TR-70-19, January, 1970.

CHAPTER 5

ISOTHERMAL UNIFORM COMPRESSION TESTS FOR DETERMINING FLOW STRESS OF METALS AT FORGING TEMPERATURES

by

J. R. Douglas, T. Altan, and R. J. Fiorentino

TABLE OF CONTENTS

ISOTHERMAL UNIFORM COMPRESSION TESTS FOR DETERMINING FLOW STRESS OF METALS AT FORGING TEMPERATURES

by

J. R. Douglas, T. Altan, and R. J. Fiorentino

ABSTRACT

Loads, stresses, and energies can be determined for various forging operations if the flow stress of the forged materials is known at the temperature and strain-rate conditions existing during the forging process.

This study describes the fundamentals of uniform compression testing. This test was used to determine the flow stress of 403 stainless steel, Waspaloy, and Ti-6Al-2Sn-4Zr-2Mo in a hydraulic press and the flow stress of 403 stainless steel, Waspaloy, Ti-6Al-2Sn-4Zr-2Mo, Inconel 718, Ti-8Mo-8V-2Fe-3Al, and AISI 4340 steel in a mechanical press. The details of instrumentation, sample preparation, heating, lubrication, data recording and evaluation are given. For a given material and temperature, test results give flow stress versus strain at varying strain rates. The results indicate that these data can be used for practical applications, within a range of strain rates.

INTRODUCTION*

In designing metalforming and forging operations, it is necessary to predict, with some degree of confidence, the force, the stresses, and the energy involved in executing a given operation. For this purpose it is necessary to know, in addition to the geometry of the part being forged, (1) the flow stress of the material being forged, and (2) the friction coefficient, or the friction factor, at the die-material interface. The values of these process parameters must be known, from experimental studies, at the temperature and strain-rate conditions that exist during the actual forging operation.

The friction factor or the friction coefficient is most commonly obtained by using a ring test.(1-4) In this test, a flat, ring-shaped specimen is upset forged to a known reduction. The change in internal diameter, produced by the given amount of reduction in thickness direction, is directly related to friction conditions at the material-tool interface. The ring test is also used in the present program for estimating the friction factor in forging various alloys, as reported in Chapters 4 and 6. The flow stress of metals is usually obtained by conducting a homogeneous or uniform compression test (without barrelling) or a torsion test at the temperatures and strain rates of interest. Most recently, the ring test has been applied with considerable success also for determining the flow stress of metals.(3,4) However, the study described in this chapter concerns only the determination of the flow stress of metals by using the isothermal uniform compression test. In this test, the platens and the cylindrical sample are maintained at the same temperature so that die chilling and its influence upon metal flow is prevented. To be applicable without errors or corrections, the cylindrical sample must be compressed without barrelling, i.e., the state of uniform stress must be maintained in the sample. Barrelling is prevented by using adequate lubrication, for instance graphite in oil for aluminum alloys, and glass for steel, titanium, and high-temperature alloys.

*A detailed discussion of the flow stress of metals was given in Chapter 1. Only the most essential background aspects are reviewed here.

BACKGROUND ON ISOTHERMAL UNIFORM COMPRESSION TEST

In analyzing metal-forming problems, it is useful to define the magnitude of deformation in terms of "logarithmic" strain, $\bar{\epsilon}$. In uniform compression test:

$$\bar{\epsilon} = \int_{h_1}^{h_o} \frac{dh}{h} = \ln \frac{h_o}{h_1} \quad , \qquad (5\text{-}1)$$

where

h_o = initial sample height

h_1 = sample height at the end of compression.

The strain-rate, $\dot{\bar{\epsilon}}$, is the derivation of strain, $\bar{\epsilon}$, with respect to time or:

$$\dot{\bar{\epsilon}} = \frac{d\epsilon}{dt} = \frac{dh}{hdt} = \frac{V}{h} \quad , \qquad (5\text{-}2)$$

where

V = instantaneous compression speed

h = instantaneous height.

The flow stress of metals, $\bar{\sigma}$, is influenced by temperature, θ, strain, $\bar{\varepsilon}$, and strain-rate, $\dot{\bar{\varepsilon}}$, or

$$\bar{\sigma} = f(\theta, \bar{\varepsilon}, \dot{\bar{\varepsilon}}) \quad (5\text{-}3)$$

In most research centers, the isothermal uniform compression test is conducted at a given temperature and at a constant strain rate.(5-8) For this purpose, a plastometer is used. This machine, designed and built first by Orowan,(9) contains a cam that can be rotated at various constant speeds. As seen in Figure 5-1, the cam has an operative portion generated over 90 degrees. The cam actuating the lower platen has a curvature of logarithmic shape. Thus, for the cam rotation at a constant speed, the ram velocity varies during deformation according to Equation (5-2) such that the strain rate remains constant. In a typical experimental setup, the specimen is compressed between lower and upper platens of tungsten or titanium carbide.(5-7) To reduce temperature variations in the specimen during transfer from furnace to the plastometer, a guard ring box, made of a nickel-base alloy is used, Figure 5-2. This complete assembly is heated to the required testing temperature in an electric furnace with an argon atmosphere. The assembly is then transferred to the plastometer. A triggering mechanism activates the cam, which rotates at the desired speed, and the specimen is compressed within a few seconds after withdrawing the guard box from the furnace. The temperature variation during this time period does not exceed a few degrees and it does not distort the test conditions. During the compression test the load and the ram displacement are recorded in function of time and the flow stress-strain relationship is calculated from these data for the given material, temperature, and strain rate. To achieve true uniform compression it is necessary to completely eliminate specimen bulging and friction at specimen and platen interfaces. This is accomplished by using appropriate lubricants such as Teflon foil (up to 500 F), graphite-oil or graphite-water emulsions (up to 1000 F), and glasses at higher temperatures. A list of glass-base lubricants recommended in the literature for high deformation temperatures are given in Table 5-1.(5)

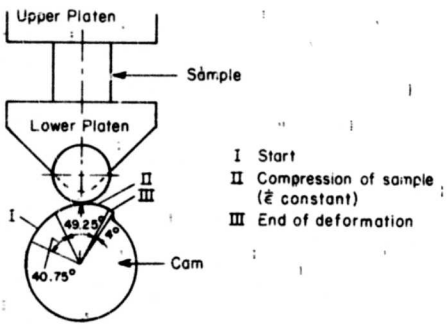

FIGURE 5-1. SCHEMATIC OF THE CAM PLASTOMETER DRIVE FOR CONDUCTING CONSTANT STRAIN-RATE COMPRESSION TESTS(7)

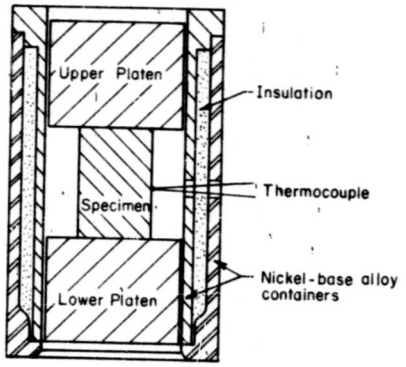

FIGURE 5-2. SCHEMATIC OF THE TOOLING USED FOR HIGH-TEMPERATURE COMPRESSION TESTS CONDUCTED IN A PLASTOMETER(5,6)

TABLE 5-1. COMPOSITIONS AND USEFUL TEMPERATURE RANGES OF GLASS LUBRICANTS USED IN ISOTHERMAL COMPRESSION TESTS IN EARLIER STUDIES(5)

Composition, percent	Glass: / Temperature Range, F:	A 850-1100	B 1100-1400	C 1500-1800	D (Pyrex) 1800-2000	E 2000-2200
SiO_2		--	27.3	69	80	55
B_2O_3		20	--	1.2	12	7
BaO		--	--	--	--	3
Al_2O_3		--	--	3.4	3	21
CaO		--	--	6.1	--	14
MgO		--	--	3.2	--	--
PbO		30	71	--	--	--
Na_2O		--	--	16.2	4	--
K_2O		--	1.5	0.7	0.3	--

EQUIPMENT, INSTRUMENTATION, AND TOOLING

Equipment

In conducting the present study, a cam plastometer was not available for constant strain-rate compression tests. Therefore, the experimental work was performed in two presses installed at the Metalworking Laboratory of Battelle's Columbus Laboratories. The presses are a 700-ton hydraulic press and a 500-ton mechanical forging press. In the compression tests performed in these presses the strain rates varied during a deformation stroke. However, average values of strain rates can still be considered in using the experimental flow-stress data for practical applications.

The vertical 700-ton hydraulic press, Figure 5-3, is direct driven, uses hydraulic oil as a working medium, and has an adjustable ram speed of 0.1 to 80 ipm. In the trials conducted in this study, the press operated at two nominal pressing speeds: 20 ipm and 80 ipm. At the start of a pressing cycle, this press operates by free falling of the ram until the upper platen contacts the specimen to be upset forged. The velocity of the ram during this free-fall period has been measured to be within 250 to 1000 ipm, depending on the setting of press speed; the impact of the ram at this velocity was adequate to completely upset forge some test specimens. Usually, however, after contact was made with the specimen, a dwell time existed while the hydraulic oil driving the press ram was pressurized. Deformation then proceeded at a relatively constant rate.

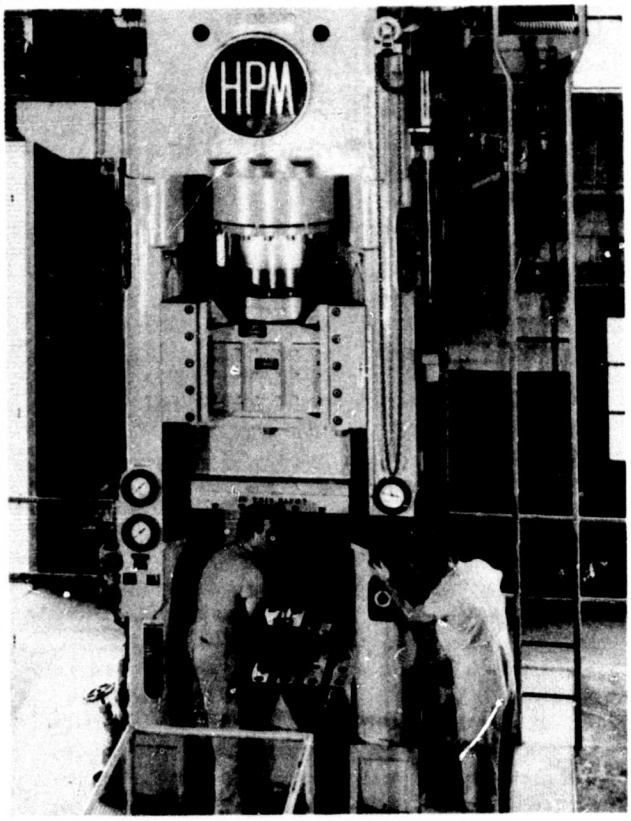

FIGURE 5-3. BATTELLE'S 700-TON, DIRECT-DRIVE, VARIABLE-SPEED HYDRAULIC PRESS USED IN ISOTHERMAL UNIFORM COMPRESSION TESTS

The mechanical press, seen in Figure 5-4, is a forging press of Scotch-yoke design. This press is rated 500 tons at 0.25 inch before bottom dead center, has a stroke of 10 inches and has a forging rate equivalent to 90 strokes per minute. The drive of this press is basically a slider-crank mechanism that translates rotary into reciprocating linear motion. The eccentric shaft is connected through an air-operated, multiplate friction clutch directly to the flywheel. The flywheel, driven by an electric motor and "V" belts, stores energy that is used only during a small portion of the crank revolution, namely during deformation of the forged material. The constant clutch torque is available at the eccentric shaft which transmits the torque and the flywheel energy to the slide, through the Scotch-yoke mechanism.

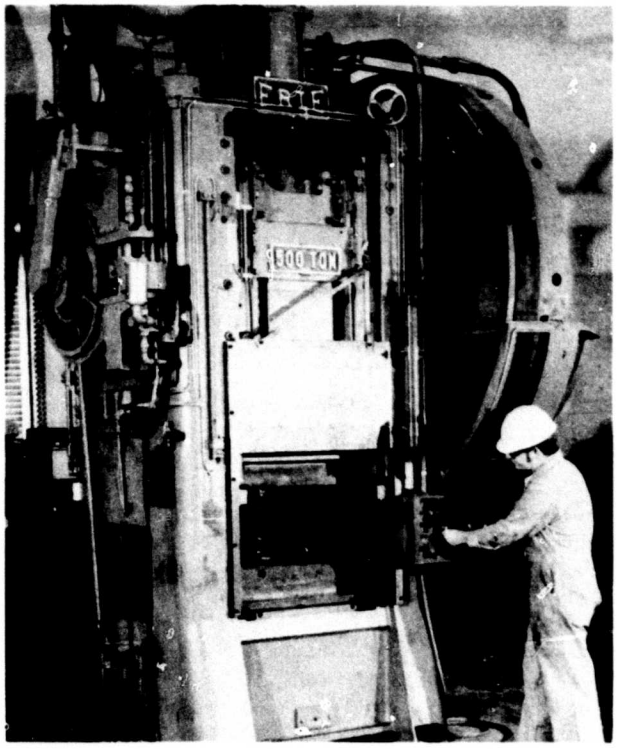

FIGURE 5-4. BATTELLE'S 500-TON SCOTCH YOKE MECHANICAL PRESS USED IN ISOTHERMAL UNIFORM COMPRESSION TESTS

Instrumentation*

In both presses, load and displacement were measured during the flow-stress trials. The displacement measurements were made using a linear variable differential transformer (LVDT). The load measurements were made via a 25-ton load cell placed under the tooling.

In the mechanical press the core of the LVDT was fixed relative to the ram of the press and moved through the center of the LVDT coils which were attached to the press frame. To accomplish this relative motion, the core was suspended between brass rods (nonmagnetic) which were in turn attached to the press frame. Thus, the motion of the core was completely dependent on the motion of the ram. In the hydraulic press an LVDT having a spring-loaded core was used.

*An extensive description of general press instrumentation is given in Chapter 2.

This transducer was placed to the rear of the press bolster and the core was actuated by a bracket attached to the moving ram.

The load cell used in these trials was a Model 35-133-BCF manufactured by the Toroid Corporation. It was a combination compression-tension load cell using bonded strain gages as its strain-sensing mechanism. The load cell was designed for use to 50,000 pounds with safe overload to 150 percent of capacity.

For forging in the hydraulic press, the output signals from the two transducers (LVDT and load cell) were recorded on a two-channel Brush Model 280 oscillographic recorder. For load measurement the recorder was set up so that a full-scale deflection represented either 50,000 pounds or 100,000 pounds. The displacement output was adjusted so that approximately 2 inches of ram displacement was represented by a full-scale deflection on the recorder.

Because of the higher forging rate in the mechanical press, the transducer outputs were recorded on a multichannel high-speed, light-beam recorder (Century Electronics Model 470). The scale magnifications were set up to give a sweep of 5 inches for either 50,000 or 100,000 pounds load on the load cell and a 1-inch sweep for 1-inch movement of the displacement transducer. The time variable was established by time lines recorded each 0.01 second.

Specimens and Tooling

The specimens used in these compression tests were all 1-inch-diameter and 1-1/2 inches high. The ends were machined flat and perpendicular to the axis of the specimen. A 1/16-inch radius was machined on the specimen edges, and a spiral groove, about 0.010 inch deep, was cut on each end to trap lubricant and assist in minimizing friction losses.

The specimens were heated in an insulated container that also held the platens (Figure 5-5). The container was constructed from Inconel alloy 601 (60.5 Ni – 23 Cr – 14.1 Fe – 1.35 Al) which was selected for its excellent resistance to oxidation at high temperature. The platens were cemented titanium carbide (Kentanium K162B supplied by Kennametal, Inc.) which was selected on the basis of its excellent strength and hardness at high temperature. A ceramic material made up of 98 percent Al_2O_3 was also considered for the platen material but was found unsatisfactory due to its poor resistance to thermal shock.

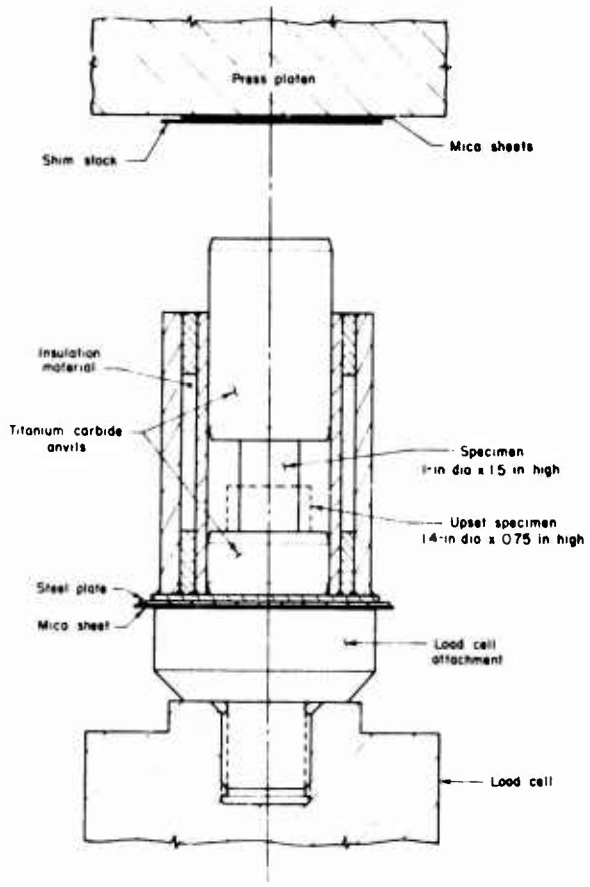

FIGURE 5-5. PRESS SETUP AND FIXTURE USED IN HEATING AND ISOTHERMAL UNIFORM UPSETTING OF CYLINDRICAL SAMPLES

(Initial sample size 1.0-inch diameter x 1.5 inches high)

The titanium carbide platens suffered serious erosion when exposed to the glass lubricant in air at high temperatures (1600 to 2200 F). To explore this problem a number of tests were run in an electric furnace without atmospheric control. In these tests a small amount of a particular glass was put on a carbide platen and placed in the furnace and maintained at different temperatures (1800 F, 1900 F, 2000 F, 2100 F) for various lengths of time (15 minutes to 1 hour). These tests illustrated more clearly the nature of the erosion and the preventive measures that might be taken. As a result of these tests the following observations were made.

- The erosion occurred regardless of the glass composition. However, the magnitude of erosion increased with increasing temperature and decreasing glass viscosity
- The erosion was limited to the edges of the puddle of molten glass indicating that the combined exposure to molten glass and atmosphere was necessary for the erosion to occur.

- The amount of erosion could be greatly reduced if the titanium carbide was placed in a container that was flooded with argon. This indicated that the reaction of the glass with the titanium carbide required the presence of air (probably the oxygen in air) and that the reaction could be prevented if the platens were not exposed to air simultaneously with the glass.

The basic chemical phenomenon involved in this erosion problem was not further investigated since that task was not within the scope of the present study. As a result of the tests described above, the fixture, seen in Figure 5-5, and the test cylinders were heated in an argon atmosphere. However, in performing the compression tests over several hours, it was found that some erosion of the carbide platens still occurred. Thus, in addition to argon atmosphere, the surface of the bottom anvil was protected by flooding it with molten glass while heating the entire assembly in the furnace. The top anvil could not be protected easily, consequently, its forging surface was reground as necessary.

ISOTHERMAL UNIFORM COMPRESSION TESTS

In an upset test to obtain flow-stress data, the specimen must deform uniformly, without any bulging. Then, the instantaneous forging pressure is equal to the instantaneous flow stress of the sample material at temperature, strain-rate, and strain conditions present at that instant of deformation. Bulging can be prevented and uniform deformation conditions can be achieved by eliminating die chilling and friction effects at the die-sample interface. Die chilling is avoided by maintaining the tooling and the sample at the same temperature, friction effects are minimized by having adequate lubrication. The uniform compression test discussed in the present work is called isothermal because the tooling and the sample are at the same temperature at the start of deformation. However, during deformation heat is generated and isothermal conditions do not exist in a strict sense.

The effect of lubrication in metal flow in upsetting is illustrated in Figure 5-6. The lubricant application must be sufficient but not too heavy, otherwise the reverse bulging seen in Figure 5-6c may result. Excess lubricant at the interface builds a film which is heavier at the center and thinner towards the edges. The nonuniformity of lubricant thickness generates local lateral stresses which push the edges of the sample further out than the rest of the material A detailed study of this phenomenon is given elsewhere.[10]

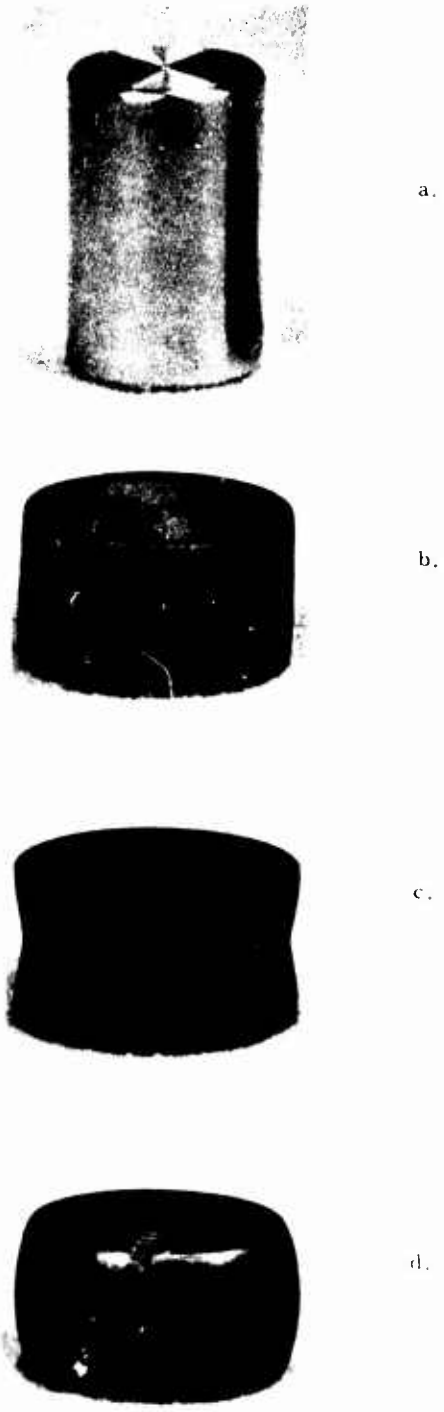

FIGURE 5-6. CYLINDRICAL SAMPLES USED IN ISOTHERMAL UNIFORM COMPRESSION TESTS

(a) Prior to deformation (1-inch diameter by 1.5 inches high)
(b) Upset with adequate lubrication
(c) Upset with excessive lubrication
(d) Upset with poor lubrication.

Experimental Procedure

The upset trials were conducted in the heated insulated container, seen in Figure 5-5. The principal purposes in using this container were to minimize cooling of the sample during transfer from furnace to the forging press, and to maintain truly isothermal conditions by heating the carbide anvils to the forging temperature.

Before conducting any compression trials, it was necessary to determine the magnitude of temperature drop in the compression cylinder after removal from the furnace and prior to forging. For this purpose, a cylinder with a thermocouple in a hole drilled to the cylinder center, was put in the container with the anvils in place, Figure 5-5. The container was then placed in the furnace directly over a thermocouple on the furnace hearth. The temperature was monitored from both of these thermocouples as well as from the furnace-control thermocouple and it was possible to determine the relationship between furnace, hearth, and cylinder temperatures during heating. When the container assembly attained a uniform temperature, it was removed from the furnace and carried to the press simulating the time lapse during a compression test. The time lapse to forging based on this test simulation, was found to be approximately 15 seconds. The temperature drop in the cylinder was found to be 10 F in about 30 seconds after removal of the container assembly from the furnace. Thus, it was concluded that the variation in forging temperatures during the tests could be conservatively estimated at less than 10 F.

For the compression tests, the cylinders were first lubricated at room temperature by dipping them in a slurry of glass in isopropyl alcohol and allowed to dry. They were then placed in the furnace next to the protective container and heated to the forging temperature. Approximately 15 minutes prior to each test, the sample was placed on the lower anvil of the container, and the top anvil was inserted. The entire assembly was then returned to the furnace and reheated to the forging temperature. While the glass-slurry coating on the sample minimized oxidation, it was inadequate to provide sufficient lubrication during the upset test. Therefore, additional powdered glass was sprinkled on the bottom anvil and on the top of the specimen, after placing it into the container. This technique worked well and allowed uniform upsetting of the cylindrical samples, Figure 5-6.

To minimize the possibility of thermal shock to the titanium carbide anvils, the container and the anvils were placed in the cold furnace at the start of each series of tests and were brought to temperature with the furnace. Since the platens of the press could chill the anvils rapidly during forging and possibly cause anvil cracking because of the large temperature gradients, insulation was placed above and below the container in the press. On the top press platen, thin sheets of mica were held in place by a thin sheet of steel taped to the platen. On the bottom, the container rested on an attachment to the load cell, and the possible thermal shock was minimized by placing a mica sheet and a thin steel sheet between the container and the load cell attachment, Figure 5-5.

After a cylinder had been upset forged, it was quickly removed from the container and replaced by a preheated unforged cylinder. During the reloading period, the average temperature of the container dropped about 500 to 600 F. Occasionally it was necessary to replenish the glass on the bottom anvil. The container was then returned to the furnace to be reheated to the forging temperature.

Materials and Lubrication

The isothermal uniform compression tests conducted in the present study are summarized in Table 5-2. Among the several glass-base lubricants used in this study, two gave the best lubrication conditions. The composition and the useful temperature range of application for these two glasses are given in Table 5-3. As discussed earlier, prior to heating, the samples were dipped into a glass slurry. After heating, powdered glass was applied upon the flat surfaces of the samples as well as on the anvils of the tooling.

TABLE 5-2. TEMPERATURES (IN DEGREES F) USED IN ISOTHERMAL UNIFORM COMPRESSION OF VARIOUS MATERIALS IN A 700-TON HYDRAULIC PRESS AND A 500-TON MECHANICAL PRESS

	Hydraulic Press Preset Speed, in./min		Mechanical Press
	20	80	
AISI 403 Stainless			1800
	1950	1950	1950
	2050	2050	2050
Waspaloy	1950		1950
	2050		2050
			2100
Ti-6Al-2Sn-4Zr-2Mo	1675	1675	1600
	1750		1675
			1750
Inconel Alloy 718			2000
			2100
Ti-8Mo-8V-2Fe-3Al			1650
			1850
			2000
AISI 4340 Steel			1900
			2000

TABLE 5-3. COMPOSITION AND USEFUL TEMPERATURE RANGE FOR GLASS LUBRICANTS USED IN THIS STUDY

Glass Type and Temperature Range	Composition, percent by weight								
	Fe_2O_3	SiO_2	B_2O_3	Al_2O_3	Na_2O	K_2O	CaO	MgO	SO_3
Pyrex (1850-2000 F)		80	12	3	4	0 3			
Window Glass (1650-1800 F)	0 1	72		0 9	14	0 1	9	3 4	0 3

Experimental Results

For each test condition given in Table 5-1, at least two samples were used. The upset samples that exhibited bulging were discarded in data evaluation. When two or more uniformly deformed samples were available the load-displacement data for these samples did not show any marked deviation from each other. Thus, only one of the oscillograph recordings was evaluated.

To obtain the flow-stress-versus-strain curve, a relatively simple computer program was developed and the data were processed as follows. The coordinates, in the vertical and horizontal direction, of load and displacement recordings on the oscillograph were read off in inches, as seen in Figure 5-7. These coordinates and the calibration factors indicating the actual value of 1-inch sweep in terms of load, displacement, and time, represented the input data for the computer program This program calculated, at small time or deformation steps, the flow stress (load divided by instantaneous area), the strain (natural logarithm of the ratio of initial sample height to instantaneous sample height), and the strain rate (instantaneous velocity divided by instantaneous height). The results are plotted by the Calcomp plotter in form of flow-stress-versus-strain, and strain-rate-versus-strain curves.

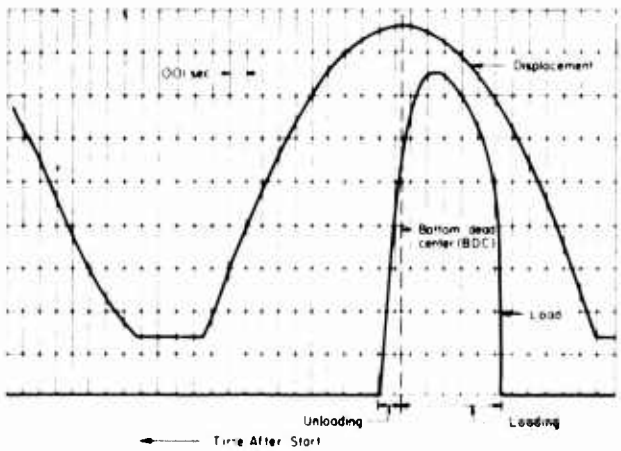

FIGURE 5-7. A TYPICAL OSCILLOGRAPH RECORDING OBTAINED IN CONDUCTING ISOTHERMAL UNIFORM COMPRESSION TESTS IN A MECHANICAL PRESS

In evaluating the data for the tests conducted in the mechanical press, the ram displacement was determined using the following relation:

$$w = s\,(1 - \cos\alpha)/2 \quad , \qquad (5\text{-}4)$$

where

w = distance from bottom dead center

s = press stroke = 10 inches

α = angle of rotation, measured from bottom dead center position.

Since the mechanical press used in the present study was of Scotch yoke design, Equation (5-4) accurately represented the displacement behavior of the ram. The ram position predicted by Equation (5-4) was compared with the displacement data obtained from the oscillograph and excellent agreement – within less than 1 percent – was found. The derivative of Equation (5-4) with respect to α gave the velocity variation during deformation and this velocity was used in calculating the strain rates. This procedure helped to avoid the irregularities in velocity curves obtained by numerical differentiation of experimental displacement data. These irregularities occur because the numerically differentiated velocity curve is much more sensitive to data-reading errors than the displacement curve itself. The ram velocity at the start of deformation was within a range of 22 to 26 in./sec at the start of deformation. The velocity decreases, following a sine curve toward the end of deformation, to reach the value zero.

In evaluating the data for the tests conducted in the hydraulic press, the strain-rate curves plotted by the computer showed some irregularities which were smoothed out by hand. This smoothing, however, is within the range of strain-rate variation encountered during the compression tests and did not impair the quality of the flow stress-strain data obtained in hydraulic press tests.

The results of uniform isothermal compression tests are given in Figures 5-8 through 5-16 for tests conducted in the hydraulic press, and in Figures 5-17 through 5-22 for tests conducted in the mechanical press. Each figure shows, in addition to the curve for flow stress versus strain at a particular temperature, the variation of strain rate, during deformation of the test samples.

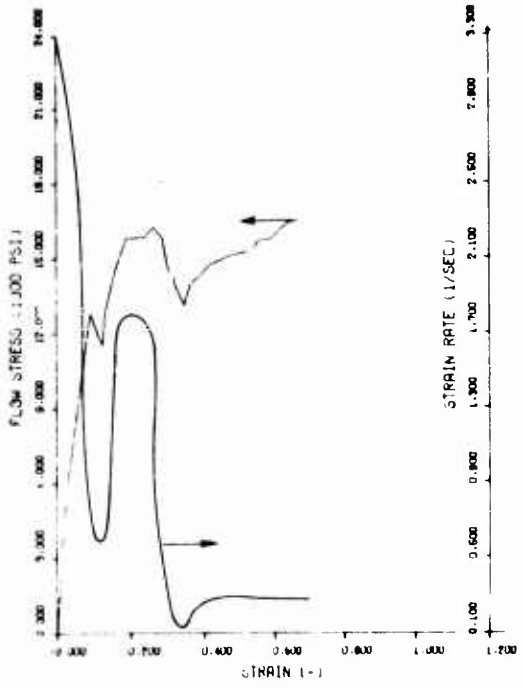

FIGURE 5-8. FLOW STRESS, $\bar{\sigma}$, VERSUS STRAIN, $\bar{\epsilon}$, FOR 403 STAINLESS STEEL OBTAINED FROM ISOTHERMAL UNIFORM COMPRESSION TEST

(Hydraulic press, 20 ipm, 1950 F)

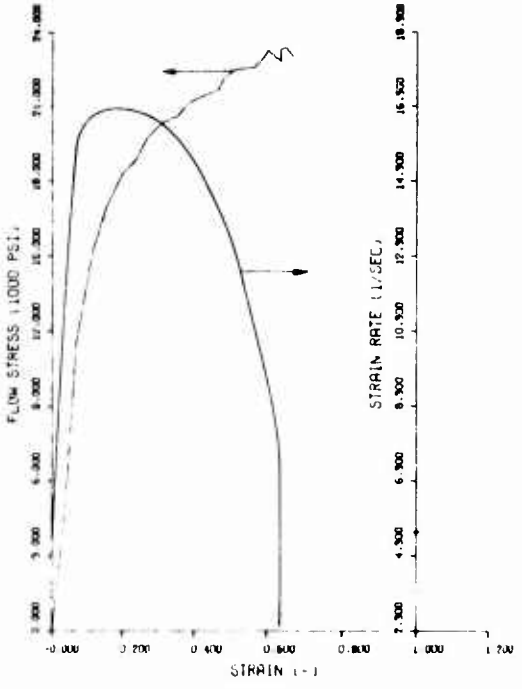

FIGURE 5-10. FLOW STRESS, $\bar{\sigma}$, VERSUS STRAIN, $\bar{\epsilon}$, FOR 403 STAINLESS STEEL OBTAINED FROM ISOTHERMAL UNIFORM COMPRESSION TEST

(Hydraulic press, 80 ipm, 1950 F)

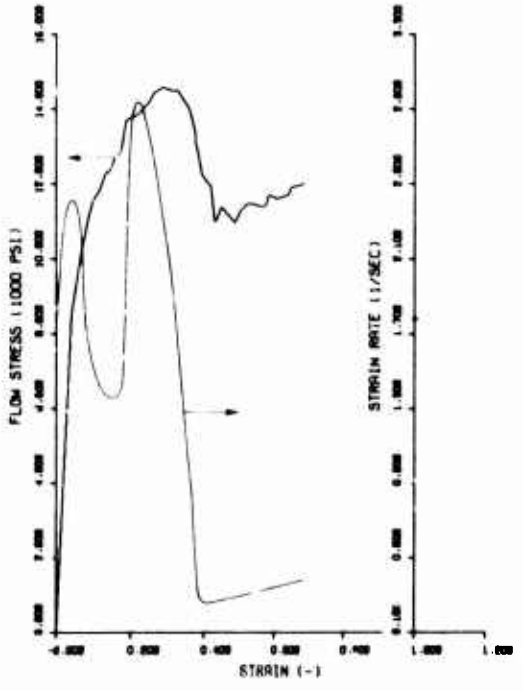

FIGURE FLOW STRESS, $\bar{\sigma}$, VERSUS STRAIN, $\bar{\epsilon}$, FOR 403 STAINLESS STEEL OBTAINED FROM ISOTHERMAL UNIFORM COMPRESSION TEST

(Hydraulic press, 20 ipm, 2050 F)

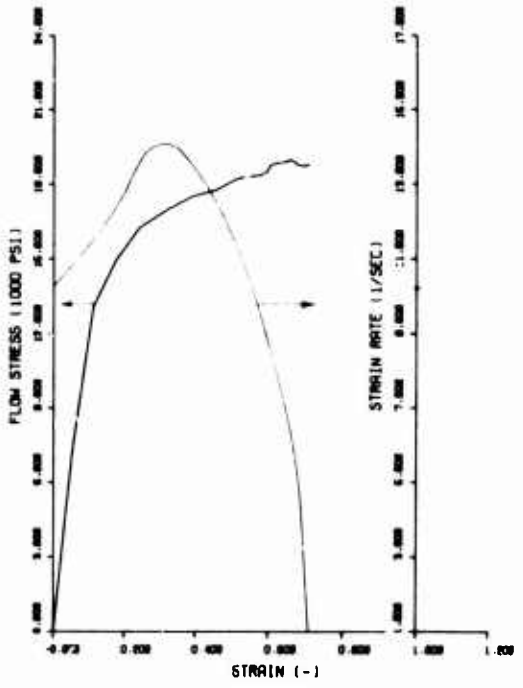

FIGURE 5-11. FLOW STRESS, $\bar{\sigma}$, VERSUS STRAIN, $\bar{\epsilon}$, FOR 403 STAINLESS STEEL OBTAINED FROM ISOTHERMAL UNIFORM COMPRESSION TEST

(Hydraulic press, 80 ipm, 2050 F)

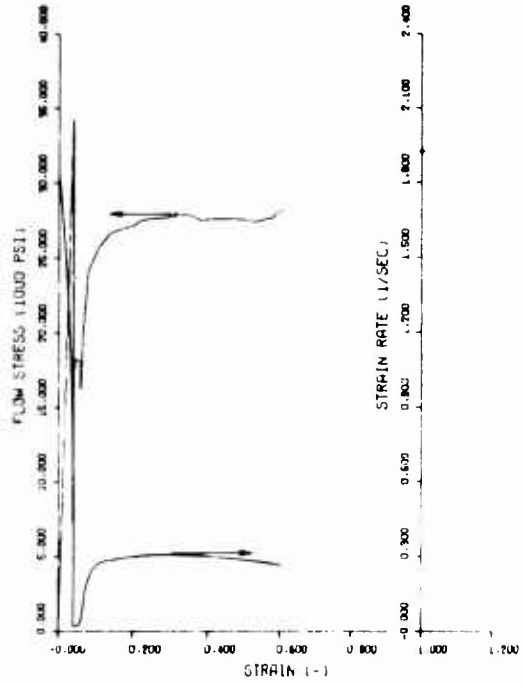

FIGURE 5-12. FLOW STRESS, $\bar{\sigma}$, VERSUS STRAIN, $\bar{\epsilon}$, FOR WASPALOY OBTAINED FROM ISOTHERMAL UNIFORM COMPRESSION TEST

(Hydraulic press, 20 ipm, 1950 F)

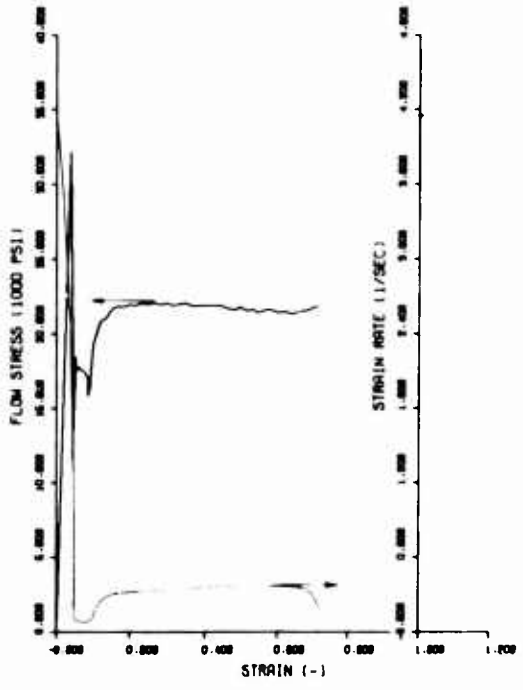

FIGURE 5-13. FLOW STRESS, $\bar{\sigma}$, VERSUS STRAIN, $\bar{\epsilon}$, FOR WASPALOY OBTAINED FROM ISOTHERMAL UNIFORM COMPRESSION TEST

(Hydraulic press, 20 ipm, 2050 F)

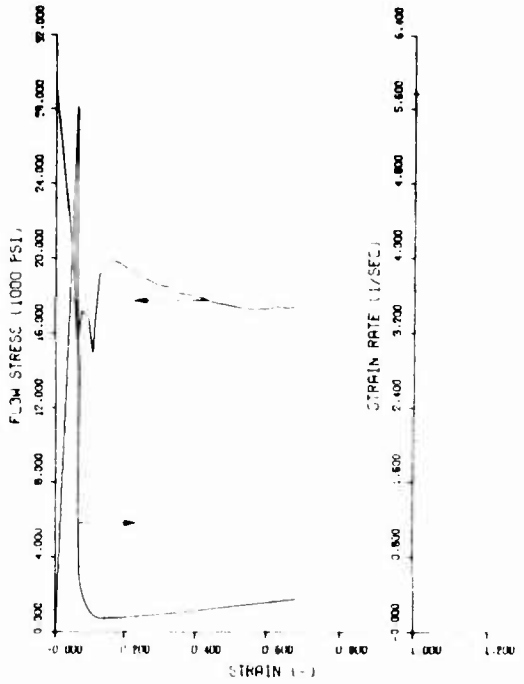

FIGURE 5-14. FLOW STRESS, $\bar{\sigma}$, VERSUS STRAIN, $\bar{\epsilon}$, FOR Ti-6Al-2Sn-4Zr-2Mo OBTAINED FROM ISOTHERMAL UNIFORM COMPRESSION TEST

(Hydraulic press, 20 ipm, 1675 F)

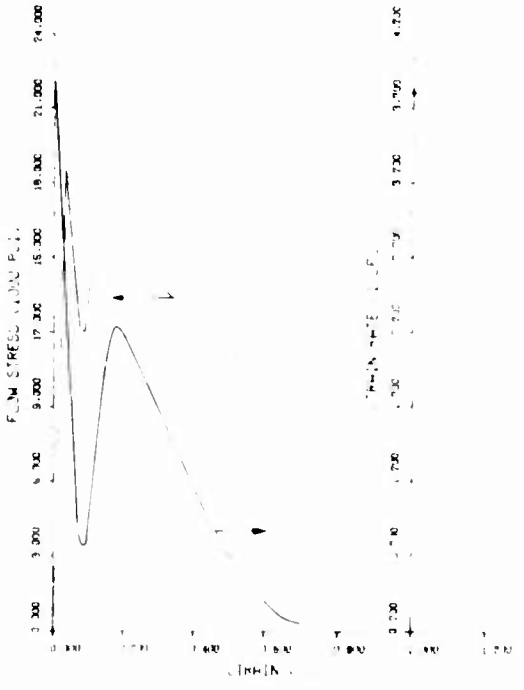

FIGURE 5-15. FLOW STRESS, $\bar{\sigma}$, VERSUS STRAIN, $\bar{\epsilon}$, FOR Ti-6Al-2Sn-4Zr-2Mo OBTAINED FROM ISOTHERMAL UNIFORM COMPRESSION TEST

(Hydraulic press, 20 ipm, 1750 F)

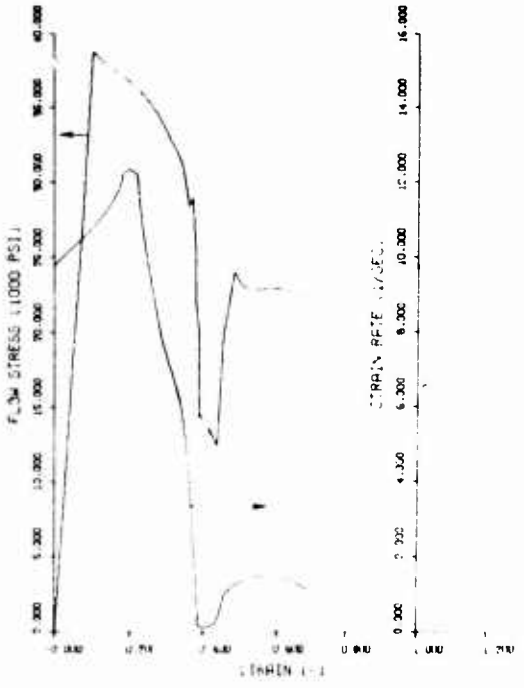

FIGURE 5-16. FLOW STRESS, $\bar{\sigma}$, VERSUS STRAIN, $\bar{\varepsilon}$, FOR Ti-6Al-2Sn-4Zr-2Mo OBTAINED FROM ISOTHERMAL UNIFORM COMPRESSION TEST

(Hydraulic press, 80 ipm, 1675 F)

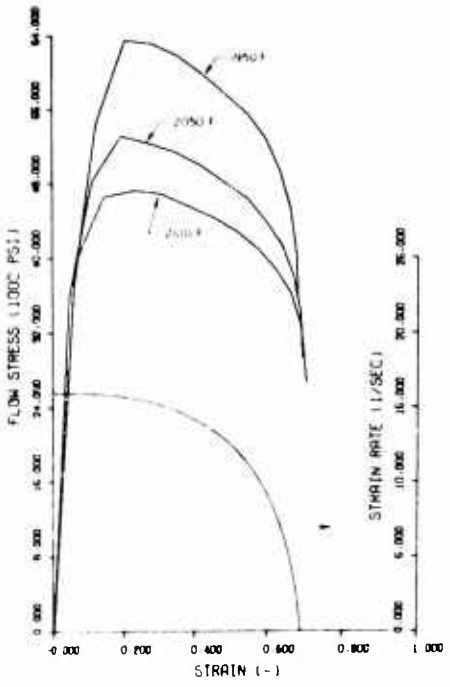

FIGURE 5-18. FLOW STRESS, $\bar{\sigma}$, VERSUS STRAIN, $\bar{\varepsilon}$, FOR WASPALOY AT 1950 F, 2050 F, AND 2100 F OBTAINED FROM ISOTHERMAL UNIFORM COMPRESSION TESTS CONDUCTED IN A MECHANICAL PRESS

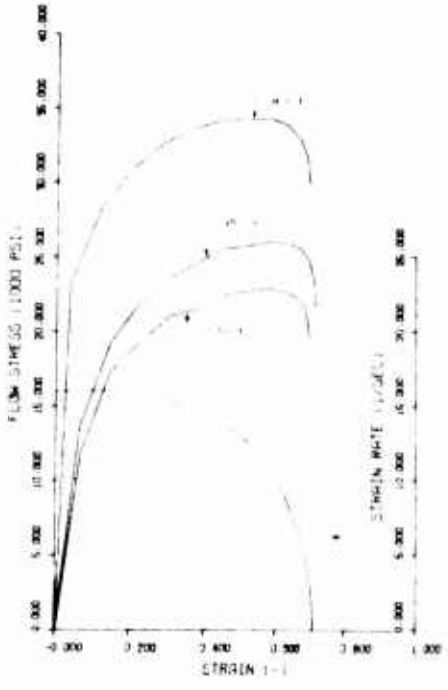

FIGURE 5-17. FLOW STRESS, $\bar{\sigma}$, VERSUS STRAIN, $\bar{\varepsilon}$, FOR 403 STAINLESS STEEL AT 1800 F, 1950 F, AND 2050 F OBTAINED FROM ISOTHERMAL UNIFORM COMPRESSION TESTS CONDUCTED IN A MECHANICAL PRESS

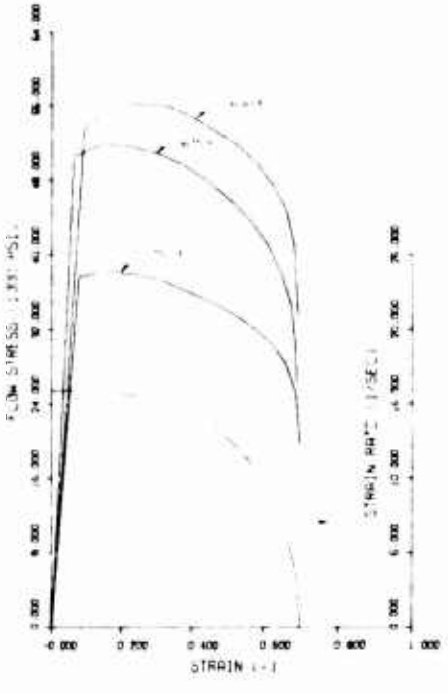

FIGURE 5-19. FLOW STRESS, $\bar{\sigma}$, VERSUS STRAIN, $\bar{\varepsilon}$, FOR Ti-6Al-2Sn-4Zr-2Mo AT 1600 F, 1675 F, AND 1750 F OBTAINED FROM ISOTHERMAL UNIFORM COMPRESSION TESTS CONDUCTED IN A MECHANICAL PRESS

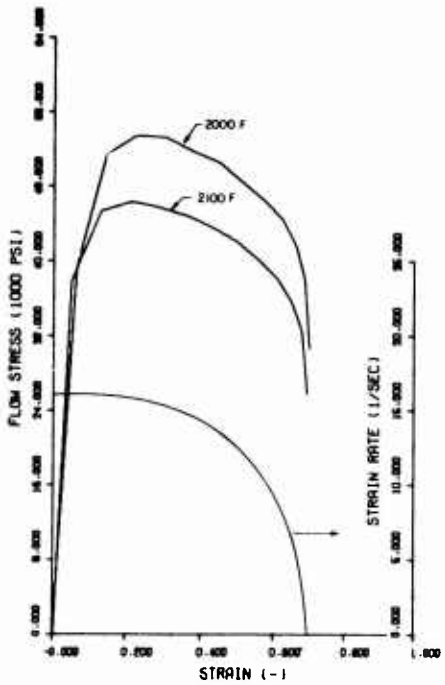

FIGURE 5-20. FLOW STRESS, $\bar{\sigma}$, VERSUS STRAIN, $\bar{\epsilon}$, FOR INCONEL 718 AT 2000 F AND 2100 F OBTAINED FROM ISOTHERMAL UNIFORM COMPRESSION TESTS CONDUCTED IN A MECHANICAL PRESS

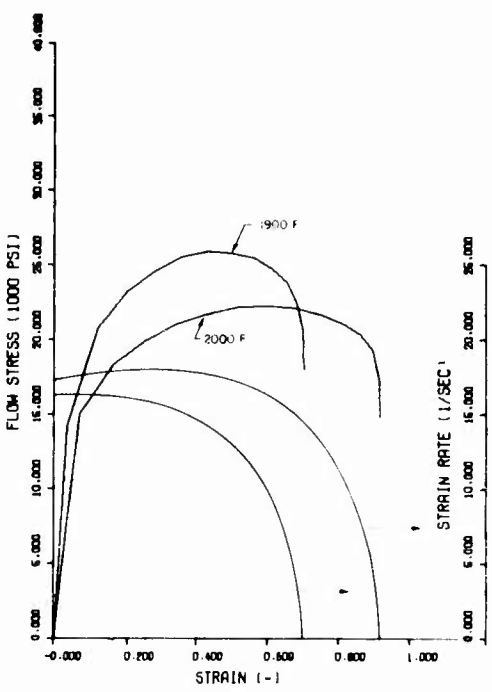

FIGURE 5-22. FLOW STRESS, $\bar{\sigma}$, VERSUS STRAIN, $\bar{\epsilon}$, FOR AISI 4340 STEEL AT 1900 F AND 2000 F OBTAINED FROM ISOTHERMAL UNIFORM COMPRESSION TESTS CONDUCTED IN A MECHANICAL PRESS

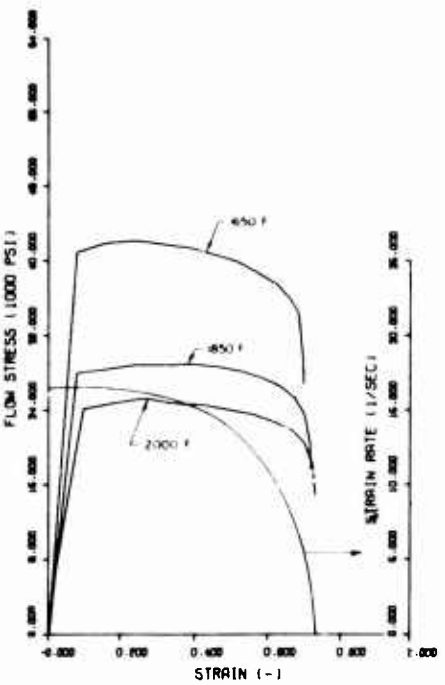

FIGURE 5-21. FLOW STRESS, $\bar{\sigma}$, VERSUS STRAIN, $\bar{\epsilon}$, FOR Ti-8Mo-8V-2Fe-3Al AT 1650 F, 1850 F, AND 2000 F OBTAINED FROM ISOTHERMAL UNIFORM COMPRESSION TESTS CONDUCTED IN A MECHANICAL PRESS

SUMMARY AND DISCUSSION

The isothermal uniform compression tests were conducted under a hydraulic and a mechanical press. As the velocity behavior of these two machines is drastically different from each other, it is necessary to review the tests conducted in each press separately.

Hydraulic Press Tests

As discussed earlier, the hydraulic press used in the present studies was direct driven. Thus, at the start of the pressing cycle, the action of the press ram falling freely on the tooling is similar to that of the ram of a hammer. In some tests, this impact had sufficient energy to completely deform the test cylinder to approximately 50 percent reduction in height. In others, the cylinder was only partially deformed during the initial impact, and after the ram slowed down drastically, it was again accelerated by the pump pressure and the compression of the cylinder proceeded. This phenomenon is well illustrated for 403 stainless steel in Figure 5-8 and 5-9, and for Waspaloy in Figures 5-12 and 5-13, where the strain-rate exhibits a rather erratic variation, due to the irregular acceleration and deceleration of the press ram. However, it is

interesting to note that the flow stress follows approximately the variation in strain rate, i.e., it increases with increasing strain rate and vice versa. As expected, the flow stress is lower at higher temperatures and lower strain rates, as illustrated in Figures 5-8 through 5-11 for 403 stainless steel. A similar observation is made for Ti-6Al-2Sn-4Zr-2Mo in Figures 5-14 through 5-16. The comparison of Figures 5-11 and 5-16 illustrate that at a comparable range of strain-rates, 10 to 14/sec and at respective deformation temperatures, the flow stress for 403 stainless steel increases with increasing strain while that for Ti-6Al-2Sn-4Zr-2Mo decreases with increasing strain. This is because the heat generation and thermal softening are significant in the titanium alloy. This observation, made also in the mechanical press experiments, will be discussed again later.

Mechanical Press Tests

In mechanical press experiments, with increasing strain, the strain rate decreases following a curve similar to a trigonometric function, as seen in Figures 5-17 through 5-22. This is expected considering the displacement-stroke behavior of a mechanical press. The decrease in strain rate is initially small, from $\bar{\epsilon} = 0$ up to $\bar{\epsilon} = 0.4$ or 0.5, but it is drastic toward the end of deformation, i.e., toward $\bar{\epsilon} \simeq 0.7$, which corresponds to about 50 percent reduction in height of the compressed samples. The large drop in strain rate toward the end of deformation, is accompanied with a sudden drop in flow stress for all materials and test temperatures. This is because, at higher temperature, the flow stress of metals decreases with decreasing strain rate.

For practical purposes the very sharp, nearly vertical, drop in flow stress values, for drastically decreasing strain rate, can be ignored. (The flow-stress data at very low strain rates are significant only in isothermal forging, in which heated dies allow advantage to be taken of the relatively low forging pressures.) It is then observed that, in 403 stainless steel and 4340 steel, flow stress continues to increase and becomes uniform over the practical strain range, up to strain $\bar{\epsilon} \simeq 0.7$. This observation is in good agreement with the fact that flow-stress values for steels obtained at constan strain rate, given in literature, do not vary with strain.

For example, in Table 1-4 of Chapter 1, the C values (of equation $\bar{\sigma} = C\,\dot{\bar{\epsilon}}^{m}$) given for 403 SS, for 1470 F, 1830 F, and 2190 F, show hardly any variation with strain. This is because flow stress values of steels being relatively low at hot forming temperatures (20,000 to 30,000 psi), the heat generation and softening due to the heat-up are relatively insignificant. Thus, for steels, the maximum values given in flow-stress-versus-strain curves can be used as practical values for the existing strain-rate, $\dot{\bar{\epsilon}}$, range, namely $\dot{\bar{\epsilon}} \simeq 10$ to 15/second.

For titanium alloys above 1650 F (Table 1-7 of Chapter 1), the C values decrease slightly with increasing strain, although these data are obtained from constant-strain-rate tests, conducted on a plastometer. This decrease of C with increasing strain is due to heat-up effects during the test. A similar observation is made in Figures 5-18 through 5-20, where the flow stress values are relatively high, in the range of 40,000 to 60,000 psi. In Figure 5-21, for Ti-8Mo-8V-2Fe-3Al, the flow stress values are in the range of 24,000 to 40,000 psi and they do not significantly decrease with increasing strain. Thus, it can be concluded that for Waspaloy, Inconel 718, and Ti-6Al-2Sn-4Zr-2Mo, the slight decrease of flow stress with increasing deformation is largely due to internal heat generation and it cannot be explained solely with strain-rate effect.

The internal heat generation encountered during the uniform compression test was discussed in detail, in Chapter 1. The temperature increase due to heat generation, $\Delta\theta$, can be estimated from

$$\Delta\theta = \frac{\bar{\epsilon}\,\bar{\sigma}_a}{J\,c\,\rho} \cdot \beta \quad , \qquad (5\text{-}5)$$

where, using the metric system,

$\Delta\theta$ = temperature increase due to deformation heat, degree C

c = heat capacity, cal/g degree C

ρ = density, g/cm^3

J = conversion factor from mechanical to thermal energy, $J = 4.27$ kg mm/Kcal

β = percentage of mechanical deformation energy transformed into heat, $\beta \simeq 0.95$

Equation (5-5) illustrates that the temperature increase, $\Delta\theta$, due to heat generation is directly proportional to the average flow stress, and inversely proportional to the product of heat capacity and specific gravity. As an example, let us assume the value of $\bar{\sigma}$ at $\bar{\epsilon} = 0.3$ as an average value for the entire compression test, i.e., for about 50 percent reduction in height, or for $\bar{\epsilon} = 0.7$. The temperature increase for 403 stainless steel, $\Delta\theta_S$, at 1800 F and for the titanium alloy, Ti-6Al-2Sn-4Zr-2Mo at 1600 F, $\Delta\theta_T$, can be estimated by using Equation 5-5. The following approximate values are used;

TABLE 5-4. AVERAGE FLOW-STRESS VALUES SUGGESTED FOR USE IN PREDICTING LOADS AND STRESSES IN PRACTICAL FORGING OPERATIONS

(These Data are Summarized From Figures 5-8 Through 5-22)

Material	Flow Stress, 10^3 psi	Temperature, F	Range of Strain, $\ln \frac{l_0}{l_1}$	Range of Strain Rate, 1/sec	From Figure[a]
403 Stainless Steel	33.0	1800	0.3-0.7	10.0-14.0	5-17 M
	16.0	1950	0.1-0.7	0.2-1.6	5-8 H
	23.0	1950	0.4-0.7	16.0-17.0	5-10 H
	25.0	1950	0.3-0.7	10.0-14.0	5-17 M
	14.0	2050	0.2-0.4	1.3-2.8	5-9 H
	11.5	2050	0.4-0.7	0.2-0.4	5-9 H
	18.0	2050	0.4-0.7	2.0-12.0	5-11 H
	21.0	2050	0.3-0.7	10.0-14.0	5-17 M
Waspaloy	27.5	1950	0.1-0.6	0.3	5-12 H
	62.0	1950	0.2-0.4	13.0-15.0	5-18 M
	56.0	1950	0.4-0.6	10.0-13.0	5-18 M
	22.0	2050	0.1-0.7	0.3-0.4	5-13 H
	52.0	2050	0.1-0.3	13.0-15.0	5-18 M
	48.0	2050	0.3-0.6	10.0-13.0	5-18 M
	46.0	2100	0.1-0.3	13.0-15.0	5-18 M
	42.0	2100	0.3-0.6	10.0-13.0	5-18 M
Ti-6Al-2Sn-4Zr-2Mo	56.0	1600	0.1-0.4	13.0-15.0	5-19 M
	52.0	1600	0.4-0.6	10.0-13.0	5-19 M
	18.0	1675	0.1-0.7	0.2-0.4	5-14 H
	23.0	1675	0.4-0.7	0.1	5-16 H
	34.0	1675	0.1-0.3	8.0-12.0	5-16 H
	52.0	1675	0.1-0.4	13.0-15.0	5-19 M
	46.0	1675	0.4-0.6	10.0-13.0	5-19 M
	13.0	1750	0.1-0.4	1.5-2.0	5-15 H
	11.0	1750	0.4-0.6	0.4-1.2	5-15 H
	38.0	1750	0.1-0.4	13.0-15.0	5-19 M
	34.0	1750	0.4-0.6	10.0-13.0	5-19 M
Inconel 718	54.0	2000	0.1-0.4	13.0-15.0	5-20 M
	48.0	2000	0.4-0.6	10.0-13.0	5-20 M
	46.0	2100	0.1-0.4	13.0-15.0	5-20 M
	40.0	2100	0.4-0.6	10.0-13.0	5-20 M
Ti-8Mo-8V-2Fe-3Al	40.0	1650	0.1-0.6	10.0-15.0	5-21 M
	28.0	1850	0.1-0.6	10.0-15.0	5-21 M
	24.0	2000	0.1-0.6	10.0-15.0	5-21 M
AISI 4340	25.0	1900	0.2-0.7	10.0-14.0	5-22 M
	21.0	2000	0.3-0.8	12.0-17.0	5-22 M

(a) H designates hydraulic press tests, M designates mechanical press tests.

for titanium alloy $\sigma_{aT} \simeq 56,000$ psi $\simeq$ 39.5 kg/mm^2

$c_T \simeq 0.1125$ cal/g degree C

$\delta_T \simeq 4.53$ g/cm^3

for steel $\bar{\sigma}_{as} \simeq 32,000$ psi $\simeq 22.5$ kg/mm^2

$c_s \simeq 0.16$ cal/g degree C

$\delta_s \simeq 7.86$ g/cm^3

Thus, the estimated temperature increases would be

for titanium alloy $\Delta\theta_T \simeq 124$ C $\simeq 225$ F

for steel $\Delta\theta_s \simeq 30$ C $\simeq 50$ F

Considering that the flow stress of the titanium alloy is much more temperature dependent than steel, the above approximate calculations illustrate why the flow stress of titanium alloy, in this instance, decreases with increasing strain.

Note that the temperatures calculated above are only estimates. In reality, heat generation, heat loss to the anvils, and decrease of flow stress take place simultaneously, thus the temperature values given above should be considered maximum upper limits.

Summary of Flow-Stress Data Obtained in the Present Study

The flow-stress-versus-strain data, given in Figures 5-8 through 5-22, may be used for practical purposes for an average strain rate and range of strains. These data, summarized in Table 5-4 in the form of average values, clearly illustrate the well-known fact that the flow stress increases with increasing strain rate and decreasing temperature. The data obtained in the hydraulic press, although in general not directly comparable, are essentially consistent with those obtained in the mechanical press.

For 403 stainless steel at 1950 F, a tenfold increase in $\bar{\epsilon}$ results in 50 percent increase in $\bar{\sigma}$. For Waspaloy at 1950 F, a fivefold increase in $\dot{\bar{\epsilon}}$ results in about 100 percent increase in $\bar{\sigma}$. For Ti-6Al-2Sn-4Zr-2Mo at 1675 F, a tenfold increase in $\dot{\bar{\epsilon}}$ results in about 100 percent increase in $\bar{\sigma}$. Similar trends are observed at other temperatures. Thus, it appears that, the order of strain-rate dependency of flow stress for these three materials is: Waspaloy, titanium alloy, and 403 stainless steel.

REFERENCES

(1) Male, A. T., and Cockroft, M. G., "A Method for the Determination of the Coefficient of Friction of Metals Under Conditions of Bulk Plastic Deformation", J. Institute of Metals, 93, 1964-65, p. 38.

(2) Male, A. T., and DePierre, V., "The Accuracy of Mathematical Solutions for Determining Friction From the Ring Test", ASME paper 69-WA/lub-8.

(3) Saul, G., Male, A. T., and DePierre, V., "A New Method for the Determination of Material Flow Stress Values Under Metalworking Conditions", Technical Report AFML-TR-70-19, January, 1970, Air Force Materials Laboratory, Wright-Patterson Air Force Base, Ohio, 45433.

(4) Lee, C. H., and Altan, T., "Influence of Flow Stress and Friction Upon Metal Flow in Upset Forging of Rings and Cylinders", ASME paper 71-WA/Prod-9.

(5) Alder, J. F., and Phillips, V. A., "The Effect of Strain-Rate and Temperature of the Resistance of Aluminum, Copper, and Steel to Compression", J. Institute of Metals, 83, 1954-55, p. 80.

(6) Cook, P. M., "True Stress-Strain Curves for Steel in Compression at High Temperatures and Strain Rates, for Application to the Calculation of Load and Torque in Hot Rolling", Institution of Mechanical Engineers, Conference on Properties of Materials at High Rates of Strain, May, 1957.

(7) Kienzle, O., and Bühler, H., "The Plastometer, A Material Testing Machine for the Compressive Characteristics of Metals" (in German), Zt. F. Metallkunde, 55, 1969, p. 668.

(8) Hockett, John E., "Compressive Stress Versus Strain at Constant Strain Rates", Applied Polymer Symposia, 1967, No. 5, p. 205.

(9) Orowan, E., British Iron and Steel Research Association Report No. MW/F/22/50, London, 1950.

(10) Hsu, T. C., "A Study of the Compression Test for Ductile Materials", ASME Paper No. 67-WA/Met 11.

CHAPTER 6

RING COMPRESSION TESTS FOR DETERMINING FLOW STRESS AND FRICTION AT FORGING TEMPERATURES

by

J. R. Douglas and T. Altan

TABLE OF CONTENTS

CHAPTER 6

RING COMPRESSION TESTS FOR DETERMINING FLOW STRESS AND FRICTION AT FORGING TEMPERATURES

by

J. R. Douglas and T. Altan

ABSTRACT

In hot forging, the metal flow, the forging load, and the forging energy are determined largely by (1) the flow stress of the deforming material, (2) the friction and cooling effects at die-material interface, and (3) the geometry of the forging. The ring-compression test offers the possibility of simultaneously determining both the friction and the flow stress under temperature and strain-rate conditions that exist during forging.

This study describes the fundamentals of the ring-compression test. This test was used to obtain simultaneously the friction shear factor and the flow stress in upsetting of 6061 aluminum, Ti-7Al-4Mo, 403 stainless steel, Waspaloy, 17-7PH stainless steel, Ti-6Al-4V, Inconel 718, Ti-8Al-1Mo-1V, 7075 aluminum, and Udimet 700 at hot-forging temperatures. The details of instrumentation, sample preparation, lubrication, data recording, and evaluation are given. The experimental program has been designed such that the effects of ring thickness, initial temperature, and rate of deformation could be investigated. For given material, temperature, and forging speed, test results give flow stress versus strain at varying strain rates. The results indicate that these data can be used for practical applications, within a given range of strain rates.

INTRODUCTION

In metalforming processes, the flow of metal determines the final shape of the product, the mechanical properties related to local deformation, and the formation of defects such as cracks or folds at the surface or at the center. The local metal flow during a forming process is essentially influenced by

- Factors related to the material of the workpiece: prior history of deformation, grain size and distribution, dependency of flow stress upon strain, strain rate, temperature, and anisotropy
- Factors related to tooling: geometrical shape, lubrication conditions at the tool-workpiece interface, and tool temperatures
- Factors related to forming equipment used: deformation speed and contact times under load.

In cold forming, i.e., room-temperature forming, the equipment behavior does not significantly influence the metal flow unless the material is strain-rate dependent at room temperature and the friction conditions vary greatly with deformation speed. However, the velocity characteristics of equipment in hot forming greatly influence the metal flow and the deformation process because most materials are strain-rate dependent in the hot-forming temperature range and the friction conditions vary drastically with temperature. In hot forming, die chilling acts like increased friction and significantly influences metal-flow behavior. Thus, in hot forging, the metal flow and die fill are largely determined by (1) the resistance of the forging material to flow, (2) the friction and cooling effects at the die-material interface, and (3) the complexity of the forging shape. The influence of these factors upon the forging process is discussed at length in earlier studies.[1,2]

Flow stress increases with increasing strain rate or ram velocity and with decreasing temperature. The magnitude of these variations depends upon the specific forging material. Thus, the flow stress is essentially a material-dependent factor. However, in hot forging, in addition to the flow stress of material, the metal flow is influenced by the frictional conditions at the tool-material interface. Since the material is forced to flow because of the pressure exerted by the tooling, it is not possible to separate the effects of friction from the flow behavior of the material. Consequently, to determine the flow properties and behavior of materials it is necessary, in addition to flow stress, to investigate the frictional conditions at various temperature and strain-rate conditions.

BACKGROUND ON RING COMPRESSION TEST

In predicting load, stress, and energy in deformation processes, the flow stress and friction factor (or the friction coefficient) must be reasonably well estimated. The ring test has proved to be very useful in predicting the friction factor under various temperature, lubrication, and strain-rate conditions.[3,4]

The ring test consists of compressing a flat ring-shaped specimen to a known reduction, Figure 6-1. The change in internal and external diameters of the forged ring is very much dependent upon the friction at the tool-specimen interface. The internal diameter of the ring is reduced if the interface friction is large; increased if friction is low. Thus, the change in the internal diameter represents a simple method for evaluating interface friction.

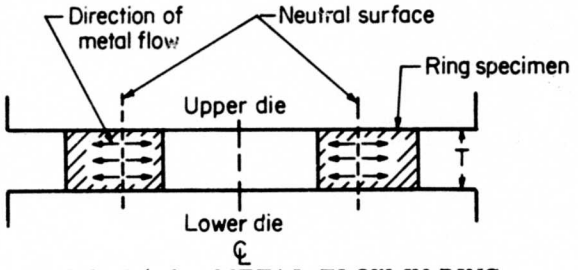

FIGURE 6-1. METAL FLOW IN RING COMPRESSION

In hot forming, as die temperatures usually are lower than billet temperatures, die chilling results. This effect influences the frictional conditions, and it is included in the measurement of the friction factor by using the ring test at hot-forging temperatures. Die chilling, however, also influences the temperature of the deforming billet and, consequently, its flow stress. It, therefore, is difficult to estimate the actual flow stress, $\bar{\sigma}$, and the friction factor, f, (or the shear factor, m) under practical forging conditions. Once these two values are known, shear stress, τ, is given by:

$$\tau = \bar{\sigma} \frac{m}{\sqrt{3}} \quad . \qquad (6\text{-}1)$$

Recently, Saul, Male, and Depierre[5] suggested that the ring test can be used for simultaneously determining flow stress ($\bar{\sigma}$) and shear factor (m). They used the upper-bound analysis of the ring compression without bulging and showed that thin rings (with OD:ID:thickness ratios of 6:3:0.5 and 6:3:1) gave good results in room-temperature studies. In the present study this principle has been further developed and applied to determine simultaneously the flow stress, $\bar{\sigma}$, and the shear factor, m, in forging various materials at different temperatures. The details of the analysis, used for theoretically simulating the ring-compression test, are discussed in Appendix 6-A.[6]

The Use of Ring Test for Determining Friction

To obtain the magnitude of the friction, the internal diameter of the compressed ring must be compared with the values predicted by using various friction factors, f, or shear factors, m. For this purpose, the upper-bound analysis and the associated computer program were used. The computer program mathematically simulates the ring-compression process for given shear factors, m, by including the bulging of the free surfaces. Thus, ring dimensions for various reductions in height and shear factors (m) can be determined. This is the conventional way of representing theoretical calibration curves used in evaluating friction with the ring test. Such calibration curves are given in Figure 6-2 for rings having OD:ID:thickness ratio of 6:3:2, 6:3:1, and 6:3:1/2, respectively. The internal diameters used in Figure 6-2 are the diameters at the internal bulge. In determining the value of the shear factor (m) for a given experimental condition, the measured dimensions (reduction in height and variation in internal diameter) are placed on the appropriate calibration figure. From the position of that point with respect to theoretical curves given for various m's, the value of the shear factor (m), which existed in the experiment, is obtained.

This procedure assumes that the experimental m value remained constant. This assumption is not necessarily correct and represents only a practical approximation. For a detailed study of given forging conditions (e.g., lubrication, die and sample temperatures, forging speed) it is necessary to conduct ring tests at various reductions. Thus the variation of m with the reduction in height will be determined experimentally. This variation can then be compared with a calibration curve that is also developed by using a shear factor (m) varying with reduction in height.

The Use of Ring Test For Determing Flow Stress

In predicting forging loads and energies, the flow stress of the deforming material must be estimated at the temperature and strain-rate conditions, that exist during the actual forging process. Estimating average strain-rate values is not too difficult since, within approximations, the velocity of the forging equipment and the average height of the forging are known during the process. However, it is far more difficult to estimate the temperatures in the forging during deformation because heat transfer depends upon initial die and stock temperatures, contact time, and the heat-transfer coefficient at the die-material interface. All these factors are very difficult to estimate, and they materially influence the accuracy of temperature calculations. It is, therefore, practical to use a ring-compression test to simulate the forging operation by employing

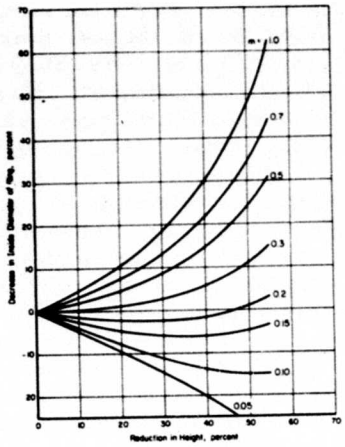

a. 6:3:2 Ratio

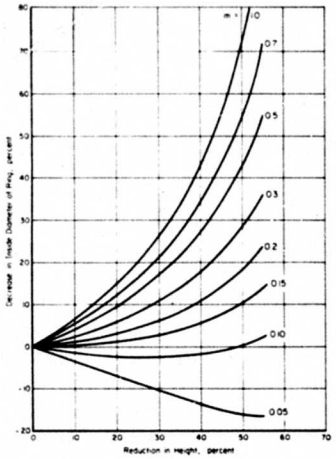

b. 6:3:1 Ratio

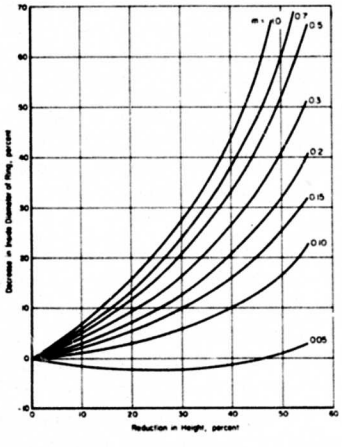

c. 6:3:0.5 Ratio

FIGURE 6-2. THEORETICAL CALIBRATION CURVES FOR UPSETTING A RING HAVING INDICATED OD, ID, AND THICKNESS RATIOS

identical initial temperatures, deformation rates, and lubrication conditions. Thus, the flow stress measured in the ring test will include the effects of temperature variations. For this purpose, rings of various volume to surface ratios can be used and, possibly, more reliable values of flow stress ($\bar{\sigma}$) and shear factor (m) can be obtained simultaneously from a single test.

The brief discussion given above explains the practical significance of the ring test in determining the flow-stress data. These data can then be used for predicting load and energy in actual hot-forming operations.

In order to use the ring-compression test for determining the flow stress from experimental data, the analysis of the ring test has been slightly modified, and a computer program has been written for this purpose. Using the m values and the load versus reduction data determined with the ring upsetting experiment, this modified computer program calculates the average flow stress, $\bar{\sigma}$, at various reductions. In this procedure, it is assumed that m remains constant throughout the deformation process. This assumption is useful in simplifying the experimental work, in reducing the amount of necessary computations, and gives approximate, but practical, results. For a more detailed and precise analysis it is necessary to consider the variation of m during compression process.

Thus, the average flow stress can be determined by using the experimental data as well as the theoretically determined ratios R = Load/$\bar{\sigma}_{ave}$.[6]

EQUIPMENT, INSTRUMENTATION, AND EXPERIMENTAL PROCEDURE

The equipment and the instrumentation used in conducting the ring compression tests, although the same as those used in performing the isothermal compression tests described in Chapter 5, are briefly reviewed below.

Equipment and Instrumentation

The ring-compression tests were conducted in a mechanical forging press of scotch-yoke design. This press, rated 500 tons at 0.25 inch before bottom dead center, has a 10-inch stroke and a forging rate equivalent to 90 strokes per minute. The drive of this press is basically a slider-crank mechanism that translates rotary into reciprocating linear motion. The eccentric shaft is connected, through an air-operated, multiplate friction clutch, directly to the flywheel. The flywheel, driven by an electric motor and "V" belts, stores energy that is used only during a small portion of the crank revolution, namely during deformation of the forged material. The

The constant clutch torque is available at the eccentric shaft which transmits the torque and the flywheel energy to the slide, through the Scotch-yoke mechanism.

During the ring-compression tests, the load was measured on the strain bars attached on four columns of the press. The displacement measurements were made using a linear variable differential transformer (LVDT). The core of the LVDT, fixed relative to the ram of the press, moved through the center of the LVDT coils attached to the press frame. To accomplish this relative motion, the core was suspended between brass rods (nonmagnetic) which were in turn attached to the press frame. Thus, the motion of the core was completely dependent on the motion of the ram. The outputs from the LVDT and the strain bars were recorded on a multichannel high-speed, light-beam recorder (Century Electronics Model 470).

The press used in the present experiment had a nominal speed of 90 strokes per minute. In order to conduct compression tests at lower speeds, 70 and 60 strokes per minute, the drive motor was shut off after the flywheel reached its nominal speed and the flywheel speed, which was then decreasing, was monitored by using a d-c tachometer. When it reached the required speed of 70 or 60 rpm, the press clutch was engaged and, thus, the eccentric shaft was driven at that monitored speed.

Experimental Procedure

The ring compression tests conducted in this study are summarized in Table 6-1. These tests are divided into two groups.

(1) High-temperature tests with 403 stainless steel (SS) at 1800 F, Ti-7Al-4Mo at 1750 F, and 6061 aluminum at 800 F. In these tests the press speed was maintained constant but the thickness of the ring samples was changed. The purpose of these experiments was to investigate the combined effect of die chilling and strain rate upon the flow stress.

(2) High-temperature tests with a number of materials at different press speeds using the same sample thicknesses. The purpose of these experiments was to investigate the effect of deformation rate upon the flow stress.

In all experiments, hardened flat dies with a surface finish of about 25 microinches (CLA) were used. The flat dies were heated to 350 F so that practical forging conditions could be simulated. The 6061 aluminum samples were compressed at 800 F, and the dies were lubricated with a graphite-water spray (Deltaforge 43 of Acheson Colloids Company, Port Huron, Michigan). Samples of all the other materials, compressed at their respective forging temperatures, were dipped into the solution of a glass-base lubricant (Deltaforge 347 of Acheson Colloids Company, diluted in isopropanol with solid content of 15 percent per weight) prior to heating. In addition, the dies were lubricated with the graphite spray, Deltaforge 43. The samples were placed on the lower die, on top of a 0.030 inch-diameter mild-steel wire, in order to prevent excessive die chilling prior to deformation. The transfer time (time necessary to take the sample from the furnace and to place it on the lower die) was approximately 3 seconds.

Since the purpose of this study was primarily to develop and apply the ring-compression-test technique, no attempt was made to optimize the lubrication conditions in the experiments.

Evaluation of Experimental Results

The dimensions of compressed rings were measured. From the variation of the internal diameter, the friction shear factor, m, was determined for each sample by using the appropriate calibration curve given in Figure 6-1. The coordinates of points were read for the displacement and load from the oscillograph recordings and punched on data cards. These load-displacement data, initial and final ring dimensions, and the shear factor, m, represented the input data for the computer program. As discussed earlier, the computer program calculates $\bar{\sigma}_{ave}$ as a function of reduction from the experimental load data. The output of the computer program is obtained as Calcomp plots of flow stress versus reduction in height and of strain rate versus reduction in height. The results are given as a function of reduction in height because they are easier to use for practical application in forging process design. Thus, the problem of calculating an average strain in the nonuniformly deformed rings is also avoided.[6]

The results of the ring tests, listed in Table 6-1, are given in Figures 6-3 through 6-5. In Figure 6-3, the flow stress and strain-rate data are given for three materials. Each chart contains the information obtained for one material at one press speed using three rings of different thicknesses. These results illustrate the combined effect of die chilling and strain rate for three materials. Figure 6-4 illustrates the variation of strain rate with reduction in height at press speeds of 90, 70, and 60 strokes per minute. In all the tests ring samples with 1-inch initial

TABLE 6-1. RING-COMPRESSION TESTS CONDUCTED IN THIS STUDY AND THE AVERAGE FLOW-STRESS VALUES SUGGESTED FOR USE IN PRACTICAL APPLICATIONS

These data are summarized from Figures 6-3 through 6-5.

Material	Flow Stress, 10^3 psi	Temperature, F	Range of Strain-Rate, 1/sec	Friction Shear Factor, m	Contact Time, seconds	From Figure	Ring Ratio (RR)*
6061 Al	9	800	18-22	0.4	0.038	6-3	a
	9	800	15-17	0.31	0.047	6-3	b
	7	800	10-13	0.53	0.079	6-3	c
Ti-7Al-4Mo	48	1750	13	0.42	0.033	6-3	d
	30	1750	18-23	0.42	0.044	6-3	e
	30	1750	15-18	0.7	0.056	6-3	f
403 SS	37	1800	25-28	0.23	0.029	6-3	d
	33	1800	25-27	0.24	0.037	6-3	e
	33	1800	16-18	0.34	0.047	6-3	f
403 SS	32	1950	20	0.28	0.06	6-5	f
	28	1950	16	0.29	0.07	6-5	f
	25	2050	20	0.35	0.06	6-5	f
	19	2050	16	0.43	0.07	6-5	f
Waspaloy	55	2100	20	0.18	0.06	6-5	f
	50	2100	13-16	0.21-0.24	0.07-0.09	6-5	f
17-7PH SS	34	1950	13-20	0.22-0.28	0.06-0.09	6-5	f
	22	2100	16-20	0.35	0.06-0.07	6-5	f
	18	2100	13	0.31	0.09	6-5	f
Ti-6Al-4V	43	1700	20	0.30	0.06	6-5	f
	35	1700	13-16	0.29-0.34	0.07-0.09	6-5	f
	27	1750	16-20	0.32-0.46	0.06-0.07	6-5	f
	20	1750	13	0.38	0.09	6-5	f
Inconel 718	65	2000	16-20	0.17-0.18	0.06-0.07	6-5	f
	58	2000	13	0.18	0.09	6-5	f
	50	2100	20	0.33	0.06	6-5	f
	48	2100	13-16	0.29-0.30	0.07-0.09	6-5	f
Ti-8Al-1Mo-V	50	1750	13-16	0.22-0.26	0.07-0.09	6-5	f
	47	1750	20	0.27	0.06	6-5	f
	40	1800	13-16	0.27-0.32	0.07-0.09	6-5	f
	27	1800	20	0.27	0.06	6-5	f
7075 Al	19	700	13-20	0.36-0.42	0.06-0.09	6-5	g
	16	800	13-20	0.31-0.49	0.06-0.09	6-5	g
Udimet	65 at 10 to 30 percent reduction	2050	14-17	0.4	not measured	6-5	f

*Ring dimensions in inches, OD:ID:thickness
a - 6:3:0.5, b - 6:3:1, c - 6:3:2, d - 3:1.5:0.25, e - 3:1.5:0.5, f - 3:1.5:1, g - 5:3:1.

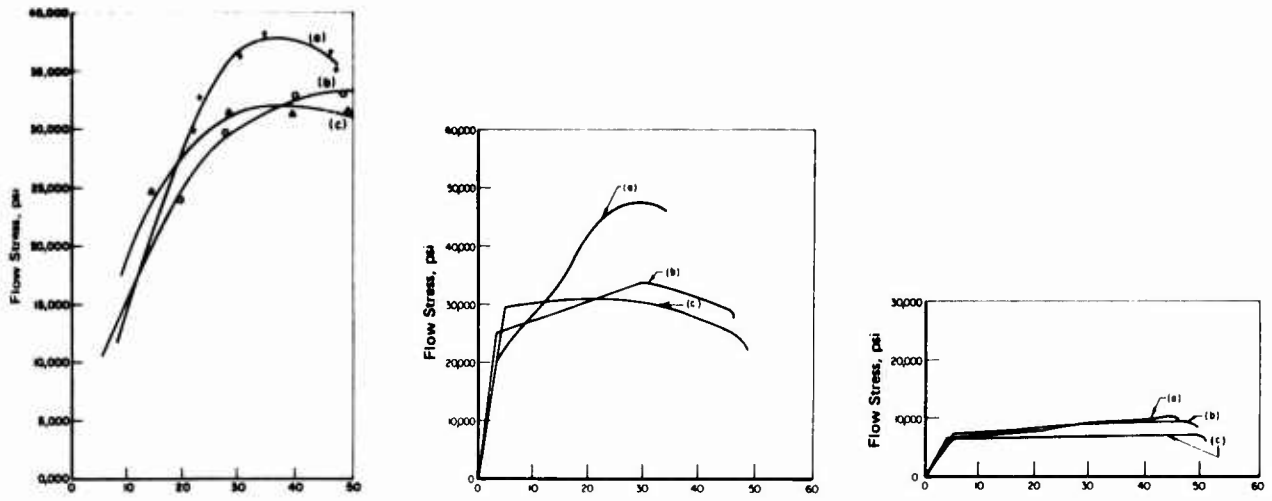

Flow Stresses

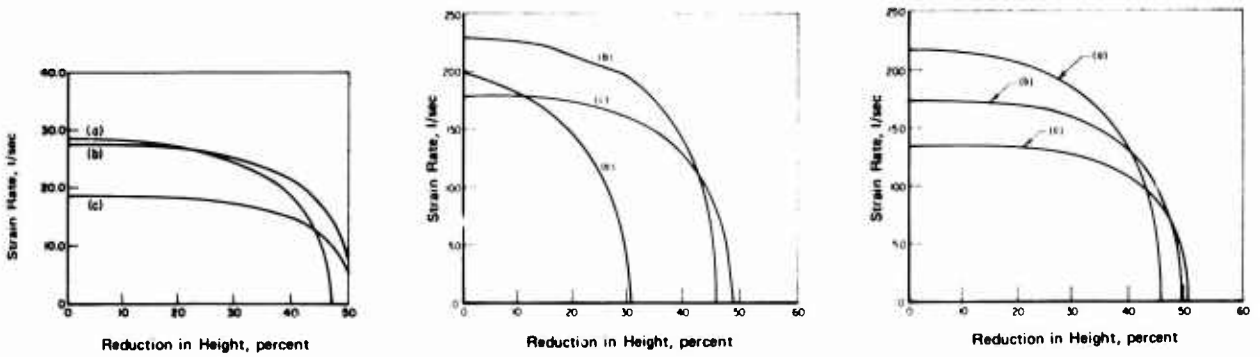

Strain Rates

403SS
Temp: 1800 F
Press Speed: 90 SPM

a. RD = 3:1.5.0.25
m = 0.23
t = 0.029

b. RD = 3:1.5:0.5
m = 0.24
t = 0.037

c. RD = 3:1.5:1
m = 0.34
t = 0.047

Ti-7Al-4Mo
Temp: 1750 F
Press Speed: 90 SPM

a. RD = 3:1.5:0.25
m = 0.42
t = 0.033

b. RD = 3:1.5:0.5
m = 0.42
t = 0.044

c. RD = 3:1.5:1
m = 0.7
t = 0.056

Aluminum 6061
Temp: 800 F
Press Speed: 90 SPM

a. RD = 6:3:0.5
m = 0.40
t = 0.038

b. RD = 6:3:1
m = 0.31
t = 0.047

c. RD = 6:3:2
m = 0.53
t = 0.079

FIGURE 6-3. FLOW STRESS AND STRAIN RATE VERSUS REDUCTION IN HEIGHT FOR RINGS OF VARIOUS THICKNESS

RD = ring dimensions in inches, OD:ID:thickness
m = friction shear factor
t = contact time, second.

height were compressed to approximately 50 percent reduction. Thus, the data on strain-rate and contact times given in Figure 6-4, are representative of the tests conducted for investigating the combined effect of press speed (or stain rate) and contact time (or die chilling) upon the flow stress of various materials.

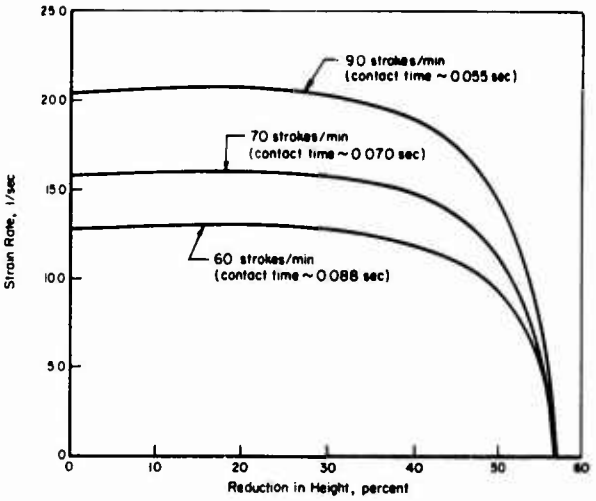

FIGURE 6-4. STRAIN RATE VERSUS REDUCTION IN HEIGHT (ABOUT 50 PERCENT) IN COMPRESSING RINGS (3 INCH OD: 1.5 INCH ID: 1.0 INCH THICK) IN A MECHANICAL PRESS AT VARIOUS SPEEDS

Press stroke = 10 inch, nominal capacity = 500 tons, nominal idle speed = 90 strokes/minute.

SUMMARY AND CONCLUSIONS

The results of the ring tests conducted in this study are given in Figures 6-3 through 6-5, and summarized in Table 6-1. This table gives

- The average flow stress values for various materials at different temperatures
- The range of strain rate for each test
- The friction shear factor, in each test
- The contact time for each test (this is the time during which the deforming ring remains in contact with the dies until the selected reduction in height is reached.)

The variation of strain rate with reduction, as seen in Figures 6-3 and 6-4, is typical for a mechanical press. The decrease in strain rate, small at the start of compression, is drastic toward the end of deformation when the press ram approaches the bottom dead center. However, for all practical purposes this sudden drop in strain rate can be ignored in selecting the approximate flow stress value for a given test.

Effect of Ring Thickness Upon Flow Stress

In the tests conducted with 6061 Al, Ti-7Al-4Mo, and 403SS, the respective test temperatures and the nominal press speed, 90 strokes per minute, were not changed, but samples of three different thicknesses were used. The ring samples had dimensional ratios, OD:ID:thickness, of 6:3:2, 6:3:1, and 6:3:1/2.

With decreasing ring thickness, the strain rate increases, the contact time decreases, but the die chilling effects are increased. As the heat content of a thinner ring is less than that of a thicker one, the effect of cooling, due to die contact, is expected to be more significant in a thin ring.

The flow-stress data, obtained by using rings of various sizes, include the combined influences of heat transfer and strain rate during deformation. Note, however, that in our experiments the strain-rate variation is not very large. Therefore, in most cases, the temperature effects are expected to be more significant. The results, which are expected to be different for different materials, can be summarized as follows.

6061 Aluminum With 6-Inch OD Rings. The results, Figure 6-3, indicate that the flow stress is lowest with the thickest sample (6:3:2). Although the contact time was also the longest, for the thickest sample the bulk temperature of the initially 2-inch-thick sample did not drop appreciably during the test. The thinner samples, (6:3:1 and 6:3:0.5), give approximately the same results. Apparently, the difference in strain rates is not significant, and the effects of cooling are approximately the same for thicker and thinner rings because the contact time increases with sample thickness and vice versa.

Ti-7Al-4Mo. As shown in Figure 6-3, the die chilling effects are most significant for the thinnest Ti-7Al-4Mo ring (dimensions in inches 3:1.5:0.5), and the increase in flow stress is rather significant. This result is expected since titanium alloys are very much temperature, as well as strain-rate, dependent. The samples (b) and (c) do not show any significant difference in flow stress. This is apparently because, in terms of heat transfer, the increase in contact time and in thickness has approximately the same effect as decrease in contact time and thickness.

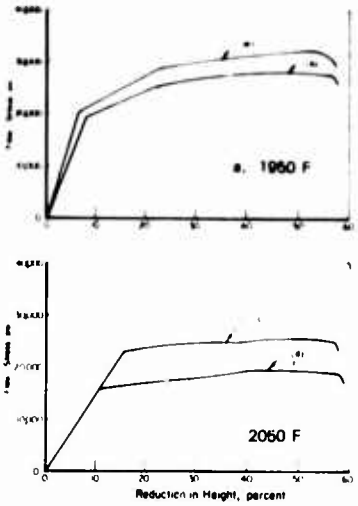

403SS

	P.S.	m
a.	90 SPM,	0.28
b.	70 SPM,	0.29
c.	90 SPM,	0.35
d.	70 SPM,	0.43

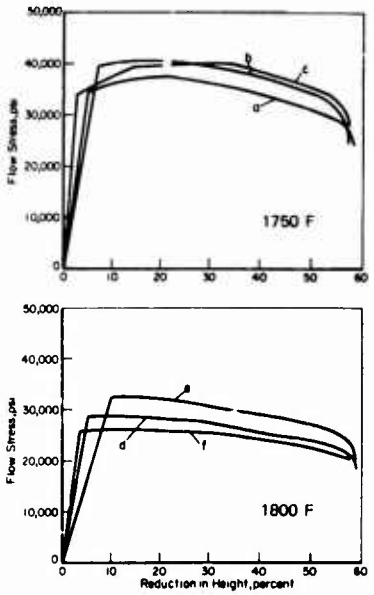

Ti-8Al-1Mo-1V

	P.S.	m
a.	90 SPM,	0.27
b.	70 SPM,	0.22
c.	60 SPM,	0.26
d.	90 SPM,	0.27
e.	70 SPM,	0.27
f.	60 SPM,	0.32

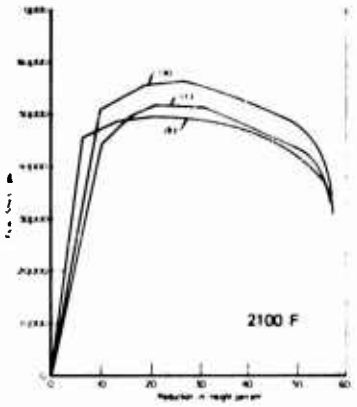

WASPALOY

	P.S.	m
a.	90 SPM,	0.18
b.	70 SPM,	0.21
c.	60 SPM,	0.24

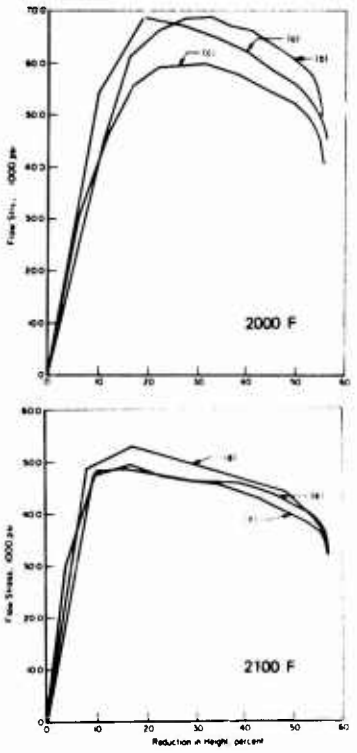

INCONEL 718

	P.S.	m
a.	90 SPM,	0.18
b.	70 SPM,	0.17
c.	60 SPM,	0.18
d.	90 SPM,	0.33
e.	70 SPM,	0.30
f.	60 SPM,	0.29

FIGURE 6-5. FLOW STRESS VERSUS REDUCTION IN HEIGHT OBTAINED IN COMPRESSING RINGS AT VARIOUS STRAIN RATES GIVEN IN FIGURE 6-4

Ring ratios were 3:1.5:1 except for aluminum which was 5:3:1
P.S. = press speed in strokes per minute
m = friction shear factor.

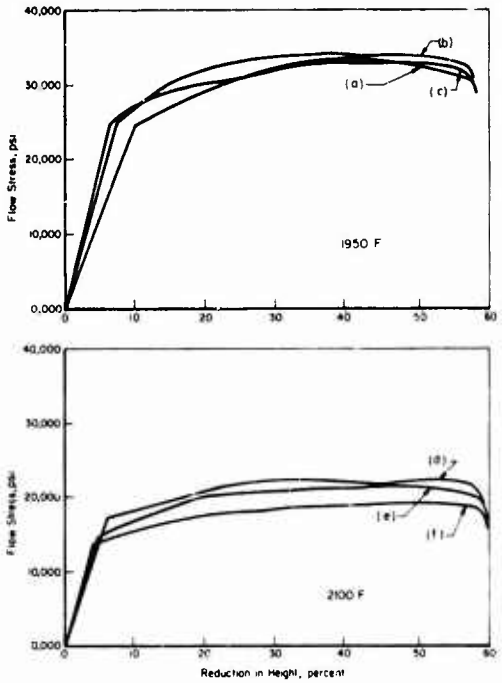

17-7 PHSS

	P.S.	m
a.	70 SPM,	0.28
b.	70 SPM,	0.26
c.	60 SPM,	0.22
d.	90 SPM,	0.35
e.	70 SPM,	0.34
f.	60 SPM,	0.31

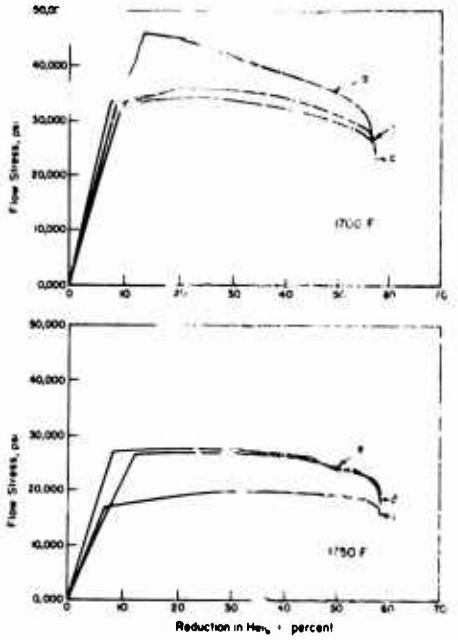

Ti-6Al-4 V

	P.S.	m
a.	90 SPM,	0.
b.	70 SPM,	0.
c.	60 SPM,	0.
d.	90 SPM,	0.46
e.	70 SPM,	0.32
f.	60 SPM,	0.38

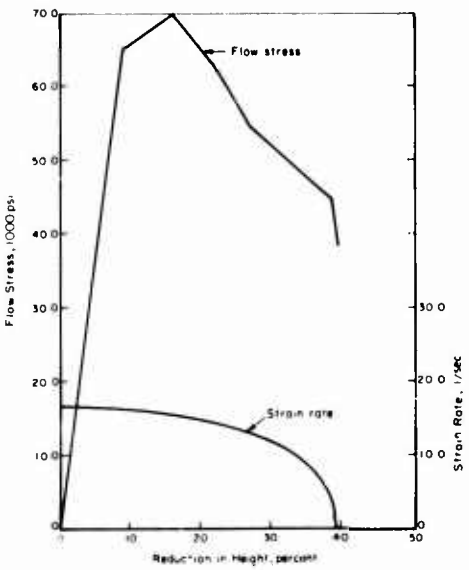

UDIMET 700

90 SPM (This alloy cracked at reductions in height greater than 40 percent.)

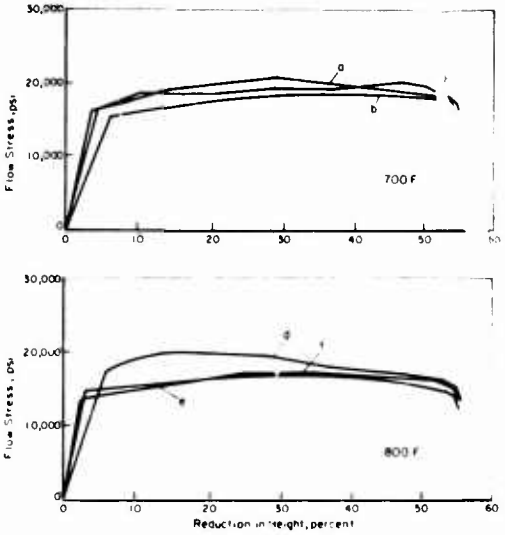

7075 ALUMINUM

	P.S.	m
a.	90 SPM,	0.37
b.	70 SPM,	0.42
c.	60 SPM,	0.36
d.	90 SPM,	0.31
e.	70 SPM,	0.40
f.	60 SPM,	0.49

FIGURE 6-5. (CONTINUED)

403SS. Results for 403SS rings (3:1.5:05) shown in Figure 6-3, are essentially similar to those for Ti-7Al-4Mo. The thinnest ring, Sample (a), gives the highest flow stress values. However, the percentage increase due to chilling is not as large as it is with the titanium alloy. This is expected since the flow stress of stainless steels is not as temperature dependent as that of titanium alloys.

Effect of Temperature and Press Speed Upon Flow Stress

The results of the tests conducted using only one size ring but different temperatures and press speeds are given in Figure 6-5. As expected, in most of these high-temperature tests, the flow stress does not vary significantly with reduction except in a few materials in which heat generated during deformation contributes to the decrease in flow stress as compression ends. The important aspects of these ring tests can be summarized as follows.

403SS at 1950 F and 2050 F. Figure 6-5 shows that the strain rate effect is significant for 403SS at test temperatures. A slight difference in contact times (0.055 to 0.07 sec) does not influence the flow stress values.

Waspaloy. Waspaloy Sample (a) in giving the highest flow stress value, illustrates a slight strain-rate effect (see Figure 6-5). However, Samples (b) and (c), giving approximately the same results, show that strain rate and temperature effects tend to cancel each other.

17-7PH SS. Figure 6-5 shows that strain-rate or chilling does not appear to exert a strong influence at 1950 F – 2100 F. A similar observation is valid for Inconel 718, at 2000 F and 2100 F.

Ti-6Al-4V. Different results are obtained at 1700 F and 1750 F for Ti-6Al-4V. Note in Figure 6-5 that at 1700 F, the strain and heat up effects are significant in Sample (a), while at lower deformation rates the chilling and strain-rate effects tend to cancel each other. At 1750 F the strain-rate effect is still predominant for Sample (f), which gives the lowest flow stress. A similar observation cannot be made for Ti-8Al-1Mo-1V. For this alloy, at 1750 F and 1800 F, the combined effects of chilling and strain rate are such that the flow stress remains approximately unchanged at all press speeds.

7075 Aluminum. A strong strain rate effect is observed for 7075 aluminum at 800 F only at the highest press speed. All other results in Figure 6-5 for this metal show that temperature and strain rate effects counteract each other, and the flow stress remains unchanged at various press speeds.

Udimet 700. Udimet 700 could not be upset more than 40 percent reduction in height without cracking. (Figure 6-5). In practice, this alloy is forged using 15-20 percent reduction in height at each forging operation. The flow stress decreases with increasing deformation, or strain. This can be explained by internal heat generation due to deformation which lowers the flow stress by increasing the temperature of the sample. The large amount of heat generated during deformation can also explain why Udimet 700 is so much susceptible to cracking in forging.

The present study had the dual purpose of (a) obtaining values of stress and friction shear factor in practical forging conditions, and (b) investigating the influence of forging speed, in mechanical press, upon the flow stress of selected materials. The deformation rates used in the tests were selected to correspond to practical speed ranges encountered in mechanical press forging. The results of the investigation showed the influence of forging thickness, press speed, and forging temperature upon the flow stress of selected materials. These results can be used by the forging engineers for prediction of loads and energies in forging, and for comparing the resistance of materials to flow in practical forging conditions.

REFERENCES

(1) Altan, T., et al., "A Study of Mechanics of Closed-Die Forging" Chapter 5, Final Report to Army Materials and Mechanics Research Center, prepared by Battelle's Columbus Laboratories, August, 1970, AD 711544.

(2) Altna, T., and Gerds, A. F., "Temperature Effects Closed-Die Forging" ASM Report No. C70-30.1, October, 1970.

(3) Male, A. T., and Cockcroft, M. G., "A Method for the Determination of the Coefficient of Friction of Metals Under Conditions of Bulk Plastic Deformation." Journal of the Institute of Metals, Vol 93 p. 38, (1964)

(4) Male, A. T., and DePierre, V., "The Validity of Mathematical Solutions for Determining Friction From the Ring Compression Test." ASME Paper No. 69-WA/Lub-8.

(5) Saul, G., Male, A. T., and DePierre, V., "A New Method for the Determination of Material Flow Stress Values Under Metalworking Conditions." Technical Report AFML-TR-70-19, January, 1970

(6) Lee, C. H., and Altan, T., "Influence of Flow Stress and Friction Upon Metal Flow in Upset Forging of Rings and Cylinders." ASME Transactions, Journal Engr. Ind., Vol 94, No. 3, August 1972, p. 775.

APPENDIX 6-A

DEVELOPMENT OF AN APPROXIMATE METHOD FOR THE THEORETICAL SIMULATION OF THE RING TEST*

To obtain the magnitude of the friction, as expressed by the shear factor, m, the internal diameter of the experimentally compressed ring must be compared with the values predicted theoretically by using various values of m. For this purpose, an analysis developed at Battelle's Columbus Laboratories was used.(6) This analysis is based on the upper-bound method which is a practical technique for theoretical study of metal flow in metal-forming processes.

The Principles of the Upper-Bound Method

For describing the metal flow, the upper-bound method considers an admissible velocity field that satisfies the incompressibility, continuity, and the velocity boundary conditions. Based on this velocity field, the deformation, the shear (if velocity discontinuities are present), and the friction energies are computed to give the total forming energy and also the forming load. Based on limit theorems, this calculated forming load is necessarily higher than the actual load and it, therefore, represents an upper bound to the actual forming load. Thus, the lower this upper-bound load, the better is the prediction. Often the velocity field considered includes one or more parameters that are determined by minimizing the total forming energy with respect to those parameters. Thus, the determined values of the parameters give a somewhat better upper-bound velocity field. In general, with an increasing number of parameters in the velocity field, the solution improves while the computations become more complex. Consequently, for practical use of the upper-bound method, practical compromises are made in selecting an admissible velocity field.

When applying the upper-bound method, the following assumptions are usually made:

(1) The deforming material is isotropic and incompressible

(2) The elastic deformations are neglected

(3) The inertial forces are small and neglected (i.e., high-energy-rate forming is not considered)

(4) The friction shear stress, τ, is constant at the die-material interface and is given by a constant shear factor, f, or by a friction factor, m:

$$\tau = f\,\bar{\sigma} = \frac{m\bar{\sigma}}{\sqrt{3}} \quad , \qquad (6A\text{-}1)$$

(5) The material flows according to von Mises' flow rule

(6) The flow stress, $\bar{\sigma}$, is constant.

In the present study, this last assumption is eliminated and the predictions are made by considering, at each small deformation step, the distribution of $\bar{\sigma}$ and an average value for $\bar{\sigma}$. As the deformation proceeds, a new distribution, or a new value for $\bar{\sigma}_{ave}$, is calculated at each step according to:

$$\bar{\sigma}_{ave} = \int_V \bar{\sigma} dV/V \quad , \qquad (6A\text{-}2)$$

where

V = total volume of deforming material.

Velocity Field for Ring Upsetting

When a ring is compressed between two flat, parallel platens, the internal diameter of the ring increases if the friction is low and decreases if the friction is high. This dependency of metal-flow behavior on friction has been extensively used for testing lubricants, lubrication conditions, and for determining the interface-friction factor or the coefficient of friction.

The two modes of deformation which occur in ring compression are illustrated in Figure 6A-1, in which the symbols and the coordinate system are also given. The two platens move toward each other with the same absolute velocity, $V_o/2$. Due to symmetry, only the top right quadrant of the sample is considered. The axial velocity component, v, which incorporates bulging is given by

$$v = -2Az\left(1 - \beta z^2/3\right) \quad , \qquad (6A\text{-}3)$$

where β is a parameter representing the severity of the bulge; the constant, A, is determined from the following velocity-boundary condition for

*The information presented in this appendix has been developed at Battelle's Columbus Laboratories under an internally sponsored project and it was originally discussed in Reference (6).

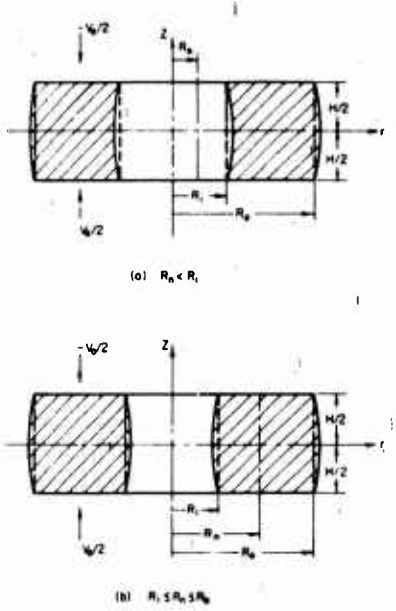

FIGURE 6A-1. TWO MODES OF DEFORMATION IN RING COMPRESSION

$z = H/2$, $v = V_o/2$, or from Equation (6A-3):

$$A = \frac{V_o}{2H\left(1 - \beta \frac{H^2}{12}\right)} \quad . \qquad (6A\text{-}4)$$

The incompressibility condition is given by

$$\frac{\partial u}{\partial r} + \frac{u}{r} + \frac{\partial v}{\partial z} = 0 \quad . \qquad (6A\text{-}5)$$

Equations (6A-3) and (6A-4) give, after integration, the radial velocity component u:

$$u = A\left(1 - \beta z^2\right) r + \frac{C(z)}{r} \quad , \qquad (6A\text{-}6)$$

where C(z) is determined from the following velocity-boundary conditions: The neutral surface at radius $r = R_n$ is defined as the surface that does not move in radial direction at a given time during deformation. Therefore,

$$\text{for } r = R_n,\ u = 0 \quad . \qquad (6A\text{-}7)$$

Introducing condition (6A-7) in Equation (6A-6) we have

$$C(z) = -A\left(1 - \beta z^2\right) R_n^2 \quad . \qquad (6A\text{-}8)$$

The strain-rate components are now obtained from the velocity components, Equations (6A-3) and (6A-6), by introducing the values of the integration constants A and C(z). Thus,

$$\dot{\epsilon}_r = \frac{\partial u}{\partial r} = A\left(1 - \beta z^2\right)\left[1 + \left(\frac{R_n}{r}\right)^2\right] \quad , \qquad (6A\text{-}9a)$$

$$\dot{\epsilon}_t = \frac{u}{r} = A\left(1 - \beta z^2\right)\left[1 - \left(\frac{R_n}{r}\right)^2\right] \quad , \qquad (6A\text{-}9b)$$

$$\dot{\epsilon}_z = \frac{\partial v}{\partial z} = -2A\left(1 - \beta z^2\right) \quad , \qquad (6A\text{-}9c)$$

$$\dot{\gamma}_{rz} = \frac{\partial u}{\partial z} + \frac{\partial v}{\partial r} = -2A\beta z r\left[1 - \left(\frac{R_n}{r}\right)^2\right] \quad , \qquad (6A\text{-}9d)$$

$$\dot{\gamma}_{tz} = \dot{\gamma}_{rt} = 0 \quad . \qquad (6A\text{-}9e)$$

It is seen that the velocity (or the strain rate) field satisfies the symmetry requirements, i.e., for $r = 0$ or $z = 0$, $\dot{\gamma}_{rz} = 0$.

The effective strain rate, $\bar{\dot{\epsilon}}$, is given by

$$\bar{\dot{\epsilon}} = \left[\frac{2}{3}\left(\dot{\epsilon}_r^2 + \dot{\epsilon}_t^2 + \dot{\epsilon}_z^2 + \frac{1}{2}\dot{\gamma}_{rz}^2\right)\right]^{1/2}$$

or

$$\bar{\dot{\epsilon}} = \frac{2A}{\sqrt{3}}\left\{\left(1 - \beta z^2\right)\left[3 + \left(\frac{R_n}{r}\right)^4\right] + \left(\beta r z\right)^2\left[1 - \left(\frac{R_n}{r}\right)^2\right]^2\right\}^{1/2} \quad . \qquad (6A\text{-}10)$$

The equations describing the velocity and strain-rate fields include two unknowns, β and R_n. At a given deformation stage, β and R_n are determined from the condition that the total energy-dissipation rate $\dot{E}$ (or the upsetting pressure), must be minimum; i.e.,

$\frac{\partial \dot{E}}{\partial \beta} = 0$ gives the value of β

and

$\frac{\partial \dot{E}}{\partial R_n} = 0$ gives the value of R_n.

Prediction of Load Versus Displacement and Bulge Profile

In compressing a ring, the total energy dissipation rate, $\dot{E}$, including deformation, and friction is given by

$$\dot{E} = 2\pi \int\int_V \bar{\sigma}\,\bar{\dot{\epsilon}}\, r\, dr\, dz + \frac{4\pi m}{\sqrt{3}} \int_{R_i}^{R_o} u_s\, \bar{\sigma} r\, dr \quad , \qquad (6A\text{-}11)$$

where

u_s = velocity at the material-die interface, for $z = H/2$

$$u_s = A\left(1 - \frac{\beta H^2}{4}\right)\left(1 - \frac{R_n^2}{r^2}\right) r \, .$$

In Equation (6A-11), the first term represents the volume integral over the volume, V, of the material, or the rate of dissipated deformation energy. Local variations of flow stress,

$\bar{\sigma}$, in the deformed material are included in the calculations. Therefore, the integral is evaluated numerically by using a computer program. The same is valid for the second term in Equation (6A-11) which represents the friction-energy rate.

The energy rate, $\dot{E}$, given by Equation (6A-11) is minimized with respect to β and R_n to determine these values. Then, the minimum energy, $\dot{E}_{min}$, is calculated. The upsetting load is given by

$$L = \frac{\dot{E}_{min}}{V_o} \quad , \qquad (6A-12)$$

and the average upsetting pressure, P_{ave}, is obtained from

$$P_{ave} = \frac{L}{\pi\left(R_o^2 - R_i^2\right)} \quad . \qquad (6A-13)$$

The block diagram of the computer program, which carries out the above calculations, is given in Figure 6A-2. Because of symmetry, only the upper right quadrant of the sample is analyzed. As seen in Figure 6A-3, this deformation region is divided into a number of radial and axial guidelines, which are perpendicular to each other initially and which deform as the deformation proceeds.

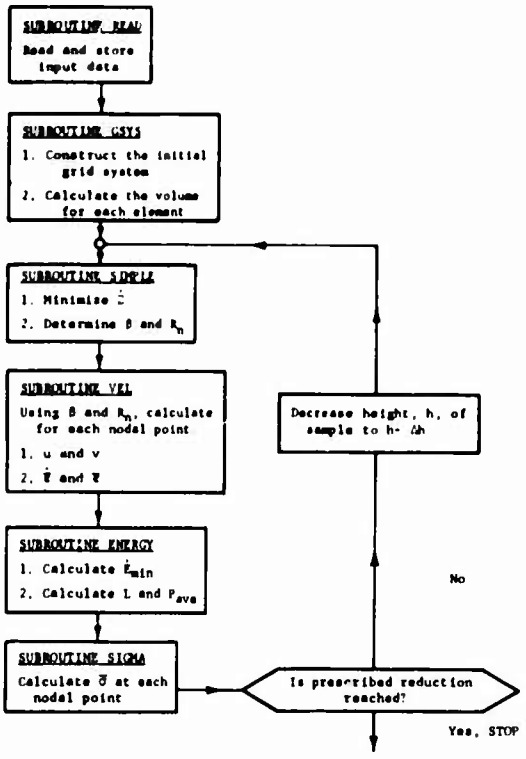

FIGURE 6A-2. SIMPLIFIED BLOCK DIAGRAM OF COMPUTER PROGRAM FOR PREDICTING LOAD AND BULGE PROFILE IN RING COMPRESSION

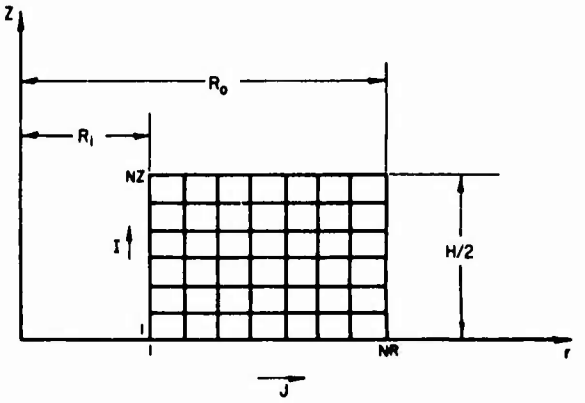

FIGURE 6A-3. INITIAL GRID SYSTEM USED IN COMPUTER ANALYSIS OF RING COMPRESSION

During deformation, each nodal point has a different flow stress, $\bar{\sigma}$, strain $\bar{\varepsilon}$, and strain rate, $\dot{\bar{\varepsilon}}$. The upsetting process is considered in small steps, Δh. At each step, new velocity, strain rate, and strain distributions are calculated. The strain, $\bar{\varepsilon}$, is determined by integrating $\dot{\bar{\varepsilon}}$ with respect to time during each deformation step. From the stress-strain curve, the known strain, $\bar{\varepsilon}$, at each nodal point is used to obtain the flow stress, $\bar{\sigma}$, at that nodal point. The minimization of $\dot{E}$ with respect to β and R_n is accomplished by using the numerical simplex minimization technique. The computer program is written in a general way so that, if desired, an average flow stress, $\bar{\sigma}_{ave}$, could also be used at each deformation step. In this case of course the value of $\bar{\sigma}_{ave}$ increases during deformation because of increase in strain or in strain rate.

The Use of Ring-Compression Analysis for Determining Friction and Flow Stress

The analysis of the ring-compression test, described above, is used to simulate the ring-compression process from the start to a specified reduction in height. Thus, for a given friction shear factor, m, the internal diameter of the deformed ring and the deformation load are calculated at each small reduction step. Consequently, by performing additional simple calculations, the variation of the internal ring diameter can be obtained for each reduction. This information, plotted in the appropriate form, represents the calibration curves used in determining the friction shear factor from a compression test.

Similarly, for a given shear factor, m, the ratio R = Load/$\bar{\sigma}_{ave}$ is easily determined for each reduction in height. Using the experimental load values, L, at each reduction, the average flow stress at a given reduction is then obtained as

$$\bar{\sigma}_{ave} = \frac{L}{R} \quad . \qquad (6A-14)$$

CHAPTER 7

PREDICTION AND MEASUREMENT OF FORGING LOAD UNDER PRODUCTION CONDITIONS

by

T. Altan, J. R. Douglas, and H. Akgerman

TABLE OF CONTENTS

CHAPTER 7

PREDICTION AND MEASUREMENT OF FORGING LOAD UNDER PRODUCTION CONDITIONS

by

T. Altan, J. R. Douglas, and N. Akgerman

ABSTRACT

In using presses for forging operations, adequate selection of the forging press requires the prediction of the forging load. Once the press is selected, it is necessary to measure and monitor the forging loads during actual forging under production conditions. Thus (a) the accuracy of load predictions is determined, (b) the excessive equipment overloading is prevented during set-up, and (c) variations in forging load due to material, temperature, or lubrication are monitored and corrective action is taken, if necessary.

Several empirical methods for predicting forging loads are reviewed, a nomogram is developed for load and energy predictions, and a simple method of load calculation in forging is described. The monitoring of forging load and ram displacement under production conditions are illustrated by the forging trials conducted at (a) Westinghouse Electric Corporation, Winston-Salem, North Carolina (screw press), (b) Steel Improvement and Forge Company, Cleveland, Ohio (screw press), and (c) Ontario Corporation, Muncie, Indiana (mechanical press).

INTRODUCTION

Closed-die forging is an extremely complex forming process with respect to deformation mechanics. The nonsteady state and nonuniform material flow, the considerable interface friction, and the heat transfer between the deforming material and the tooling are very difficult to analyze. This is why there is no general, accurate method of estimating forging loads.

Three broadly defined methods are used in estimating forging loads, namely:

Applied experience. The estimates for each new part are based on observations made on a variety of forging shapes in similar materials. Sometimes, very simple formulas that are developed for average forming loads are helpful in applying experience with one part to sharpen up the predictions for succeeding parts.

Empirical procedures. In some forging companies, the formulas derived from experience are based on detailed observations made during forging of a few selected parts. More comprehensive empirical formulas which are then derived take into account such factors as flow stress, average strain, circumscribing part dimensions, and friction. Some investigators have carried their derivations to the point where they incorporate a mathematically derived "shape factor" to account for wide ranges of shape complexity. The accuracy of the empirical procedures depends largely on the accuracy of the observations.

Analytical procedures. When a forging is viewed as being composed of several components, it is possible to first analyze the individual subsections and then estimate the forces required for deforming each component. A further analysis then takes into account the distribution of pressures over the die surfaces. Recently, plasticity theory has been applied to some relatively simple forging problems to obtain approximate predictions of forging loads. The approximate theory most widely reported in the literature is the "Sachs" or "slab method" of analysis.

EMPIRICAL METHODS FOR PREDICTING THE MAXIMUM FORGING LOAD

The maximum load for forging a given part can be estimated by an empirically established formula. The results are usually sufficiently accurate for estimating average forging pressures and maximum forging loads under practical shop conditions. No detailed information on stress distributions, on material flow, and/or forging mechanics can be obtained from these empirical predictions. They do not generally contribute to the advancement or refinement of forging know-how since they are not based on the fundamental phenomena of material deformation and flow.

AISI - Schey

In a review prepared for the American Iron and Steel Institute, Schey[1] presented the following expression for calculating the forging load:

$$P_t = C_1 \cdot \bar{\sigma}_a A_t \quad , \qquad (7\text{-}1)$$

where

C_1 = a factor depending on the complexity of the forging, as given in Table 7-1

A_t = cross-sectional area of the forging in the parting line, complete with flash

$\bar{\sigma}_a$ = average flow stress at the given average forging temperature θ_a and average strain rate $\bar{\epsilon}_a$. If the material is strain dependent, then $\bar{\sigma}_a$ must be obtained at the average strain

$$\bar{\epsilon}_a = \ln\left(\frac{h_o A_t}{v}\right)$$

v = volume of the forging

h_o = initial height of the stock material.

In calculating the energy requirement:

$$E = C_2 \, V \, \bar{\epsilon}_a \cdot \bar{\sigma}_a \quad , \qquad (7\text{-}2)$$

where

C_2 = factor given in Table 7-1

$\bar{\epsilon}_a$ = average strain = $\ln\left(\frac{h_o A_t}{v}\right)$.

TABLE 7-1. MULTIPLYING FACTORS FOR ESTIMATING FORCE AND ENERGY REQUIREMENTS[1]

Mode of Deformation	Factors C_1	Factors C_2
Compression of cylinder between flat platens		
$\bar{\epsilon} = 0.5$	1.2	1.2
$\bar{\epsilon} = 0.8$	1.5-2.5	1.5
Impression die forging of simple shape		
Without flash formation	3-5	2.0-2.5
With flash formation	5-8	3.0
Impression die forging of complex shape (High Rib) with flash formation	8-12	4.0

It is seen from Table 7-1 that the selection of the values for Factors C_1 and C_2 used in Equations (7-1) and (7-2) can be very approximate and must be based on experience. The predictions thus obtained can be accepted only with a relatively large margin of error. The accuracy of predictions made with this procedure will depend on the experience of the user.

Geleji

In his most recent book, Geleji[2] reports on an empirical method suggested by Kurrein[3]. According to this suggestion, the total forging load, P_t, is given by:

$$P_t = C \, \bar{\sigma}_a \cdot A_t \quad . \qquad (7\text{-}3)$$

The shape factor, C, is dimensionless and must be obtained from Figure 7-1.

The values of the shape factor, C, given in Figure 7-1 are valid for forgings with diameters from 100 to 300 mm (4 to 12 in.). The value of the shape factor, C, for a given disk diameter, D, increases with decreasing web thickness, S, with decreasing shaft diameter, d, and with increasing height of any shaft or rib that might be present. The calculation of the forging load for the part shown in Figure 7-2 is the example given by Geleji[2] and illustrates the use of this method. At the forging temperature of 1000 C (1830 F), for the type of steel being forged, a value of

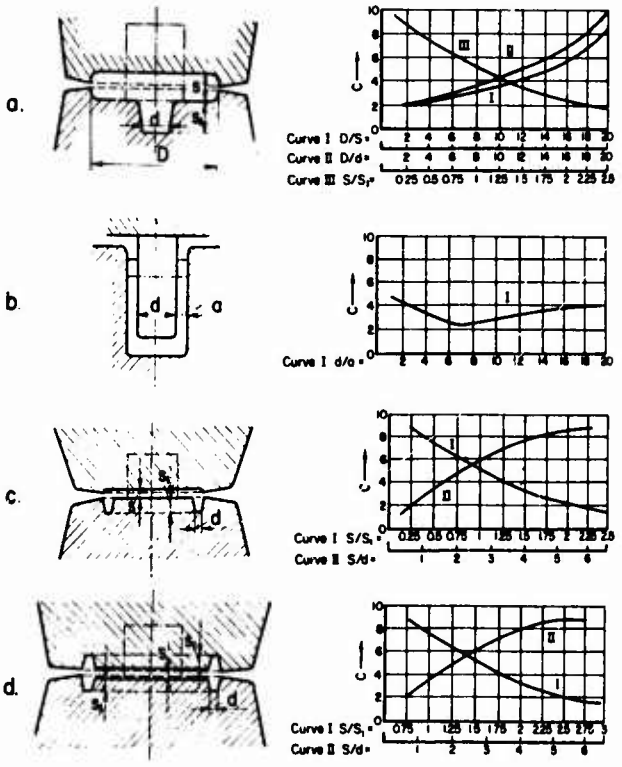

FIGURE 7-1. CALCULATION OF SHAPE FACTOR C FOR CLOSED-DIE FORGING[3]

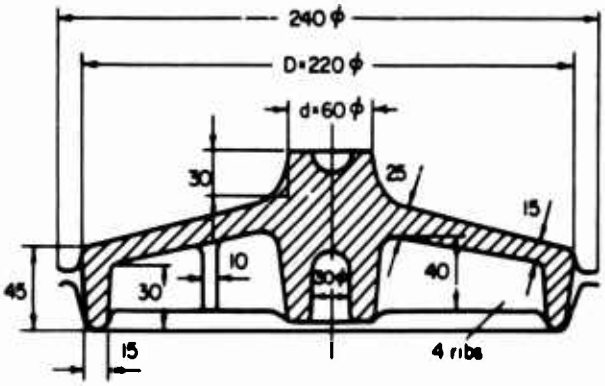

(Dimensions in mm, 1 mm = 0.040 inch)

FIGURE 7-2. EXAMPLE FOR CALCULATING THE FORGING LOAD[2]

520 kg/cm^2 (7400 psi) can be assumed for $\bar{\sigma}_a$. The flash thickness is about 5 mm (0.2 in.):

For a disk 220 mm in diameter and 15 mm thick (Figure 7-1a, Curve I) D/S = 14.7 C = 5.0

Periphery is 45 mm high and 15 mm thick, i.e.,

For a disk 15 mm thick, with a rib 30 mm high (Figure 7-1c, Curve I) S/S_1 = 0.5 C = 7.4

For a disk 15 mm thick, with a rib 15 mm thick (Figure 7-1d, Curve II) S/d = 1.0 C = 2.9

Radial ribs

For a disk 15 mm thick, with a rib 10 mm thick (Figure 7-1d, Curve II) S/d = 1.5 C = 4.0

For a disk 15 mm thick, with a rib 40 mm high (Figure 7-1c, Curve I) S/S_1 = 0.375 C = 8.0

The highest value for C represents the most difficult-to-forge feature in the forging. In this example, 8.0 is the shape factor criterion for calculating the upsetting force required for the entire die forging; thus the vertical load acting on the plane of the die cavity:

$$P_d = 8.0\,\bar{\sigma}_a \frac{22^2\pi}{4}, \text{ i.e.,}$$

$$P_d = 1,580,000 \text{ kg } (3,480,000 \text{ lb}).$$

With the same considerations used for the cavity, the shape factor for the flash is 6.0, assuming that the flash temperature is lower and consequently the flow stress is higher:

$$\bar{\sigma}_a = 1100 \text{ kg/cm}^2 \text{ (15,600 psi)}.$$

The upsetting load, P_f, in the flash is:

$$P_f = 6 \times 1100\,(24^2 - 22^2)\frac{\pi}{4} = 476,000 \text{ kg } (1,050,000 \text{ lb}).$$

Thus, the total forging load, P_t, is:

$$P_t = P_d + P_f = 2,050,000 \text{ kg } (4,500,000 \text{ lb}).$$

In this procedure, the experience and the intuition of the user will obviously influence the selection of simple analogue shapes in order to evaluate Factor C from Figure 7-1.

Neuberger and Pannasch

Neuberger and Pannasch[4] conducted forging experiments with various carbon steels (up to 0.6 percent carbon) and with low-alloy steels using flash ratios, w/t (w, flash land width; t, flash thickness), from 2 to 4. They found the variable that influences the forging load most to be the average height, h_a, of the forging. The average height (h_a) is determined from the weight (Q), from the total projected area (A_t) of the forging, and from the specific weight (ρ) of the forging material:

$$h_a = \frac{Q}{A_t \cdot \rho} \quad . \qquad (7\text{-}4)$$

The maximum total forging load is expressed as:

$$P_t = A_t p_a \quad , \qquad (7\text{-}5)$$

where p_a represents average forging pressure, including friction.

On the basis of their experimental data, Neuberger and Pannasch[4] suggested using the diagram shown in Figure 7-3 for predicting the forging pressure, p_a. The lower curve in Figure 7-3 is described by the equation

$$(\text{kg/mm}^2)\; p_a = 14 + \frac{618}{h_a} \text{ (metric)} \qquad (7\text{-}6a)$$

or

$$l_a \quad 1422\left(14 + \frac{618}{25.4\,h_a}\right) \text{ (English)} \qquad (7\text{-}6b)$$

where p_a is in psi and h_a in inch scale.

The upper curve in Figure 7-3 is described by

$$(\text{kg/mm}^2)\ p_a = 37 + \frac{781}{h_a} \quad \text{(metric)} \quad (7\text{-}7a)$$

or

$$(\text{psi})\ p_a = 1422 \left(37 + \frac{781}{24.5\ h_a} \right) \quad \text{(English)}. \quad (7\text{-}7b)$$

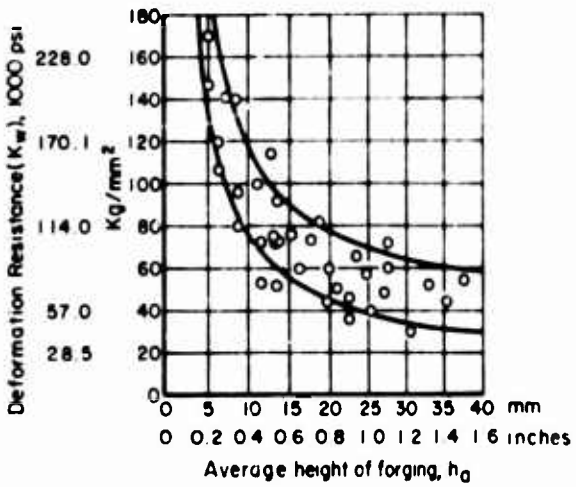

FIGURE 7-3. FORGING PRESSURE, p_a, VERSUS THE AVERAGE FORGING HEIGHT, h_a, FOR FORGINGS INVESTIGATED[4]

Equation (7-6) is used for less-intricate parts, Equation (7-7) is used for more-difficult-to-forge parts.

Nomograms for Predicting Load and Energy in Steel Forging

Neuberger and Pannasch[4] further extended their findings and gave two diagrams, seen in Figures 7-4 and 7-5, for predicting load and energy in forging carbon and low alloy steel parts.

Nomogram for Load Prediction

The nomogram, seen in Figure 7-4 can be used for predicting the load in forging low alloy steel parts. The description and the use of this nomogram are discussed below.

Example: In the nomogram, Figure 7-4, a series of lines, are drawn to indicate the determination of the load for the following forging:

Weight of forging - 2.9 kg

Surface area without flash - 160 cm^2

Sharp contoured cross-sectional shape, type C in Region II

Forging temperature - 1100 C

Surface area with flash - 200 cm^2

Predicted forging load - p = 1100 M_p (metric tons).

Nomogram for Energy Prediction

The nomogram, seen in Figure 7-5, can be used for predicting the energy in forging steel components. The description and the use of this nomogram are discussed below.

Example: The prediction of the forging energy is illustrated in Figure 7-5 for an example forging. The example is the same as that used for predicting the forging load.

Weight of forging = 2.9 kg

Surface area without flash = 160 cm^2

Sharp contoured cross-sectional shape

Forging temperature = 1100 C

Ratio $h_{mA}/h_{mE} = 3$

Predicted forging energy = 7800 mkp.

SUGGESTED METHOD FOR CALCULATING THE FORGING LOAD IN PRACTICAL CONDITIONS

Most empirical methods, summarized in terms of simple formulas or nomograms are not sufficiently general to predict the forging load for a variety of parts and materials. Consequently, a nomogram such as the one seen in Figure 7-4, may be useful for carbon and low-alloy steels but cannot be applied for titanium and high-temperature alloys. It is, therefore, necessary to establish a practical method for calculating the forging load.

Round or Nearly Round Forgings

In round forgings, or in those which can be considered as round, the approximate forging load is predicted by calculating separately the forging stresses due to deformation of the flash and of the material in the die cavity. The detailed steps, without describing the theory involved, are illustrated by using the example given in Figure 7-6.

Step 1. Establish the average thickness, h, for the metal flowing in the cavity towards the flash. If the metal in the cavity flows by sliding over the die surfaces, h is equal to the average cavity height, i.e., h equals H in Figure 7-6. In this case, the friction factor $f \simeq 0.2$ to 0.4.

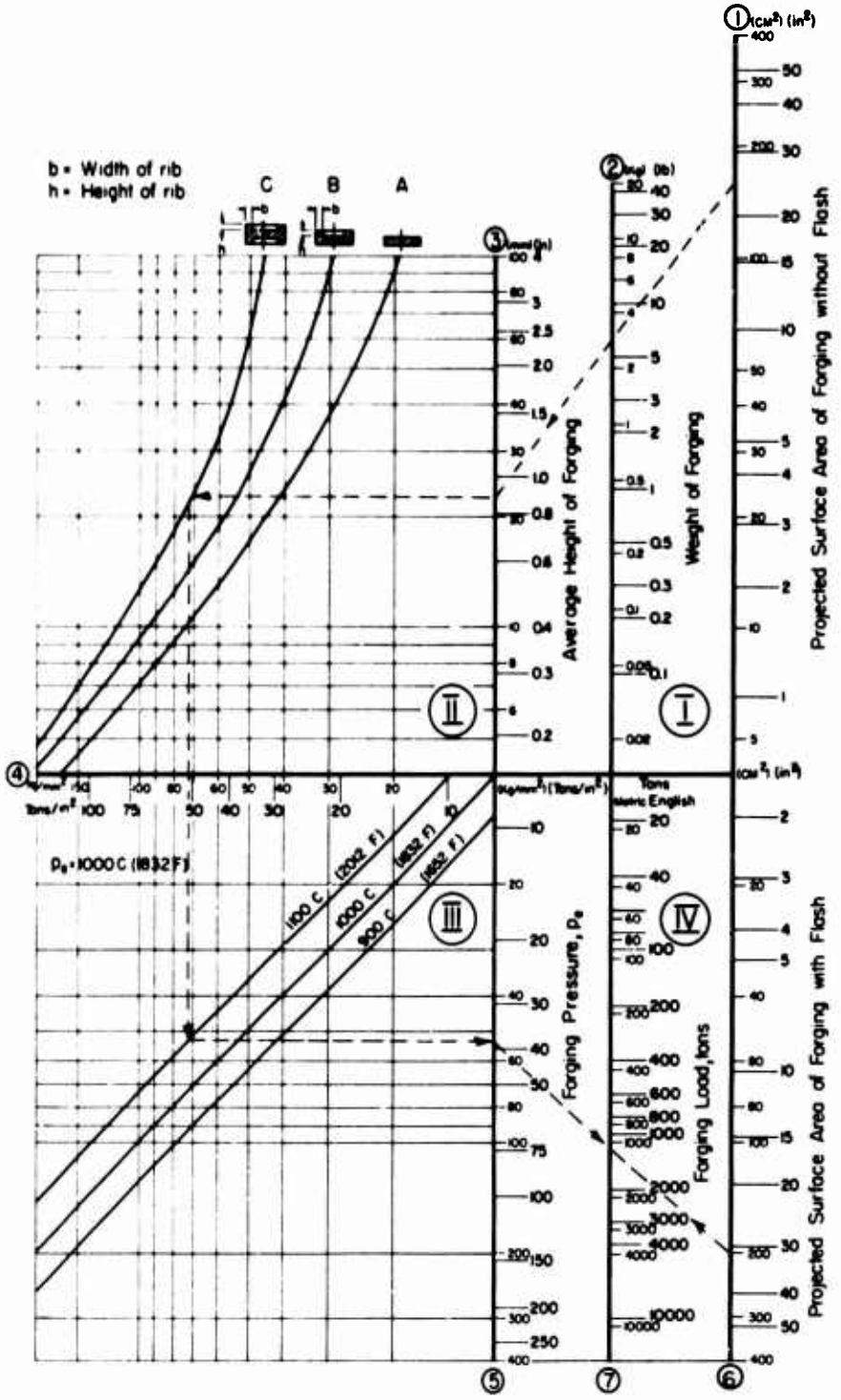

Region I - The projected surface area of the forging without flash, is specified on Axis 1. The weight of the forging is specified on Axis 2. Thus, the average height of the forging is obtained on Axis 3.

Region II - In this region the basic type of forging configuration must be taken into account. Each of the three basic forging types, A, B, and C are represented with a line in this region.

Region III - In this region the influence of temperature upon forging pressure is considered. Each of the three temperatures, 900 C (1650 F), 1000 C (1830 F), and 1100 C (2010 F) is represented by a line. The maximum forging pressure, p_e, at 1000 C (1830 F) is obtained on Axis 4, at the line separating the Regions II and III. Using one of the three temperature lines in Region III, the maximum forging pressure at a given temperature is obtained on Axis 5.

Region IV - In this region the total maximum forging load is obtained by relating the forging pressure, p_e, on Axis 5, and the projected surface area of the forging including flash, on Axis 6. Thus, the total load is obtained on Axis 7.

FIGURE 7-4. NOMOGRAM FOR PREDICTING LOAD IN CLOSED-DIE FORGING OF CARBON AND LOW-ALLOY STEELS IN MECHANICAL PRESSES[4]

A = Forgings without sharply contoured cross sections or preformed cross sections and intermediate forms.

B = Forgings the final shape of which does not require preforming;

$$\frac{h}{b} < 1.2$$

C = Forgings with sharply contoured cross sections, $\frac{h}{b} > 1.2$.

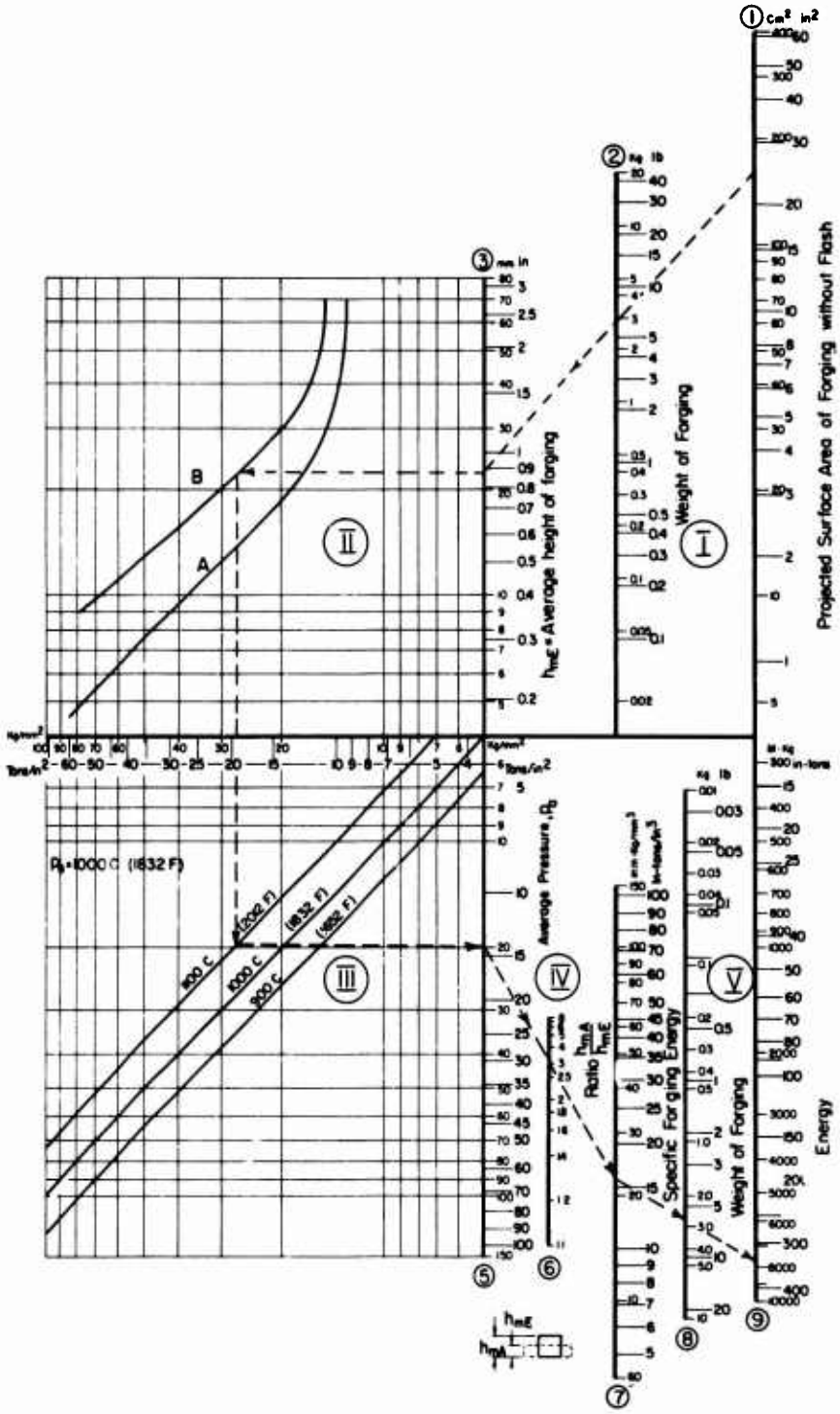

Region I - The projected surface area of the forging without flash is specified on Axis 1. The weight of the forging is specified on Axis 2. Thus, the average height of the forging is obtained on Axis 3.

Region II - In this region two types of forging are considered, each is designated by a line. Line A represents forgings without sharply contoured cross sections or preformed cross sections. Line B represents forgings with sharply contoured cross sections.

Region III - In this region the influence of temperature is considered. Each of three temperatures is represented by a line: 900 C (1650 F), 1000 C (1830 F), 1100 C (2010 F). The average forging pressure, p_a, (pressure averaged over the forging stroke) on Axis 4, is modified according to the forging temperature to give the pressure, p_a, on Axis 5.

Region IV - In this region, the average pressure, p_a, on Axis 5 is related to the ratio h_{mA}/h_{mE}, on Axis 6 to obtain the energy per unit weight on Axis 7 (h_{mA} = average height of the stock or preform, h_{mE} = average height of the completely forged part).

Region V - The specified energy obtained on Axis 7 is related to the forging weight, on Axis 8 to predict the total forging energy on Axis 9.

FIGURE 7-5. NOMOGRAM FOR PREDICTING ENERGY IN CLOSED-DIE FORGING OF CARBON AND LOW-ALLOY STEEL IN MECHANICAL PRESSES[4]

A = Forgings without sharply contoured cross sections or preformed cross sections and intermediate forms

B = Forgings with sharply contoured cross sections.

However, if the metal flow in the die cavity is by shearing, as indicated by broken lines in Figure 7-6, then the average thickness in the cavity, h, must be estimated. For this purpose, using the symbols of Figure 7-6, we calculate[5]

$$h = 0.8t\left(\frac{L}{t}\right)^{0.9} . \qquad (7\text{-}8)$$

For $h \geq H$, then we set $h = H$. For $h < H$, we use the value of h calculated by Equation (7-8). In this latter case, the metal flow is by shearing, and the friction factor $f = 0.577$.

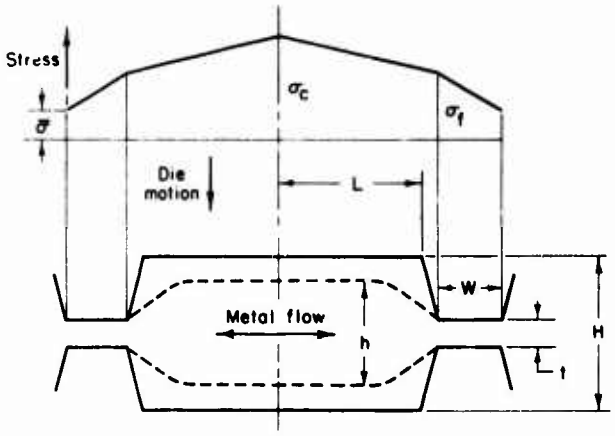

FIGURE 7-6. SCHEMATIC OF A SIMPLE ROUND CLOSED-DIE FORGING AND THE DISTRIBUTION OF FORGING STRESS

Step 2. Calculate the stress σ_e at the entrance to flash from die cavity is:

$$\sigma_e = \frac{2\,f\bar{\sigma}}{t}\,w + \bar{\sigma}_F , \qquad (7\text{-}9)$$

where

$\bar{\sigma}_F$ = flow stress in the flash zone

t = flash thickness

w = flash width

f = friction factor, 0.2 to 0.4 .

Step 3. Calculate the total forging load. The forging load P_F due to deformation and friction in the flash zone is, Figure 7-6.

$$P_F = \left[\frac{-2\tau_F}{t}\left(\frac{R^3 - L^3}{3}\right) + \left(\frac{2\tau R}{t} + \bar{\sigma}_F\right)\left(\frac{R^2 - L^2}{2}\right)\right], \qquad (7\text{-}10)$$

where

θ = angle of the sector, in radians, describing the round forging area. (In a completely round forging $\theta = 2\pi$, in a round section of an irregular forging θ is obtained from forging drawing.)

τ_f = friction shear stress in flash zone

$= f\,\bar{\sigma}_F$

$\bar{\sigma}_F$ = flow stress of the flash material at the strain rate and temperature conditions existing in the flash zone

R = L + W, Figure 7-6.

The forging load, P_c, due to deformation and friction in the die cavity is given by:

$$P_c = \theta\left[\frac{-2\tau}{h}\,\frac{L^3}{3} + \left(\frac{2\tau L^3}{h} + \sigma_f\right)\frac{L^2}{2}\right], \qquad (7\text{-}11)$$

where, in addition to the symbols discussed earlier,

τ = friction shear stress in cavity

$= f\,\bar{\sigma}_c$ for $h \geq H$ in Step 1

$\bar{\sigma}_c$ = flow stress in the die cavity, for the strain rate and temperature conditions existing in the die cavity

h = average cavity height

= H for $h \geq H$

= h, as calculated by Equation (7-8) .

Finally, the total forging load, P_T is:

$$P_T = P_F + P_C . \qquad (7\text{-}12)$$

Relatively Long Forgings

In relatively long forgings the predominant metal flow is lateral, except at the corners of the forging. Thus, the metal flow is essentially plane strain. In this case, the stress distribution illustrated in Figure 7-6 is still valid with the exception that at the free end of flash the stress is equal to $\frac{2}{\sqrt{3}}\bar{\sigma}$ instead of $\bar{\sigma}$. The steps to be followed are similar to those discussed for round forgings. Equation (7-8) is still valid for determining the average height, h, of the deformation zone in the die cavity.

The stress σ_e at the entrance to flash from cavity is:

$$\sigma_e = \frac{2f\bar{\sigma}}{t} w + \frac{2\bar{\sigma}_F}{\sqrt{3}} \quad . \qquad (7\text{-}13)$$

The flash load, P_F, per unit depth is:

$$P_F = w\left(\frac{2\bar{\sigma}_F}{\sqrt{3}} + \frac{\tau w}{t} \right) , \qquad (7\text{-}14)$$

where

$$\tau = f\bar{\sigma}_F$$

The cavity load, P_c, per unit depth is:

$$P_c = L \left(\sigma_e + \frac{\tau L}{h} \right) . \qquad (7\text{-}15)$$

In evaluating Equation (7-15), the same considerations as for round forgings are still valid for determining the friction shear stress τ and the average height h. The total load is again given by Equation (7-12) for unit depth.

Practical Application

In applying the equations discussed above in practical determination of forging load, two major parameters must be estimated: the friction factor, f, for die-material friction and the flow stress, $\bar{\sigma}$, for the strain, strain-rate, and temperature conditions existing during forging. Often average strain-rate and temperature values must be estimated separately for flash and cavity. The details of predicting the flow stress for given forging conditions are described in Chapter 1. Experience[6, 7] shows that the interface friction factor has a value of 0.2 to 0.4. Thus, a good value for a first estimate is f = 0.3.

Most forgings cannot be classified as only round or long. It is often necessary to consider a forging as having round (axisymmetric) as well as long (plane strain flow) sections. Detailed discussion on dividing a forging into smaller components, for the purpose of analysis, is given elsewhere[7].

FORGING TRIALS UNDER PRODUCTION CONDITIONS

As part of the present study, various forging operations were investigated under production conditions. For this purpose forging trials were conducted in a Weingarten screw press at the Westinghouse Electric Corporation's plant in Winston-Salem, North Carolina; in a Hasenclever screw press at Steel Improvement and Forge Company in Cleveland, Ohio; and in a mechanical press at Ontario Corporation in Muncie, Indiana.

Forging Trials at Westinghouse Electric Corporation

Equipment and Instrumentation

The screw press used in this investigation was a Weingarten PZS 630 with electric drive geared directly to the flywheel. This press, using an electric drive to accelerate the flywheel and screw assembly converts the angular kinetic energy into the linear energy of the ram. Two reversible electric motors are attached to the press frame and drive the flywheel. The screw is threaded into the ram and does not move vertically. During the down stroke, the motors accelerate the flywheel and the screw, and the ram starts its downward motion. The flywheel energy and the ram speed continue to increase until the ram hits the workpiece. Thus the load necessary for forging is built up and transmitted through the ram, the screw, and the bed to the press frame. During forging, the entire energy of the flywheel is used up in deforming the workpiece and elastically deflecting the press, the flywheel, and the screw. Once the flywheel has stopped, the elastic loading of the frame and the axial and torsional straining of the screw cause the flywheel and the screw to rotate in the reverse direction and the ram disengages from the workpiece. The electric motors are then reversed and lift the ram to its initial position.

This screw press, seen in Figure 7-7, has a nominal rating of 4000 metric tons (4400 U. S. tons), and a nominal energy capacity of 71,000 kgm (3100 ton-inch). The maximum ram velocity of the press is 0.6 m/sec (24 inches/second) and its static stiffness, as measured by the manufacturer, is 1280 metric tons/mm (35,200 tons/inch).

The displacement measurements during the forging trials were made using an inductive type of transducer (LVDT). The transducer, manufactured by the Daytronic Corporation, had a maximum stroke of 4 inches. The load measurements were made using strain gages attached directly to the tie rods of the press. These strain gages were connected into a Wheatstone bridge arrangement so that the small changes in resistance of the strain gages could be easily monitored.

As the Westinghouse press had not been calibrated for load previously, it was necessary to do so in order to properly interpret the data obtained. The calibration was done using the 3000-ton load cell that was designed and built earlier in this program (see Chapter 2). Since the press was to be calibrated using a load cell of much smaller capacity than the press capacity, it was imperative that the energy expended during the calibration blow be relatively small

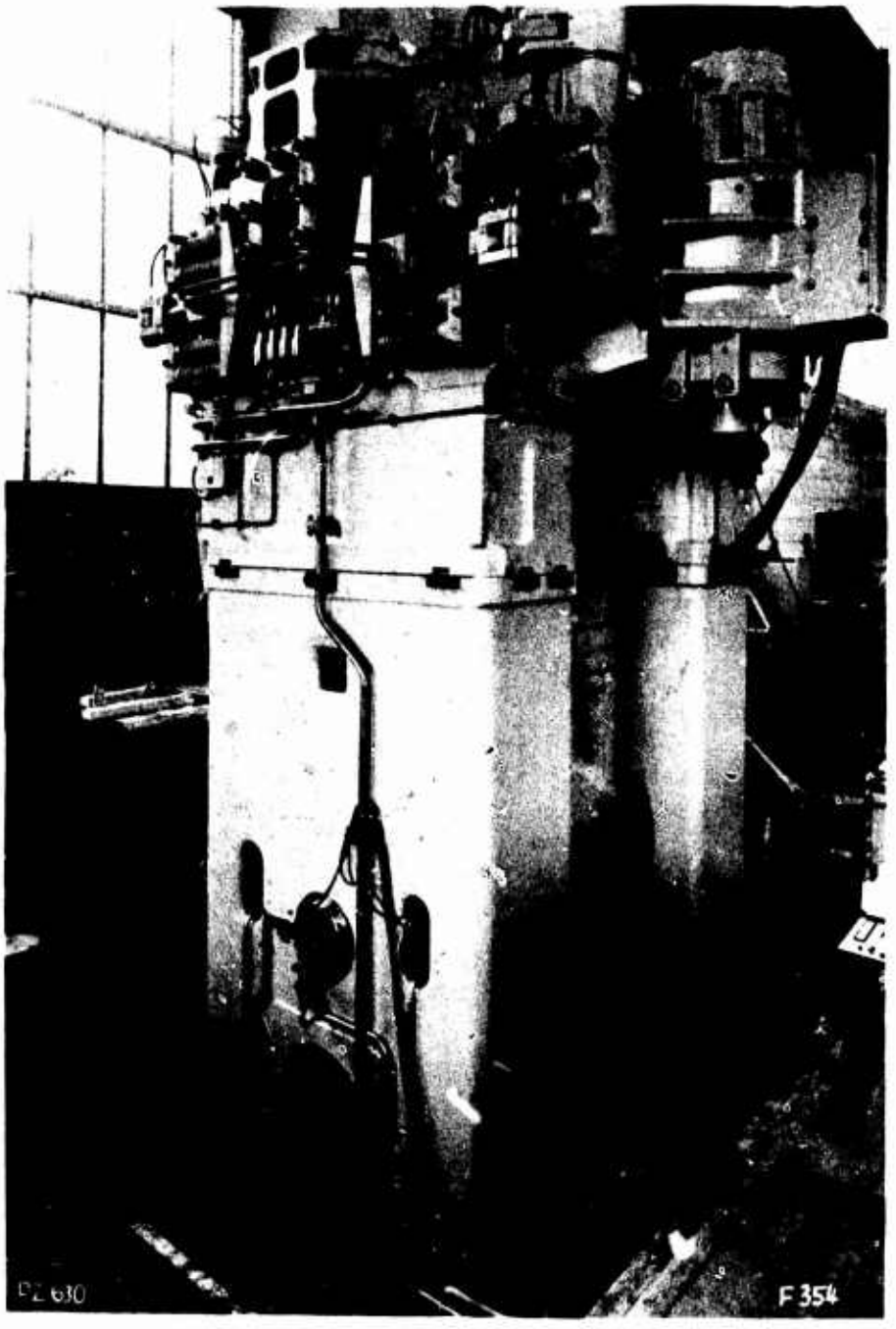

FIGURE 7-7. 4000-TON WEINGARTEN SCREW PRESS IN WHICH FORGING TRIALS WERE CONDUCTED AT WESTINGHOUSE ELECTRIC CORPORATION IN WINSTON-SALEM, NORTH CAROLINA

compared to the maximum possible energy. For this calibration, the ram was allowed to fall onto the load cell from several inches above the load cell without the use of the electric drive motors. When the falling distance of the ram was increased, the velocity of the ram and the flywheel was also increased. The increased velocities resulted in increased kinetic energies and higher loads were obtained. Initially, the ram was dropped from 4 inches above the load cell, and a load of 1730 tons was obtained. Subsequently, the ram was dropped from several different positions. A 5-inch drop resulted in a load of 2140 tons, and a 1-inch drop gave a load of 910 tons. During this calibration the output from the load cell was monitored simultaneously with the output from the strain-gage bridge on the tie bars of the press. Thus, it was possible to relate the output of the press bridge to an obtained load.

During the forging trials, output from the load and displacement transducers were recorded on a high-speed light-beam oscillographic recorder (Century model 470). The signals from the transducers were electronically amplified so that most of the width of the chart paper was used in recording the data. This was done to

improve resolution so that small changes in load or displacement could be easily distinguished. The recorder, which records the data as a function of time, was operated at a relative high chart speed (either 10 or 20 inches per second) so the time relationship of the data could be easily distinguished.

Forging Trials

Figure 7-8 illustrates the type of part forged in the screw press at the Westinghouse Corporation. This part is of 403 stainless steel and was forged from a preform at 2050 F. The preform configuration was achieved by reducer rolling and exhibited a large head, for forging the root of the blade, and a reduced straight portion having an approximately round cross section. In these trials the preform was not lubricated or coated prior to forging. The dies, however, were lubricated with a commercial water-base graphite lubricant and were also heated to about 400 F.

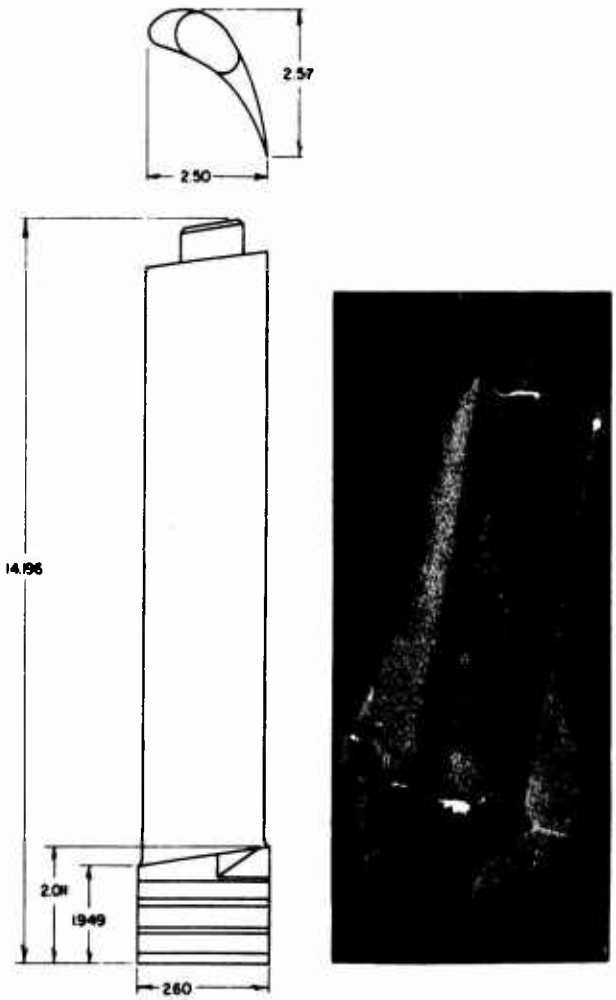

FIGURE 7-8. 403 STAINLESS STEEL BLADE FORGED IN 4400 TONS WEINGARTEN SCREW PRESS AT WESTINGHOUSE

The energy delivered by a screw press can be controlled by the position from which the downward motion of the ram begins. This is because over the longer strokes the flywheel achieves a higher velocity and therefore, contains more energy. This is true both when the ram falls under its own weight (as was described for the calibration of this screw press) and when the flywheel is driven by the electric motors. Thus, the energy available at the ram can be related to the press stroke.

For the trials conducted in the Westinghouse press, it was felt desirable to forge blades at several different energy settings. Thus, the starting position of the ram was changed for each forging in these trials. The initial portion of the load-displacement relationship was found to be much the same whether the blade was forged with

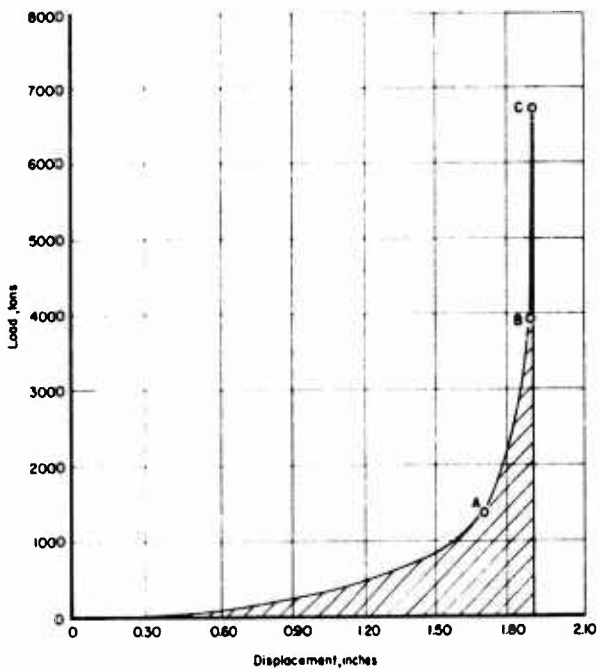

FIGURE 7-9. LOAD-DISPLACEMENT RELATIONSHIP FOR FORGING A 403 STAINLESS STEEL TURBINE BLADE IN THE WESTINGHOUSE SCREW PRESS

Point A indicates the load and displacement achieved when inadequate energy was supplied for forging the blade.

Point B indicates the load and displacement achieved when just adequate energy was supplied for forging the blade.

Point C indicates the load and displacement achieved when a large excess of energy was supplied for forging the blade.

excess energy or whether the energy was inadequate and the part was not completely forged. This is shown in Figure 7-9 for three blades; one that was forged with a large excess of energy, a second that had just adequate energy, and a third that did not have sufficient energy. Obviously, when excess energy is available in the machine, the load continues to increase after the forging is completed. Thus, excess machine energy is transformed into elastic deflection energy by straining the dies and the press. In order to protect the tooling it is necessary to reduce the amount of this excess energy by using energy metering.

The energy required for the forging, graphically shown as the shaded area in the figure, was determined to be about 975 inch-tons. At the highest energy setting, the velocity of the upper die at the start of forging was 16.7 inch/second and the contact time during forging (including load buildup and release) was about 0.120 second.

Forging Trails at Ontario Corporation

Equipment and Instrumentation

The mechanical press used in these trials was a 1300-ton Bliss press located in Ontario Corporation's plant in Muncie, Indiana. The drive of this press is based on a slider-crank mechanism which translates rotary to linear motion. Since the load available in a mechanical press varies with the stroke position, it is important to know the load versus stroke curve. For the Bliss press, the nominal load capacity of 1300 tons corresponds to a stroke position of 0.040 inch before bottom dead center. This press has an 11-inch stroke and an idling speed of 75 strokes/min. The idling velocity of the flywheel largely determines the rate of forging.

Load measurements in the mechanical press were made using strain bars similar to those shown in Chapter 2. These strain bars are attached to the press frame and are designed to mechanically amplify the strain in the press frame when the press is loaded. The strain amplification is achieved by designing a stress concentration into the bar so that the strain in that area is increased. The amplified strain is then monitored by strain gages connected into a wheatstone bridge arrangement. The displacement was measured using the inductive transducer (LVDT) as for the screw press at Westinghouse. The outputs of the strain bars and of the LVDT were recorded using the same high-speed light-beam recorder.

Forging Trials

The Ti-6Al-4V blade shown in Figure 7-10 was forged in the 1300-ton Bliss press at the Ontario Corporation. During the observed trials, blades were forged to the finish configuration by two procedures. One procedure involved forging the finish shape in one blow from the preform (bottom of Figure 7-10). The second procedure involved forging the preform to an intermediate size before finishing. This intermediate size was forged in the finishing die but the die was not allowed to close to the finish dimension. Thus, an intermediate configuration that was obtained looked much like the finish forging, but it was thicker than the finish forging by about 0.030 inch.

Load and displacement were measured only during forging to finish configuration from the preform, seen in Figure 7-10 and from the intermediate size. It was not possible to monitor the forging of the intermediate shape, discussed above, because of production-scheduling problems. In preparation for forging, the preforms (and the intermediate pieces) were coated by spraying with a commercial glass forging lubricant. They were then heated to about 1700 degrees F in a gas-fired rotary-hearth furnace. The dies were heated to about 400 F and were lubricated using a commercial water-base graphite lubricant.

Figure 7-11 illustrates a typical load displacement relationship for forging these blades from both the intermediate shape and the preform. As seen in Figure 7-11, the maximum load during the forging of the preform was about 1100 tons. The energy required for the forging, graphically illustrated as the shaded area in

FIGURE 7-10. THE PREFORM AND THE FINISH FOR Ti-6Al-4V BLADE FORGED AT THE ONTARIO CORPORATION

Figure 7-11, was determined to be about 145 inch-tons. The contact velocity of the upper die for these trials was 19 inch/second and time duration for forging, only during load buildup, was 0.053 second.

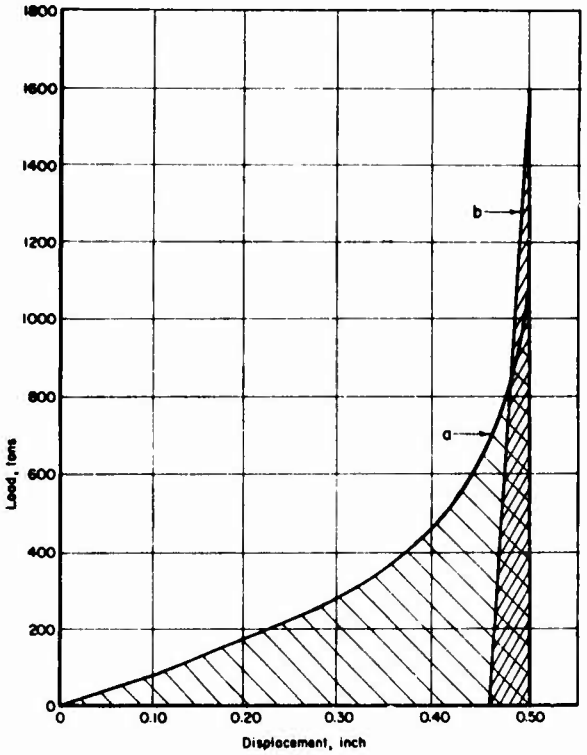

FIGURE 7-11. LOAD-DISPLACEMENT RELATIONSHIP FOR FORGING THE Ti-6Al-4V BLADE IN THE 1300-TON MECHANICAL PRESS AT THE ONTARIO CORPORATION

Curve a is the load-displacement relationship for forging the blade from the preform (see Figure 7-10).
Curve b is the load-displacement relationship for forging the blade from the intermediate shape.

Forging from the intermediate shape required a much higher load, about 1620 tons, Figure 7-11. The energy required for forging from the intermediate shape, again the area beneath the load-displacement curve, was determined to be about 29 inch-tons. The contact velocity of the upper die for this forging operation was 7 inch/second and the time duration for forging, only during load buildup was 0.031 second.

Forging Trials at Sifco

Forging trials were also monitored on the Hasenclever screw press at the Sifco plant in Cleveland, Ohio. This press uses a hydraulic drive to accelerate the flywheel and screw assembly. The angular kinetic energy of these components is then converted into linear energy of the ram in the same manner as for the electrically driven screw press at Westinghouse (described above).

This screw press has a nominal rating of 3150 metric tons (3460 U. S. tons) and a net energy capacity of about 43,000 kg-m (1800 inch-tons). The maximum ram velocity of the press is about 0.8 meter/second (31.5 inches/second) and its stiffness, determined by Hasenclever, is 820 metric tons/mm (~22,500 U. S. tons/inch).

Displacement was measured during the forging trials using the same LVDT described for the other trials. However, because the stroke of the press under load was quite small, the resolution was poor and the displacement data were considered to be of no value.

This press had been calibrated for load by the Hasenclever personnel when the press was installed. In addition, a recorder was provided that recorded the peak load for each forging cycle. The load was monitored via Wheatstone bridge arrangement made up of 600-ohm strain gages placed on the tie-bars of the press. For the forging trials monitored it was necessary only to connect the existing bridge to the Battelle recorder and use the calibration established by the Hasenclever personnel. Again, the output from the load and displacement transducers were recorded on a high-speed light-beam oscillographic recorder (Century model 470).

Blades of a superalloy similar to that illustrated in Figure 7-12, were forged in these trials.

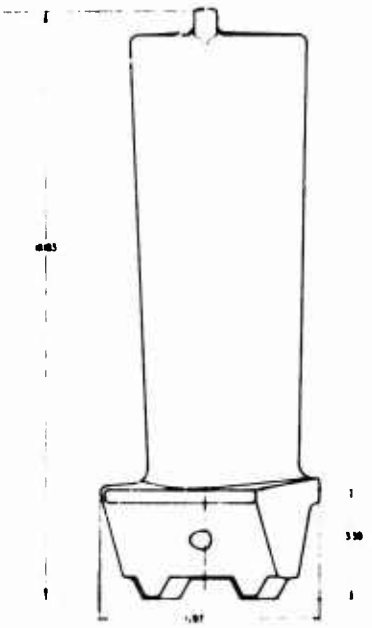

FIGURE 7-12. THE SUPERALLOY BLADE FORGED ON THE HASENCLEVER SCREW PRESS AT THE SIFCO PLANT IN CLEVELAND, OHIO

The forging was a finishing operation in which the blades were sized using the same dies they had been forged on earlier. Thus, the reduction in thickness was small. Before the forging blow the dies were lubricated with an oil-base graphite lubricant.

The peak load for this operation was 3900 tons or about 113 percent of nominal capacity. The ram velocity prior to contact was about 25.8 inches/second (0.64 meters/second) and the contact time during forging (including load buildup and release) was about 0.032 seconds.

SUMMARY AND DISCUSSION

Chapter 7 consists essentially of two parts. The first part represents a review of the literature on empirical methods for predicting forging loads, the second part of this chapter discusses the details of forging trials conducted in two screw presses (at Sifco and Westinghouse) and in a mechanical press (at Ontario).

Review of Prediction Methods

The first part also includes (a) the description of a nomogram useful in predicting forging loads and energies in steel forgings and (b) a relatively simple method, based on elementary plasticity analysis, for calculating stress distribution, average pressure, and load in forging. The empirical methods have been developed by analyzing forging load data for a variety of parts produced from a certain material, mostly from carbon and low alloy steels. Consequently, their application will be limited to those materials unless a correction factor, which is based on the flow stress of steels and of other materials, is used in evaluating the results. The simple mathematical method is somewhat more cumbersome and would require the use of a calculator, however, it can be applied to any material as long as the flow stress at forging conditions (strain, strain-rate and temperature) and the friction factors are known. Such information is given in Chapter 1, and in Chapters 5 and 6 of this Final Report.

Forging Trials

The screw presses used in the forging trials had nominal capacities of 4400 tons (Weingarten at Westinghouse Electric Corporation's Winston-Salem, North Carolina plant) and 3500 tons (Hasenclever at Sifco's Cleveland, Ohio plant). The mechanical press (Bliss at Ontario's Muncie, Indiana, plant) had a nominal capacity of 1300 tons. The parts forged in these presses (two screw and one mechanical), were different in size and in material (stainless steel at Westinghouse, superalloy at Sifco, and titanium alloy at Ontario). Consequently, as seen in Table 7-2 a direct comparison of parameters such as forging performance, deformation speeds, contact times (loading and unloading), load and energy variations because of machine characteristics, accuracy characteristics cannot be made. Nevertheless, certain overell observations are given below:

TABLE 7-2. CONTACT TIMES MEASURED DURING FORGING IN THREE DIFFERENT PRESSES

The data given in this table cannot be used for direct comparison of machine characteristics because the machine capacities and the forged parts were different in all three cases.

Press	Company	Maximum Measured Load, tons	Contact Velocity, in./sec	Approximate Stroke Under Load, inch	Contact Times, second		
					Load Buildup	Load Release	Total
4400-Ton Weingarten Screw	Westinghouse	3900(a)	10.3	2.5(c)/0.9	0.215(c)/ 0.140	0.085	0.30(c)/ 0.225
3500-Ton Hasenclever Screw	Sifco	3900(b)	25.2	>0.080(d)	0.019	0.013	0.032
1300-Ton Bliss Mechanical	Ontario Corporation	1110(a)	19.0	0.50	0.053	0.023	0.076
		1620(b)	7.0	0.03	0.031	0.023	0.054

(a) Forging from preform.
(b) Forging from intermediate shape (or blocker).
(c) Data related to forging blade root.
(d) As forging stroke was difficult to measure, the value shown is only approximate.

(1) The Ti-6Al-4V blade, Figure 7-10, was forged from a preform (extruded and upset) in one blow and also from a preformed intermediate shape (or blocker). The forging stroke for the blocker was approximately 0.030 inch. In forging from the preform, the maximum load was 1110 tons, while in forging from the intermediate shape, the maximum load was 1620 tons. This difference is explained by the following facts:

(a) For the preform, the initial heat losses in the material are small (small surface-to-volume ratio in a round cross section, as seen in Figure 7-10), the forging stroke and the forging energy are large. Thus, the heat generated during deformation maintains the flow stress of the titanium alloy, which is very sensitive to temperature, at a low level. This results in a relatively low forging load.

(b) The preformed shape (or blocker) has large surface-to-volume ratio. This results in heat losses during transport of the part from furnace to the press and during the initiation of the stroke. The deformation energy and the heat generation are relatively low, therefore, the material temperature during forging is also low. This results in higher flow stress and forging load.

(2) The contact velocity in the 4400-ton Weingarten press is relatively low. Because the energy available in the press was much more than that required by the relatively small forging, the energy level and the ram speed had to be lowered. As a result, the contact times, both for load buildup and release, are relatively long.

(3) The 3500-ton Hasenclever press was operated near its maximum energy and speed level. Thus, for a relatively small stroke the contact times are very small.

(4) In the mechanical press, the load release times are not influenced by the magnitude of the forging load, as it was observed in earlier studies (in Chapter 4, where a screw press and a mechanical press of similar capacities were compared). It appears that, in comparison, the measurements for the 3500-ton Hasenclever screw press gives shorter total contact times although it has a larger capacity.

REFERENCES

(1) Schey, J. A., "Principles of Forging Design" prepared by IITRI for The American Iron and Steel Institute.

(2) Geleji, A., "Forge Equipment, Rolling Mills, and Accessories", Akademiai Kiado, Budapest (1967), Chapter 2.

(3) Kurrein, M., "Tools and Processes in Presses" (in German), Springer Verlag, Berlin 1926.

(4) Neuberger, F., and Pannasch, S., "Material Consumption in Die Forging of Steel" (in German), Fertigungstechnik und Betrieb, 12, 1962, p. 775-79.

(5) Altan, T., and Fiorentino, R. J., "Prediction of Loads and Stresses in Closed-Die Forging", ASME Transactions, J. of Engr. for Industry, May, 1971, p. 477.

(6) Akgerman, N., Altan, T., and Fiorentino, R. J., "Manufacturing Methods for a Computerized Forging Process for High-Strength Materials", Interim Progress Reports IR-222-1(I), IR-222-1(II), IR-222-1(III), and IR-222-1(IV), Air Force Contract No. F33615-71-C-1689, Battelle's Columbus Laboratories, October, 1971; January, 1972; April, 1972; and July, 1972.

(7) Akgerman, N., and Altan, T., "Modular Analysis of Geometry and Stresses in Closed-Die Forging: Application to a Structural Part", ASME Paper No. 72-Prod-9, will be published in Transactions.